

Empirical Relationships for Peak Ground Acceleration in Indian Earthquakes

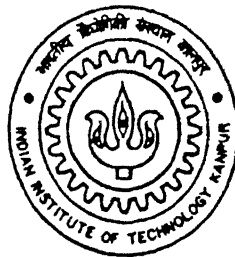
702701

A Thesis Submitted
In Partial Fulfillment of the Requirements
for the Degree of

MASTER OF TECHNOLOGY

by

Roshan A. D.
Roll number 9710328



DEPARTMENT OF CIVIL ENGINEERING
INDIAN INSTITUTE OF TECHNOLOGY KANPUR
August 2000

19 JUL. 2001/CE

पुरुषोत्तम लाल शर्मा केलकर पुस्तकालय
भारतीय प्रौद्योगिकी संस्थान कानपुर
अवाप्ति क्र० A...**134265**.....-

TH

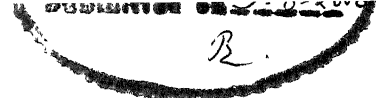
CE/2222/11

R7



A134265

CERTIFICATE



It is certified that the work contained in this thesis entitled "*Empirical Relationships for Peak Ground Acceleration in Indian Earthquakes*" by Mr. Roshan A.D. (Roll Number: 9710328), has been carried out under our supervision and this work has not been submitted elsewhere for a degree.

(Dr. Prabir C. Basu)

Head, Civil & Structural Engineering Division
Atomic Energy Regulatory Board
Niyamak Bhavan, Mumbai

(Dr. Sudhir K. Jain)

Professor
Department of Civil Engineering
Indian Institute of Technology, Kanpur

July, 2000

ABSTRACT

Himalayan region in India is one of the most seismically active regions in the world. About 120 recordings from Strong Motion Accelerographs (SMAs) are now available from the recent Himalayan earthquakes in the magnitude (M) range of 5.2 to 7.3 with the epicentral distances (R) ranging from 3 to 350kms. About 260 records from Structural Response Recorders (SRRs) from 5 Himalayan earthquakes are also available (M : 5.5-7.3; R : 4-770kms). SRRs record spectral acceleration at natural periods of 0.4sec, 0.75sec and 1.25sec, for damping ratios of 5% and 10% of critical. The strong motion database available for Indian earthquakes can be enhanced by making use of records from SRRs.

The compatibility of responses from SRRs and SMAs from Indian earthquakes has been studied and the peak ground acceleration has been estimated from SRR recordings. The estimates of peak ground acceleration from SRRs are in line with those from SMAs. The peak ground accelerations in Indian earthquakes are compared with those predicted by the existing attenuation relationships. It is seen that the relationships provide reasonable estimates for the earthquakes in Central Himalayas, but underestimate the motion for earthquakes in North-East India and Indo-Gangetic plains. It is seen that based on attenuation characteristics, the Himalayan earthquakes can be grouped into four categories: (a) events of Central Himalayas, (b) non-subduction earthquakes of North-East India, (c) subduction events of North-East India, and (d) Earthquakes in Indo-Gangetic plains.

Separate attenuation relationships for peak ground acceleration are derived for earthquakes in Central Himalayas, Indo-Gangetic plains, North East Indian Non-subduction zone earthquakes and North East Indian subduction zone earthquakes.

Acknowledgement

I express my deep sense of gratitude to my thesis supervisors, Professor Sudhir K. Jain and Dr. Prabir C. Basu, for their valuable and unbiased guidance, critical discussions, continuous encouragement, and support during the thesis program. Their constant surveillance and suggestions have helped me in the critical stages of the thesis. I am especially indebted to Professor Jain for keeping a special interest on the topic and helping me complete my work well in time. Without the helpful guidance from Dr. Debasis Kundu, it would not have been possible for me to tackle the problems related to statistics.

I am also deeply indebted to Professors Sudhir Misra and C.V.R. Murty for the constant support and encouragement they have provided throughout my course. I thank the faculty at IIT Kanpur, without whose help it would not have been possible for me to cover many of the unfamiliar territories in my subject.

The moments I spent with my classmates Kiran, Ranjith, Siju, Dada, Vishnu, Naram, Piyush, Rajesh, Mukul, Srikanth, and Madhu will always be one of the most memorable periods in my life. It would not have been possible for me complete this endeavor without the great amount of help I got from Jaswant. Bajpaiji has always been a source of inspiration. I thank him for the help he provided. Its been a pleasure to be with my juniors Pavan, Joshi, Moitra, Diptesh, Pdasg, Samit, Gandhi, Vijay, Manojku, Choubey and my friends Groverji and Hemant. I also thank all my colleagues in *Malayali samajam* for the great support they provided.

I gratefully acknowledge the help provided by Department of Earthquake Engineering, University of Roorkee for supplying strong motion data. I also thank Atomic Energy Regulatory Board for granting me leave for completion of thesis and the constant encouragement provided throughout the period.

Roshan A. D.

Table of Contents

Certificate	i
Abstract	ii
Acknowledgements	iii
Table of Contents	iv
List of Tables	vi
List of Figures	viii
List of Symbols	xiii
Chapter 1: Introduction	
1.0 General	1
1.1 Seismic hazard analysis	1
1.1.1 Deterministic Seismic Hazard Assessment	1
1.1.2 Probabilistic Seismic Hazard Assessment	2
1.2 Scope of Study	3
1.3 Organisation	3
Chapter 2: Review of Existing Attenuation Relationships	
2.0 Introduction	7
2.1 Estimation of Ground Motion	7
2.2 Attenuation Relationships for Peak Ground Acceleration (PGA)	8
2.2.1 Nature of PGA Values	8
2.2.2 Propagation Parameters	9
2.2.2.1 Distance	9
2.2.2.2 Site Geology	12
2.2.3 Effect of Magnitude	14
2.2.4 Source Mechanism	16
2.2.5 Method of Regression Analysis	16
2.2.5.1 Method of Least Squares	16
2.2.5.2 Two Step Regression Analysis	17
2.2.5.3 Method of Maximum Likelihood	20
2.2.6 Validity of Result and Treatment of Uncertainty	21
2.2.6.1 Analysis of Residuals	21
2.2.6.2 Multiple Correlation Coefficient	21
2.2.6.3 Uncertainty in Prediction	22
2.3 Literature Review of Attenuation Relationships	22
2.3.1 Boore et al. (1997)	22
2.3.2 Campbell (1997)	23
2.3.3 Sadigh et al. (1997)	25
2.3.4 Spudich et al. (1997)	26
2.3.5 Atkinson and Boore (1997b)	26
2.3.6 Youngs et al. (1997)	27
2.3.7 Crouse (1991)	28
2.3.8 Ambraseys (1995)	29
2.3.9 Tenta et al. (1992)	30
2.3.10 Fukushima and Tanaka (1990)	30
2.3.11 Caillot and Bard (1993)	30
2.3.12 Anders et al. (1990)	31

Chapter 3 Strong Motion Data from Indian Earthquakes

3.0 Introduction	39
3.1 Seismo-Tectonics of Himalayan Region	39
3.2 Instrumentation and Availability of Data	40
3.2.1 Shillong Array in Meghalaya	41
3.2.2 Bihar Array in Bihar	41
3.2.3 Uttar Pradesh Array in North-Western Uttar Pradesh	41
3.2.4 Kangra Array in Himachal Pradesh	42
3.2.5 Arunachal Pradesh Array in Arunachal Pradesh	42
3.3 Earthquake Parameters	42
3.3.1 Calculation of Epicentral Distance	43
3.4 Analysis of SRR Data	44
3.4.1 Resultant Response Spectrum	44
3.4.2 SRR Data versus SMA Data	45
3.4.3 Removal of Outliers	46
3.4.4 Observations on Data Analysis	48
3.4.5 Statistical Analysis of Data	50
3.4.6 Spectral Acceleration versus Distance	51
3.5 PGA from SRR Data	52
3.5.1 Spectrum Amplification Factor	53
3.5.2 PGAs from Recorded RSAs	55
3.5.2.1 Method Based on Median of Analysis	56
3.5.2.2 Method Based on Median of Analysis and Weight Functions	56
3.5.2.3 Method Based on Mean of Analysis	57
3.5.2.4 Method Based on Mean of Analysis and Weight Functions	57
3.5.2.5 Best-Fit Method	58
3.5.3 Spread in Predicted PGAs	59

Chapter 4 Development of Attenuation Relationships

4.0 Introduction	107
4.1 Indian Strong Motion data Versus Existing Attenuation Relationships	107
4.2 Development of Attenuation Model	111
4.2.1 Selection of Parameters	111
4.2.1.1 Earthquake Parameters	111
4.2.1.2 Source Parameters	112
4.2.1.3 Propagation Parameters	112
4.2.1.4 Site Parameters	112
4.2.1.5 Data Selection	112
4.2.2 Selection of Attenuation Model	113
4.3 Attenuation model for Himalayan Earthquakes	115
4.3.1 Preliminary analysis of data	116
4.3.2 Study of Outliers	117
4.3.3 Observations on variation of PGA of different events	119
4.4 Development of Attenuation Relationships	121
4.5 Adequacy of Model	123
4.5.1 Analysis of Residuals	123
4.5.2 Significance Testing of Coefficients	123

Chapter 5 Summary and Conclusions

References

Appendix A

Appendix B

List of Tables

<i>Table</i>	<i>Title</i>	<i>Page</i>
2.1	Comparison between the parameters obtained by one-stage maximum likelihood method, the two-stage method and the ordinary least squares method applied to Fukushima and Tanaka's data for the model $\log(y) = a + bM + c \log R$ [Joyner and Boore, 1993]	32
3.1(a)	Earthquake events considered in this study.	61
3.1(b)	Earthquake events considered and number of recordings.	61
3.2	Correlation of epicentral distances with average peak ground acceleration.	62
3.3(a)	Results of statistical analysis for the ratios of the data of 6 August 1988 Shillong earthquake	63
3.3(b)	Results of statistical analysis for the ratios of the data of 21 August 1988 Bihar-Nepal earthquake.	63
3.3(c)	Results of statistical analysis for the ratios of the data of 20 October, 1991 Uttarkashi earthquake.	64
3.3(d)	Results of statistical analysis for the ratios of the data of 29 March, 1999 Chamoli earthquake.	64
3.3(e)	Results of statistical analysis for the ratios of the data of 26 April, 1986 Kangra earthquake.	65
3.4	Correlation between spectral acceleration and epicentral distance.	66
3.5	Statistical parameters for the amplification factors ($SA_{\text{resultant}}/PGA_{\text{average}}$) for the different earthquakes.	66
3.6	Spectrum amplification factors for horizontal elastic response (from Newmark and Hall, 1982).	67
3.7	Correlation of amplification factors and distance for different earthquakes.	67
3.8	Error between PGA_{observed} and $PGA_{\text{predicted}}$ using different weighing factors and amplification factors.	67
3.9	Coefficient of variation among the six PGA calculated from SA values of SMAs and SRRs (Weights equal to unity).	68
4.1	Average error of prediction from the observed data for different attenuation relationships.	125
4.2	Coefficients of regression for the model given in Eq. (4.10), using the database containing accelerations from all the events.	125
4.3	Coefficients of regression for the model given in Eq. (4.13), using the database after the removal of records obtained from August 20, 1988 Bihar-Nepal earthquake.	126
4.4	Coefficients of regression for the model given below using the accelerations recorded by 1986 NE M5.2, 1987 NE M5.9 and 1988 NE M5.8. $\ln Y = b_1 + b_2M + b_3R + b_4 \ln R$	126
4.5	Coefficients of regression for the model given below using the database of accelerations recorded by 1986 NE M5.2, 1987 NE 5.9 and 1988 NE M5.8. $\ln Y = b_1 + b_2M + b_3 \ln R$	126
4.6	Coefficients of regression for the model given below using the database of accelerations recorded by Uttarkashi, Chamoli and Kangra earthquakes. $\ln Y = b_1 + b_2M + b_3R + b_4 \ln R$	127

4.7	Coefficients of regression for the model given below with only subduction zone event (1988 NE M7.3). $\ln Y = b_1 + b_2 R + b_3 \ln R$	127
4.8	Coefficients of regression for the model given below with only 1988 Bihar-Nepal M6.8. $\ln Y = b_1 + b_2 R + b_3 \ln R$	127
4.9	Average error of prediction from the observed data for different attenuation relationships.	128

List of Figures

<i>Figures</i>	<i>Title</i>	<i>Page</i>
1.1	Figure 1.1 Basic steps of a deterministic hazard assessment (Bommer, 1999)	5
1.2	Figure 1.2 Basic steps in probabilistic seismic hazard assessment (Bommer, 1999)	6
2.1	Different definitions of distances used in the attenuation relationships [Abrahamson and Shedlock, 1997].	33
2.2	Different definitions of distances used in the attenuation relationships [Campbell, 1985].	34
2.3	Relationship Between moment magnitude and various magnitude scales [Kramer, 1996].	35
2.4	Histogram showing distribution of distance coefficients for individual earthquakes and average value along with coefficients obtained by non-stratified (one step) and two-step analyses [Fukushima and Tanaka, 1990].	36
2.5	Comparison of predictive curves for peak acceleration from two-stage and one-stage regression. (a) Predicted equations without considering focal depth, (b) Predicted equations when focal depth is considered in the analysis [Ambraseys, 1995].	37
2.6	Variation of Standard Deviation (σ_{ln}) of Peak Ground Acceleration with respect to magnitude for different attenuation relationships..	38
3.1	Tectonic features of the different regions considered in this study [modified from Rajendran <i>et. al.</i> , 1992].	69
3.2	Relative position of arrays used in this study [modified from Chandrasekaran and Das, 1992].	70
3.3 (a)	Photograph of a SRR [Agarwal, 1991].	71
3.3 (b)	A typical SRR record.	72
3.4 (a)	Location of stations in the Shillong array.	73
3.4 (b)	Location of stations in the Bihar array.	74
3.4 (c)	Location of stations in the Uttar Pradesh array.	75
3.4 (d)	Location of SMA and SRR stations in the Kangra region.	76
3.5 (a)	Location of epicenters as reported by different agencies along with the recording stations activated for the Shillong earthquake of 10 September 1986.	77
3.5 (b)	Location of epicenters as reported by different agencies along with the recording stations activated for the Shillong earthquake of 14 May 1987.	78
3.5 (c)	Location of epicenters as reported by different agencies along with the recording stations activated for the Shillong earthquake of 6 February 1988.	79
3.5 (d)	Location of epicenters as reported by different agencies along with the recording stations activated for the Shillong earthquake of 6 August 1988.	80
3.5 (e)	Location of epicenters as reported by different agencies along with the recording stations activated for the Shillong earthquake of 9 January 1990.	81
3.5 (f)	Location of epicenters as reported by different agencies along with the recording stations activated for the Bihar-Nepal earthquake of 21 August 1988.	82

3.5 (g)	Location of epicenters as reported by different agencies along with the recording stations activated for the Uttar Pradesh (Uttarkashi) earthquake of 20 October 1991.	83
3.5 (h)	Location of epicenters as reported by different agencies along with the recording stations activated for the Uttar Pradesh (Chamoli) earthquake of 29 March 1999.	84
3.5 (i)	Location of epicenters as reported by different agencies along with the recording stations for activated the Kangra earthquake of 26 April 1986.	85
3.6	Schematic representation for the calculation of the resultant two-dimensional acceleration from the SMA records.	86
3.7 (a)	Distribution of ratios of $SA_{T_1, \zeta=5\%} / SA_{T_2, \zeta=5\%}$ for August 6, 1988 event for SRRs and SMAs	87
3.7 (b)	Distribution of ratios of $SA_{T_1, \zeta=10\%} / SA_{T_2, \zeta=10\%}$ for August 6, 1988 event for SRRs and SMAs	88
3.7 (c)	Distribution of ratios of $(SA_{0.4 \text{ sec}, \zeta=5\%} / SA_{0.4 \text{ sec}, \zeta=10\%})$, $(SA_{0.75 \text{ sec}, \zeta=5\%} / SA_{0.75 \text{ sec}, \zeta=10\%})$ and $(SA_{1.25 \text{ sec}, \zeta=5\%} / SA_{1.25 \text{ sec}, \zeta=10\%})$ for August 6, 1988 event.	89
3.7 (d)	Distribution of ratios of $SA_{T_1, \zeta=5\%} / SA_{T_2, \zeta=5\%}$ for October 20, 1990 Uttarkashi event for SRRs and SMAs	90
3.7 (e)	Distribution of ratios of $SA_{T_1, \zeta=10\%} / SA_{T_2, \zeta=10\%}$ for October 20, 1990 Uttarkashi event for SRRs and SMAs	91
3.7 (f)	Distribution of ratios of $(SA_{0.4 \text{ sec}, \zeta=5\%} / SA_{0.4 \text{ sec}, \zeta=10\%})$, $(SA_{0.75 \text{ sec}, \zeta=5\%} / SA_{0.75 \text{ sec}, \zeta=10\%})$ and $(SA_{1.25 \text{ sec}, \zeta=5\%} / SA_{1.25 \text{ sec}, \zeta=10\%})$ for October 20, 1990 Uttarkashi event for SRRs and SMAs.	92
3.7 (g)	Distribution of ratios of $SA_{T_1, \zeta=5\%} / SA_{T_2, \zeta=5\%}$ for August 21, 1988 Bihar event for SRRs	93
3.7 (h)	Distribution of ratios of $SA_{T_1, \zeta=10\%} / SA_{T_2, \zeta=10\%}$ for August 21, 1988 Bihar event for SRRs	94
3.7 (i)	Distribution of ratios of $SA_{T_1, \zeta=5\%} / SA_{T_2, \zeta=5\%}$ for March 29, 1999 Chamoli event for SRRs and SMAs.	95
3.7 (j)	Distribution of ratios of $SA_{T_1, \zeta=10\%} / SA_{T_2, \zeta=10\%}$ for March 29, 1999 Chamoli event for SRRs and SMAs.	96
3.7 (k)	Distribution of ratios of $SA_{T_1, \zeta=5\%} / SA_{T_2, \zeta=5\%}$ for April 26, 1986 Kangra event for SRRs and SMAs.	97
3.7 (l)	Distribution of ratios of $SA_{T_1, \zeta=10\%} / SA_{T_2, \zeta=10\%}$ for April 26, 1986 Kangra event for SRRs and SMAs.	98

3.8	The histograms for average values of $(SA_{0.4 \text{ sec}, \zeta=5\%} / SA_{0.4 \text{ sec}, \zeta=10\%})$, $(SA_{0.75 \text{ sec}, \zeta=5\%} / SA_{0.75 \text{ sec}, \zeta=10\%})$ and $(SA_{1.25 \text{ sec}, \zeta=5\%} / SA_{1.25 \text{ sec}, \zeta=10\%})$	99
3.9	Schematic representation for the confidence interval for the null hypothesis, H_0 .	100
3.10 (a)	Amplification factor of the resultant Spectral Acceleration versus epicentral distance for the August 6, 1988 Shillong earthquake, best fit line used $y = a \ln x + b$.	101
3.10(b)	Amplification factor of the resultant spectral acceleration versus epicentral distance for the October, 1991 Uttarkashi earthquake, best fit line used $y = a \ln x + b$.	102
3.10(c)	Amplification factor of the resultant spectral acceleration versus epicentral distance for the March, 1999 Chamoli earthquake, best fit line used $y = a \ln x + b$.	103
3.10(d)	Amplification factor of the resultant spectral acceleration versus epicentral distance for the April, 1986 Kangra earthquake, best fit line used $y = a \ln x + b$.	104
3.11	Variation of amplification factors for spectral acceleration from different attenuation relationships available in the literature ($\zeta = 5\%$ of critical).	105
3.12	Peak ground acceleration versus distance for different earthquakes.	106
4.1(a)	Distribution of peak ground acceleration for 10 September 1986, NE India earthquake and the predicted values of PGA using different relationships available for interplate earthquakes.	129
4.1(b)	Distribution of peak ground acceleration for 14 May 1987, NE India earthquake and the predicted values of PGA using different relationships available for interplate earthquakes.	129
4.1(c)	Distribution of peak ground acceleration for 6 February 1988, NE India earthquake and the predicted values of PGA using different relationships available for interplate earthquakes.	130
4.1(d)	Distribution of peak ground acceleration for 6 August 1988, NE India earthquake and the predicted values of PGA using different relationships available for interplate earthquakes.	130
4.1(e)	Distribution of peak ground acceleration for 10 January 1990, NE India earthquake and the predicted values of PGA using different relationships available for interplate earthquakes.	131
4.1(f)	Distribution of peak ground acceleration for 20 October 1991, Uttarkashi earthquake and the predicted values of PGA using different relationships available for interplate earthquakes.	131
4.1(g)	Distribution of peak ground acceleration for 29 March 1999, Chamoli earthquake and the predicted values of PGA using different relationships available for interplate earthquakes.	132
4.1(h)	Distribution of peak ground acceleration for 26 April 1986 Kangra earthquake and the predicted values of PGA using different relationships available for interplate earthquakes.	132
4.1(i)	Distribution of peak ground acceleration for 21 August 1988, NE India earthquake and the predicted values of PGA using different relationships available for interplate earthquakes.	133

4.2(a)	Distribution of peak ground acceleration for 10 September 1986, NE India earthquake and the predicted values of PGA using different relationships available for intraplate earthquakes.	134
4.2(b)	Distribution of peak ground acceleration for 14 May 1987, NE India earthquake and the predicted values of PGA using different relationships available for intraplate earthquakes.	134
4.2(c)	Distribution of peak ground acceleration for 6 February 1988, NE India earthquake and the predicted values of PGA using different relationships available for intraplate earthquakes.	135
4.2(d)	Distribution of peak ground acceleration for 6 August 1988, NE India earthquake and the predicted values of PGA using different relationships available for intraplate earthquakes.	135
4.2(e)	Distribution of peak ground acceleration for 10 January 1990, NE India earthquake and the predicted values of PGA using different relationships available for intraplate earthquakes.	136
4.2(f)	Distribution of peak ground acceleration for 20 October 1991, Uttarkashi earthquake and the predicted values of PGA using different relationships available for intraplate earthquakes.	136
4.2(g)	Distribution of peak ground acceleration for 29 March 1999, Chamoli earthquake and the predicted values of PGA using different relationships available for intraplate earthquakes.	137
4.2(h)	Distribution of peak ground acceleration for 26 April 1986 Kangra earthquake and the predicted values of PGA using different relationships available for intraplate earthquakes.	137
4.2(i)	Distribution of peak ground acceleration for 21 August 1988, NE India earthquake and the predicted values of PGA using different relationships available for intraplate earthquakes.	138
4.3(a)	Distribution of peak ground acceleration for 6 August 1988, NE India earthquake and the predicted values of PGA using different relationships available for subduction zone earthquakes.	139
4.3(b)	Distribution of peak ground acceleration for 10 January 1990, NE India earthquake and the predicted values of PGA using different relationships available for subduction zone earthquakes.	139
4.4	Scatter-graph of the epicentral distances from stations and magnitude of each event recorded by them.	140
4.5	Plot of the variation of accelerations recorded in the different earthquakes with respect to the epicentral distance. This includes database consisting accelerations from all events	141
4.6	Distribution of h_i with respect to epicentral distance for the data set considered in the analysis. The dashed line gives theoretical cutoff for the data.	142
4.7	Plot of the variation of accelerations recorded in the different earthquakes with respect to the epicentral distance. This includes database consisting accelerations from all events after removal of outliers.	143
4.8	Plot of the variation of accelerations recorded in the NE Indian earthquakes with respect to the epicentral distance.	144
4.9	Plot of the variation of accelerations recorded in the N Indian earthquakes (Uttarkashi, Chamoli and Kangra).	145
4.10	Plot of the variation of accelerations recorded in the Bihar- Nepal earthquake with respect to the epicentral distance.	146

4.11	Plot of the best fit line of the accelerations recorded for each events with respect to the epicentral distance	147
4.12	The predicted values of acceleration using the new attenuation relationships plotted for different events along with the existing attenuation relationships	148
4.13	Comparison of the proposed equations for the four tectonic categories for a M7.0 event	149
4.14	Plot of residues of the regression analysis for NE, non-subduction zone earthquakes.	150
4.15	Plot of residues of the regression analysis for NE, subduction zone earthquake (August 6, 1988).	150
4.16	Plot of residues of the regression analysis for Central Himalayan earthquakes.	151
4.17	Plot of residues of the regression analysis for Bihar-Nepal earthquake.	151

List of Symbols

<i>Symbol</i>	<i>Description</i>
$\left. \begin{matrix} b_1 \\ b_2 \\ . \\ b_n \end{matrix} \right\}$	Coefficients used in regression analysis
g	Acceleration due to gravity
$\{h\}$	Diagonal terms of hat matrix
$[H]$	Hat matrix
H	Depth of focus of the earthquake
H_0	Null hypothesis
H_1	Alternate hypothesis
La_m, Lo_m	Latitude and Longitude of station 'm'
m_b	Body wave magnitude of earthquake
M_l	Local magnitude of earthquake
M_S	Surface wave magnitude of earthquake
M_W	Moment magnitude of earthquake
r_{jb}	Closest distance to surface projection of fault
R	Distance from source to site in km
r_{rup}	Closest distance to fault rupture.
T_n	Natural period of the SDOF system
V_s	Shear wave velocity of the medium of propagation
X	Matrix of explanatory variables
y_i	Observed value of dependant variable, PGA
\hat{y}_i	Predicted value of dependant variable
z	Test statistic for normal distribution
σ	Standard deviation of the sample
μ	Mean of the sample
δ	Difference in population means
ζ	Damping value

Chapter 1

Introduction

1.0 General

The Probabilistic Risk Assessment (PRA) of a Nuclear Power Plant (NPP) is conducted to develop an appreciation of plant behavior, understand most likely accident sequences, identify the dominant risk contributors etc. The contribution to the total plant risk can be divided into two parts: (1) Risk due to internal events, (2) Risk due to external events. The risk due to seismic activity is considered to be a major contributor in the total risk due to external events. This is because of the unique ability of an earthquake to initiate an accident and simultaneously fail a number of otherwise redundant components required for mitigating the accident. The elements of a seismic risk analysis can be identified as analyses of:

1. the seismic hazard at site
2. response of plant systems and structures
3. component fragilities
4. accident sequences
5. consequences

1.1 Seismic hazard analysis

The seismic hazard assessment can be carried out either deterministically or probabilistically.

1.1.1 Deterministic Seismic Hazard Assessment

The most straightforward approach to seismic Hazard assessment is deterministic. A Deterministic Seismic Hazard Assessment (DSHA) is based on identifying scenario events and determining the resulting ground motions at site. The basic steps of DSHA are illustrated in Figure 1.1. The size of the design earthquake may

be determined from the length of faults, assuming that a certain portion will rupture and estimating the magnitude from empirical relationships. When this is not possible, it is common practice to estimate the maximum credible earthquake magnitude, not from the physical dimensions of the fault but by simply adding an increment to the largest earthquake in the seismic catalogue [Bommer, 1999].

Having fixed the design magnitude for each source and corresponding distance from source, it is a simple matter to calculate the resulting ground motion at site with the help of attenuation relationships. The most severe case is then chosen as design earthquake. But a major difficulty with DSHA is that the level of conservatism of the design event is unknown.

1.1.2 Probabilistic Seismic Hazard Assessment

The problems associated with defining design earthquake are bypassed in Probabilistic Seismic Hazard Assessment (PSHA) (Figure 1.2).

The major elements of the hazard analysis are:

1. Identification of the sources of earthquakes such as faults and seismotectonic provinces. The assumption is made that earthquakes have an equal probability of occurring at any location within the source, so it is not necessary to fix the location of the design earthquake.
2. Evaluation of the earthquake history of the region to assess the frequencies of occurrence of earthquakes of different magnitudes.
3. Development of an attenuation relationship to estimate the intensity of earthquake induced ground motion (e.g., peak ground acceleration) at the site.
4. Integration of all these information to generate the frequencies with which different values of selected ground motion parameter would exceed.

Thus, the attenuation of ground motion parameter depending on the distance from the source and the magnitude of the earthquake is one of the important parameters used in seismic hazard evaluation of site.

The ground motion parameter predicted by the attenuation relation can be peak ground acceleration, peak ground velocity, peak ground displacement, intensity of shaking, or shape of the response spectrum.

The attenuation relationships developed are constantly updated based on the availability of new data for the particular region. In Indian subcontinent, the attenuation relationships commonly used for major projects are based on the data from Western United States of America (e.g., Chandrasekaran and Das, 1992). In recent years, strong motion data has been recorded by the strong motion instrumentation during several earthquakes in Northern India (e.g., Chandrasekaran and Das, 1990; Chandrasekaran and Das, 1992).

1.2 Scope of Study

A methodology is developed to calculate the peak ground acceleration from the response of structural response recorders. Based on this, a new attenuation relationship for peak ground acceleration is proposed using the Strong Motion Accelerograms and Structural Response Recordings of earthquakes experienced in the Himalayan region from 1986 to 1999.

1.3 Organisation

The work has been presented in five chapters including this one. In Chapter 2, various parameters, which control the attenuation of acceleration are discussed along with different solution schemes available. A review of various attenuation models available in the literature for different regions of the world is also presented. Chapter 3 discusses the various types of strong motion records available for Indian earthquakes and

formulates methods of extraction of peak ground acceleration from these records. A brief comparison of the observed peak ground acceleration with some of the published attenuation equations is presented in Chapter 4. A set of new attenuation relationships is also developed for the Himalayan region. A brief summary and conclusions of the study are presented in Chapter 5. The database used in the present study is given in Appendices A and B.



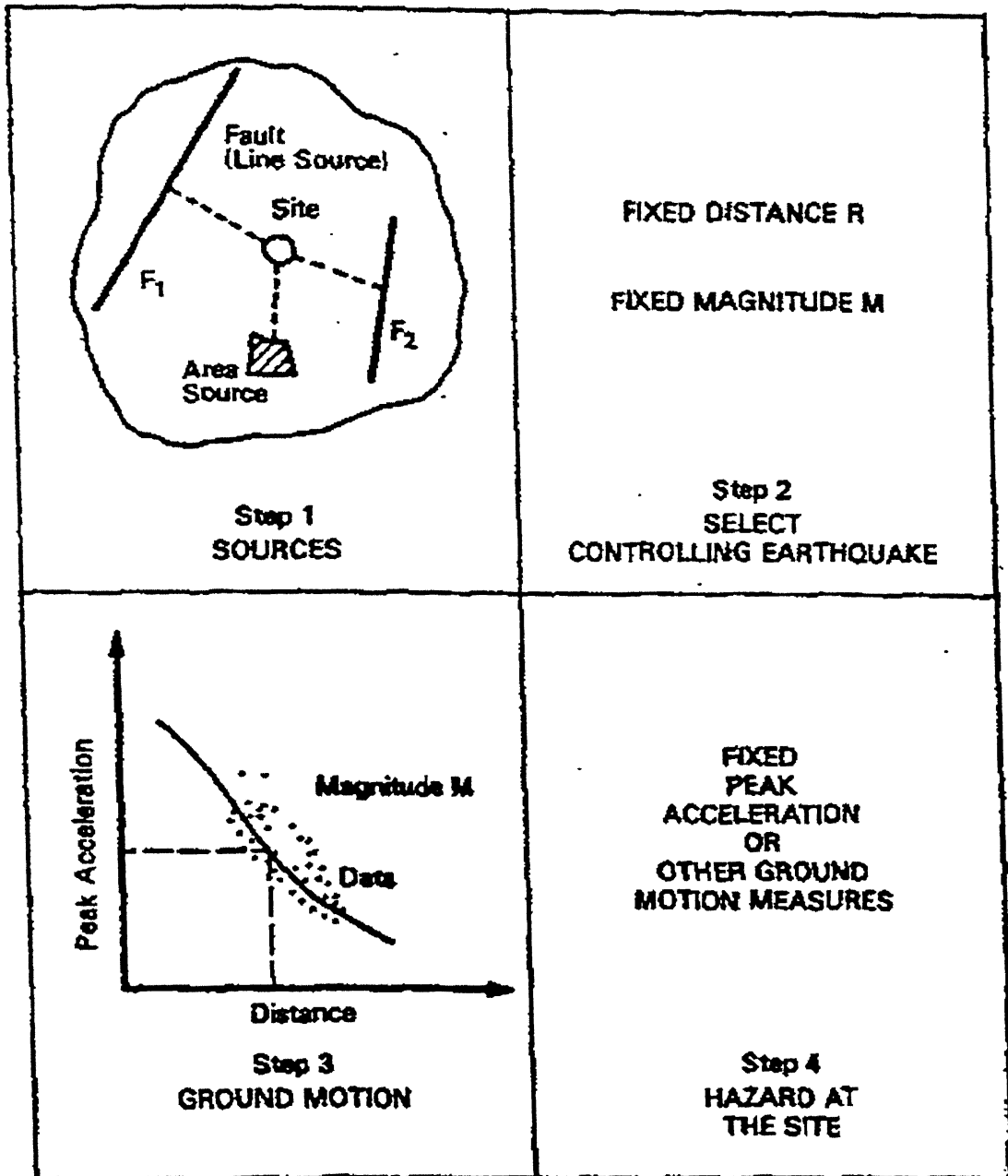


Figure 1.1 Basic steps of a deterministic hazard assessment (Bommer, 1999)

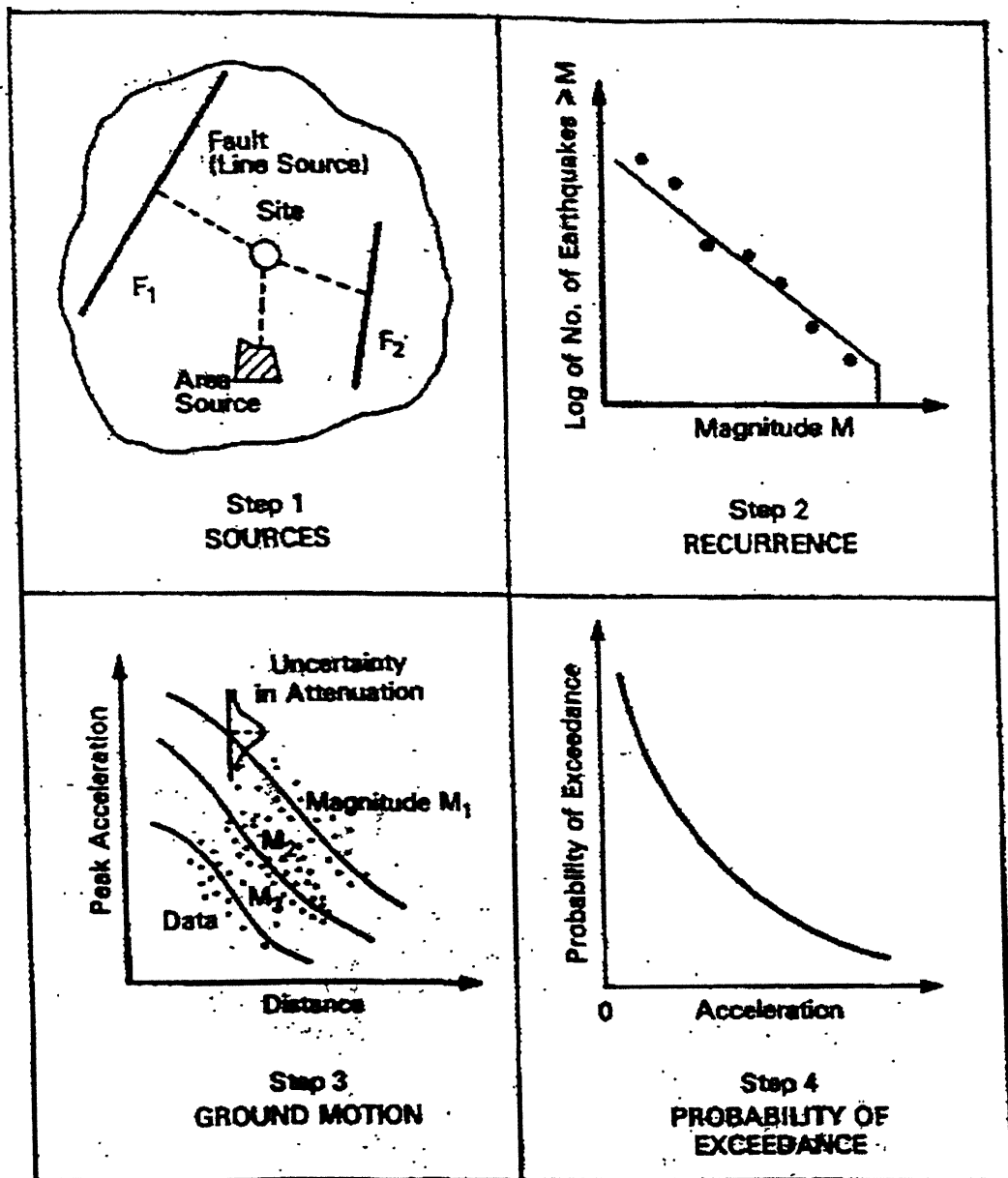


Figure 1.2 Basic steps in probabilistic seismic hazard assessment (Bommer, 1999)

Review of Existing Attenuation Relationships

2.0 Introduction

Seismic hazard assessment may be performed deterministically and probabilistically. Both approaches require the use of ground motion attenuation models for prediction of ground motion parameters. Most of the attenuation models are based on statistical analysis of recorded ground motions, which are updated as new strong motion data becomes available. This chapter reviews some of the attenuation relationships available in the literature for calculation of peak ground acceleration and spectral ordinates of response spectra.

2.1 Estimation of Ground Motion

The ground motion at a site depends on magnitude of the earthquake (M), distance (R), site conditions (S), type of faulting (F) etc. Different source-to-site distance measurements used by different researchers are given in Figure 2.1 and 2.2. Different type of site classification schemes ranging from qualitative descriptions of the base surface material [Calliot and Bard, 1993] to very quantitative definitions based on shear wave velocity [Boore *et al.*, 1997] are used.

With the availability of more strong motion data, separate relationships have been developed for different categories of regional ground motion characteristics. These include shallow crustal earthquakes in active tectonic regimes, shallow crustal earthquakes in stable continental regions, subduction zone earthquakes, and earthquakes in extensional regimes. Regardless of the tectonic regime, rupture directivity also affects ground motion attenuation relationships [Somerville *et al.*, 1997]

Attenuation relationships are available for predicting not only the peak ground

acceleration, but also the spectral ordinates of the response spectrum. In all the available relationships, the ordinates of response spectrum are calculated for 5% of critical damping.

2.2 Attenuation Relationships for Peak Ground Acceleration (PGA)

2.2.1 Nature of PGA Values

The strong motion accelerographs provide three components of ground motion: two horizontal (longitudinal and transverse) and one vertical. For earthquake resistant design, one is usually more interested in estimation of horizontal acceleration. There are a number of methods for defining even a simple parameter like PGA since each accelerogram has two horizontal components.:

1. The two horizontal components are considered as separate and independent records during the regression analysis [Crouse, 1990]. This method corresponds to a randomly oriented component and hence allows statistical treatment of the variation in the orientation of the shaking with respect to the axes of the structure. But, this procedure may lead to erroneous results due to high correlation that exists between these two components [Campbell, 1985].
2. The largest of the two horizontal components is considered for the regression analysis [Joyner and Boore, 1981; Anders *et al.*, 1990; Tento *et al.*, 1992; Ambraseys, 1995; Loh *et al.*, 2000]. It has been reported that on an average, the larger value of the peak acceleration exceeds the mean value of the acceleration by about 13 percent [Joyner and Boore, 1981].
3. The arithmetic mean of the two horizontal components is considered in the regression analysis [Fukushima and Tanaka, 1990; Boore *et al.*, 1997; Campbell, 1997; Sadigh *et al.*, 1997]. The regression analysis using this method results in almost identical

predicted values as those obtained by using both components of PGA, but artificially reduces scatter in the regression [Bommer, 1999].

4. The geometric mean of the two components is used in the regression analysis [Young *et al.*, 1997].

2.2.2 Propagation Parameters

The ground motion attenuation is dependent on the propagation parameters of the medium as well as the source parameters. Propagation parameters characterize the wave scattering, geometrical attenuation, and inelastic attenuation of the ground motion as it travels from the source to the site.

2.2.2.1 Distance

The variable that is generally used to characterize the propagation parameter is distance. The earthquake rupture can extend over tens to hundreds of kilometers, and a number of distance measures have come into use. The various distance measures used in the literature are (Figure 2.1): (a) epicentral distance (R_e), (b) hypocentral distance (R_{hypo}), (c) distance to zone of energy release (R_z), (d) closest distance to rupture (R_{rup}), (e) closest distance to surface projection of rupture (r_{jb}). These are briefly described below.

Epicentral distance (R_e):

It is the distance on the ground surface between an observer or site and the epicenter. Many relationships derived prior to 1985 were based on epicentral distance. Ambraseys (1995) has also used the epicentral distance because only a few earthquakes in the database had the information about associated surface faulting. When the information about the fault dimensions were available, the shortest distance to surface projection of the fault (r_{jb}) was used as the distance measure and in the case of events where the fault parameters were not known, r_{jb} was assumed equal to epicentral distance.

Hypocentral distance (R_{hypo}):

Atkinson and Boore (1997a) have used hypocentral distance as the distance

parameter for modeling the ground motion attenuation in the Cascadia region. The study conducted by Joyner and Boore (1981) suggest that a fault distance based measure is more appropriate in arriving at an attenuation relationship compared to the one based on distance to focus or epicenter. It was observed in their study that the closest distance to rupture zone is most suitable representation of the distance especially in the near source region. However, due to uncertainties in the depth estimation, this factor can be replaced by distance to surface projection of fault [Calliot and Bard, 1993]. Their study compared the results of regression using hypocentral distance with those using distance to surface projection of fault as the distance measure. It was found that the different distance definitions show very little variation in the statistical parameters of the results especially for events with magnitude less than 6.5.

Distance to zone of energy release (R_z):

During the fault rupture, the maximum amount of energy released may be originating from a small zone in the fault plane. The distance to this zone can be used as a distance measure in the attenuation relationship. During the development of attenuation relationship for subduction zone earthquakes, Crouse (1991) used the distance to center of energy release as the distance measure. Tiento et al., (1992) considered R_z to be equivalent to $R = \sqrt{d^2 + h^2}$ Where, d is the closest distance to fault and h is hypocentral depth. In the study, the use of R as the distance measure resulted in lesser scatter of the data compared to that using d as the distance measure.

Closest distance to plane of rupture (R_{rup}):

The shortest distance between the site and fault rupture was used as the distance measure in the development of some attenuation relationships [Fukushima and Tanaka, 1990; Abrahamson and Silva, 1997; Sadigh *et al.*, 1997]. Based on the recordings obtained from Chi-Chi earthquake of Taiwan, 21 September 1999, Loh *et al.*, (2000)

developed an attenuation relationship with the shortest distance to plane of rupture being used as the distance measure. Campbell (1994) used distance to seismogenic rupture (R_{SEIS}) in the derivation of attenuation relationship. The seismogenic rupture zone was determined from the location of the surface fault rupture, the spatial distribution of aftershocks, earthquake modeling studies, regional crustal velocity profiles, and geologic data. This distance measure was used under the assumption that the fault rupture within the upper sediments and within 2 to 4 km of the fault is primarily non-seismogenic and does not contribute significantly to the recorded ground motion at frequencies of engineering interest.

Closest distance to surface projection of fault rupture (r_{jb}):

Joyner and Boore (1981) have used closest distance to surface projection of fault rupture as the distance measure. Therefore, this distance is also known as Joyner-Boore distance (r_{jb}). The epicentral distance or distance to center of rupture was not used in their analysis because during the Parkfield (1966) and Imperial Valley (1979) earthquakes the recording sites were located close to rupture but far from epicenter, and rupture center recorded high values of acceleration. Though the distance to point on the rupture would have been a more appropriate measure of distance, it was not used in their relationship because of the difficulties involved in determination of that point. Many of the recent relationships [Spudich *et al.*, 1997; Toro *et al.*, 1997] also use this as the distance measure in their calculations.

For the sites located several source dimensions from the earthquake (far source records), there is little difference between the results obtained using different distance measures. But for shorter distances (near source records), the difference in results using different distance measures become more significant. In the near source region, where predictions are of greatest concern, the use of epicentral or hypocentral distance leads to

considerably greater scatter in estimates of strong ground motion. Use of a fault-distance measure can lead to biased predictions, especially if the strong-motion stations included in the analysis have a non-random distribution around the fault, or if the strong motions come from a localized source (or sources) then on the fault [Campbell, 1985]. The concept of a distance to localized source is represented by M3 in Figure 2.2.

If the strong motion radiates from small areas of the fault rupture surface, then a fault-distance measure would tend to underestimate the actual distance to these localized sources. It may be possible to identify these areas for some past earthquakes, but it is virtually impossible to anticipate their locations during future events. Because of this, most earthquake scenarios, whether for probabilistic or deterministic applications, use the closest approach to the fault, tectonic structure, or earthquake rupture as the representative distance of the hypothesized earthquake. If an analysis hypothesizes earthquake sources to be equally distributed along a fault or within an area, then epicentral distance, hypocentral distance, or distance to the energy center would be the more appropriate measure to use. In this case, attenuation relations in terms of fault distance will underestimate the true ground motions. This is because, for a fault under consideration the distance measures like epicentral distance, hypocentral distance or distance to energy center will vary based on the originating point of rupture whereas closest distance to surface projection of fault will remain same.

2.2.2.2 Site Geology

Site parameters in a model are related to geologic descriptions of recording stations. The recorded ground motion may be affected by the nature of soil on which the recording station is situated. A large amplification (as much as a factor of two) in accelerations was observed to be associated with shallow deposits for sites located near the source of small to moderate earthquakes [Campbell, 1985]. The classification of these

sites as rock can significantly increase estimates of strong ground motion if enough of these sites are included in the analysis. The different classification schemes used by researchers divide the sites into hard rock, soft rock, shallow alluvium, deep alluvium, stiff soils, deep cohesionless soils, soft soils, etc. The classification is based on the depth of the soil deposit, age of the deposit, shear wave velocity of the medium, etc.

The soil response can be modeled either as a function of peak ground acceleration or by using an amplification factor, which predicts the soil site response based on the corresponding motion in the rock. Thus, a single attenuation relationship can be used for both soil and rocky strata. It is also possible to use separate functional forms for soil and rock resulting in separate regression analysis for soil and rock site recordings. Youngs *et al.* (1997) classified the sites into rock, shallow soil, and deep soil. Separate relationships were provided for rocky and deep soil sites. For an earthquake of magnitude 5.0, the predicted accelerations on deep soil sites were 50% higher than that for rocky sites. This difference increased to 65% for an earthquake of magnitude 7.0. Abrahamson and Silva (1997) classified the sites into rock and deep soil, which was based upon geomatrix soil classification. The amplification factor for soil was predicted as a nonlinear function of PGA in rocky strata. The predicted relationship showed an higher PGA in rocky sites compared to soil sites up to a distance of 40 km. After 40km, predicted PGA was higher for soil sites. The difference in predicted PGA for soil sites varied from -30% at 5km to +30% at 300km with respect to rocky sites for an earthquake of magnitude 7.0

Boore *et al.* (1997) used shear wave velocity of upper 30m of the crust to characterize the sites into 5 groups namely NEHRP site class B, class C, class D, rock and soil. When compared with the response predicted by NEHRP class B; NEHRP site class C, class D, rock and soil predicted the PGAs, which were higher by about 30%, 71%, 22% and 58% respectively. Campbell (1997) classified the sites into alluvium or

firm soil with depth of layer greater than 10m, soft rock, and hard rock. As per this classification, for an earthquake of magnitude 7.0, acceleration predicted for soil site was 96% higher than that of the rocky sites. This was reduced to 35% in the case of sites with soft rocky strata. The site dependent amplification factor used by Campbell (1997) was a function of both magnitude and distance.

2.2.3 Effect of Magnitude

The parameter mostly used to characterize the earthquake size in strong motion attenuation relationships is earthquake magnitude. It is the only source parameter routinely reported by seismographic networks. Earthquake magnitude although routinely reported and universally used as a measure of earthquake size has a few limitations. The variety of magnitude scales that exist can lead to confusion in comparing various predictions. There is also a clear tendency for all scales, except moment magnitude, to saturate as the size of the earthquake increases (Figure 2.3).

Currently, the following different types of magnitude scales are being used

1. Richter Local Magnitude (M_L): This magnitude scale is based on the maximum trace amplitude of the Wood-Anderson seismometer. Commonly used for shallow, local earthquakes.
 2. Surface Wave magnitude (M_S): The amplitude of Rayleigh waves is used to calculate surface wave magnitude. The surface wave magnitude is commonly used to describe the size of shallow focus, distant, moderate to large earthquakes.
 3. Body wave magnitude (m_b): For deep focus earthquakes, surface waves are often too small to permit reliable evaluation of the surface wave magnitude. The body wave magnitude scale is based on the amplitude of the first few cycles of p-waves (usually with a period of 1sec) which are not strongly influenced by the focal depth.
-

4. Moment magnitude (M_W): The ground shaking characteristics does not increase at the same rate at which the total energy released increases during an earthquake. For strong earthquakes, the measured ground shaking characteristics become less sensitive to the size of the earthquake, than for smaller earthquakes. The body wave and Richter local magnitudes saturate at magnitudes of 6.0 to 7.0 and the surface wave magnitude saturates at about $M_S = 8.0$. In order to overcome this drawback, a magnitude scale based on the seismic moment was developed. This magnitude scale is known as moment magnitude. Figure 2.3 gives the comparison of different magnitude scales being used worldwide with moment magnitude.

An important element in the choice of scale is related to the specification of the magnitude of a future earthquake. Generally, surface wave magnitudes are not reliably determined for magnitudes less than 6.0 and because of saturation m_b become relatively independent of earthquake size for magnitudes near 7.0.

Most of the recent attenuation relationships [Boore *et al*, 1997; Youngs *et al*., 1997; Joyner and Boore, 1981; Crouse, 1991] make use of moment magnitude. Since M_L is approximately equal to M_W for $M_L < 6.5$ and M_S is approximately equal to M_W for M_S ranging from 6.0 to 8.0, Campbell (1997) made use of M_L and M_S magnitudes in the interval as specified above considering them as equal to M_W . Ambraseys (1995) while developing attenuation relationships for European earthquakes, used the events which had their surface wave magnitude (M_S) between 4.0 and 7.3. Calliot (1993) made use of M_S if (M_S and M_L) > 6.0 and M_L if (M_S or M_L) < 6.0 as the magnitude term. Fukushima and Tanaka (1990) used M_J , the magnitude defined by Japan Meteorological Agency for earthquakes with $M_J > 6.0$.

2.2.4 Source Mechanism

Different tectonic environments give rise to different ground motion attenuation characteristics. Recent studies [Campbell, 1997] on ground motions show that normal-faulting earthquakes located in extensional stress regimes are associated with lower ground motions than either strike-slip or reverse faulting earthquakes located in compressional stress regimes. For distances greater than 50km from the earthquake rupture, ground motions from subduction zone earthquakes are substantially larger than those from shallow crustal earthquakes [Crouse, 1991].

The distinction between ground motions from strike slip and reverse faults has become common in recent relationships [Campbell and Bozorgnia 1994; Abrahamson and Silva, 1997]. The amplification due to style of faulting can be modeled as a value independent of both source-to-site distance and magnitude [Boore *et al.*, 1997], as a function of only magnitude [Abrahamson and Silva, 1997] or as a function of the distance measure and magnitude [Campbell, 1997]. Boore *et al.* (1997) predicted an increase in acceleration by 21% in the case of reverse faults compared to strike-slip faults. As per Abrahamson and Silva (1997), the increase was 30% for reverse faults and 15% for oblique faults compared to strike slip events with a magnitude of 7.0.

2.2.5 Method of Regression Analysis

Different methods of regression analysis are being used by researchers to arrive at the attenuation relationships:

2.2.5.1 Method of Least Squares

In the past, most of the regression analyses for curve fitting were performed using a least-squares procedure. This procedure minimizes the sum of the squared errors

$\sum_{i=1}^n w_i (\hat{y} - y_i)^2$, where \hat{y} is the predicted value of y_i and w_i is the weight assigned to each

observation y_i . Ambraseys (1995) used this method for the development of attenuation

relationship for European earthquake data. If the equation is linear with respect to the coefficients to be determined, then standard linear least-squares procedure can be used. Otherwise non-linear methods of analysis should be used. Campbell (1997) and Crouse (1991) used generalised non-linear least square analysis to derive the attenuation relationships. Stage-wise regression procedures are useful to decide the important variables controlling the resultant parameter. If the model is non-linear, distribution of the nonlinear coefficients must be developed empirically using Monte-Carlo simulation [Campbell, 1985].

Biased estimates of the coefficients will be obtained if many recordings from a few earthquakes or recording sites dominate the data. This bias can be reduced by restricting the data sample to no more than a certain number of recordings from a given earthquake for a given site, and with the use of weighted regression procedures to equalise the impact of the recordings from individual earthquakes or from specified ranges of magnitude and distance [Caillot and Bard, 1993]. In order to increase the impact of larger values of Y , some researchers have carried out the regression analysis on Y rather than $\ln Y$ [Bolt and Abrahamson, 1982].

2.2.5.2 Two Step Regression Analysis

Two-step regression procedure de-couples the determination of magnitude dependence from determination of distance dependence. This procedure is also known as two-step stratified regression analysis. The variables considered in regression equations usually can take values over some continuous range. Occasionally a factor is to be introduced, which has two or more distinct levels. For example, data may arise from three machines, or two factories etc. In such case we cannot set up a continuous scale for the variable “machine”, or “factory”. We must assign these variables some levels in order to

take account of the fact that these variables may have separate and distinct effects on the response. Such variables are usually-called dummy variables.

Two-step regression analysis introduces a dummy variable E_i for each earthquake. This variable, E_i will take a value equal to '1' for all the records obtained from the i^{th} event and '0' for the records from all other events. This procedure de-couples the determination of magnitude dependence from determination of distance dependence. In the first stage, the regression is carried out using the form of equation as given below.

$$\log y = \sum_{i=1}^N a_i E_i + b_1 \log R + b_2 R + b_3 S \quad (2.1)$$

where N is the total number of earthquakes in the data sample, E_i is the dummy variable whose value is equal to '1' for earthquake ' i ' and '0' otherwise. The values a_i , b_1 , b_2 and b_3 are determined using method of least squares. After a_i values are determined, they are used to fit a first or second order polynomial by least squares to represent the magnitude dependence.

$$a_i = \alpha + \beta M + \gamma M^2 \quad (2.2)$$

The advantages of this method are [Joyner and Boore, 1981]:

1. The data from a single earthquake is typically recorded over a limited range of distance. If the regression analyses were done simultaneously including the magnitude and distance terms, errors in measuring magnitude would affect the distance coefficient obtained from regression and vice versa.
2. This method causes each earthquake to have the same weight in determining the magnitude dependence and each recording to have the same weight in determining the distance dependence.

The standard error σ_y of the residuals from the regression is given by

$$\sigma_y = (\sigma_s^2 + \sigma_a^2)^{1/2} \quad (2.3)$$

where σ_s is the standard error from the first stage of regression and σ_a is the standard error obtained from the second stage of regression. Many of the recent attenuation relationships are based on two-stage methods *e.g.*, Joyner and Boore (1981); Fukushima and Tanaka (1990); Anders *et al.* (1990), Tento *et.al.* (1992); Caillot and Bard (1993); Boore *et al.* (1997). Fukushima and Tanaka (1990) showed that for the data set considered for regression analysis, one-stage ordinary least square results (non-stratified regression analysis) were seriously erroneous. The error was attributed to the strong correlation between magnitude and distance and the resulting trade-off between magnitude dependence and distance dependence. The correct distance dependence, given by the two-stage method and verified by analyzing individual earthquakes separately, showed a much stronger decay of PGA with distance than that predicted by the one-stage ordinary least squares method. The model used for the analysis was $\log(y) = aM - b \log R + c$. The distance coefficients were calculated for individual events as well as by one stage and two stage methods, and it was shown that the two-stage regression was giving closer value to the average distance coefficient of the data (Figure 2.4).

Campbell (1985) and Caillot and Bard (1993) reported that the two-step regression procedure precludes the optimum fit of the data and gives only a local minima of the regression surface. Moreover, it fails to account for the magnitude saturation at near source distances. The analysis of the data obtained from European earthquakes showed that for the database under consideration, one-stage and two-stage methods produced almost same shape of attenuation curve (Figure 2.5(a), 2.5(b)) [Ambraseys, 1995]. The model used to derive the particular attenuation relationship was

$$\log(y) = a + bM_s + cR + d \log R. \quad (2.4)$$

2.2.5.3 Method of Maximum Likelihood

The method of maximum likelihood is a general method of finding estimated (fitted) values of parameters. The underlying concept is that the best estimate of a parameter is that giving the highest probability that the observed set of measurements will be obtained. The estimation process involves considering the observed data values as constants and the parameter to be estimated as a variable, and then using differentiation to find the value of the parameter that maximizes the likelihood function.

Let $f(x, \theta)$ be the density function of the random variable x and let θ be the parameter of the density function. If we observe a random sample of X_1, X_2, \dots, X_N , then the maximum likelihood estimator of θ is that value which maximises the density function $f(x, \theta)$. The maximum likelihood estimator has several desirable properties

- a) The estimator is efficient in the sense that there is no estimator with smaller variance.
- b) The estimator approaches the true population parameter asymptotically as the number of observations increases. The maximum likelihood method works best for large samples, where it tends to produce estimators with the smallest possible variance.

The maximum likelihood estimate for the slope and intercept in simple linear regression is the same as the least squares estimates when the underlying distribution for Y is normal [e.g., Gujarati, 1995]. In general, however, the maximum likelihood and least square estimates need not be the same. Method of maximum likelihood can be used to calculate the estimated value of a coefficient in either one-stage or two-stage regression analysis instead of using least square methods. Abrahamson and Silva (1997) and Boore *et al.* (1997) have used maximum likelihood method to develop the attenuation relationships. Joyner and Boore (1993) reported that using Fukushima and Tanaka's data, the one-stage maximum likelihood method gave essentially same results as the two-stage

method. But, these results did not match with the parameters obtained using ordinary least square method (Table 2.1).

2.2.6 Validity of Result and Treatment of Uncertainty

2.2.6.1 Analysis of Residuals

Different methods for regression analyses are derived based on the assumption that the random error term ε_i is normally distributed. This error term is represented by the residuals obtained after regression. The normality assumption of the residuals is checked by χ^2 [Chi-Square] test. The adequacy of the model with respect to the fitted variables are then checked by plotting the residuals against the independent variables M , R , etc. If these plots do not show any apparent trend, the model can be considered adequate.

2.2.6.2 Multiple Correlation Coefficient

The goodness of the fit can be evaluated by the multiple correlation coefficient. The expression for multiple correlation coefficient is [e.g., Caillot and Bard, 1993]:

$$R_c = \sqrt{1 - \frac{\sum_{i=1}^n w_i (y_i - \hat{y}_i)^2}{\sum_{i=1}^n w_i (y_i - \bar{y})^2}}, \quad (2.5)$$

where w_i is the weight assigned to each observation, \hat{y}_i is the predicted value of the parameter \bar{y} is the mean of observations y_i . R_c varies from 0 to 1 (perfect correlation).

The proportion of the variability of y_i 's explained by the regression is given by R_c^2 . If R_c^2 is less than 0, the regression form used is unable to explain the variation in the data.

Caillot and Bard (1993) reported that the value of R_c varied from 0.4 to 0.5 when two-stage regression analysis was used to predict both PGA and spectral acceleration.

2.2.6.3 Uncertainty in Prediction

In addition to median ground motion estimates, the uncertainty (standard deviation) is also important for seismic hazard analyses. The uncertainty in the prediction of the strong motion parameters is represented with the help of standard deviation (σ) of the predicted variables. The predicted dependence of standard deviation is different for different models, and also depends on the data set. The standard deviation is reported as a constant value or as a value dependant on the predicted amplitude or dependant on the magnitude of the earthquake predicted. Usually a linear relationship with respect to the magnitude or amplitude of motion is used to denote the uncertainty in the prediction of ground motion [Campbell, 1997; Sadigh *et al.*, 1997]. The attenuation models having magnitude dependant standard deviation predicts smaller standard deviations for the events with larger magnitudes, than smaller magnitude events. This trend is evident from Figure 2.6. The reported values of the standard deviation of $\log(y)$ ranges from 0.4 to 0.9

2.3 Literature Review of Attenuation Relationships

There are many strong motion attenuation relationships that have been proposed throughout the years. Some of the recent relationships, which address the attenuation of peak ground acceleration, are summarized below. These empirical equations have been arrived at based on different solution procedures, for different types of tectonic regimes, site conditions, different distance definitions, and ranges of magnitudes.

2.3.1 Boore *et al.* (1997)

Boore *et al.* (1997) studied the peak ground acceleration for shallow earthquakes from western North America. The ground motion data consisted of horizontal PGAs of 271 records obtained from 19 earthquakes. The average of two horizontal components of acceleration was used in the regression analysis. The distance range was from 0 to 118 km and the magnitudes of the recorded events varied from 5.2 to 7.7. Moment magnitude

(M_w) was used as a measure of earthquake size and the closest distance from the station to a point on the earth's surface, which lies directly above the rupture (r_{jb}) was used as the distance measure.

A cutoff distance was introduced in the analysis to account for the triggering of instruments due to local site effects at a particular station. The cut off distance was set to least of the following:

- a) Distance to the first digitized record triggered by S wave;
- b) Distance to closest non-digitized recording;
- c) Distance to an operational non-triggered instrument.

Two types of faulting were considered, namely strike-slip and reverse-slip faults. The site classification was based on shear wave velocity up to 30m depth. A two-stage maximum likelihood method was adopted. The attenuation relationship for the peak ground acceleration (g) is given by

$$\ln Y = b_1 + 0.527(M - 6) - 0.778 \ln r - 0.371 \ln \frac{V_s}{1396}, \quad (2.6)$$

where

$$b_1 = \begin{cases} -0.313 & \text{for strike - slip faults} \\ -0.117 & \text{for reverse - slip faults} \\ -0.242 & \text{if mechanism is not specified} \end{cases}$$

and V_s is the average shear wave velocity which depends on the site class. The standard deviation of the predicted acceleration is given as $\sigma_{\ln Y} = 0.520$. The relationship was found to give best results when used to predict motions at distances less than 80 km and magnitude range 5.5 to 7.5.

2.3.2 Campbell (1997)

Campbell (1997) developed attenuation relationship for mean PGA with majority of the earthquakes recorded in California. Some events from Middle East and South America were also used in the study. A total of 645 recordings from 47 earthquakes were

used for arriving at the attenuation relationship. Moment magnitude (M_W) was used as the measure of the earthquake size. The range of magnitudes considered in the study was 4.7-8.0. Closest distance from the station to seismogenic rupture (R_{SEIS}) (Figure 2.1) was used as the distance measure and its range was 3.0-60.0 km. This distance was used under the assumption that fault rupture within softer sediments and within the upper 2 to 4 km of the fault zone is primarily non-seismogenic and does not contribute to recorded ground motions at periods of engineering interest.

Two types of faulting, namely strike-slip and reverse-thrust were used to characterise the source mechanism. All the earthquakes considered were shallow crustal earthquakes (focal depth <25 km). The sites were classified into alluvium or firm soil, soft rock, and hard rock and two variables were introduced in the model to represent the site conditions. The recommended relationship for PGA (g) is given by

$$\begin{aligned} \ln(A_H) = & -3.512 + 0.904M - 1.328 \ln \sqrt{R_{SEIS}^2 + \left[0.149e^{(0.647M)^2}\right]} \\ & + [1.125 - 0.112 \ln(R_{SEIS}) - 0.0957M]F \\ & + [0.440 - 0.171 \ln(R_{SEIS})]S_{SR} \\ & + [0.405 - 0.222 \ln(R_{SEIS})]S_{HR} + \varepsilon \end{aligned} \quad (2.7)$$

where

$$F = \begin{cases} 0.0 & \text{for strike - slip faulting} \\ 0.5 & \text{for normal faulting} \\ 1.0 & \text{for reverse, thrust, reverse - oblique, and thrust - oblique faulting} \end{cases}, \text{ and}$$

$S_{HR} = S_{SR} = 0$ for alluvium or firm soil; $S_{HR} = 0$ and $S_{SR} = 1$ for soft rock; and $S_{HR} = 1$ and $S_{SR} = 0$ for hard rock.

The regression analysis was done in stages. In the first stage, all selected recordings were used to determine the regression coefficients using unweighted, generalized nonlinear least-square method. A distance threshold was calculated based on magnitude, distance, style of faulting, site conditions, and trigger level of strong motion

recorders. In the second stage, the records that did not meet the calculated distance threshold were removed from the set and the regression was repeated.

Two estimates of standard deviation in the prediction were obtained. The first estimate, based on the amplitude of PGA is given by

$$\sigma = \begin{cases} 0.55, & A_H < 0.068g \\ 0.173 - 0.140 \ln(A_H), & 0.068g \leq A_H \leq 0.21g \\ 0.39, & A_H > 0.21g \end{cases} \quad (2.8)$$

The second estimate of σ is based on magnitude M and is given by the expression

$$\sigma = \begin{cases} 0.889 - 0.0691M, & M < 7.4 \\ 0.38, & M \geq 7.4 \end{cases} \quad (2.9)$$

The second estimate for standard deviation was found to be statistically more robust.

2.4.3 Sadigh *et al.* (1997)

Sadigh *et al.* (1997) proposed attenuation relationships for peak ground acceleration based on Californian earthquakes. Two major source mechanisms, namely strike-slip and reverse faulting were used to classify the records. The relationships were developed for rock and deep firm soil deposits. Rock sites are defined as those with bedrock less than 1m from the surface. Earthquake size was characterized by moment magnitude (M_w) and distance was defined as the closest distance to rupture surface. The distance range of the records used in the analysis was 2.5-261 km and the magnitude of the events varied from 3.8-7.4. The regression coefficients for mean PGA was calculated from 121 recordings from 40 earthquakes. The attenuation model of PGA for rock sites is given by

$$\ln(y) = b_1 + b_2 M + b_3 (8.5M)^{2.5} + b_4 \ln(r_{rup} + e^{(b_5 + b_6 M)}) + b_7 \ln(r_{rup} + 2), \quad (2.10)$$

where

$$b_1 = -0.624, b_2 = 1.0, b_3 = 0.0, b_4 = -2.10, b_5 = 1.29649, b_6 = 0.25 \text{ and } b_7 = 0.0 \text{ for } M \leq 6.5,$$

and

$b_1 = -1.274, b_2 = 1.1, b_3 = 0.0, b_4 = -2.10, b_5 = 0.48451, b_6 = 0.524$ and $b_7 = 0.0$ for $M > 6.5$,

with standard deviation given by

$$\sigma_{\ln y} = \begin{cases} 1.39 - 0.14M & \text{for } M < 7.21 \\ 0.38 & \text{for } M \geq 7.21 \end{cases} \quad (2.11)$$

For deep soil sites the attenuation relationship is given by

$$\ln(y) = b_1 + b_2 M - b_3 \ln(r_{rup} + b_4 e^{b_5 M}) + b_6 + b_7 (8.5 - M)^{2.5}, \quad (2.12)$$

where

$b_1 = -2.17$ for strike-slip, -1.92 for reverse and thrust earthquakes; $b_2 = 1.0$; $b_3 = 1.70$

$$b_4 = \begin{cases} 2.1863 & \text{for } M \leq 6.5 \\ 0.3825 & \text{for } M > 6.5 \end{cases}, b_5 = \begin{cases} 0.32 & \text{for } M \leq 6.5 \\ 0.5882 & \text{for } M > 6.5 \end{cases}, \text{ and } b_6, b_7 = 0 \text{ for PGA,}$$

with the standard deviation given by

$$\sigma_{\ln y} = 1.52 - 0.16M. \quad (2.13)$$

2.3.4 Spudich *et al.* (1997)

Extensional regimes are the regions in which the lithosphere is expanding aerielly.

Spudich *et al.* (1997) developed an attenuation relationship for PGA from worldwide data of 129 recordings from 20 earthquakes in the extensional tectonic regimes. Two site classifications, namely rock and soil were used. The magnitude of the earthquakes varied from 5.1 to 6.9 and the distance (r_{jb}) of recordings ranged from 0 to 102 km. Relationship for peak ground acceleration is given by

$$\log_{10} y = 0.156 + 0.229(M - 6) - 0.945 \log_{10} R + 0.077\Gamma, \quad (2.14)$$

$$\text{where } R = \sqrt{r_{jb}^2 + 5.57^2}, \text{ and } \Gamma = \begin{cases} 0 & \text{for rock} \\ 1 & \text{for soil} \end{cases}.$$

The standard deviation of the observations is $\sigma_{\log_{10} y} = 0.216$, which is equivalent to a value of 0.497 in terms of natural logarithms.

2.3.5 Atkinson and Boore (1997b)

Due to low seismicity rates in stable continental regions, there are very few strong motion records available for this tectonic regime. As a result, attenuation relationships are

obtained using numerically simulated ground motions instead of recorded ground motions.

Based on the numerical simulations for Eastern North America (ENA), Atkinson and Boore (1997b) developed an attenuation model for peak ground acceleration. The regression is based on thousands of records from hundreds of simulated ENA earthquakes in the magnitude range from 3 to 7 recorded at distances (r_{jb}) from 10 to 1000km. The digital data used are from hard rock sites. No distinction of focal mechanism type was made in the study. The attenuation relationship for PGA (g) is given by

$$\ln(y) = 1.841 + 0.686(M - 6) - 0.123(M - 6)^2 - \ln R - 0.00311R. \quad (2.15)$$

The standard deviation of the observation is found to be equal to 0.62.

2.3.6 Youngs *et al.* (1997)

Youngs *et al.* (1997) developed an attenuation relationship for subduction zone interface and intraslab earthquakes using the data from Alaska, Chile, Cascadia, Japan, Mexico, Peru and Solomon Islands. The rate of attenuation of the ground acceleration is less in subduction zone earthquakes as compared to shallow focus earthquakes. The attenuation models indicate that for large events at large distances, the peak motions from subduction zone earthquakes will be larger than those predicted using attenuation relationship for shallow crustal earthquakes. The difference increases as the size of earthquake increases. Most subduction zone events are recorded at large distances because the events tend to be deep and off shore in most of the cases. In the analysis, the events that occurred at a depth less than 50km were considered to be interface earthquakes.

The data used for the regression analysis consisted of geometric mean of two horizontal components of 481 recordings from 163 earthquakes. The moment magnitudes (M_w) of the events varied from 5 to 8.4 and the closest distance to rupture surface ranged

from 8.5 to 550 km. The regression of the sample was carried out using random effects model [Abrahamson and Youngs, 1992]. The random effects model is a maximum likelihood method that accounts for correlations in the data recorded by a single earthquake. The attenuation relationship for rock sites is given by

$$\ln(y) = 0.2418 + 1.414M - 2.552 \ln(r_{rup} + 1.7818e^{0.554M}) + 0.0060H + 0.3846Z_T, \quad (2.16)$$

where H is the depth of focus in km and Z_T is the term denoting the source type. It takes a value equal to 0 for interface 1 for intraface earthquakes.

the standard deviation of the predicted motion given by

$$\sigma_{\ln} = 1.45 - 0.1M. \quad (2.17)$$

For soil sites the PGA (g) is given by

$$\begin{aligned} \ln(y) = & -0.6687 + 1.438M - 2.329 \ln(r_{rup} + 1.097e^{0.617M}) \\ & + 0.00648H + 0.3643Z_T \end{aligned} \quad (2.18)$$

$$\text{and } \sigma_{\ln} = 1.45 - 0.1M \quad (2.19)$$

2.3.7 Crouse (1991)

Based on the recordings of peak ground acceleration from 697 components Crouse (1991) calculated an attenuation relationship for subduction zone earthquakes in Cascadia region. The magnitude of the earthquakes varied from 4.8 to 8.2 and the distance to center of energy release varied from 8-866 km. The distance to center of energy release was assumed to be equal to hypocentral distance for events with moment magnitude (M_w) less than 7.5. For larger events, the closest distance to centroid of fault plane defined by after shocks was taken as the distance to energy release. The PGA (gals) is given by

$$\ln(PGA) = 6.36 + 1.76M - 2.73 \ln(R + 1.58e^{0.608M}) + 0.00916H \quad (2.20)$$

with the standard deviation (σ_{\ln}) of the observations equal to 0.773. It was observed during the analysis that introduction of a quadratic term of magnitude in the attenuation relationship did not have any statistical significance. The solution of the regression equation was done using a generalised nonlinear regression code.

2.3.8 Ambraseys (1995)

Based on the data collected from earthquakes in Eurasia and Middle East, Ambraseys (1995) developed an attenuation relationship for shallow crustal earthquakes. The database consisted of 1,667 triaxial records generated during 865 earthquakes. The moment magnitude of majority of earthquakes ranged from 2 to 7.3 and the recorded distances ranged from 0 to 260 km. For larger events in the database ($M_S > 6.0$) and for earthquakes for which results from special focal studies are available, $d=r_{jb}$ was used as the distance measure. For smaller events epicentral distance ($d=R_e$) was used as the distance measure. When the events with magnitude > 4.0 was considered for the analysis (828 records from 332 earthquakes) the following empirical equation for peak ground acceleration (g) was obtained.

$$\log(y) = -1.06 + 0.245M_S - 0.00045r - 1.016\log(r), \quad (2.21)$$

where $r = \sqrt{d^2 + h^2}$ and h is the depth of focus of the earthquake.

The standard deviation of the prediction is given by $\sigma_{\log_{10}} = 0.254$, which is equivalent to $\sigma_{\ln} = 0.585$.

Two-stage regression procedure was adopted for the analysis of the data. It was also observed that the predicted attenuation curves using one stage regression and two-stage regression do not differ very much. One-stage regression values were slightly higher at distances less than 10 km and slightly lower at distances greater than 100 km.

2.3.9 Tento *et al.* (1992)

The data from Italian earthquakes until 1991 was used by Tento *et al.* (1992) to develop the attenuation relationship for PGA. A two-stage regression analysis was carried out. The local magnitude was used in the study with hypocentral distance as the distance measure. The resulting equation is as follows

$$\ln(y) = 4.73 + 0.52M - \ln R - 0.00216R, \quad (2.22)$$

where $R = \sqrt{r_{jb}^2 + H^2}$ and H is the depth of focus.

The standard deviation (σ_{\ln}) of the model is equal to 0.67.

2.3.10 Fukushima and Tanaka (1990)

Fukushima and Tanaka (1990) developed an attenuation relationship for near source region in Japan based on 1,372 horizontal components of PGA from 28 earthquakes in Japan and 15 earthquakes from other countries. The estimated ground motion equation is given as

$$\log_{10} y = 1.3 + 0.41M_S - \log_{10}(R + 0.032 \times 10^{0.4M_S}) - 0.0034R, \quad (2.23)$$

where R is the shortest distance between site and fault rupture (R_{rup}).

The standard deviation of the model was $\sigma_{\log_{10}} = 0.391$ i.e., $\sigma_{\ln} = 0.90$.

2.3.11 Caillot and Bard (1993)

Data collected from Italian sites were used to establish empirical relations between spectral acceleration, magnitude, hypocentral distance and site conditions. Total of 115 records from earthquakes of magnitude between 3.2 and 6.8 with epicentral distance less than 60 km and focal depth less than 30 km were used. The records belonged to three different site categories namely, rock (S_0), thin alluvium with thickness less than 20m (S_1), and deep alluvium (S_2). The form of the equation is given by

$$\ln(y) = -3.692 + 0.507M - 0.483 \ln(R_{hypo}) + 0.271S, \quad (2.24)$$

where $S = 0$ for site category S_0 and 1 for site category S_1 . Since the data coming under site category S_2 was too heterogeneous, it was not considered in the study.

For the data considered in the study, regression analysis was done using two multi-linear regression methods: (i) two stage regression analysis which de-couples the spatial dependence of acceleration from that of magnitude, and (ii) weighted multi-linear regression procedure where weighing is aimed at correcting the non-uniform magnitude-distance distribution for each site-specific data set. It was observed that the two-stage regression procedure does not reduce the initial variance (stage 1) of the data ($(R_c)^2 < 0$). It was due to the fact that the two successive regressions correspond to a local non-absolute minimum and not the minima of the whole surface.

2.3.12 Anders *et al.* (1990)

Andres *et al.* (1990) developed an attenuation relationship based on the 87 strong motion recordings from 56 intraplate earthquakes that occurred in North America, Europe, China and Australia. A two-stage regression was used. Hypocentral distance was taken as the distance parameter and the surface wave magnitude (M_s) was used as the measure of size. The largest horizontal component of the horizontal PGA was used for the analysis. The relationship is given by

$$\ln A = -1.471 + 0.849M - 0.00418R + \ln G(R, R_o) \quad (2.25)$$

$$\text{with } \sigma_{\ln} = 0.984. \text{ Here, } G(R, R_o) = \begin{cases} R^{-1} & \text{for } R \leq R_o \\ R_o^{-1} \left(\frac{R_o}{R} \right)^{5/6} & \text{for } R > R_o \end{cases}. \text{ The recommended}$$

value for R_o is 100km.

• • •

Table 2.1: Comparison between the parameters obtained by one-stage maximum likelihood method, the two-stage method and the ordinary least squares method applied to Fukushima and Tanaka's data for the model $\log(y) = a + bM + c \log R$ [Joyner and Boore, 1993]

<i>Parameter</i>	<i>One-stage Maximum-likelihood</i>	<i>Two-stage Maximum-likelihood</i>	<i>Ordinary Least-squares</i>
a	2.20	2.20	2.22
b	0.44	0.44	0.26
c	-1.73	-1.76	-1.19
$\hat{\sigma}_r$	0.26	0.26	-
$\hat{\sigma}_e$	0.19	0.21	-
$\hat{\sigma}$	0.33	0.34	0.33

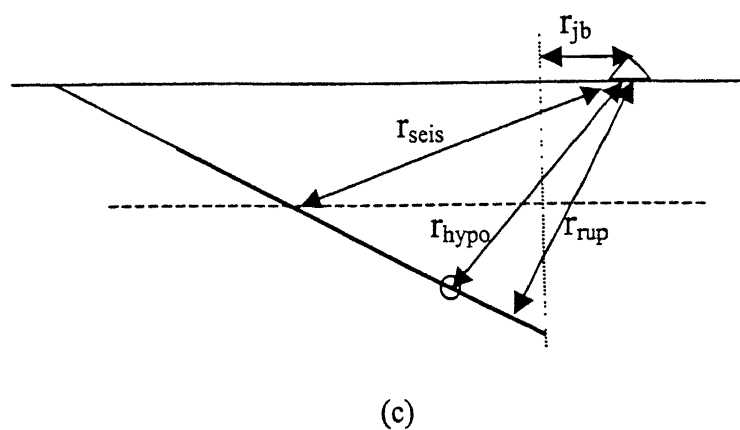
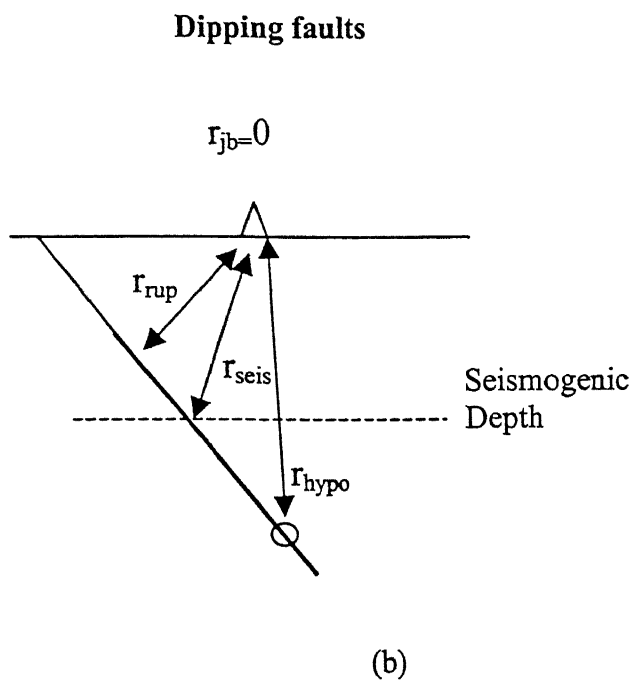
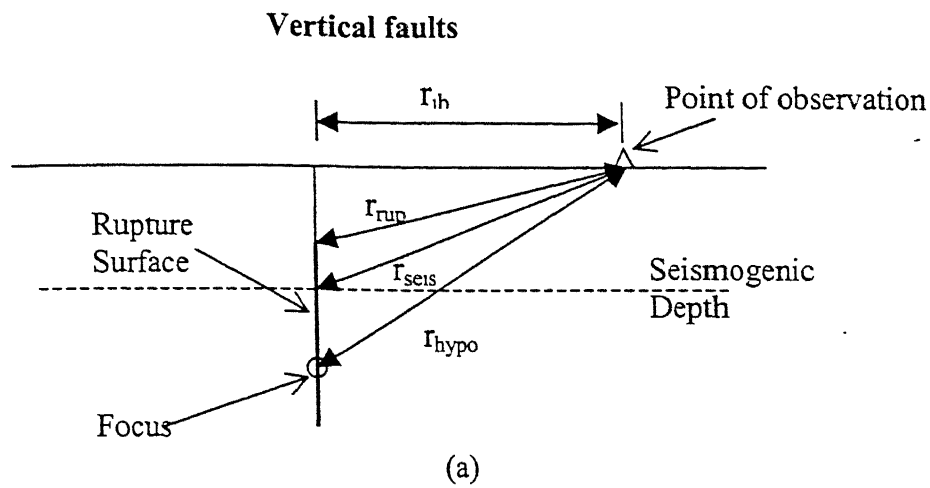
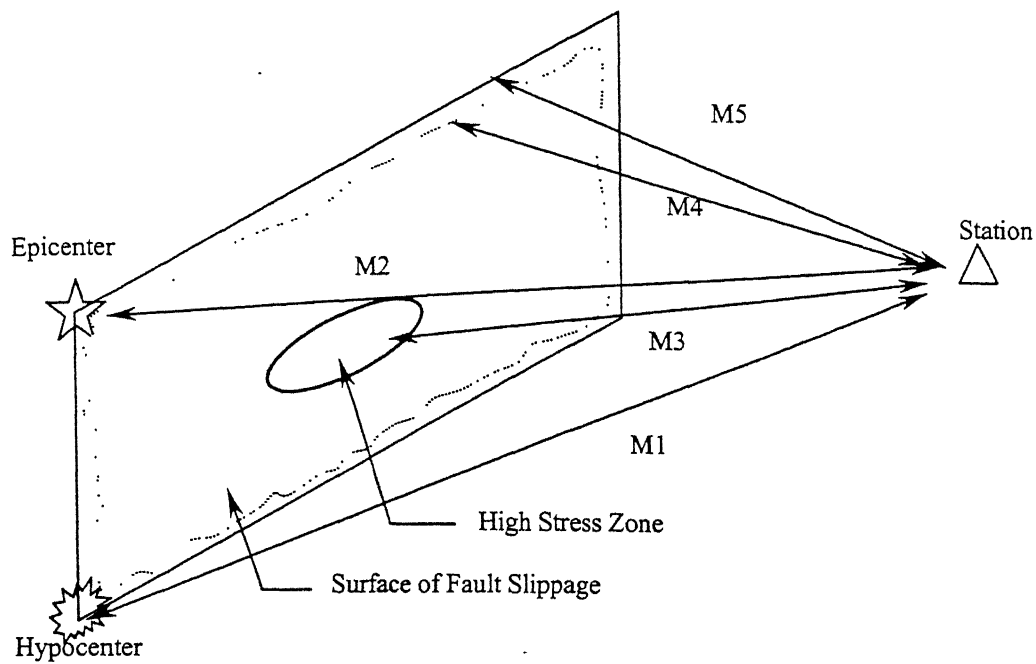


Figure 2.1: Different definitions of distances used in the attenuation relationships [Abrahamson and Shedlock, 1997].



- M1: Hypocentral Distance;
M2: Epicentral Distance;
M3: Distance to Zone of energy release;
M4: Closest Distance to rupture;
M5: Closest Distance to surface projection of Rupture

Figure 2.2: Different definitions of distances used in the attenuation relationships
[Campbell, 1985].

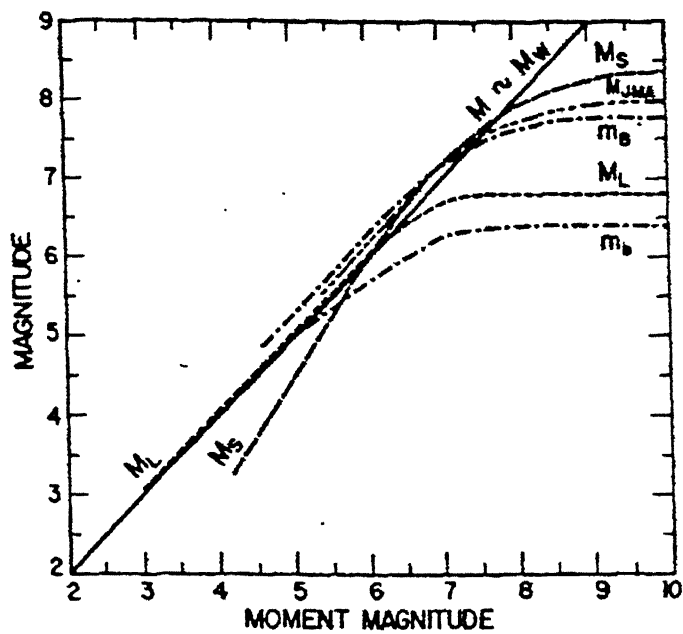


Figure 2.3: Relationship Between moment magnitude and various magnitude scales [Kramer, 1996].

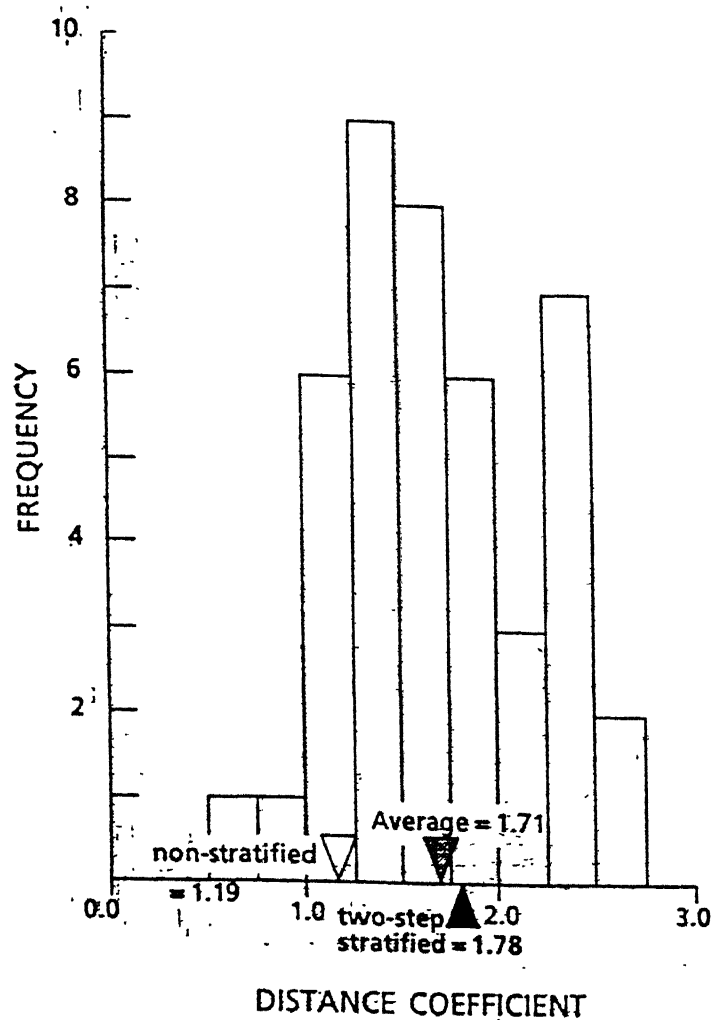
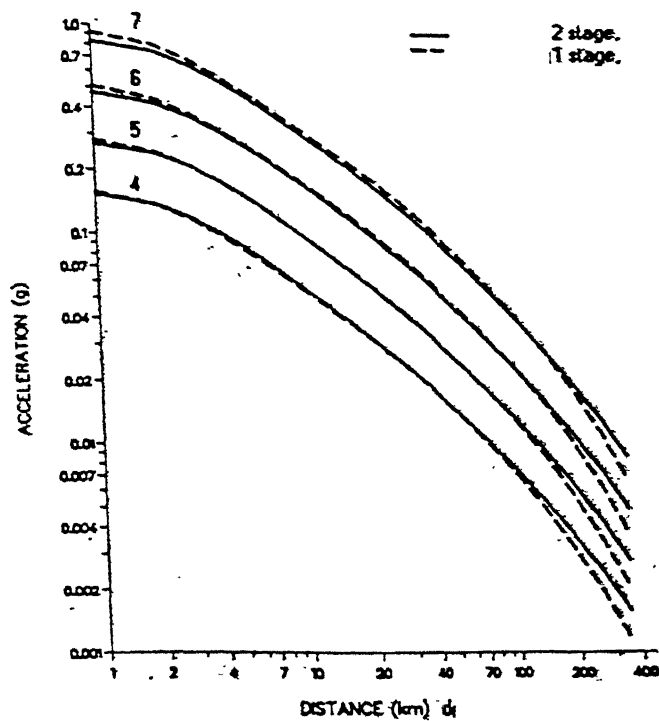
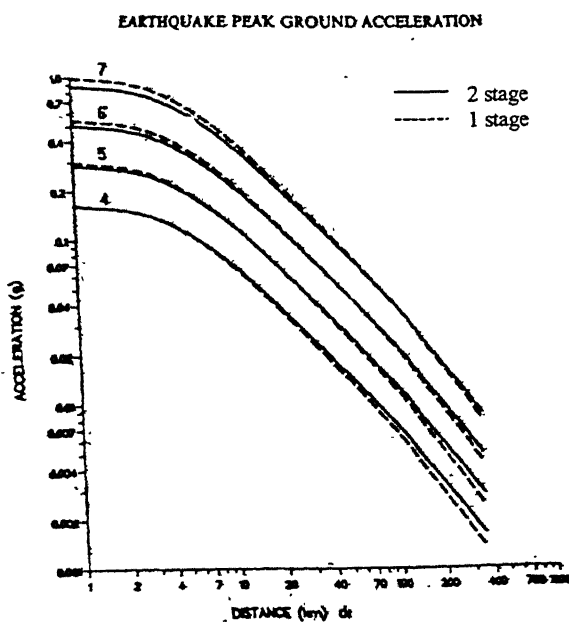


Figure 2.4: Histogram showing distribution of distance coefficients for individual earthquakes and average value along with coefficients obtained by non-stratified (one step) and two-step analyses [Fukushima and Tanaka, 1990].



(a)



(b)

Figure 2.5: Comparison of predictive curves for peak acceleration from two-stage and one-stage regression. (a) Predicted equations without considering focal depth, (b) Predicted equations when focal depth is considered in the analysis [Ambraseys, 1995].

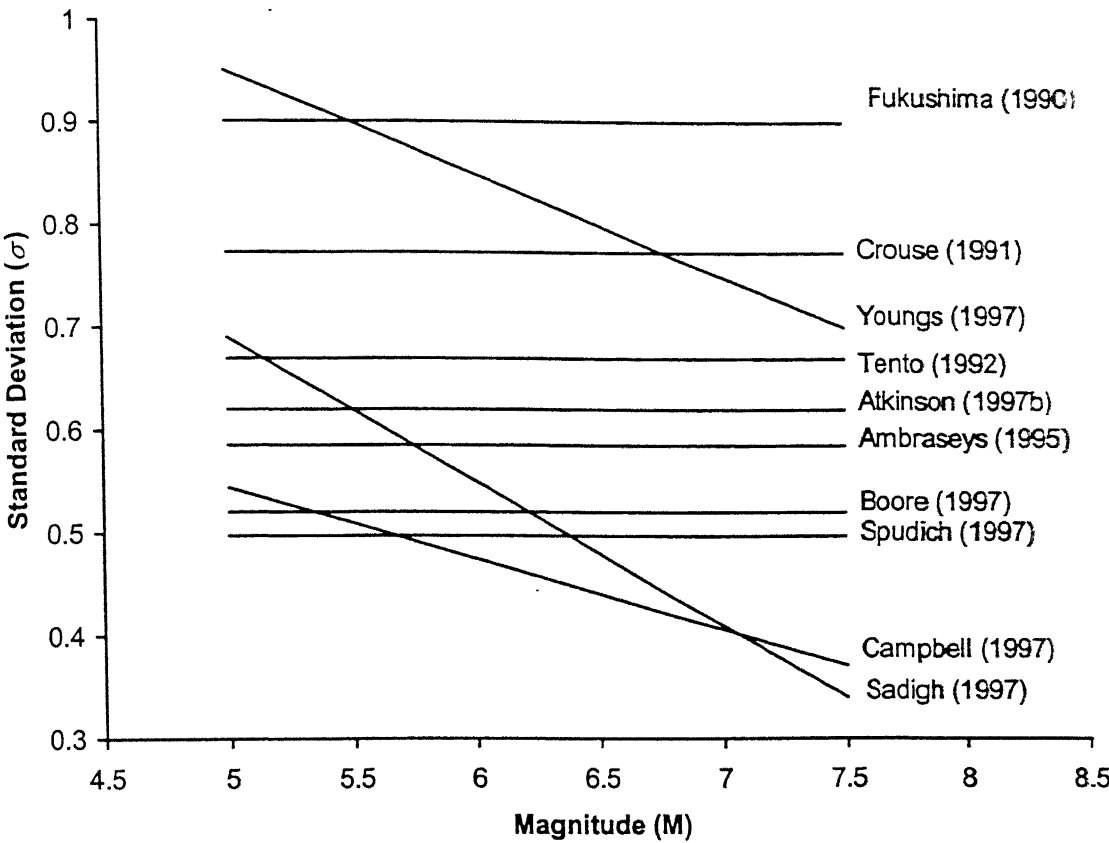


Figure 2.6: Variation of Standard Deviation (σ_{ln}) of Peak Ground Acceleration with respect to magnitude for different attenuation relationships.

Chapter 3

Strong Motion Data from Indian Earthquakes

3.0 Introduction

The Himalayan region in northern-India is a highly seismically active region. Because of the economic as well as operational constraints, only a small area in northern-India could be covered with Strong Motion Accelerographs (SMA's). Structural Response Recorders (SRR) are relatively inexpensive instruments, which are used to record the spectral accelerations during an earthquake. Due to low cost, SRRs have been installed covering a wider region. This chapter compares the characteristics shown by the recordings from SMA's and SRR's. A methodology is also developed to calculate Peak Ground Acceleration (PGA) from Resultant Spectral Accelerations (RSA's) recorded by SRR's.

3.1 Seismo-Tectonics of Himalayan Region

The northeastern region of India is an active seismic zone. An earthquake of magnitude 8.7 has occurred in the Shillong region in 1897 and in the Mishmi region of Arunachal Pradesh in 1950. Shillong plateau is bounded by the main boundary thrust in the north-west, and the Mishmi and the Lohit thrusts towards the north-east (Figure 3.1). The other two prominent tectonic features forming the boundary of the Shillong plateau are the Dhubri fault towards the west and the Dauki fault towards the south. The Dauki fault merges with the north-east trending Haflong-Disang thrust towards the east. A thrust type mechanism was suggested for the Dauki fault in a recent study [Chandra and Das, 1992]. There is also report of a subduction process along Burmese arc, which lies near the Shillong region [Mukhopadhyay, 1992].

The Bihar region consists of a tectonic basin in the east-west direction along the

southern margin of the Himalayan fold belt [Dasgupta, 1993]. The formation of this basin is attributed to the upheaval of the Himalayas along with the down warp of Indian lithosphere. The central part of this basin is called the Gangetic foredeep. The 1988 Bihar-Nepal $M6.8$ earthquake originated below the Gangetic foredeep [Dasgupta, 1993].

In the Kangra region, the major tectonic features are the Main Boundary Thrust (MBT) and the Main Central Thrust (MCT) (Figure 3.1).

3.2 Instrumentation and Availability of Data

The Himalayan region of India has been instrumented in the recent times using the Strong Motion Accelerographs (SMA) and the Structural Response Recorders (SRR). Strong Motion Accelerographs are three-component instruments installed near a potential seismo-tectonic source; these provide time history of ground acceleration in two horizontal and one vertical directions. In all, there are five major arrays of SMAs in the Himalayan region [Chandrasekaran *et al.*, 1996]. Figure 3.2 shows the relative positions of the strong motion arrays installed in different parts of the Himalayan region. Under the Indian National Strong Motion Network (INSMN) Program, Department of Earthquake Engineering (DEQ), Roorkee has installed more than three hundred SRRs in different parts of India. The multiple Structural Response Recorder (SRR) consists of six recording instruments, in the form of conical pendulums, which measure the horizontal component of motion (Figure 3.3a). These seismoscopes are relatively inexpensive instruments. Their natural periods are adjusted to 0.40sec, 0.75sec and 1.25sec and the damping provided is 5% and 10% of critical damping. The output from a SRR provides ordinates of Resultant Acceleration Spectrum (RAS) at natural periods 0.4sec, 0.75sec and 1.25sec for 5% and 10% damping. A typical SRR recording is shown in Figure 3.3(b).

3.2.1 Shillong Array in Meghalaya

This array consists of 45 strong motion accelerographs located between 24°N to 26°N and 91°E to 94°E (Figure 3.4a). About 110 SRR stations are also situated between 23°N to 28°N and 90°E to 95°E. Strong motion accelerograms recorded by the Shillong strong motion array for five earthquakes are available, viz., 10 September 1986 Meghalaya ($m_b=5.2$) earthquake (12 records), 18 May 1987 Northeast ($M_s=5.9$) earthquake (14 records), 6 Feb 1988 northeast ($m_b=5.8$) earthquake (18 records), 6 August 1988 ($M_s=7.3$) earthquake along the Indo-Burma border (33 records), and the 9 January 1990 Northeast ($m_b=6.1$) earthquake (14 records). The 6 August 1988 earthquake was also recorded by about 120 SRRs installed in the region. Figures 3.5(a) to 3.5(e) show the locations of strong motion recorders and SRRs, which have recorded these earthquakes along with the epicenter locations as per different agencies.

3.2.2 Bihar Array in Bihar

This array (Figure 3.4b) consists of five digital accelerographs (Chandra *et al.*, 1996) and about 47 SRRs. The 21 August 1988 Bihar-Nepal earthquake was recorded by 41 SRRs installed in the region (Figure 3.5f).

3.2.3 Uttar Pradesh Array in North-Western Uttar Pradesh

This array contains 40 SMA stations between 29°N to 31°N and 77.5°E to 81°E and about 70 SRR stations between 28°N to 32°N and 76.5°E to 80.5°E (Figure 3.4c). The 20 October 1991 Uttarkashi ($M_s=7.0$) and 29 March 1999 Chamoli ($M_s=6.6$) earthquakes occurred in the seismic gap lying between the rupture zones of the Great Kangra (1905) and the Bihar-Nepal (1934) earthquakes. Uttarkashi earthquake was recorded by 13 SMA stations of the Uttar Pradesh array (Figure 3.5g). 111 SRR stations including those situated at far off places like New Delhi also produced records of this

event. The Chamoli earthquake was recorded by 11 SMA stations and 16 SRR stations (Figure 3.5h).

3.2.4 Kangra Array in Himachal Pradesh

This array (Figure 3.4d) contains 50 SMAs located between 31°N to 33°N and 75°E to 78°E and about 65 SRR stations between 30.5°N to 33.5°N and 75.5°E to 78.5°E . The 26 April 1986 earthquake ($m_b=5.5$) was recorded by 9 SMAs [Chandrasekaran and Das, 1992] and 17 SRRs (Figure 3.5i).

3.2.5 Arunachal Pradesh Array in Arunachal Pradesh

The Arunachal Pradesh array consists of 20 digital accelerographs (Chandra *et al.*, 1996).

The earthquakes of which the data is analyzed in this study are listed in Table 3.1(a). The numbers of strong motion recordings obtained along with the range of epicentral distances are listed in Table 3.1(b). The peak parameters like maximum acceleration, velocity, and displacement for these earthquakes are given in Table A1 and SMA station coordinates are given in Table A2 of Appendix A. The values of spectral acceleration recordings by SRRs are listed in Table B1 and the SRR station coordinates are given in Table B2 of Appendix B.

3.3 Earthquake Parameters

Wherever available, locations of epicenters proposed by United States Geological Survey (USGS) and Indian Meteorological Department (IMD) for different events are shown in Figures 3.5(a) to 3.5(i). For some of these events, epicenter location obtained by Chandrasekaran and Das (1990) using the strong motion records are also shown; these are denoted as DEQ. Epicenters by different agencies differ significantly and sometimes the difference between these can be up to 100kms (e.g., Figure 3.5c and 3.5d). Table 3.1(a) shows the earthquake magnitudes calculated by different agencies. As the

magnitude calculations for all the earthquakes considered in this study are available from USGS, the magnitude as reported by USGS has been followed.

For all the earthquakes, the correlation coefficient between the average PGA in the two horizontal directions and the epicentral distance was calculated (Table 3.2). The epicenter that gave the best correlation coefficient has been considered in the present study.

For most earthquakes, the causative fault details are not available in the literature. Similarly, there is a significant uncertainty in the focal depth. Hence, the epicentral distance is used as the control distance to the fault.

3.3.1 Calculation of Epicentral Distance

From known coordinates of epicenter and recording station, the epicentral distance should normally be calculated by assuming shape of the earth as spheroid. However, assuming shape of the earth as a sphere introduces an error less than 0.21% for a distance of 400 km. The error will be less for smaller distances. Hence, the spherical triangle formula was used for the calculation of epicentral distances.

The spherical angle $\angle MN$ between two points M and N on the surface of earth with latitude and longitude (La_m, Lo_m) and (La_n, Lo_n) , respectively, is given by (e.g., Abramowitz and Stegun, 1972):

$$\cos(\angle MN) = \cos(90 - La_m) \cos(90 - La_n) + \sin(90 - La_n) \sin(90 - La_m) \cos(Lo_m - Lo_n) \quad (3.1)$$

The mean radius at a point on surface of the earth for the mean latitude ϕ_A is given by [e.g., Clarke, 1950]

$$R_m = \frac{a(1 - e^2)}{(1 - e^2 \sin^2 \phi_A)^{3/2}} \quad (3.2)$$

where the values $a=6,377,304$ and $b=6,356,103$ are used in India by Geological Survey of India (Everest's values) and $e^2 = 1 - (b/a)^2$. The mean latitude of stations (ϕ_A) in Shillong array was found to be $25^\circ 9'$ and this value was used in the calculation of R_m as 6346.38km. It was observed that the change in R_m due to the change in mean latitude from $25^\circ 9'$ to 32° (Kangra array) was rather low ($<0.1\%$) and hence the same value of R_m was used for all the events. For the sphere of radius 6,346.38km, the epicentral distance in km is given by:

$$R = 6346.38 \times \angle MN^c \quad (3.3)$$

3.4 Analysis of SRR Data

As seen in Table 3.1(b), for several earthquakes considerably more number of SRR recordings are available than the SMA records. Therefore, any study on ground motion attenuation must consider both SMA and SRR data. A systematic methodology has been used in this study to estimate PGA values from SRRs, and thus the database for PGA values has been considerably enhanced. However, SRR is a relatively simple instrument and it is necessary to first verify the quality of SRR data. Rest of this chapter is concerned with the following objectives: (a) To assess the degree of uniformity between the SRR data, (b) To examine the similarity between information from SMA and SRR data, and (c) To develop a methodology for the computation of PGA from SRR data.

3.4.1 Resultant Response Spectrum

The SRR produces records in a two-dimensional reference frame, i.e., any point on the SRR record results from the two-dimensional input in the horizontal plane. However, the SMA records are unidirectional ones; the input motion is recorded along

mutually perpendicular directions. Thus, before the records from SMA and SRR are compared, the SMA records have to be reduced to represent the two-dimensional input.

The time history record of ground acceleration along longitudinal direction was used as an input to calculate the response acceleration of a Single Degree Of Freedom (SDOF) oscillator with natural period T and damping $\zeta\%$ of critical. This was done with the help of program SPECTR [NICEE, 1998]. This procedure was repeated using the ground acceleration along transverse direction. The resultant of these response accelerations acting along mutually perpendicular directions was calculated by taking the vector sum of response accelerations at each time instant. This procedure is repeated covering the complete time history. The maximum value of resultant response acceleration obtained during the entire time history is taken as the Resultant Spectral Acceleration (RSA) for natural period T and damping $\zeta\%$ of critical. Figure 3.6 shows the schematic representation for the calculation of the RSA from SMA data that can be directly compared with SRR output.

3.4.2 SRR Data versus SMA Data

Since SRR record provides maximum response acceleration in any direction, it gives ordinates of the *resultant response spectrum*. These ordinates are provided at periods 0.4sec, 0.75sec and 1.25sec for 5% and 10% damping, i.e., 0.4sec and 5% damping (represented as $SA_{0.4,5\%}^r$), at period 0.75sec and 5% damping ($SA_{0.75,5\%}^r$) etc.

As the SMA and SRR are seldom located at the same location, the direct comparison of SRR and SMA data is not possible. However, if the attenuation characteristics for the region are similar for all the recording stations, the statistical ratios of recordings should show similar trends.

Nine different ratios of SRR recordings are studied and compared with those

damping ratio, for instance between periods 0.4sec and 0.75sec for 5% damping (denoted as $(SA_{0.4}^r / SA_{0.75}^r)_{\zeta=5\%}$), etc. The remaining three ratios studied are between the RSAs for the same period but for different damping values, e.g., between period 0.4sec for 5% damping and period 0.4sec for 10% damping (denoted as $(SA_{5\%}^r / SA_{10\%}^r)_{T=0.4}$), etc.

3.4.3 Removal of Outliers

The various ratios for SRRs and SMAs as discussed above were plotted to form histograms. These histograms can be divided into two categories: (1) Ratios of records with same damping ratio but with different natural periods, and (2) Ratios of records with same natural period but with different damping ratios. The histogram for a particular ratio for SMA and SRR are given side by side for ease of comparison. (Figure 3.7a to 3.7l). It can be observed from these histograms that:

- a. The shape of the frequency distribution followed by SRRs as well as SMAs is similar.
- b. For both SRRs and SMAs, the peaks of the distribution lie almost near the same value.
- c. The shape of the distribution functions are either symmetrical or skewed to the left. It can be assumed that these ratios follow either normal or lognormal distribution.
- d. The distribution follows a well-behaved form for the ratios of RSA corresponding to $(SA_{0.4}^r / SA_{0.75}^r)_{\zeta}$ and $(SA_{0.75}^r / SA_{1.25}^r)_{\zeta}$. But the dispersion in the histogram increases for the values of $(SA_{0.4}^r / SA_{1.25}^r)_{\zeta}$. This shows that, the ratios of RSAs with closely spaced natural periods show less scatter compared to the ones with much larger difference in natural frequencies.

e. For some SRR stations the ratio of response with 5% damping to that with 10% damping is less than 1.0. However, the response of a 5% damped system should be greater than that with 10% damping. Similarly, for some SRR stations the ratio appears too high.

The unusually high or low values might have resulted from some erroneous records and poor calibration of the SRR instruments. Hence, it is desirable to remove these records or outliers from the data sets before they are used in further analysis.

Figure 3.8 gives the frequency distribution of the average value of $(SA_{0.4 \text{ sec}, \zeta=5\%} / SA_{0.4 \text{ sec}, \zeta=10\%})$, $(SA_{0.75 \text{ sec}, \zeta=5\%} / SA_{0.75 \text{ sec}, \zeta=10\%})$, and $(SA_{1.25 \text{ sec}, \zeta=5\%} / SA_{1.25 \text{ sec}, \zeta=10\%})$ for SMAs and SRRs. For August 6, October 20 and August 21 events the mean value of the above frequency distribution for SRRs was found to be 1.5, 1.49 and 1.4 with standard deviations equal to 0.4, 0.37 and 0.3. In the case of SMAs, for August 6, October 20 events, these mean values were 1.3 and 1.24 with standard deviations 0.06 and 0.07 respectively. It can be seen that, the mean values obtained from SMAs are less compared to that of SRR and SD of the ratios from SRRs is very high compared to that of SMAs. One of the reasons for this unusual difference in the values may be due to inclusion of erroneous observations. In order to remove these points, the following strategy was adapted.

The average of $mean + \sigma$ values of these events was found to be equal to 1.83. So the upper cut-off point was fixed at 1.85 (U_{cut}) and the lower limit at 1.0 (L_{cut}). Based on this criteria, about 18 ($16U_{cut} + 2L_{cut}$) observations were removed from August 6, 15 ($15U_{cut}$) from October 20 and 3 ($2U_{cut} + 1L_{cut}$) from August 21 event. Removal of points for which the ratio do not lie between 1.0 & 1.85 had the following effects:

- The change in mean value of $(SA_{5\%}^r / SA_{10\%}^r)_T$ was more pronounced compared to the

U_{cut} , it meant curtailment of the tail of the distribution and this had more pronounced effect on mean than for median.

- The change in various statistical parameters of response ratios between different damping values (e.g., $(SA_{5\%}^r / SA_{10\%}^r)_T$) was more significant compared to that for response ratios across different periods (e.g., $(SA_{T_1}^r / SA_{T_2}^r)_\zeta$) for the same amount of damping. This may be due to the fact that the removal criterion is based on the response ratio for different damping values.

The rest of the analysis uses the data remained after the above removal of outliers.

3.4.4 Observations on Data Analysis

To gain more confidence on the SRR data, correlation coefficients (CC) between the variables considered in the analysis were calculated for SRR as well as SMA data. These along with the other statistical coefficients are given in Table 3.3(a) to Table 3.3(e). For the events considered in this study, the following general observations can be made:

1. The mean and median values of RSA ratios from SRR data are fairly close to those from SMA data (e.g., Tables 3.3a to 3.3e). Generally, the median values from two data sets compare better than the mean values. The average difference between median values of all the ratios is about 16% and the difference ranges from 1% to 68% whereas the average difference between mean values is less than 20%; and it ranges from 3% to 45%.
2. The mean ratios of RSAs from SRRs for different damping corresponding to a constant period $(SA_{5\%}^r / SA_{10\%}^r)_T$ are generally higher compared to the corresponding ratios obtained from SMA records (average difference of 19%).

3. The median values of the ratios of RSAs from SRRs based on different damping values $(SA_{5\%}^r / SA_{10\%}^r)_T$ show good agreement with that of SMAs (average difference of 5%). At the same time, the difference in the median values of ratios of RSAs between different natural periods with same damping $(SA_{T_1}^r / SA_{T_2}^r)_\zeta$ shows considerable difference (average difference of 25%).
4. The standard deviation of RSA ratios for different natural periods but with same damping from SRR data compares well with that from the SMA data. However, standard deviation for RSA ratios for different damping values but same natural period is much higher for the SRR data than that from the SMA data; in fact, the value from SRR data may be four to five times that from the SMA data. This is perhaps an intrinsic nature of the data. In case of SRR different oscillators record the motion for 5% and 10% damping values and there tends to be a large variation in the ratio of the two quantities. For SMA, same time history is used to computationally obtain the response for 5% and 10% damping ratios and thus there is only a limited variation in the two quantities.
5. The correlation factors of the ratios of RSAs from SMAs and SRRs show good agreement with each other for all the earthquakes. However, for 29 March Chamoli earthquake, the correlation coefficients corresponding to $(SA_{0.4}^r / SA_{1.25}^r)_{\zeta=5\%}$ and $(SA_{0.75}^r / SA_{1.25}^r)_{\zeta=5\%}$ for SRRs show large deviation from the corresponding values for SMA. This may be due to poor calibration of the instrument with period 1.25sec and 5% damping.

From the above observations, it can be concluded that the characteristics shown by SMAs and SRRs are similar in nature. The similarity between the recordings of

SMAAs and SRRs has also been studied with the help of statistical tools in the following section

3.4.5 Statistical Analysis of Data

Many of the statistical tests available need certain assumptions to be made on the nature of the distribution followed by the variables. From the plots of response ratio histograms, it can be observed that their shape resembles a normal distribution. The frequency distribution of the ratios for RSAs of SRRs obtained in the August 6, 1988 earthquake was tested to find out validity of this observation. A test which can be used to check the validity of the model is χ^2 test for goodness of fit [Kreyszig, 1979]. The χ^2 test was conducted for the sample under consideration and the assumption of distribution being normal was found acceptable with 5% level of significance.

When the underlying populations follow normal distribution, the following test statistic can be used to test the fact that the response ratio values obtained from SRRs and SMAAs have originated from the same population [Miller, F., 1977].

$$z = \frac{(\bar{x}_1 - \bar{x}_2) - \delta}{\sqrt{\frac{\sigma_1^2}{n_1} + \frac{\sigma_2^2}{n_2}}} \quad (3.4)$$

where, \bar{x}_1, σ_1 are the mean and standard deviation of the samples obtained from SRRs and \bar{x}_2, σ_2 those of SMAAs and n_1, n_2 are corresponding number of observations. δ is the difference in the population means μ_1, μ_2 which will be equal to zero if the population means are same. The assumption that the samples of SRRs and SMAAs do not come from the same parent population can be considered acceptable if test statistic (z) do not lie in the range +1.96 to -1.96 (with level of significance, $\alpha = 5\%$). The results of statistical analysis are given in table 3.3 (a) to 3.3 (e). The ratios $\left(SA_{T_1}^r / SA_{T_2}^r \right)_s$ satisfy

the hypothesis about the parent population of the two samples being same. This reinforces the assumption that the SRRs as well as SMAs are generated from the same parent population. The hypothesis is generally not satisfied for $(SA_{5\%}^r / SA_{10\%}^r)_T$ for the data considered, except for those from the 26 April 1986 Kangra earthquake. This may be because for all the other events the standard deviation for the response ratios of SMAs with same period and different damping are very low (up to $1/5^{th}$) as compared to that from the SRR data and the possible reasons for the same have been discussed earlier.

Based on the results of this comparison, one gains more confidence on the SRR data. However, one must avoid using SRR data for study of response ratio for different damping values.

3.4.6 Spectral Acceleration *versus* Distance

The variation of RSA with distance is studied by calculating the correlation coefficient (CC) between the observed RSA (from the SMA and well as the SRR data) and the epicentral distance (Table 3.4). This parameter can also be used to bring out the similarities/differences between SMA and SRR database. The following observations can be made:

1. The CCs calculated for SRRs and SMAs are quite comparable. The average value of CC is around -0.5.
2. For August 6, 1988 Shillong earthquake, the average CC for SRRs (-0.523) is found to be higher compared to that for SMA (-0.484).
3. For Uttarkashi and Chamoli earthquakes, the CCs for RSAs of SRRs (-0.397 & -0.478) are showing lower correlation when compared with the corresponding values for SMAs (-0.613 & -0.549, average difference being 30% and ranges from 15 to 55%).

पुरुषोत्तम काशीनाथ केलकर पुस्तकालय
भारतीय प्रौद्योगिकी संस्थान कानपुर
अवाप्ति क्र० A... 134265

4. In the case of Kangra earthquake, there is high correlation between the SMA spectral values and distance ($CC \approx -0.9$). But, SRR records do not show this trend ($CC \approx -0.4$). The difference between the observed correlation factors for SRRs and SMAs is maximum in this case (average difference of 55%). It is also observed that, for this event the CC corresponding to the response from the SRRs with $T=0.4$ and $\zeta=5\%$ is very low (≈ -0.1) but the CC calculated from rest of the SRRs give almost uniform value (≈ -0.45).
5. In northern Himalaya, the RSAs from SRRs are less correlated with epicentral distance compared to that from SMAs.

For most of the earthquakes CCs of SRRs are close to CCs of SMAs with respect to epicentral distance and this nature also strengthens the observation that SRRs and SMAs show similar properties.

3.5 PGA from SRR Data

Spectrum Amplification Factors (SAF) are commonly used to develop response spectrum from known PGA values. Newmark and Hall (1982) have proposed values of amplification factors for various amounts of damping (Table 3.6) and methodology of calculation of response spectrum bounds employing these values. This was based on the fact that response spectrum over certain frequency ranges is related to the peak value of ground acceleration, velocity and displacement. For calculating PGA from resultant spectral values a similar concept can be used. But, Chandak and Jain (1994) have reported that the amplification factors are significantly different from that reported in the study by Newmark and Hall (1982).

A methodology can be developed based on the characteristics of the recordings from SMAs and the validity of the procedure can be tested based on the available values of actual PGAs for SMAs. The procedure which gives the best prediction of PGAs can

be employed in conversion of SRR responses to PGA values. Before amplification factor is used as the conversion parameter, the variation of amplification factors with respect to distance and with change in geological characteristics of different regions needs to be studied.

3.5.1 Spectrum Amplification Factor

The high frequency waves of the ground motions attenuate faster than low frequency waves. This may lead to SAF being influenced by distance. In general, SA/PGA values are generally expected rise with respect to distance in velocity and displacement controlled region. The variations of Amplification Factor (AF) with distance along with the logarithmic best-fit lines are shown in Figure 3.10 (a) to 3.10 (d). Table 3.5 shows various statistical parameters calculated between RSA and average PGA from SMAs. Table 3.7 shows the correlation coefficients of various amplification factors with respect to epicentral distance $(SA/PGA, D)_{T,\zeta}$.

It can be observed from Table 3.7 that CC changes from +0.53 to -0.501 for different events and there is less negative correlation between amplification factor and epicentral distance. It is seen that the amplification factors corresponding to the same earthquake shows an increasing trend with respect to distance for some natural periods and decreasing trend for some other values (e.g., Uttarkashi, Chamoli). For some events, the trend is consistent for all periods (e.g., Shillong). The relationships for spectral acceleration available in the literature predict the relation of amplification factor with distance as one with a very weak negative dependence or a strong positive dependence (Figure 3.11). The trend predicted by all the relationships is consistent for periods 0.4sec, 0.75sec and 1.25 sec [Youngs *et al.*, 1997; Atkinson and Boore 1997; Sadigh *et al.*, 1997; Boore *et al.*, 1997], which contradicts with the observations made for Indian earthquakes. The logarithmic best fit for the data of amplification factors *versus*

epicentral distance tends to become flat (weak dependence) as the period and damping increases. Thus, from the analysis of correlation factors between $(SA/PGA)_{T,\zeta}$ and D and the trend of amplification factors $(SA/PGA)_{T,\zeta}$ versus epicentral distance D , no general conclusion can be drawn about the distance dependence of amplification factors. The records from SRRs cover large distances compared to SMAs. Thus, any distance dependant extrapolation of data based only on the observations from SMAs might lead to erroneous results. Hence $(SA/PGA)_{T,\zeta}$ is assumed independent of epicentral distance D for the regions considered in this study.

Since the amplification factor is considered independent of distance, the regional variation of the amplification factor can be studied with the help of parameters given in Table 3.5. The calculated parameters include mean ratios of RSA and average PGA at different time periods and at different damping ratios, represented as $(SA/PGA)_{T,\zeta}$, and their medians, standard deviations and correlation factors. The following observations can be made on these parameters corresponding to different events:

1. The mean SAF for these events ranges from 2.45 to 2.14, 1.0 to 1.44 and 0.45 to 0.77 corresponding to 5% damping for natural periods of 0.4, 0.75 and 1.25 sec. The corresponding values for 10% damping were found to range between 1.68 to 1.87, 0.84 to 1.07 and 0.38 to 0.61.
2. Based on the local geology, the mean values of amplification factors show significant variation from event to event (e.g., $AF_{1.25,10\%}=0.377$ for Kangra and 0.605 for Shillong earthquake). Similar trend is also shown for median values. This implies that the shape of the normalised response spectrum will be different for each event and use of a single amplification factor corresponding to all events for a particular period will be meaningless. So, in the subsequent analysis the amplification factors

used in the computation of SRRs are the ones obtained from the SMAs of corresponding events.

3. Generally, median values are lower than the mean values.
4. The standard deviation of SAF decreases as the natural period and damping ratio increases. But, the rate of decrease is different for each earthquake. Since the mean of amplification factor also decreases with increasing period, it is observed that the coefficient of variation increases with period and damping.
5. Higher value of damping produces better correlation of amplification factor with distance.
6. For 26 April 1986 Kangra earthquake and March 20, 1999 Chamoli earthquake PGA values were found to have very good correlation with RSA (ranges from 0.82 to 0.94). This implies that the ratio of RSA/PGA is not being influenced by any external elements like geology. The least correlation with PGA was observed for 6 August, Shillong earthquake. For this event, good correlation between RSA and PGA (0.88) was observed for RSA corresponding to natural frequency of 0.4. But, these were found to decrease as the natural period of the system increased (0.6 for $T=0.75$ and 0.45 for $T=1.25\text{sec}$).

Based on the above observations it can be seen that the mean or median values of SAF can be used for arriving at PGAs. The use of CCs as weighing functions can also be explored. This aspect is discussed in detail in the next section.

3.5.2 PGAs from Recorded RSAs

Different alternatives for calculation of PGA from RSA are explored in this section. All methods are based on employing SAFs to back-calculate PGAs. Since the actual PGA values are available for SMAs, the accuracy of the different procedures can be compared. The parameter known as error of estimate was used to compare the

accuracy of the predictions. This is the error in the estimate of predicted PGA as compared to the actual PGA. It is defined as

$$\text{Error} = \frac{\sqrt{\sum_{i=1}^n \left(\frac{PGA_{\text{predicted}} - PGA_{\text{observed}}}{PGA_{\text{observed}}} \right)^2}}{n}, \quad (3.5)$$

where, n is the number of stations used to estimate the error.

3.5.2.1 Method Based on Median of Analysis

In this method, the median of the $(RSA/PGA)_i$ ratios of the available records is used as the amplification factor and assuming equal weights to all observations. This can be written as

$$PGA = \frac{1}{6} \sum_{i=1}^6 (RSA/\text{median})_i. \quad (3.6)$$

When this procedure was employed, the error in prediction for different events ranged from 9.4 to 17 % (Table 3.8).

3.5.2.2 Method Based on Median of Analysis and Weight Functions

As the correlation coefficient relates the degree of dependence of RSA on PGA, this method assigns the RSA values with higher correlation with PGA more weight in the calculation of the PGA, *i.e.*, the correlation coefficients are used as *weighing* function for each RSA. The peak ground acceleration is obtained by dividing the sum of observed accelerations by the sum of weights used and written as

$$PGA_{\text{predicted}} = \frac{\sum_{i=1}^6 (w_i RSA_i / \text{median}_i)}{\sum_{i=1}^6 w_i}. \quad (3.7)$$

It is seen that the error ranges from 9.4 to 16.9 % in this procedure (Table 3.8). reduction in error is considerable in the case of August because compared to others, observation with 0.4 sec period had shown more correlation with PGA. But for all ot events this method did not result in any significant reduction in error. This is due to fact that the CCs for these events are almost equal to unity and hence this method v not produce results significantly different from the previous method.

3.5.2.3 Method Based on Mean of Analysis

The mean of the $(SA/PGA)_i^r$ ratios of the available records is used as t amplification factor and weighing functions are assumed to be unity. This can be writt as

$$PGA = \frac{1}{6} \sum_{i=1}^6 (RSA / \text{mean})_i, \quad (3.$$

where, i represent to each response from SRRs.

The use of this method resulted in significant reduction in error. For some events, th reduction was upto 4%. The error of prediction raged from 9.0 to 14.0.

3.5.2.4 Method Based on Mean of Analysis and Weight Functions

In this method, the mean is used as the amplification factor and the correlatio coefficients between RSA and PGA are used as the weighting functions. The relation i given as

$$PGA_{predicted} = \frac{\sum_{i=1}^6 (w_i RSA_i / \text{mean}_i)}{\sum_{i=1}^6 w_i}. \quad (3.9)$$

Out of all the methods discussed above, the least values of errors were obtained when this procedure was used. The error in prediction varied from 8.9 to 14.

A method based on using arbitrary weighing factors 0.90, 0.60 and 0.45 corresponding to periods 0.4, 0.75 and 1.25sec was also employed. The use of these weighing factors resulted in lesser value of error (Table 3.8). The error ranged from 8.5 to 13. For August 6, 1998 event, the values the weighing factors were approximately equal to the correlation coefficients, but these weighing functions were physically meaningless for all other events.

Since a best-fit equation will be providing the least error of prediction, an attempt was made to compare results from best fit method with the procedures discussed above.

3.5.2.5 Best-Fit Method

In this method a best-fit expression is obtained for the sample considering PGA as the dependent variable and the various SA as the independent variables. There are 6 values for the resultant SA from the SRR records, i.e., $SA_{T,\zeta}^r$ for different values of period and damping. In this study, two such models are considered.

Model I:

$$PGA = b_1 SA_{0.4,5\%}^r + b_2 SA_{0.75,5\%}^r + b_3 SA_{1.25,5\%}^r + b_4 SA_{0.4,10\%}^r + b_5 SA_{0.75,10\%}^r + b_6 SA_{1.25,10\%}^r \quad (3.10)$$

Model II:

$$PGA = b_1 + b_2 SA_{0.4,5\%}^r + b_3 SA_{0.75,5\%}^r + b_4 SA_{1.25,5\%}^r + b_5 SA_{0.4,10\%}^r + b_6 SA_{0.75,10\%}^r + b_7 SA_{1.25,10\%}^r \quad (3.11)$$

For the model I, the values of the coefficients calculated for August 6 1988 event are given below:

$$b_1 = 0.0818, \quad b_2 = 2.988, \quad b_3 = -6.303, \quad b_4 = 0.33, \quad b_5 = -4.365, \quad b_6 = 8.7965.$$

Theoretically, these values should be similar to $AF/6$ and should be greater than zero. It

can be observed from these coefficients that no general trend can be predicted about the relation of this numbers with the Resultant Spectral Accelerations. The usage of these coefficients as weighing functions was also discarded because of arbitrarily high values corresponding to some accelerations and change in signs which would imply a negative effect of a particular RSA on PGA.

For the second model described in least-square analysis, the coefficients obtained for August 6 1988 event are

$$b_1 = 0.0533, b_2 = 0.4748, b_3 = 0.5061, b_4 = -0.2177, b_5 = 0.9587, b_6 = -0.4820 \\ b_7 = -0.2835.$$

In this case, the calculated error was found to be 5.85%. For some events, model-1 predicted the least error and model-2 for some other events.

The performance of the solutions of least-square estimates when extrapolated is known to be erroneous especially when there is no physical basis for selection of parameters (Campbell 1985). Since the range of recordings by SRR are much wider compared to that of SMAs and model-2 do not have any physical basis, the use of this method for calculation of PGA from SRR values may produce misleading answers.

It was also observed that the error predicted by this procedure was not very different from the one predicted using mean as amplification factors and correlation coefficients as weighing functions (difference of 0.6 to 5). So for the back calculation of PGA from SRRs, it was decided to use mean as amplification factor and the correlation coefficient between RSA and PGA as weighing function.

3.5.3 Spread in Predicted PGAs

In order to study the spread in the predicted PGAs from SMAs and SRRs a parameter called *average Coefficient of Variation* was used. This is defined as the

average of coefficient of variation (σ/μ) observed for all the stations across the predicted values and gives average extent of spread that occurs among the six generated PGAs at each station. Since the weighing functions will also be affecting the variation, the weight was assumed equal to 1.0 for this analysis.

The coefficient of variation among the six calculated peak ground accelerations was computed for all the events (Table 3.9). It can be observed from the table that,

- (a) The spread of predictions in the case of SRRs is not very different from SMAs. The predictions based on SMAs differ from that based on SRRs by an average of 20% which ranges from 13% (Uttarkashi) to 50% (Kangra).
- (b) The spread in prediction is always more for SRRs compared to SMAs.

It can be concluded that, the spread in PGAs calculated from SRRs and SMAs do not vary significantly.

Based on these observations, it was decided to use the Mean values as conversion factors and CC as weighing functions for calculation of PGA from SRR recordings. The observed values of peak ground acceleration from SMAs for different events as well the predicted values of acceleration from the SRRs are given in Figure 3.12. It can be observed that the predicted values of acceleration seamlessly fit into the observed SMA data.



Table 3.1 (a): Earthquake events considered in this study.

Location	Array	Date	Epicenter			Depth (km)	Magnitude
			Source	Lat N	Long E		
NE. India	Shillong	10 Sep 1986	USGS	25.385	92.077	43.0	5.2 m_b
			IMD	25.200	91.600	-	5.5
			DEQ	25.562	92.187	19.5	-
NE. India	Shillong	14 May 1987	USGS	25.271	94.202	49.0	5.9 M_s
			DEQ	25.498	93.450	-	-
NE. India	Shillong	6 Feb 1988	USGS	24.467	91.517	33.0	5.8 m_b
			DEQ	25.504	91.342	-	-
NE. India	Shillong	6 Aug 1988	USGS	25.149	95.127	90.0	7.3 M_s
			DEQ	25.392	94.533		6.8
NE. India	Shillong	9 Jan 1990	USGS	24.750	95.240	119.0	6.1 m_b
N. India	-	21 Aug 1988 (Bihar-Nepal)	USGS	26.750	86.620	57.0	6.8 M_s
			ISC	26.720	86.630	-	6.4
N. India	Uttar Pradesh	20 Oct 1991 (Uttarkashi)	USGS	30.780	78.770	10.0	7.0 M_s
			DEQ	30.738	78.792	19.0	6.5
N. India	Uttar Pradesh	29 Mar 1999 (Chamoli)	USGS	30.510	79.400	15.0	6.6 M_s
			DEQ	30.410	79.420	21.0	6.8 M_l
N. India	Kangra	26 Apr 1986 (Kangra)	USGS	32.128	76.374	33.0	5.5 m_b
			IMD	32.193	76.290	9.0	5.7
			DEQ	32.183	76.266	6.6	-

Table 3.1 (b): Earthquake events considered and number of recordings.

Date	Type of EQ	Mag	SMA			SRR		
			Number of Records	Distance R (km)		Number of Records	Distance R (km)	
				Min	Max		Min	Max
10 Sep 1986	Thrust	5.2	12	6	90	-	-	-
14 May 1987	Thrust	5.9	14	90	190	-	-	-
6 Feb 1988	Thrust	5.8	18	35	176	-	-	-
6 Aug 1988	Subduction	7.3	33	99	323	122	39	772
9 Jan 1990	Subduction	6.1	14	200	300	-	-	-
21 Aug 1988 (Bihar-Nepal)	Strike-Slip	6.8	-	-	-	41	42	325
20 Oct 1991 (Uttarkashi)	Thrust	7.0	13	19	152	111	14	322
29 Mar 1999 (Chamoli)	Thrust	6.6	10	8	123	16	4	158
26 Apr 1986 (Kangra)	Thrust	5.5	9	2	28	17	5	107

Table 3.2: Correlation of epicentral distances with average peak ground acceleration.

<i>Event</i>	<i>Agency</i>	<i>Correlation Coefficient</i>	<i>Epicentral location used</i>
10 Sep 1986 Shillong	USGS	-0.586	DEQ
	IMD	-0.293	
	DEQ	-0.638	
14 May 1987 Shillong	USGS	-0.559	USGS
	DEQ	-0.548	
6 Feb 1988 Shillong	USGS	-0.411	DEQ
	DEQ	-0.708	
6 Aug 1988 Shillong	USGS	-0.408	DEQ
	IMD	-0.403	
	DEQ	-0.451	
9 Jan 1990 Shillong	USGS	-0.369	USGS
20 Oct 1991 (Uttarkashi)	USGS	-0.676	DEQ
	DEQ	-0.685	
29 Mar 1999 Chamoli	USGS	-0.619	DEQ
	DEQ	-0.619	
26 Apr 1986 Kangra	USGS	-0.417	IMD
	IMD	-0.818	
	DEQ	-0.805	
21 Aug 1988 Bihar	-	-	USGS

Table 3.3(a): Results of statistical analysis for the ratios of the data of 6 August 1988 Shillong earthquake

Event	#SMA	33	#SRR	104						
Shillong 6-Aug-88	Mean		Median		SD		CC		Test	
	SMA	SRR	SMA	SRR	SMA	SRR	SMA	SRR	Statistic	
$(SA_{0.4}^r / SA_{0.75}^r)_{\zeta=5\%}$	2.157	2.597	1.674	2.438	1.635	1.276	0.713	0.777	-1.415	
$(SA_{0.75}^r / SA_{1.25}^r)_{\zeta=5\%}$	2.280	2.212	1.957	1.856	0.982	1.622	0.845	0.710	0.291	
$(SA_{0.4}^r / SA_{1.25}^r)_{\zeta=5\%}$	4.903	5.125	4.305	4.496	3.973	3.437	0.631	0.611	-0.303	
$(SA_{0.4}^r / SA_{0.75}^r)_{\zeta=10\%}$	2.109	2.721	1.765	2.438	1.452	1.787	0.739	0.827	-1.990	
$(SA_{0.75}^r / SA_{1.25}^r)_{\zeta=10\%}$	2.016	2.227	2.011	1.842	0.710	1.759	0.874	0.716	-0.994	
$(SA_{0.4}^r / SA_{1.25}^r)_{\zeta=10\%}$	4.458	5.349	3.615	4.761	3.585	3.831	0.655	0.680	-1.223	
$(SA_{5\%}^r / SA_{10\%}^r)_{T=0.4}$	1.338	1.471	1.337	1.353	0.121	0.525	0.997	0.956	-2.391	
$(SA_{5\%}^r / SA_{10\%}^r)_{T=0.75}$	1.337	1.529	1.337	1.401	0.105	0.600	0.995	0.948	-3.116	
$(SA_{5\%}^r / SA_{10\%}^r)_{T=1.25}$	1.238	1.524	1.252	1.272	0.102	0.743	0.995	0.872	-3.814	

Table 3.3(b): Results of statistical analysis for the ratios of the data of 21 August 1988 Bihar-Nepal earthquake.

Event	#SMA	0	#SRR	38						
Bihar 21-Aug-88	Mean		Median		SD		CC		Test	
	SMA	SRR	SMA	SRR	SMA	SRR	SMA	SRR	Statistic	
$(SA_{0.4}^r / SA_{0.75}^r)_{\zeta=5\%}$	-	2.563	-	1.873	-	1.641	-	0.848	-	
$(SA_{0.75}^r / SA_{1.25}^r)_{\zeta=5\%}$	-	2.417	-	2.358	-	1.370	-	0.841	-	
$(SA_{0.4}^r / SA_{1.25}^r)_{\zeta=5\%}$	-	5.846	-	4.462	-	4.629	-	0.637	-	
$(SA_{0.4}^r / SA_{0.75}^r)_{\zeta=10\%}$	-	2.693	-	1.945	-	1.755	-	0.864	-	
$(SA_{0.75}^r / SA_{1.25}^r)_{\zeta=10\%}$	-	2.353	-	2.154	-	1.491	-	0.909	-	
$(SA_{0.4}^r / SA_{1.25}^r)_{\zeta=10\%}$	-	5.851	-	4.362	-	4.077	-	0.731	-	
$(SA_{5\%}^r / SA_{10\%}^r)_{T=0.4}$	-	1.322	-	1.266	-	0.263	-	0.955	-	
$(SA_{5\%}^r / SA_{10\%}^r)_{T=0.75}$	-	1.447	-	1.269	-	0.539	-	0.964	-	
$(SA_{5\%}^r / SA_{10\%}^r)_{T=1.25}$	-	1.434	-	1.336	-	0.407	-	0.973	-	

Table 3.3(c): Results of statistical analysis for the ratios of the data of 20 October, 1991 Uttarkashi earthquake.

Event	#SMA	13	#SRR	95						
Uttarkashi 20-Oct-91	Mean		Median		SD		CC		Test	
	SMA	SRR	SMA	SRR	SMA	SRR	SMA	SRR	Statistic	
$(SA_{0.4}^r / SA_{0.75}^r)_{\zeta=5\%}$	2.225	2.422	1.555	2.268	1.486	1.324	0.820	0.898	-0.454	
$(SA_{0.75}^r / SA_{1.25}^r)_{\zeta=5\%}$	1.910	1.677	1.890	1.375	0.700	1.188	0.943	0.967	1.026	
$(SA_{0.4}^r / SA_{1.25}^r)_{\zeta=5\%}$	4.403	3.587	3.424	2.952	3.929	2.300	0.701	0.885	0.732	
$(SA_{0.4}^r / SA_{0.75}^r)_{\zeta=10\%}$	2.047	2.580	1.795	2.245	1.166	1.693	0.879	0.924	-1.452	
$(SA_{0.75}^r / SA_{1.25}^r)_{\zeta=10\%}$	1.919	1.578	1.723	1.229	0.693	1.291	0.947	0.959	1.461	
$(SA_{0.4}^r / SA_{1.25}^r)_{\zeta=10\%}$	3.992	3.508	3.294	2.939	2.959	2.337	0.747	0.852	0.566	
$(SA_{5\%}^r / SA_{10\%}^r)_{T=0.4}$	1.274	1.518	1.229	1.313	0.154	0.628	0.991	0.986	-3.156	
$(SA_{5\%}^r / SA_{10\%}^r)_{T=0.75}$	1.220	1.556	1.238	1.372	0.111	0.596	0.998	0.988	-4.908	
$(SA_{5\%}^r / SA_{10\%}^r)_{T=1.25}$	1.236	1.410	1.240	1.297	0.123	0.415	0.997	0.992	-3.189	

Table 3.3(d): Results of statistical analysis for the ratios of the data of 29 March, 1999 Chamoli earthquake.

Event	#SMA	10	#SRR	16						
Chamoli 29-Mar-99	Mean		Median		SD		CC		Test	
	SMA	SRR	SMA	SRR	SMA	SRR	SMA	SRR	Statistic	
$(SA_{0.4}^r / SA_{0.75}^r)_{\zeta=5\%}$	2.225	2.605	2.006	2.523	0.837	0.835	0.988	0.942	-1.127	
$(SA_{0.75}^r / SA_{1.25}^r)_{\zeta=5\%}$	2.285	1.753	1.843	1.536	1.491	0.998	0.977	0.450	0.997	
$(SA_{0.4}^r / SA_{1.25}^r)_{\zeta=5\%}$	4.876	4.563	4.513	4.643	3.042	2.501	0.949	0.304	0.273	
$(SA_{0.4}^r / SA_{0.75}^r)_{\zeta=10\%}$	2.119	2.292	2.021	2.211	0.775	0.795	0.991	0.988	-0.548	
$(SA_{0.75}^r / SA_{1.25}^r)_{\zeta=10\%}$	2.074	1.785	1.977	1.708	0.975	0.961	0.988	0.949	0.739	
$(SA_{0.4}^r / SA_{1.25}^r)_{\zeta=10\%}$	4.313	3.863	4.384	3.143	2.263	2.301	0.969	0.913	0.490	
$(SA_{5\%}^r / SA_{10\%}^r)_{T=0.4}$	1.286	1.612	1.318	1.462	0.106	0.601	0.998	0.987	-2.118	
$(SA_{5\%}^r / SA_{10\%}^r)_{T=0.75}$	1.229	1.439	1.240	1.175	0.137	0.590	0.999	0.997	-1.366	
$(SA_{5\%}^r / SA_{10\%}^r)_{T=1.25}$	1.194	1.392	1.215	1.333	0.116	0.277	0.999	0.949	-2.527	

Table 3.3(e): Results of statistical analysis for the ratios of the data of 26 April, 1986 Kangra earthquake.

Event	#SMA	9	#SRR	17						
Kangra 26-Apr-86	Mean		Median		SD		CC		Test	
	SMA	SRR	SMA	SRR	SMA	SRR	SMA	SRR	Statistic	
$(SA_{0.4}^r / SA_{0.75}^r)_{\zeta=5\%}$	2.238	2.654	1.972	2.824	0.911	1.405	0.820	0.972	-0.911	
$(SA_{0.75}^r / SA_{1.25}^r)_{\zeta=5\%}$	2.606	1.808	2.583	1.533	1.027	0.865	0.859	0.946	1.988	
$(SA_{0.4}^r / SA_{1.25}^r)_{\zeta=5\%}$	5.813	4.288	4.500	4.167	3.152	2.187	0.834	0.929	1.296	
$(SA_{0.4}^r / SA_{0.75}^r)_{\zeta=10\%}$	2.088	3.152	1.970	2.514	0.526	1.934	0.905	0.891	-2.125	
$(SA_{0.75}^r / SA_{1.25}^r)_{\zeta=10\%}$	2.409	2.079	2.460	1.352	0.826	1.692	0.914	0.767	0.646	
$(SA_{0.4}^r / SA_{1.25}^r)_{\zeta=10\%}$	5.049	7.139	4.290	3.400	2.140	10.070	0.903	0.603	-0.826	
$(SA_{5\%}^r / SA_{10\%}^r)_{T=0.4}$	1.232	1.217	1.218	1.229	0.107	0.620	0.996	0.885	0.097	
$(SA_{5\%}^r / SA_{10\%}^r)_{T=0.75}$	1.195	1.635	1.182	1.242	0.108	1.181	0.994	0.978	-1.524	
$(SA_{5\%}^r / SA_{10\%}^r)_{T=1.25}$	1.133	1.359	1.115	1.182	0.135	0.697	0.993	0.871	-1.292	

Table 3.4: Correlation between resultant spectral acceleration and epicentral distance.

Event	Correlation Coefficient Between SA and Distance							
	Shillong		Bihar-Nepal		Uttarkashi		Chamoli	
	6-Aug-1988		21-Aug-1988		20-Oct-1990		29-Mar-1999	
$SA_{T,\zeta}^r, D$	SMA	SRR	SMA	SRR	SMA	SRR	SMA	SRR
$T=0.4, \zeta=5\%$	-0.446	-0.473	-	-0.502	-0.608	-0.444	-0.500	-0.334
$T=0.75, \zeta=5\%$	-0.534	-0.556	-	-0.607	-0.597	-0.429	-0.532	-0.472
$T=1.25, \zeta=5\%$	-0.455	-0.531	-	-0.631	-0.628	-0.451	-0.610	-0.536
$T=0.4, \zeta=10\%$	-0.464	-0.518	-	-0.625	-0.605	-0.357	-0.512	-0.416
$T=0.75, \zeta=10\%$	-0.523	-0.518	-	-0.589	-0.617	-0.361	-0.543	-0.475
$T=1.25, \zeta=10\%$	-0.482	-0.543	-	-0.609	-0.621	-0.341	-0.598	-0.634
Average Value	-0.484	-0.523	-	-0.593	-0.613	-0.397	-0.549	-0.478
							-0.905	-0.406

Table 3.5: Statistical parameters for the amplification factors ($SA_{\text{resultant}}/PGA_{\text{average}}$) for the different earthquakes.

$SA_{T,\zeta}^r/PGA$	Event															
	6-Aug-1988 Shillong				20-Oct-1991 Uttarkashi				29-Mar-1999 Chamoli				26-Apr-1986 Kangra			
	Mean	Median	SD	CC	Mean	Median	SD	CC	Mean	Median	SD	CC	Mean	Median	SD	CC
$T=0.4, \zeta=5\%$	2.267	2.173	1.004	0.873	2.375	2.012	1.307	0.897	2.447	2.434	1.039	0.974	2.144	2.278	0.784	0.820
$T=0.75, \zeta=5\%$	1.438	1.235	1.026	0.592	1.206	0.962	0.552	0.931	1.269	1.056	0.746	0.974	0.999	1.018	0.296	0.858
$T=1.25, \zeta=5\%$	0.771	0.549	0.739	0.435	0.768	0.588	0.535	0.813	0.697	0.575	0.481	0.973	0.446	0.391	0.284	0.834
$T=0.4, \zeta=10\%$	1.689	1.615	0.720	0.888	1.806	1.752	0.841	0.941	1.871	1.764	0.728	0.980	1.710	1.821	0.530	0.905
$T=0.75, \zeta=10\%$	1.065	0.911	0.719	0.619	0.994	0.857	0.438	0.943	1.028	0.858	0.610	0.975	0.837	0.861	0.241	0.914
$T=1.25, \zeta=10\%$	0.605	0.435	0.539	0.471	0.608	0.481	0.414	0.819	0.582	0.494	0.694	0.971	0.377	0.337	0.171	0.903

Table 3.6: Spectrum amplification factors for horizontal elastic response (from Newmark and Hall, 1982).

Damping % Critical	One Sigma (84.1%)			Median (50%)		
	A	V	D	A	V	D
0.5	5.1	3.84	3.04	3.68	2.59	2.01
1	4.38	3.38	2.73	3.21	2.31	1.82
2	3.66	2.92	2.42	2.74	2.03	1.63
3	3.24	2.64	2.24	2.46	1.86	1.52
5	2.71	2.30	2.01	2.12	1.65	1.39
7	2.36	2.08	1.85	1.89	1.51	1.29
10	1.99	1.84	1.69	1.64	1.37	1.20
20	1.26	1.37	1.38	1.17	1.08	1.01

Table 3.7: Correlation of amplification factors and epicentral distance for different earthquakes.

Correlation factor Between Amplification Factor ($SA_{resultant} / PGA_{average} \cdot D$) _{T,ζ} and Epicentral Distance D				
Event	6-Aug-1988 Shillong	20-Oct-1991 Uttarkashi	29-Mar-1999 Chamoli	26-Apr-1986 Kangra
T=0.4, ζ=5%	-0.418	+0.214	+0.437	-0.373
T=0.75, ζ=5%	-0.254	-0.358	-0.172	-0.016
T=1.25, ζ=5%	-0.105	-0.343	-0.501	-0.327
T=0.4, ζ=10%	-0.487	+0.197	+0.339	-0.326
T=0.75, ζ=10%	-0.252	-0.437	-0.336	-0.107
T=1.25, ζ=10%	-0.121	-0.349	-0.508	+0.528

Table 3.8 Error (eqn 3.5) between $PGA_{observed}$ and $PGA_{predicted}$ calculated using different weighing factors and amplification factors (e.g. eqn 3.9).

Method	Event		6-August 1988 Shillong	20-Oct- 1991 Uttar.	29-Mar- 1999 Chamoli	26-Apr- 1986 Kangra
	Ampli. Factor	Weight	Error(%)	Error(%)	Error(%)	Error(%)
a	Median	1.0	13.64	14.54	16.93	9.43
b	Median	CC between RSA's & PGA	11.68	14.20	16.92	9.38
c	Mean	1.0	10.47	11.12	14.01	9.00
e	Mean	CC between RSA's & PGA	9.41	10.91	14.00	8.96
d	Mean	0.9 _(0.40sec, 5&10% ζ) , 0.60 _(0.75sec, 5&10% ζ) , 0.45 _(1.25sec, 5&10% ζ)	9.36	10.37	13.12	8.55
f	Model 1		7.90	8.45	8.46	8.00
g	Model 2		5.85	6.98	14.33	8.36

Table 3.9 *Coefficient of variation among the six PGA calculated from SA values of SMAs and SRRs (Weights equal to unity)*

<i>Event</i>	<i>Amplification factor</i>	<i>SMA</i>	<i>SRR</i>
<i>6-August-1988 Shillong</i>	Mean	0.314	0.388
	Median	0.253	0.371
<i>20-Oct-1991 Uttarkashi</i>	Mean	0.309	0.356
	Median	0.291	0.345
<i>29-Mar-1999 Chamoli</i>	Mean	0.289	0.364
	Median	0.275	0.351
<i>26-Apr-1986 Kangra</i>	Mean	0.231	0.486
	Median	0.201	0.444
<i>21-Aug-1988 Bihar</i>	Mean	-	0.406
	Median	-	0.352

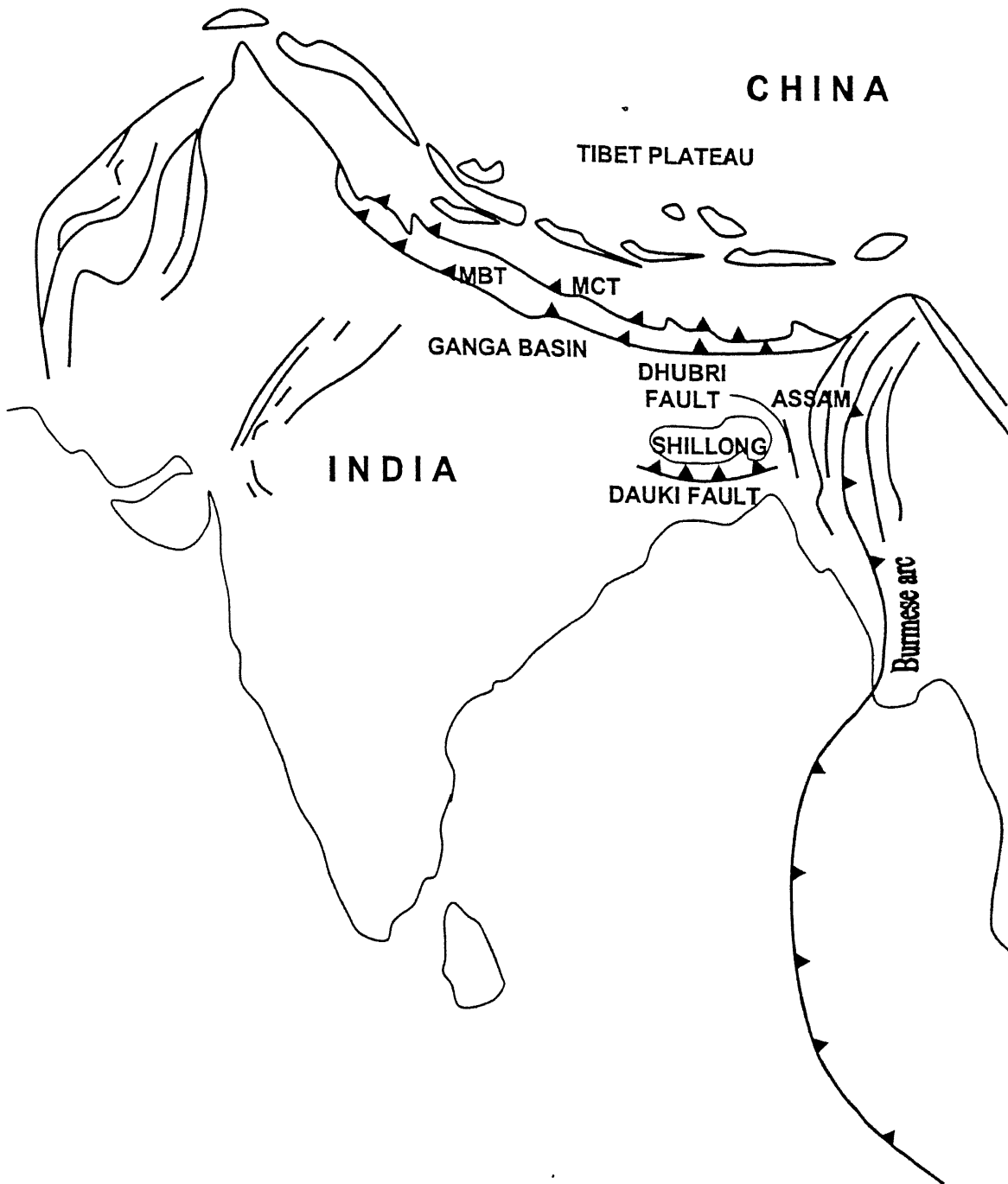


Figure 3.1: Tectonic features of the different regions considered in this study [modified from Rajendran *et. al.*, 1992].

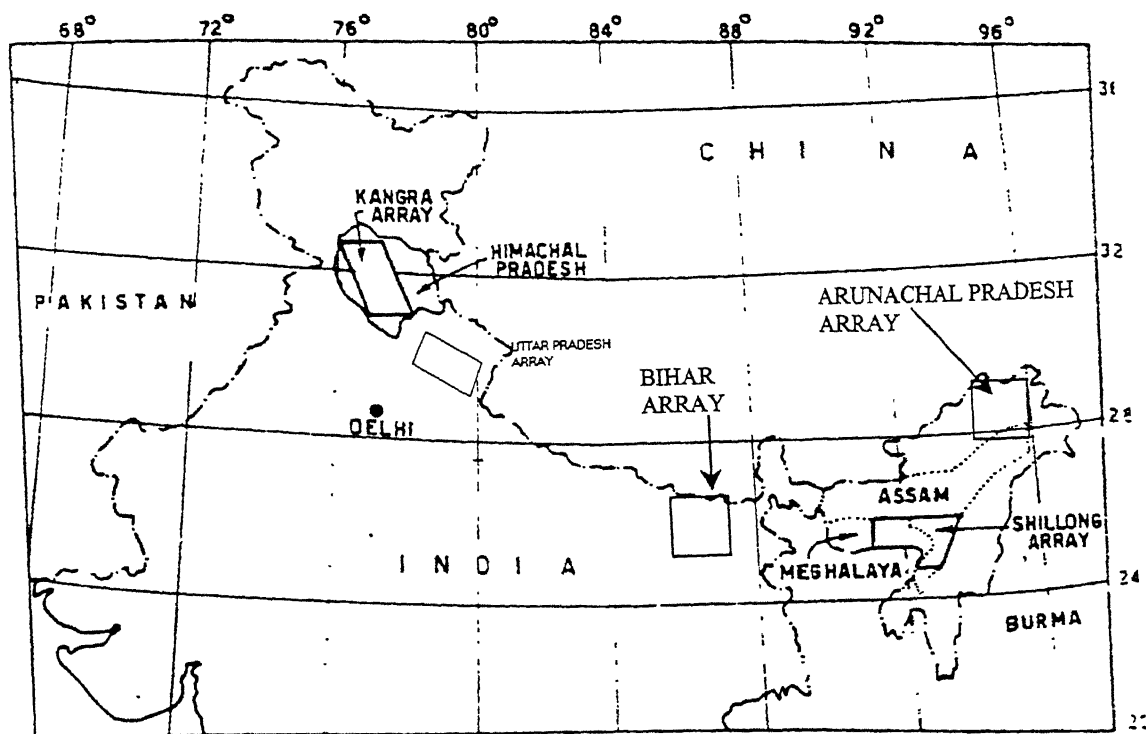


Figure 3.2: Relative position of arrays used in this study [modified from Chandrasekaran and Das, 1992].

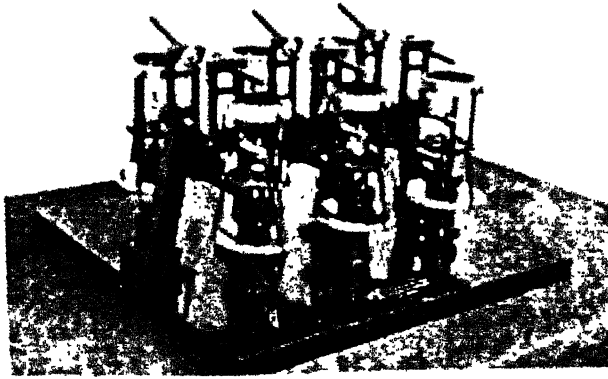


Figure 3.3(a): Photograph of a SRR [Agarwal, 1991].

5% Damping

10% Damping



Time Period = 0.4 sec

 $S_a = 211 \text{ (cm/sec}^2\text{)}$ $S_a = 183 \text{ (cm/sec}^2\text{)}$ 

Time Period = 0.75 sec

 $S_a = 98 \text{ (cm/sec}^2\text{)}$ $S_a = 87 \text{ (cm/sec}^2\text{)}$ 

Time Period = 1.25 sec

 $S_a = 36 \text{ (cm/sec}^2\text{)}$ $S_a = 31 \text{ (cm/sec}^2\text{)}$

Figure 3.3(b): A typical SRR record [DEQ 1999].

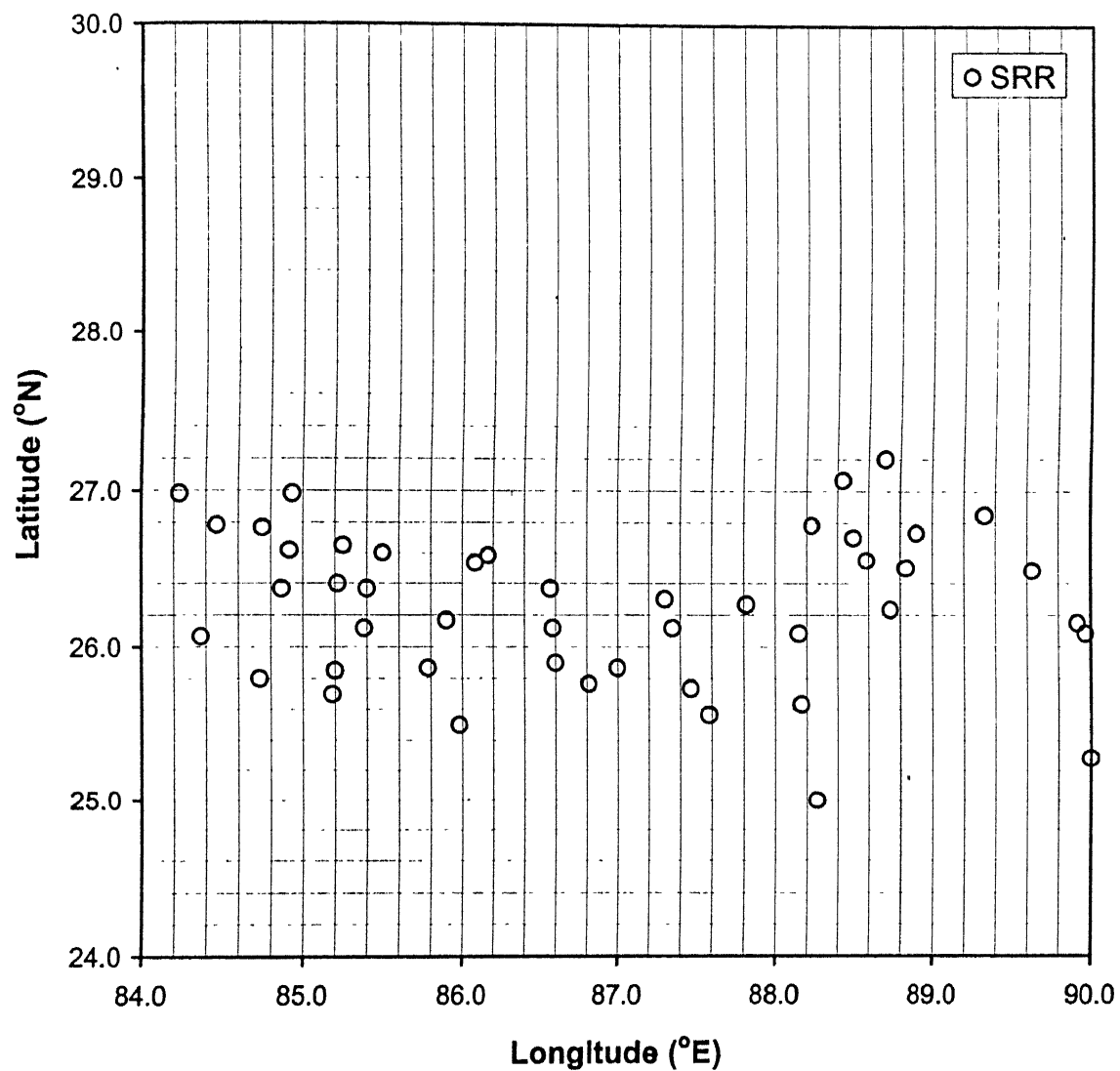
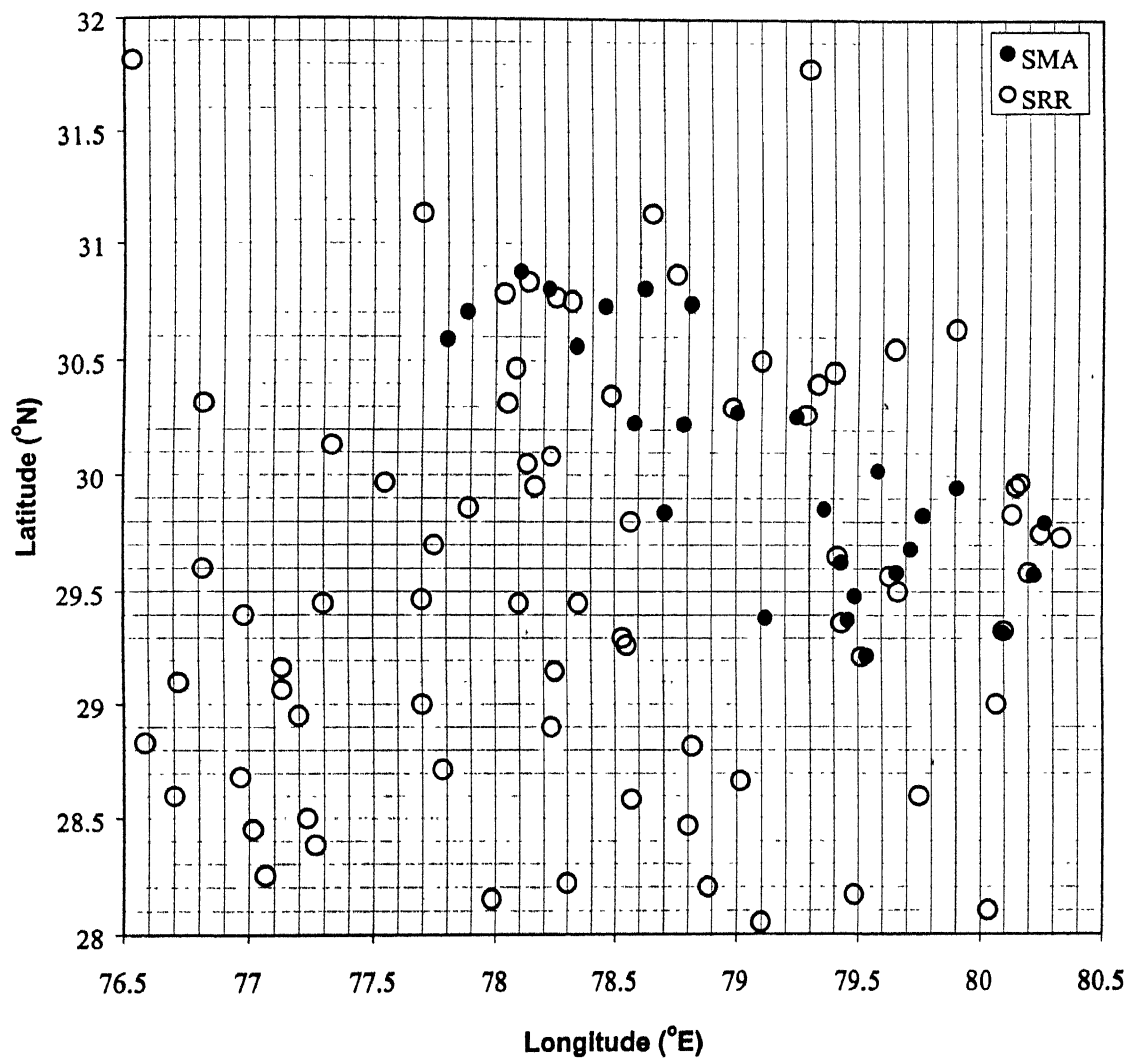
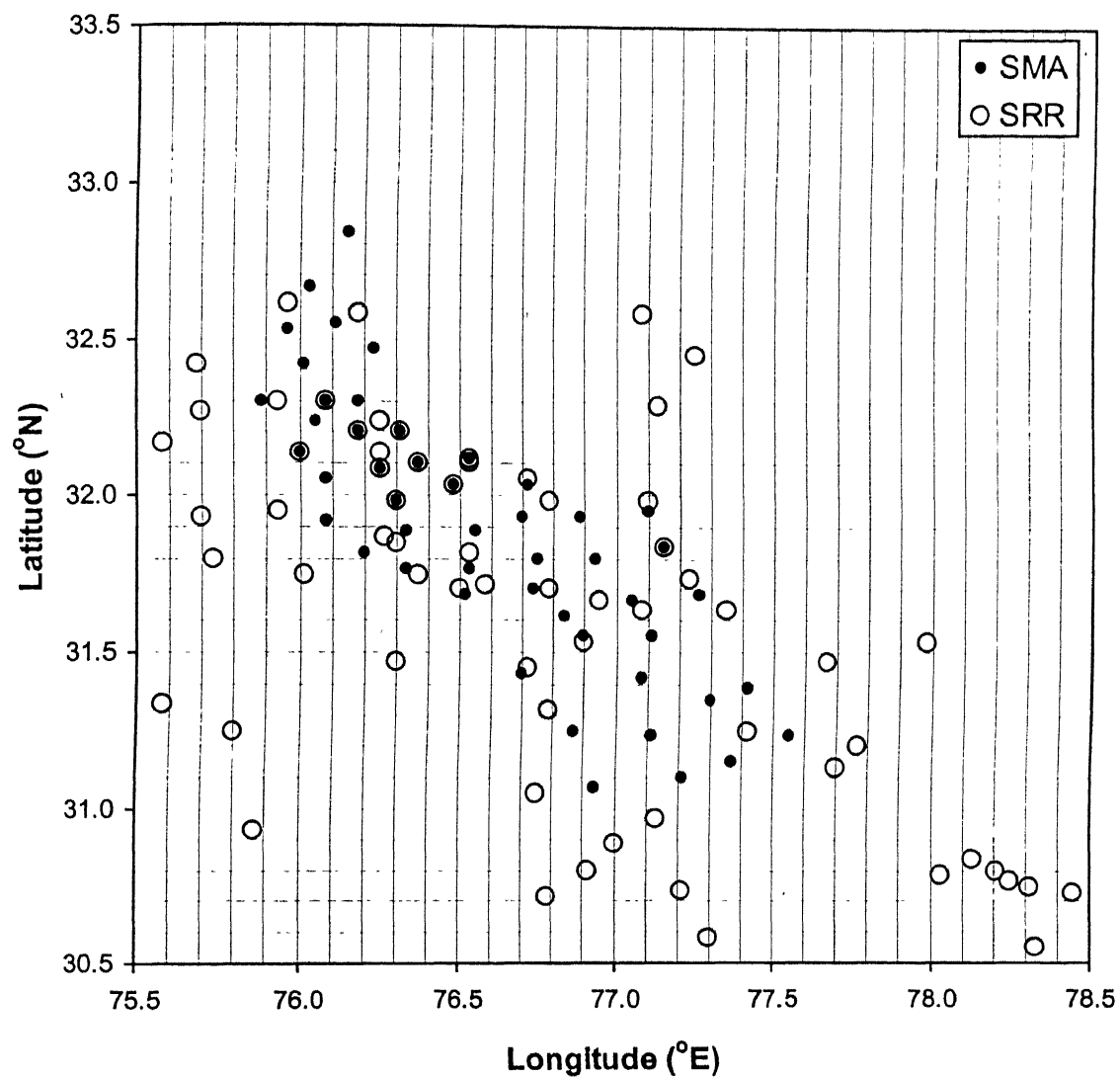


Figure 3.4(b): Location of stations in the Bihar array.





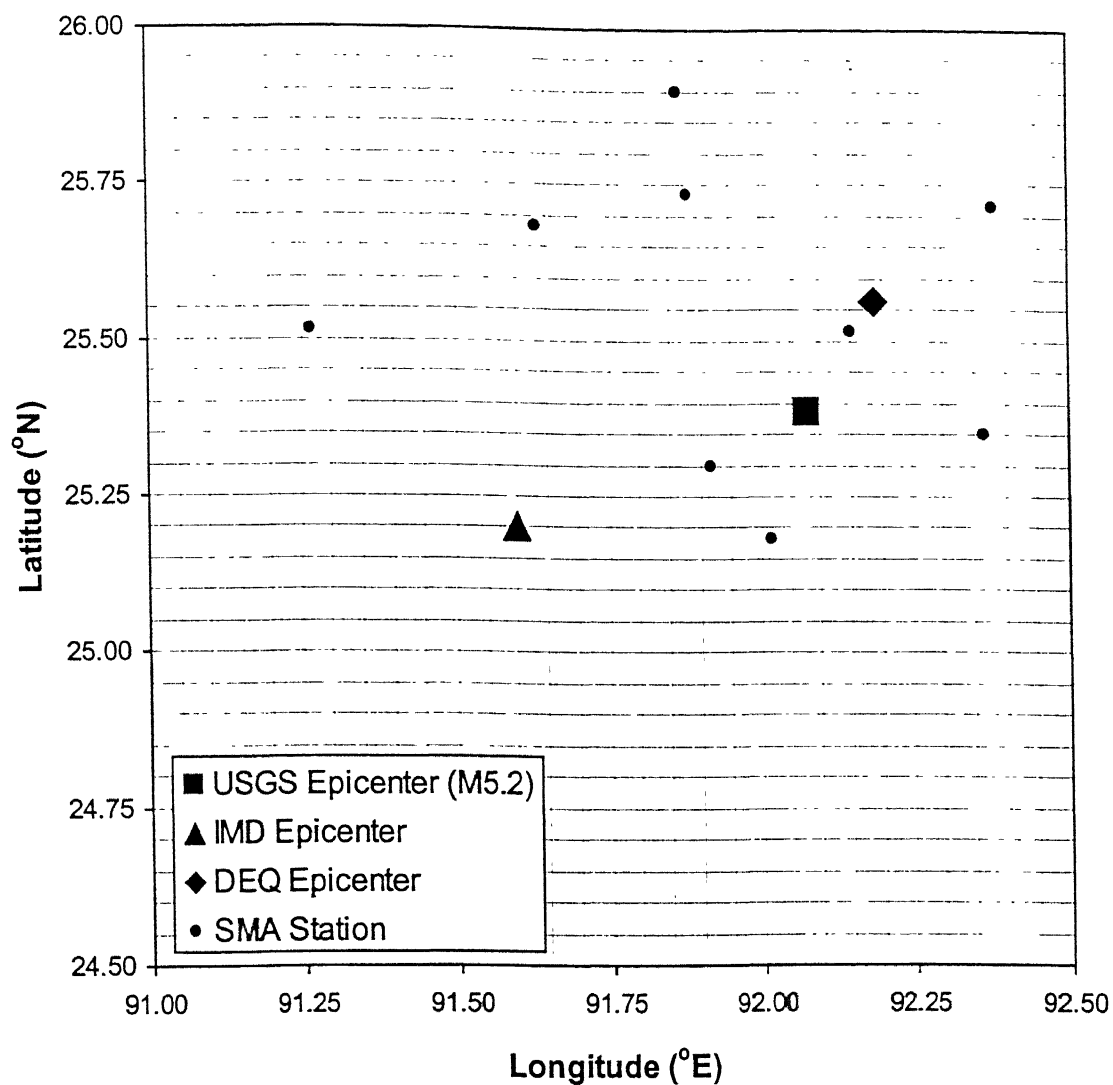


Figure 3.5(a): Location of epicenters as reported by different agencies along with the recording stations activated for the Shillong earthquake of 10 September 1986.

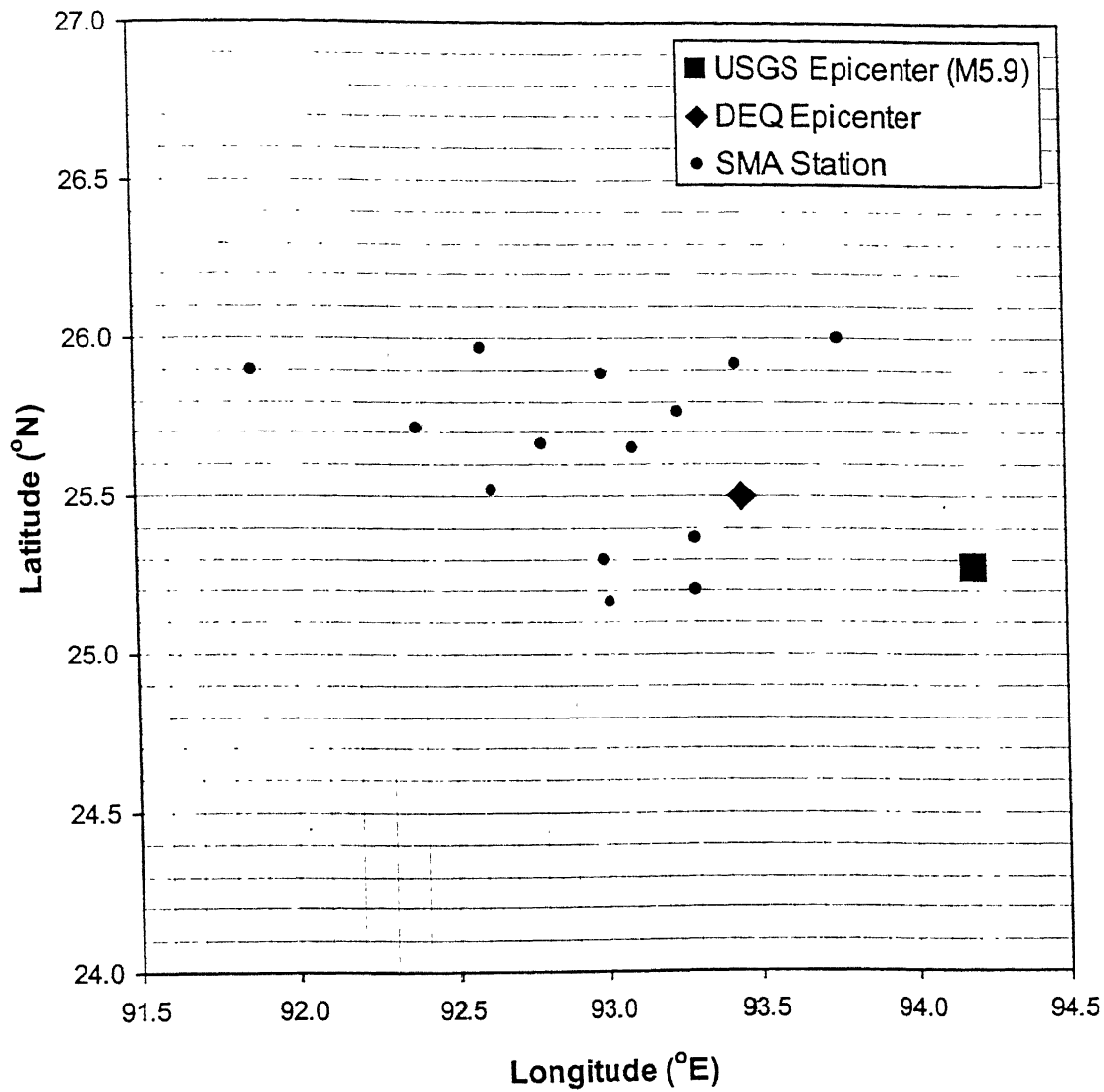


Figure 3.5(b): Location of epicenters as reported by different agencies along with the recording stations activated for the Shillong earthquake of 14 May 1987.

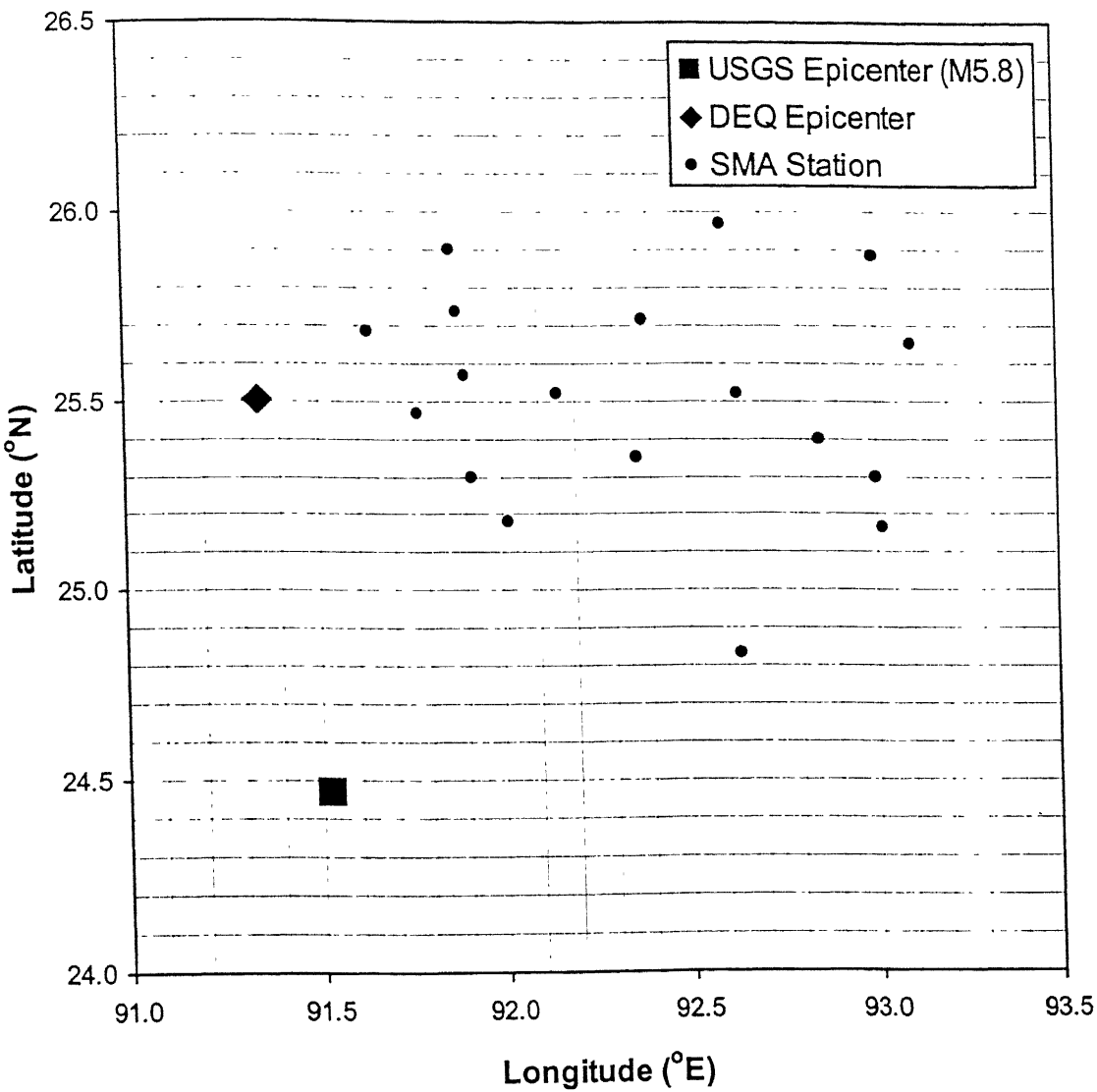


Figure 3.5(c): Location of epicenters as reported by different agencies along with the recording stations activated for the Shillong earthquake of 6 February 1988.

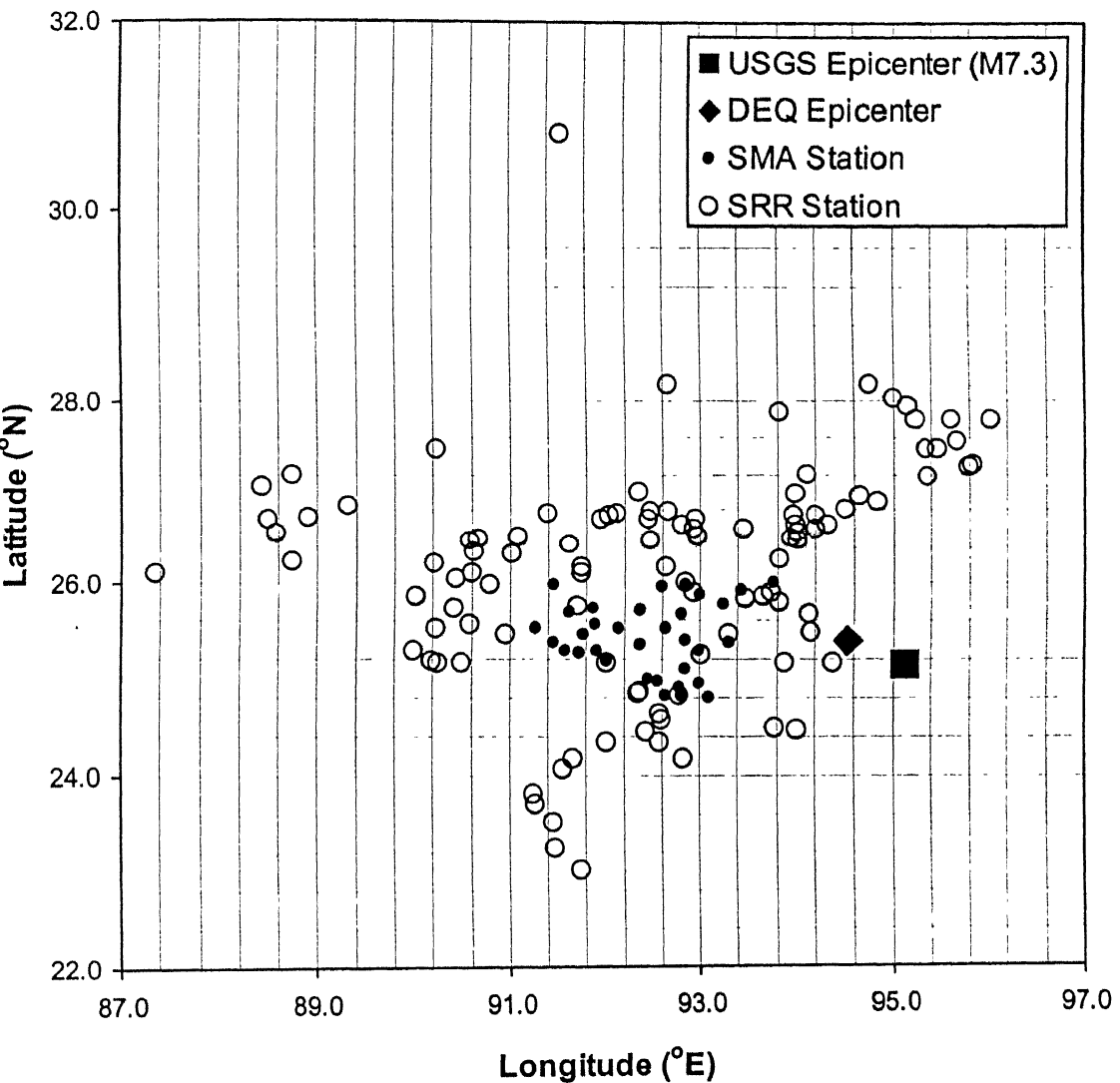


Figure 3.5(d): Location of epicenters as reported by different agencies along with the recording stations activated for the Shillong earthquake of 6 August 1988.

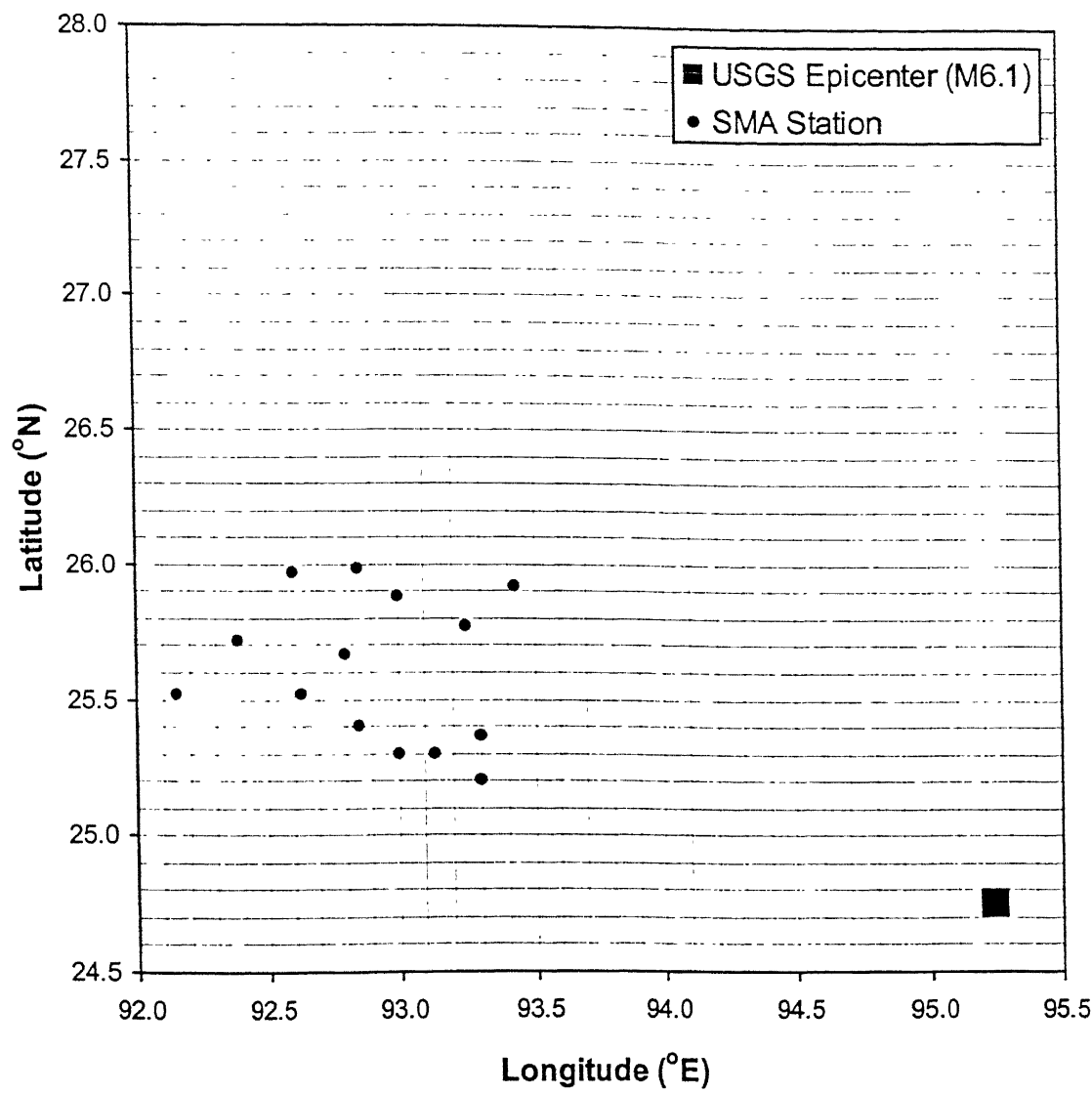


Figure 3.5(e): Location of epicenters as reported by different agencies along with the recording stations activated for the Shillong earthquake of 9 January 1990.

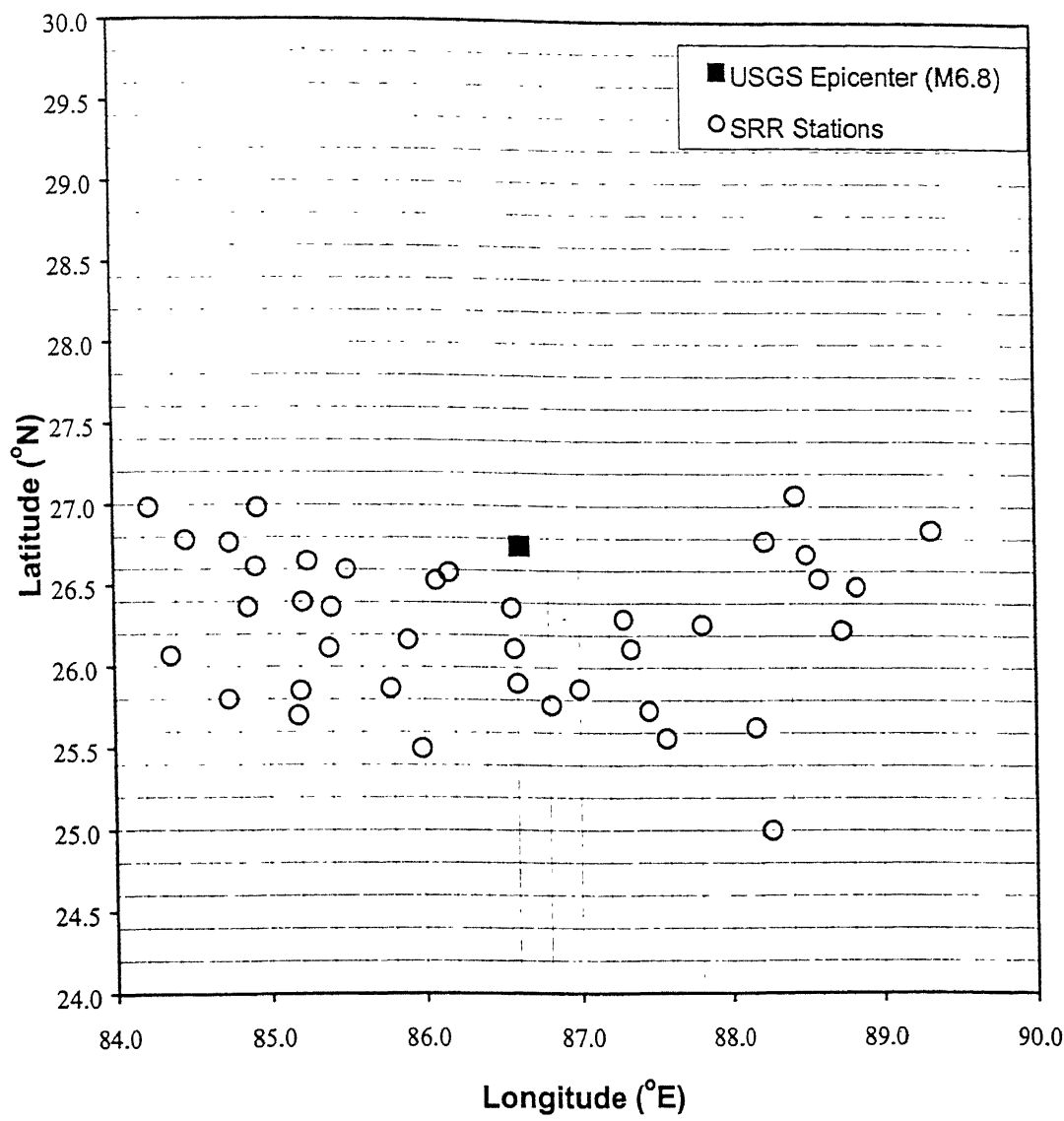


Figure 3.5(f): Location of epicenters as reported by different agencies along with the recording stations activated for the Bihar-Nepal earthquake of 21 August 1988.

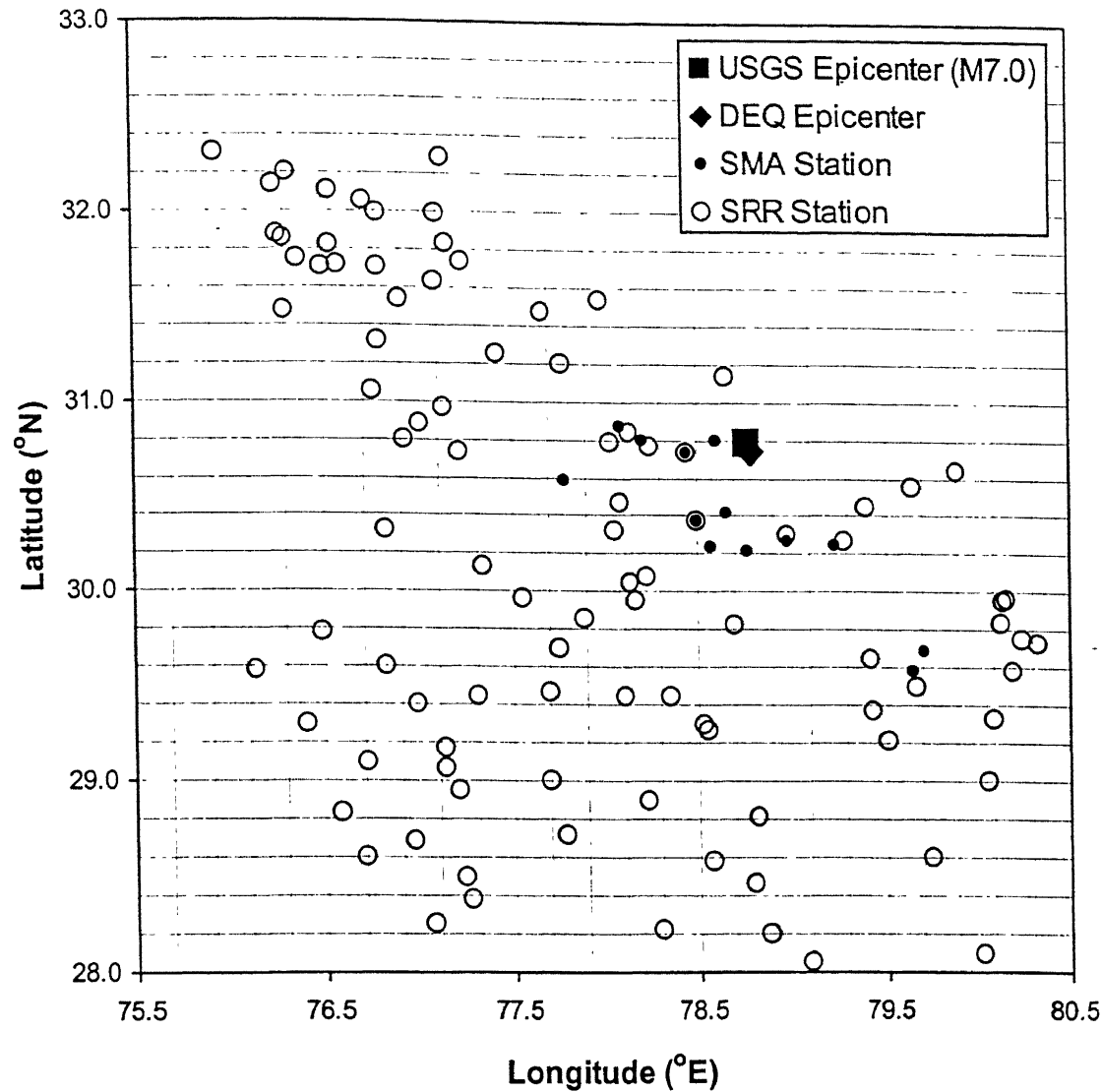


Figure 3.5(g): Location of epicenters as reported by different agencies along with the recording stations activated for the Uttar Pradesh (Uttarkashi) earthquake of 20 October 1991.

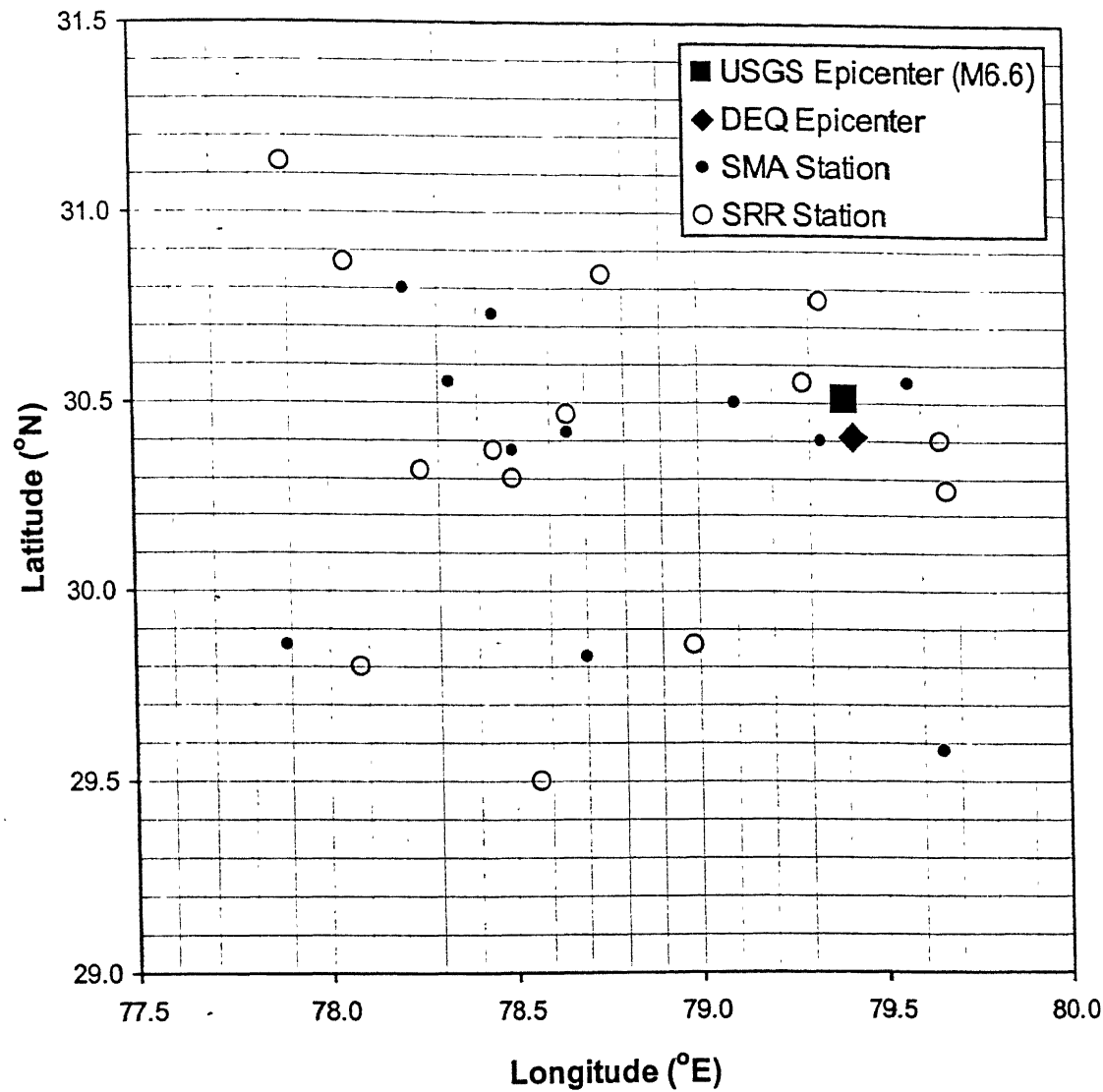
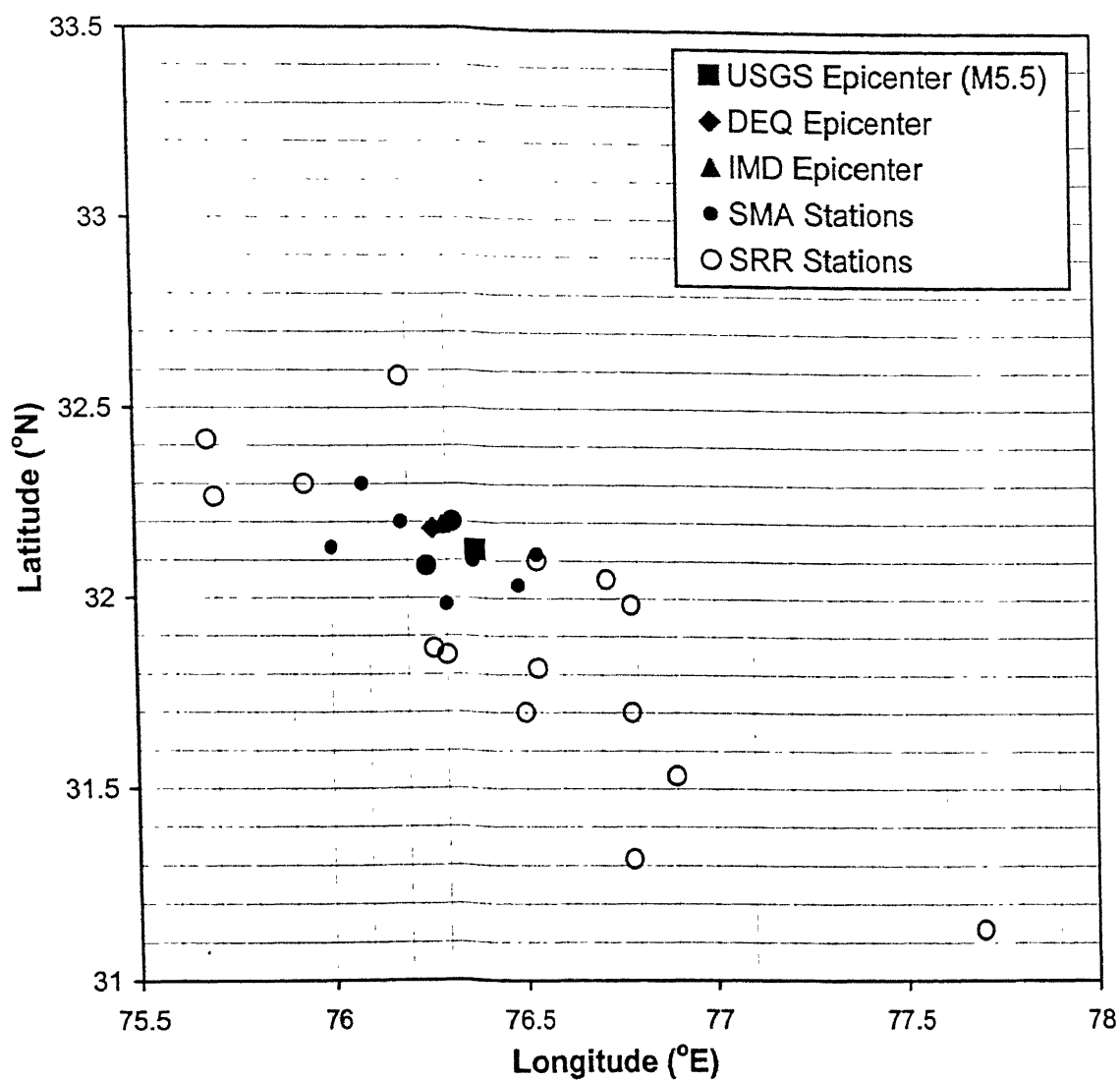


Figure 3.5(h): Location of epicenters as reported by different agencies along with the recording stations activated for the Uttar Pradesh (Chamoli) earthquake of 29 March 1999.



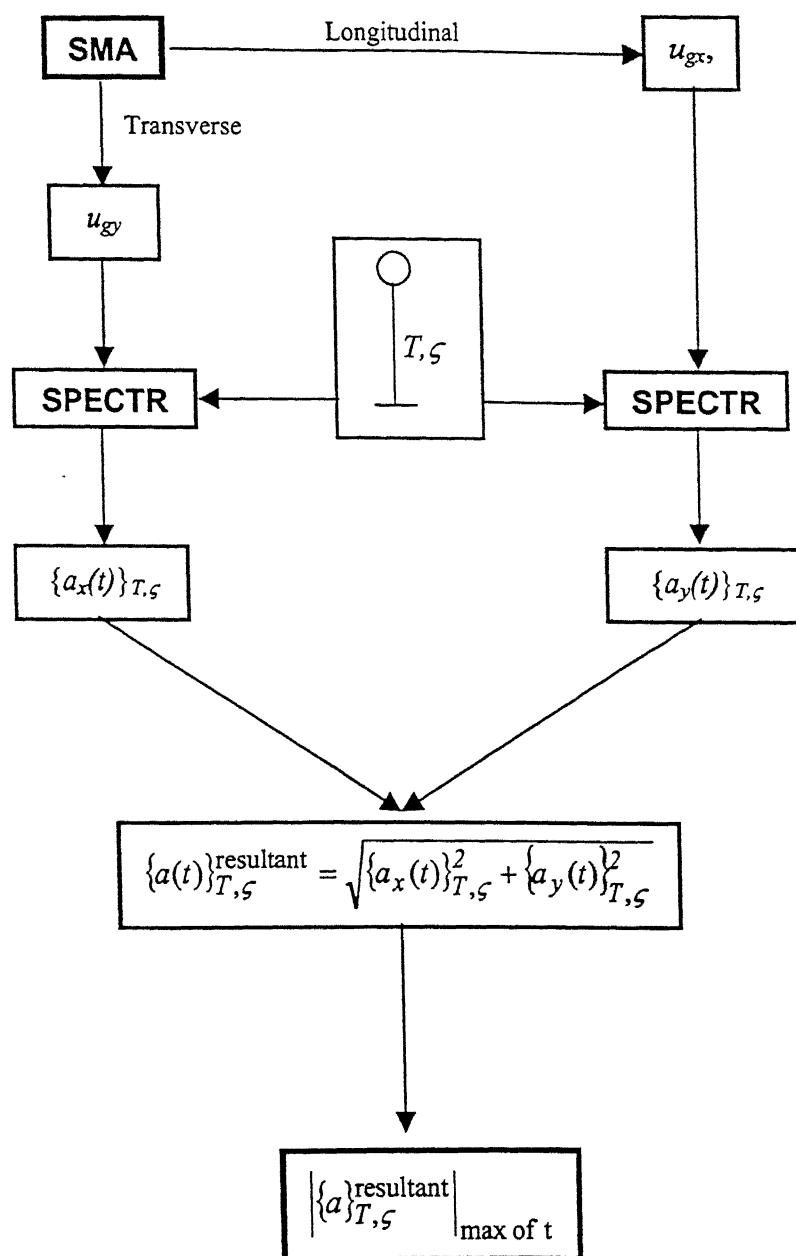
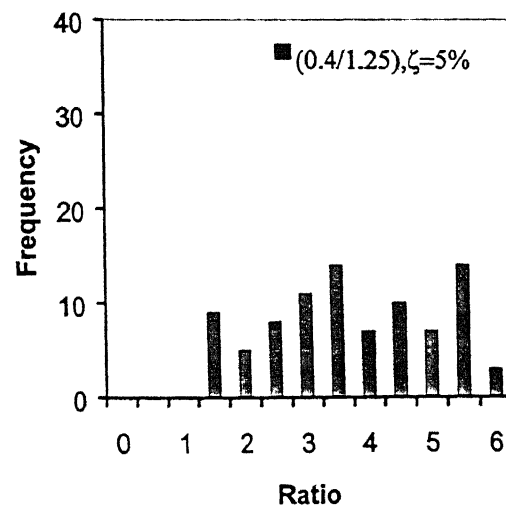
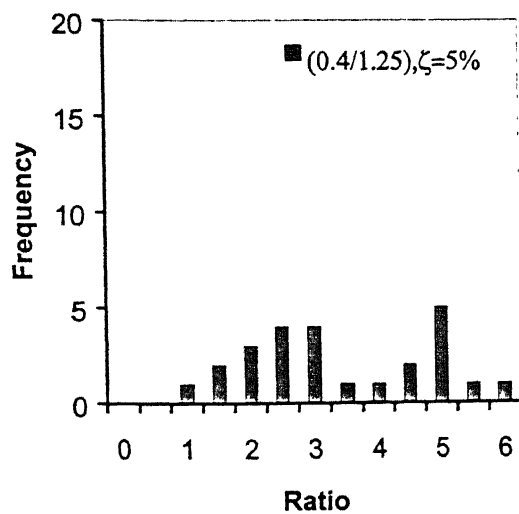
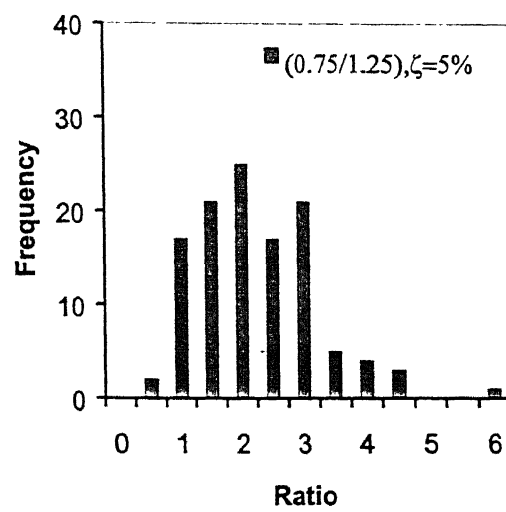
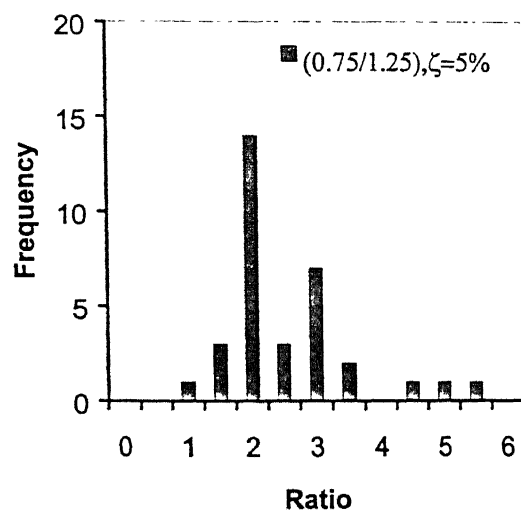
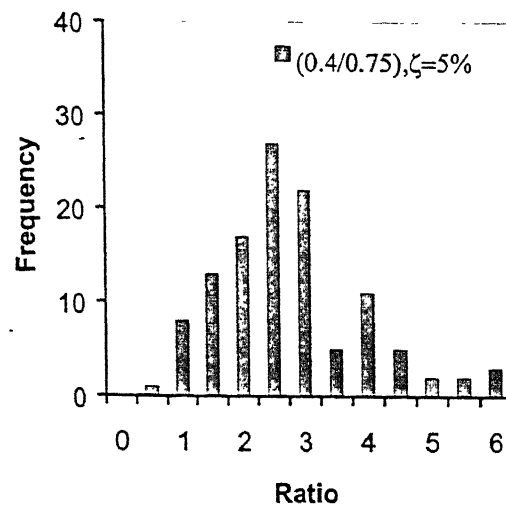
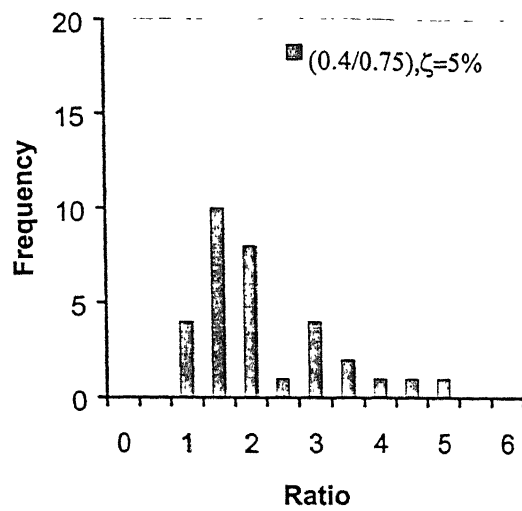


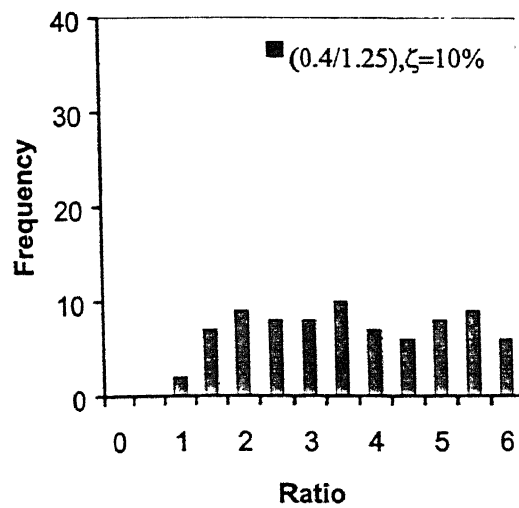
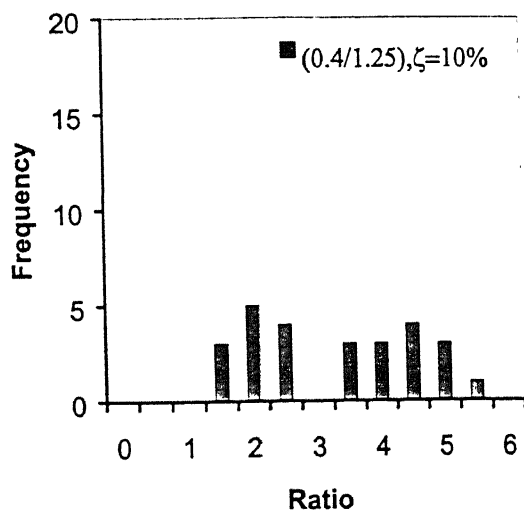
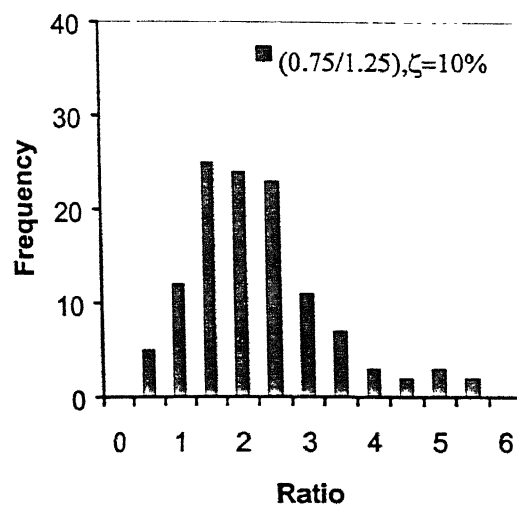
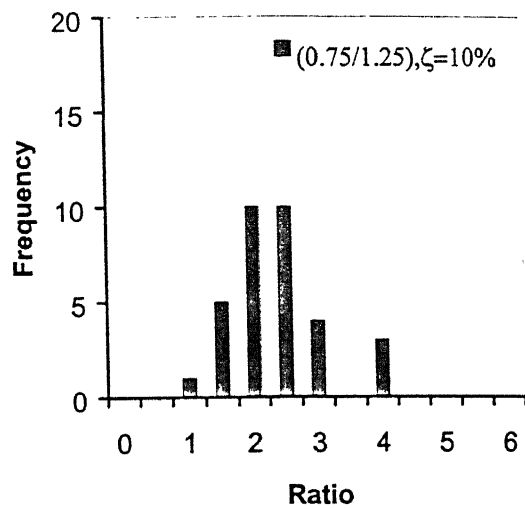
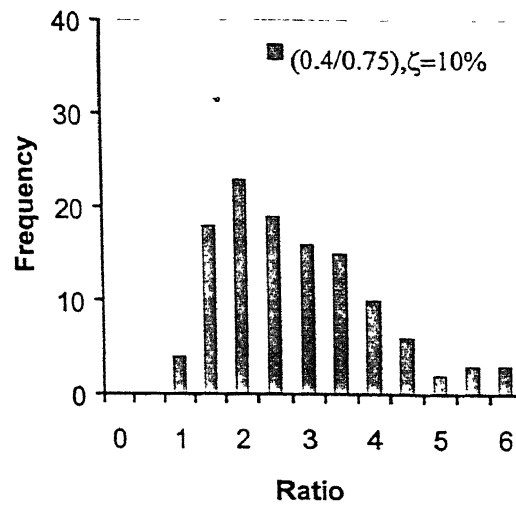
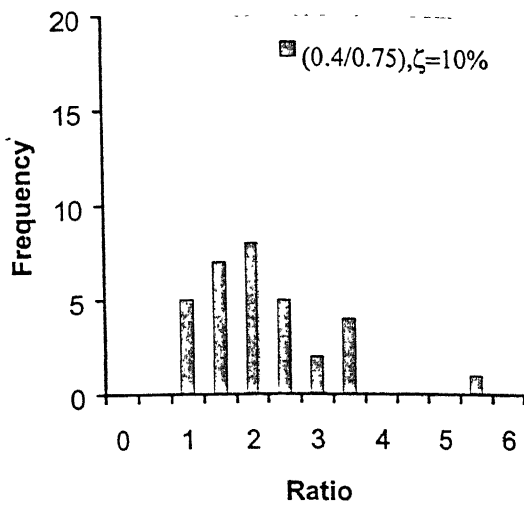
Figure 3.6: Schematic representation for the calculation of the resultant spectral acceleration from the SMA records.



(i) SMA

(ii) SRR

Figure 3.7(a): Distribution of ratios of $SA_{T_1, \zeta=5\%} / SA_{T_2, \zeta=5\%}$ for August 6, 1988 event for SRRs and SMAs.



(i) SMA

(ii) SRR

Figure 3.7(b): Distribution of ratios of $SA_{T_1, \zeta=10\%} / SA_{T_2, \zeta=10\%}$ for August 6, 1988 event for SRRs and SMAs.

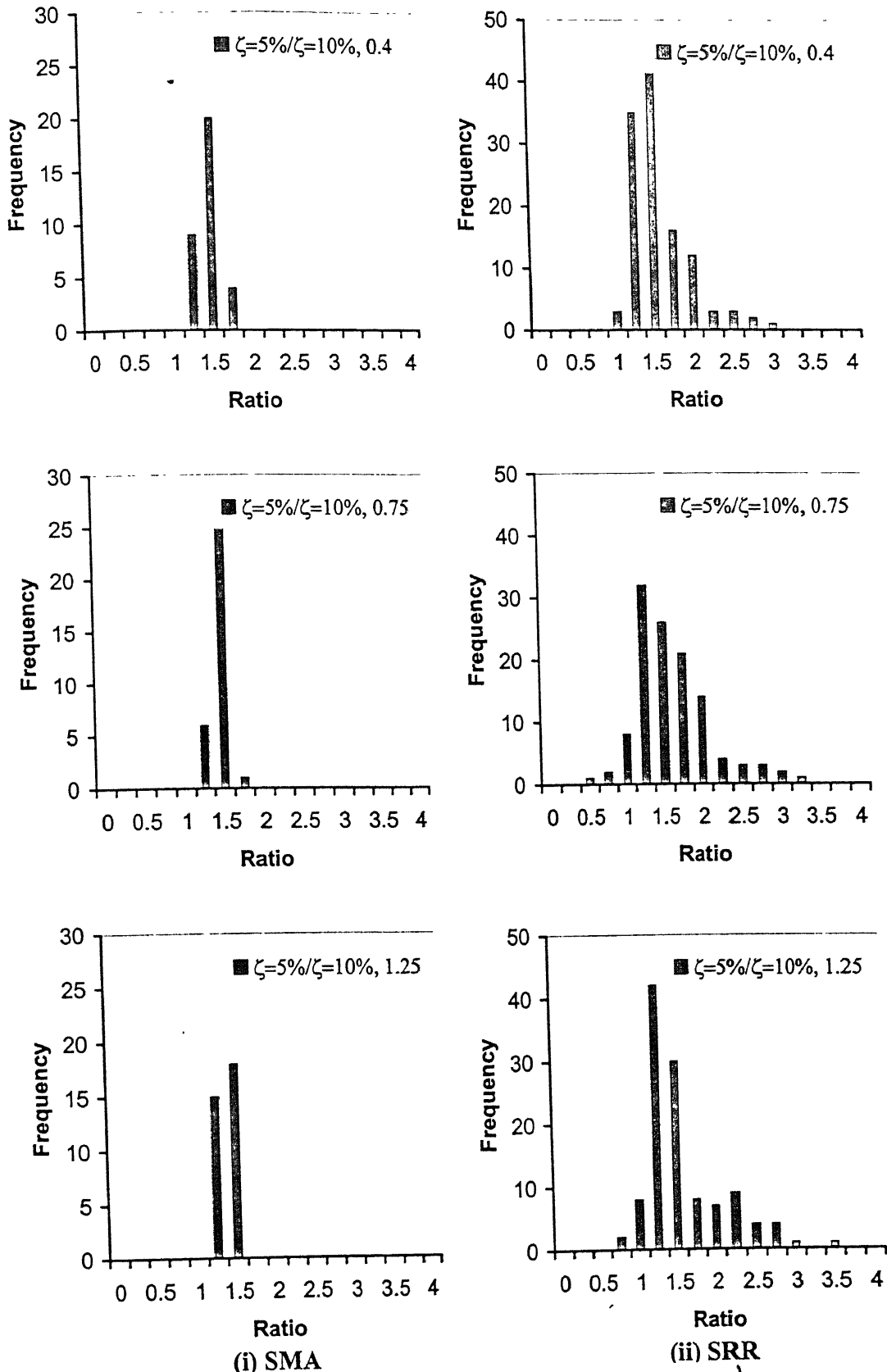


Figure 3.7(c): Distribution of ratios of $(SA_{0.4 \text{ sec}, \zeta=5\%} / SA_{0.4 \text{ sec}, \zeta=10\%})$, $(SA_{0.75 \text{ sec}, \zeta=5\%} / SA_{0.75 \text{ sec}, \zeta=10\%})$ and $(SA_{1.25 \text{ sec}, \zeta=5\%} / SA_{1.25 \text{ sec}, \zeta=10\%})$ for August 6, 1988 event.

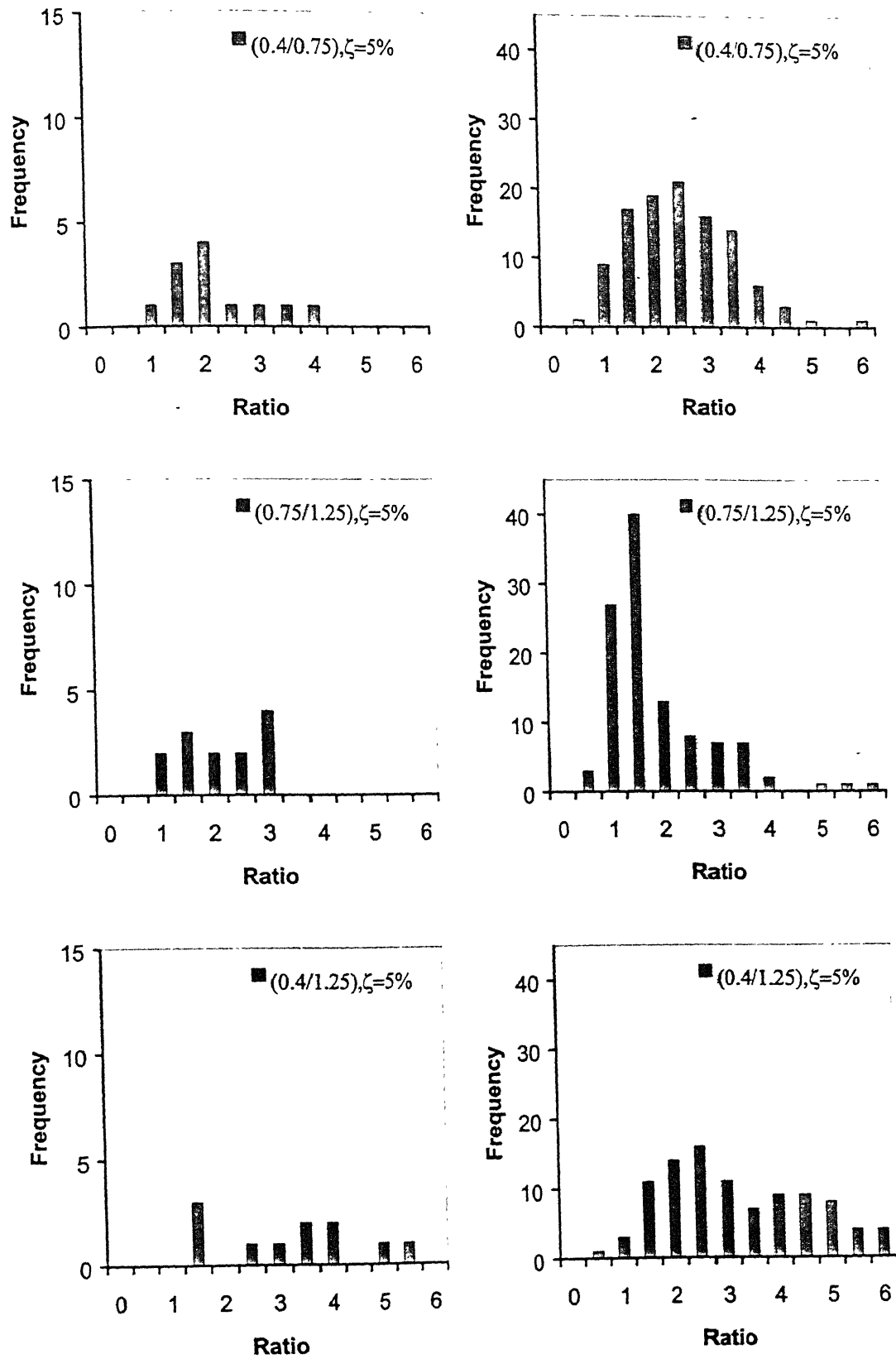


Figure 3.7(d): Distribution of ratios of $SA_{T_1, \zeta=5\%} / SA_{T_2, \zeta=5\%}$ for October 20, 1990 Uttarkashi event for SRRs and SMAs.

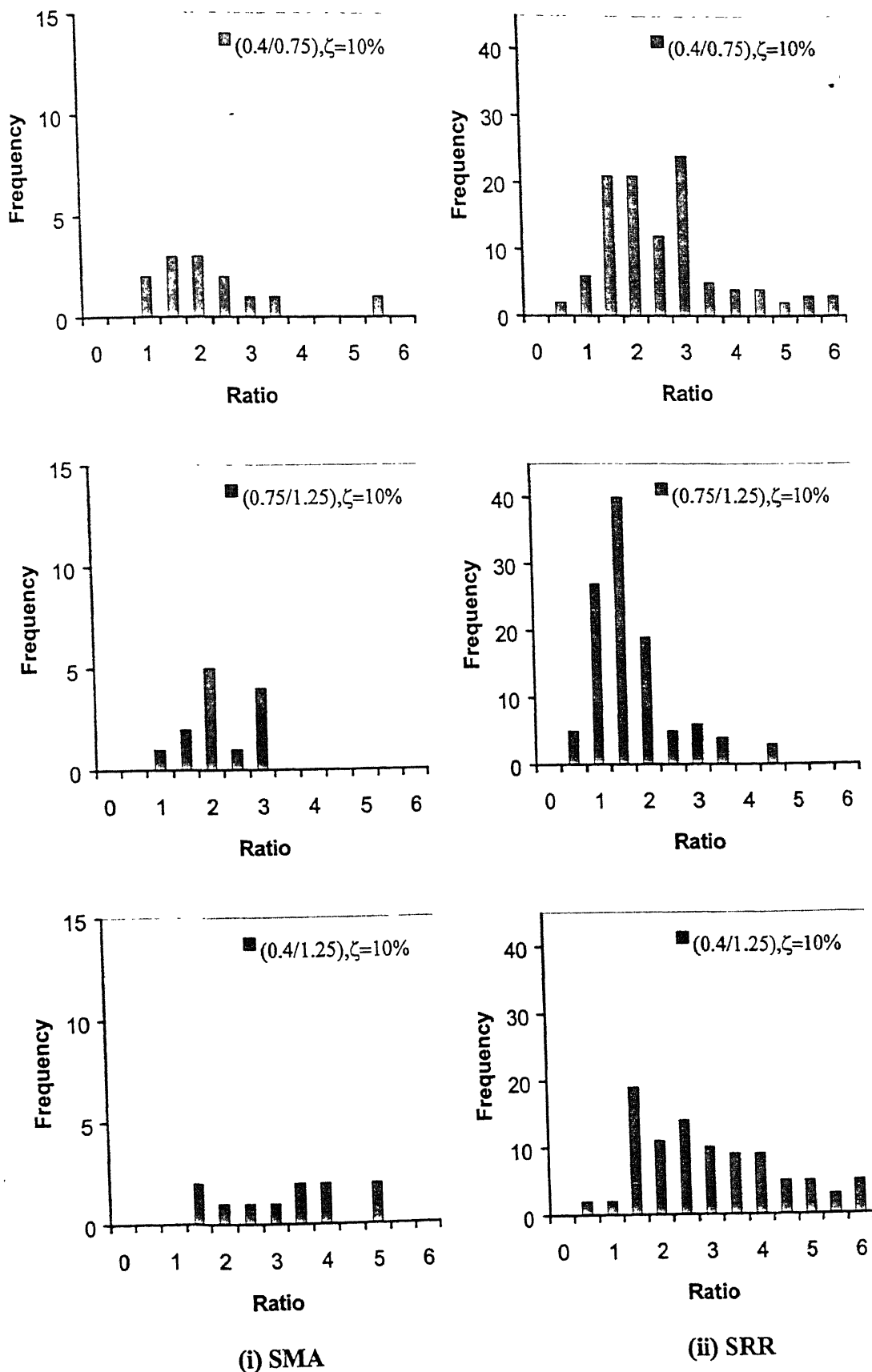


Figure 3.7(e): Distribution of ratios of $SA_{T_1, \zeta=10\%} / SA_{T_2, \zeta=10\%}$ for October 20, 1990 Uttarkashi event for SRRs and SMAs.

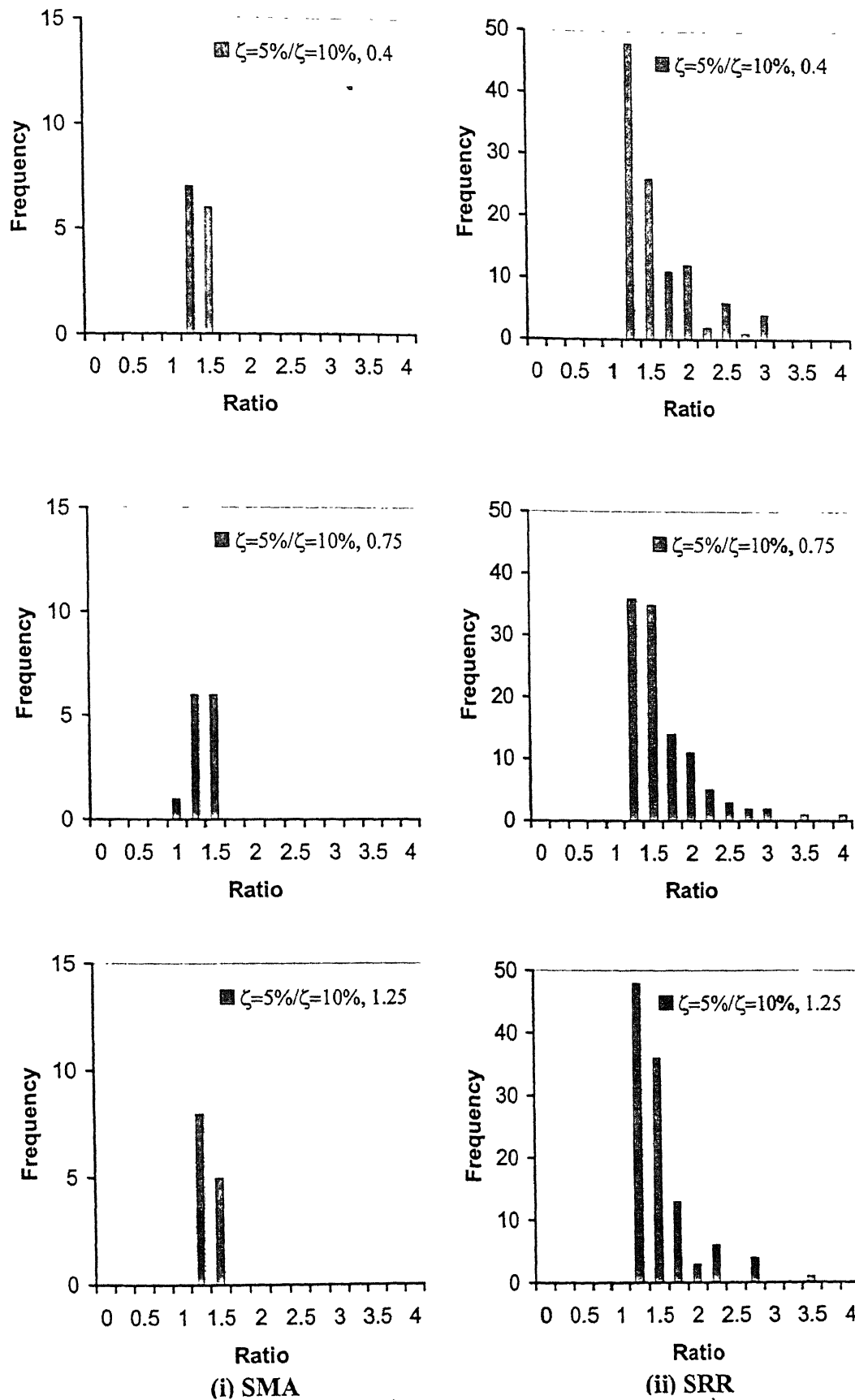
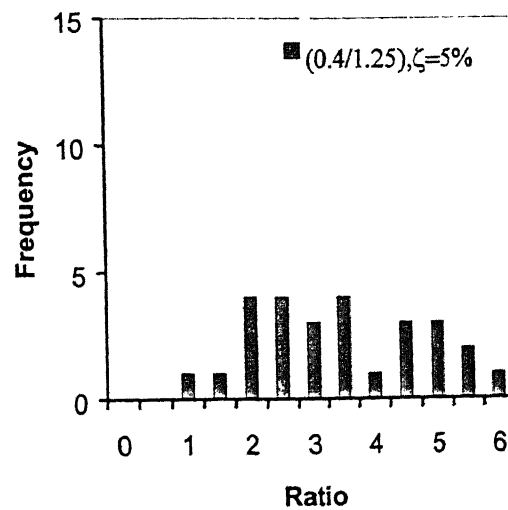
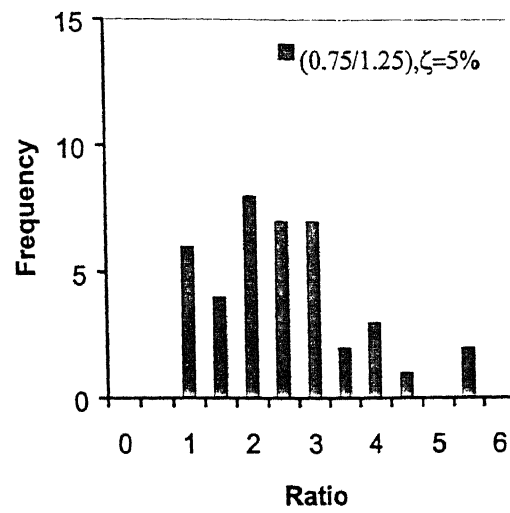
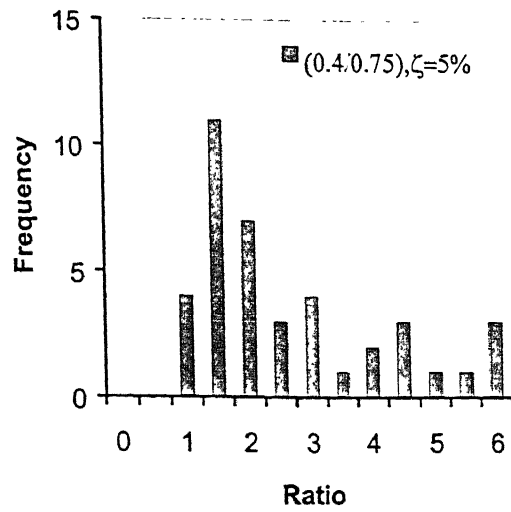
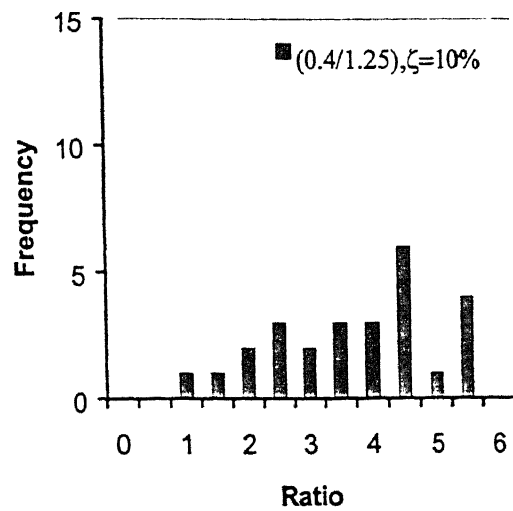
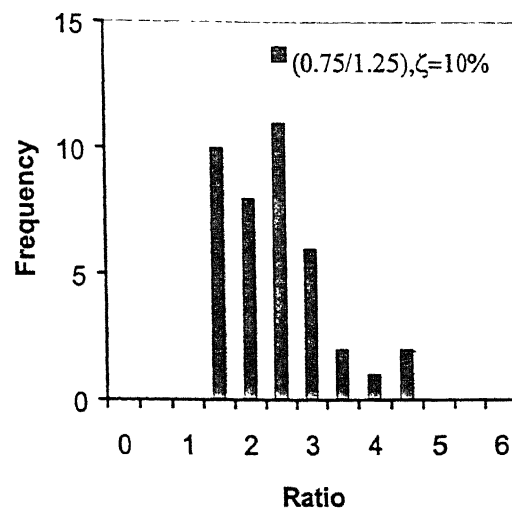
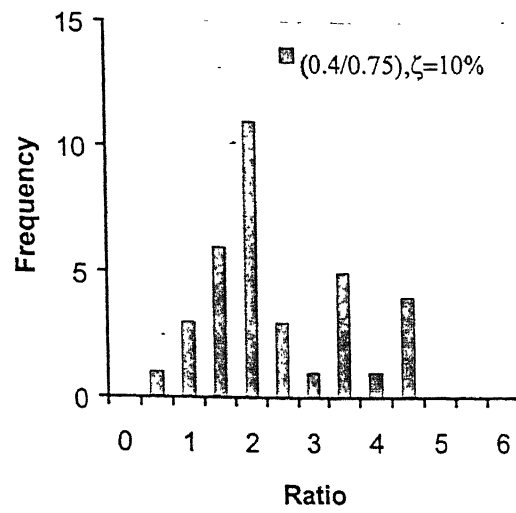


Figure 3.7(f): Distribution of ratios of $(SA_{0.4 \text{ sec}, \zeta=5\%} / SA_{0.4 \text{ sec}, \zeta=10\%})$, $(SA_{0.75 \text{ sec}, \zeta=5\%} / SA_{0.75 \text{ sec}, \zeta=10\%})$ and $(SA_{1.25 \text{ sec}, \zeta=5\%} / SA_{1.25 \text{ sec}, \zeta=10\%})$ for October 20, 1990 Uttarkashi event for SRRs and SMAs.



SRR

Figure 3.7(g): Distribution of ratios of $SA_{T_1, \zeta=5\%}/SA_{T_2, \zeta=5\%}$ for August 21, 1988 Bihar event for SRRs.



SRR

Figure 3.7(h): Distribution of ratios of $SA_{T_1, \zeta=10\%} / SA_{T_2, \zeta=10\%}$ for August 21, 1988 Bihar event for SRRs.

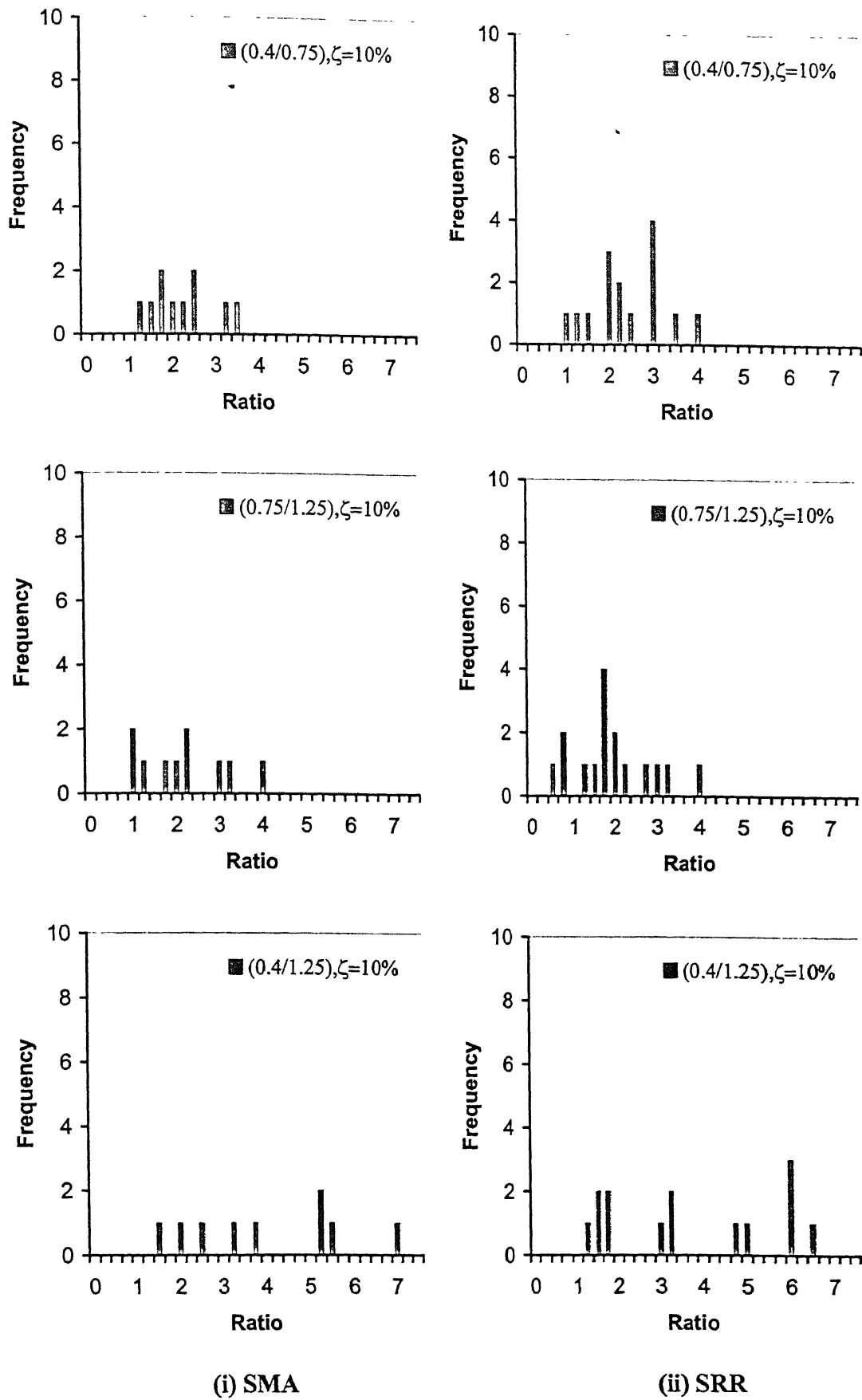


Figure 3.7(j): Distribution of ratios of $SA_{T_1, \zeta=10\%} / SA_{T_2, \zeta=10\%}$ for March 29, 1999 Chamoli event for SRRs and SMAs.

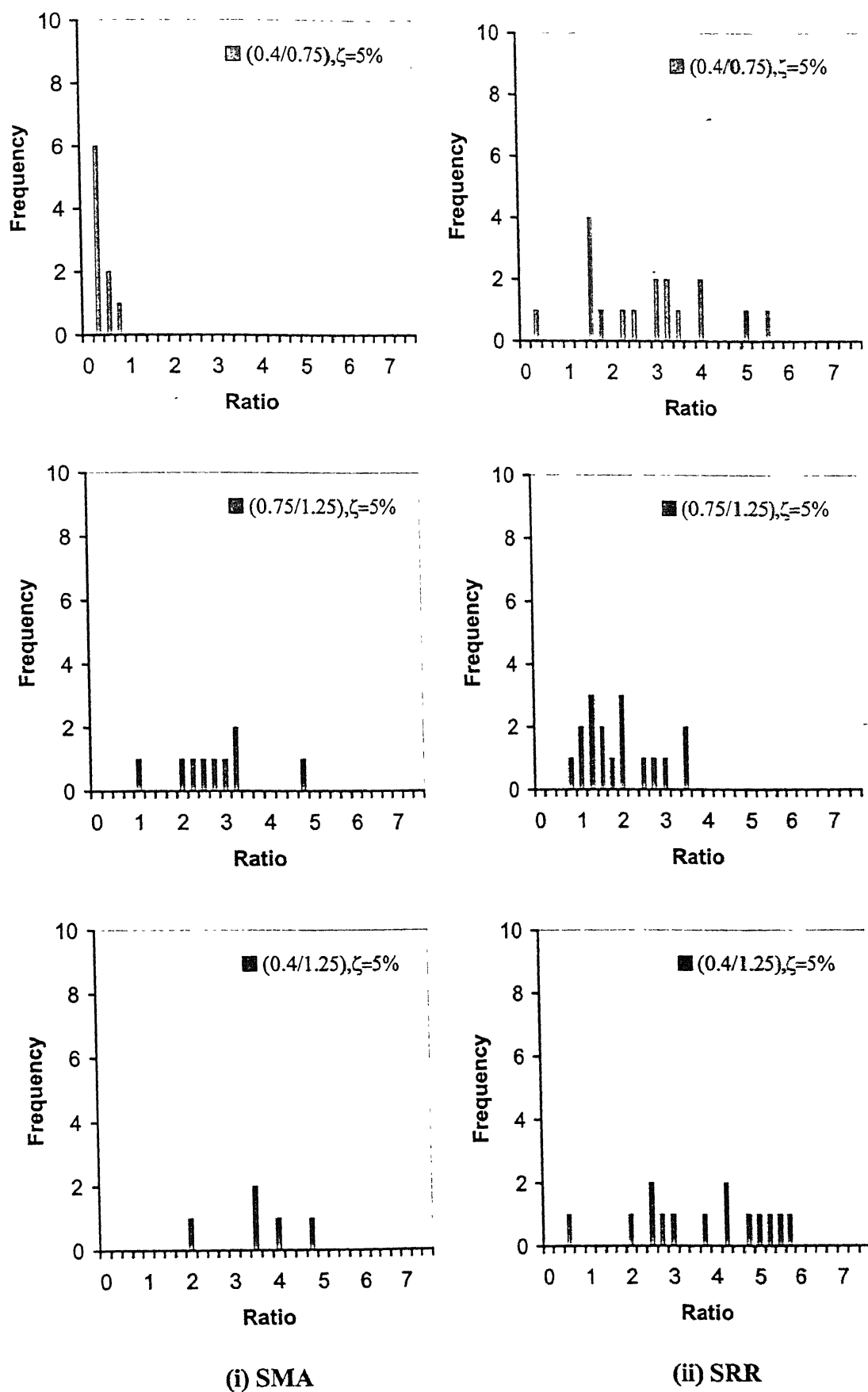


Figure 3.7(k): Distribution of ratios of $SA_{T_1, \zeta=5\%} / SA_{T_2, \zeta=5\%}$ for April 26, 1986 Kangra event for SRRs and SMAs.

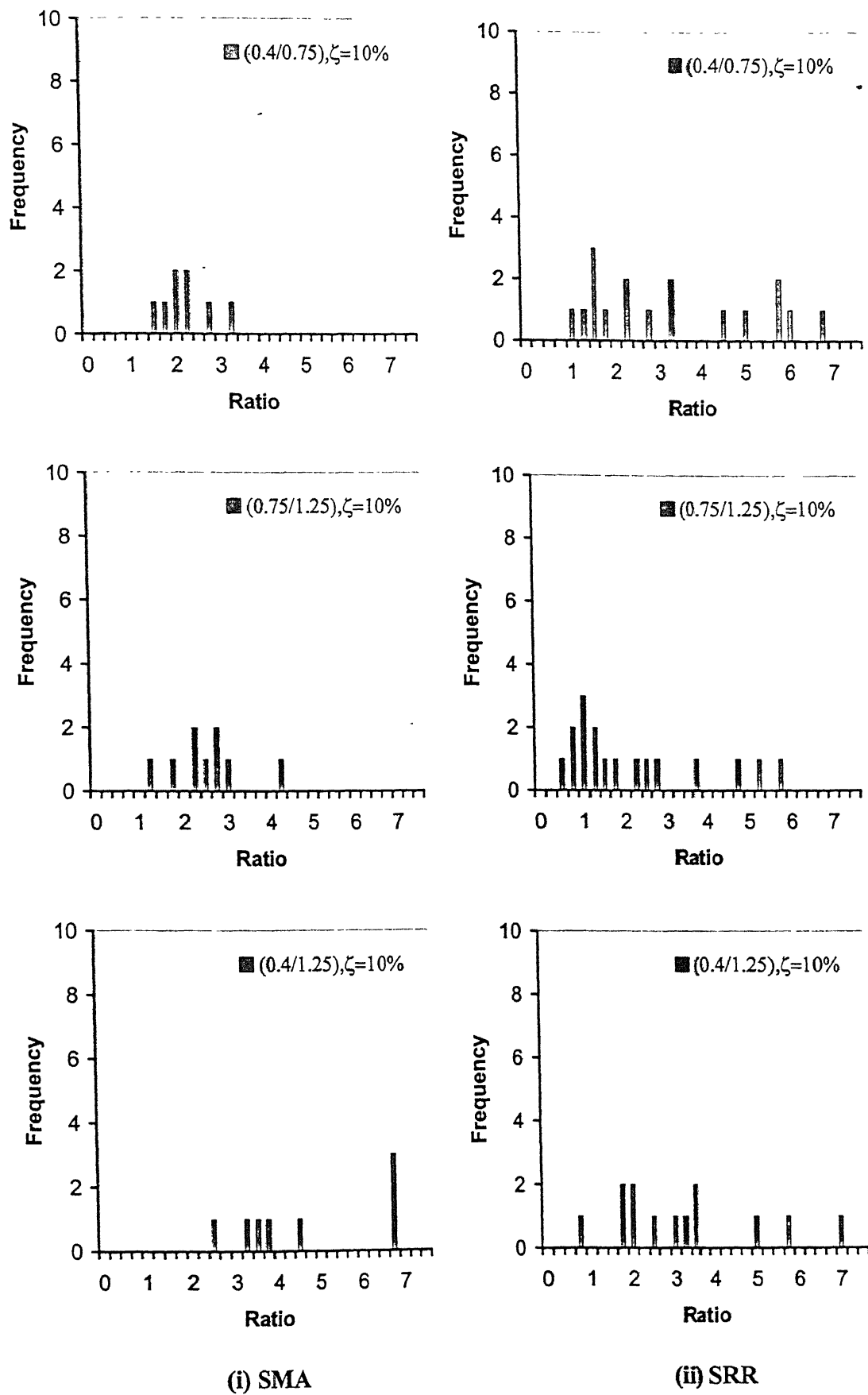
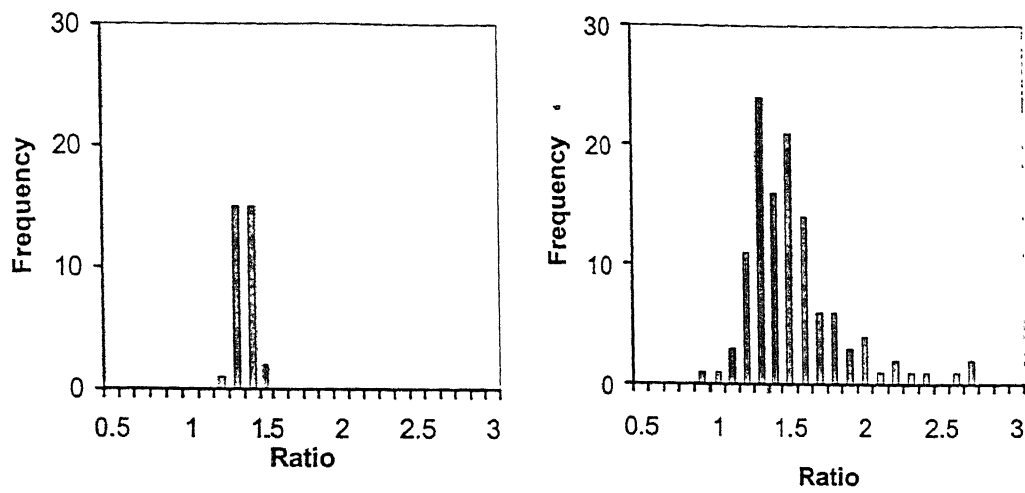
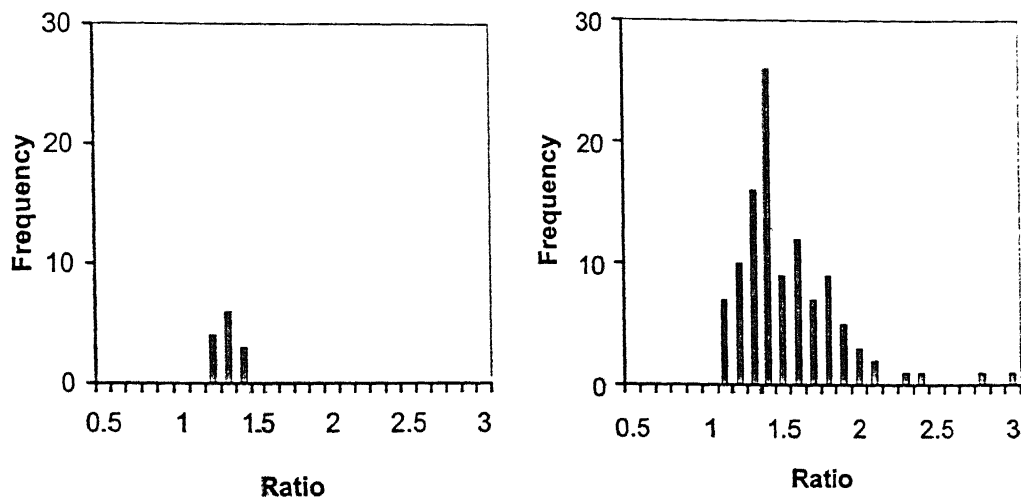


Figure 3.7(l): Distribution of ratios of $SA_{T_1, \zeta=10\%} / SA_{T_2, \zeta=10\%}$ for April 26, 1986 Kangra event for SRRs and SMAs.



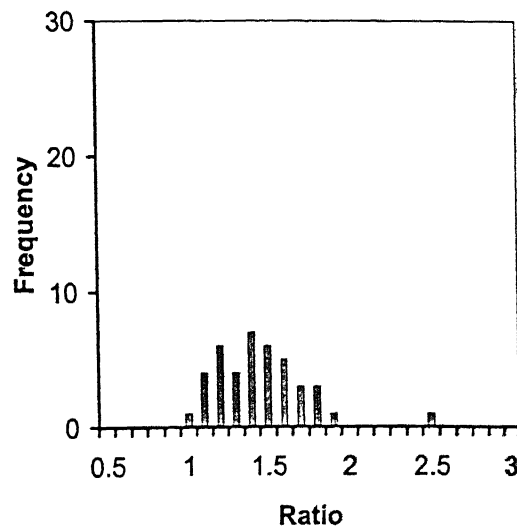
(i) August 6, 1988 NE India earthquake



(a) SMA

(b) SRR

(ii) October 20, 1991 Uttarkashi earthquake



(iii) August 21, 1988 Bihar earthquake, SRR

Figure 3.8: Histograms for average values of $(SA_{0.4 \text{ sec}, \zeta=5\%} / SA_{0.4 \text{ sec}, \zeta=10\%})$, $(SA_{0.75 \text{ sec}, \zeta=5\%} / SA_{0.75 \text{ sec}, \zeta=10\%})$ and $(SA_{1.25 \text{ sec}, \zeta=5\%} / SA_{1.25 \text{ sec}, \zeta=10\%})$.

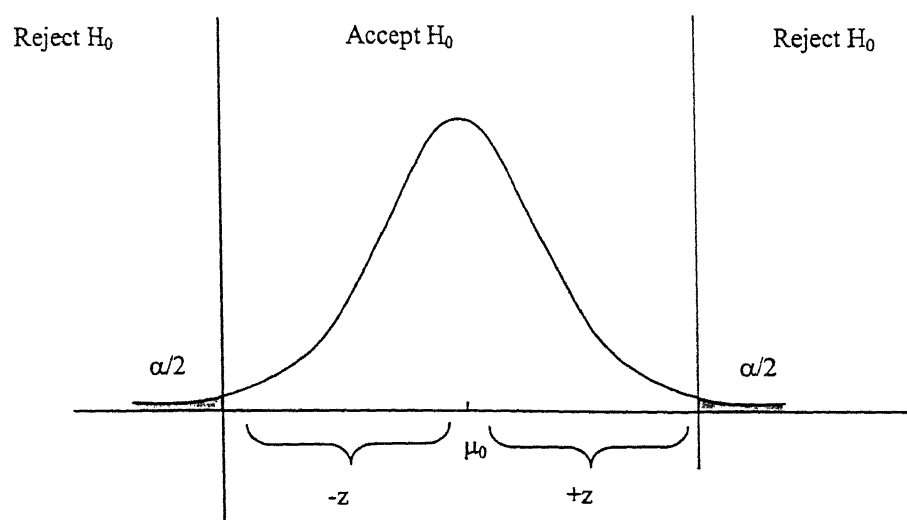


Figure 3.9: Schematic representation for the confidence interval for the null hypothesis, H_0 .

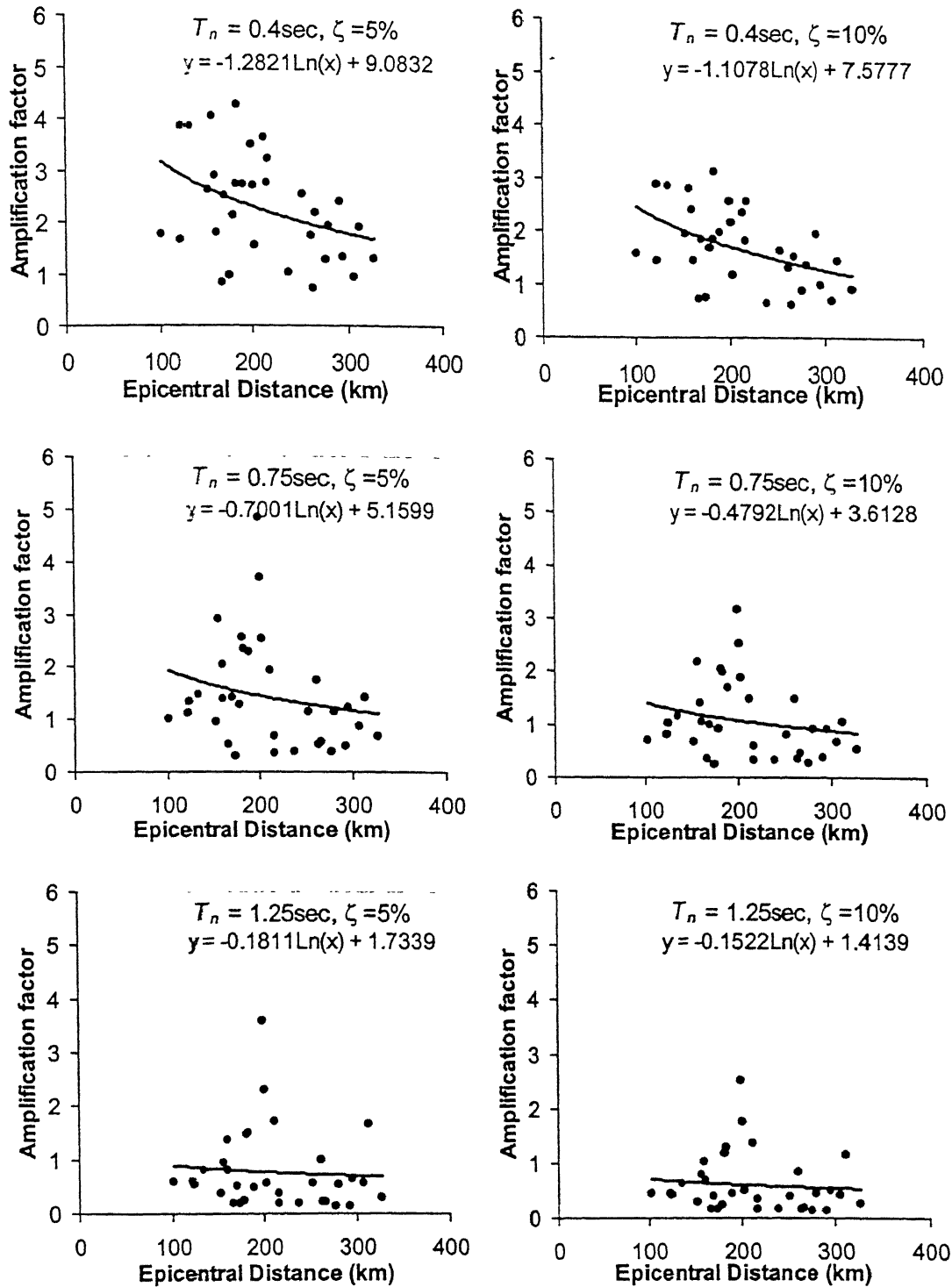


Figure 3.10(a): Amplification factor of the resultant Spectral Acceleration *versus* epicentral distance for the August 6, 1988 Shillong earthquake, best fit line used $y = a \ln x + b$.

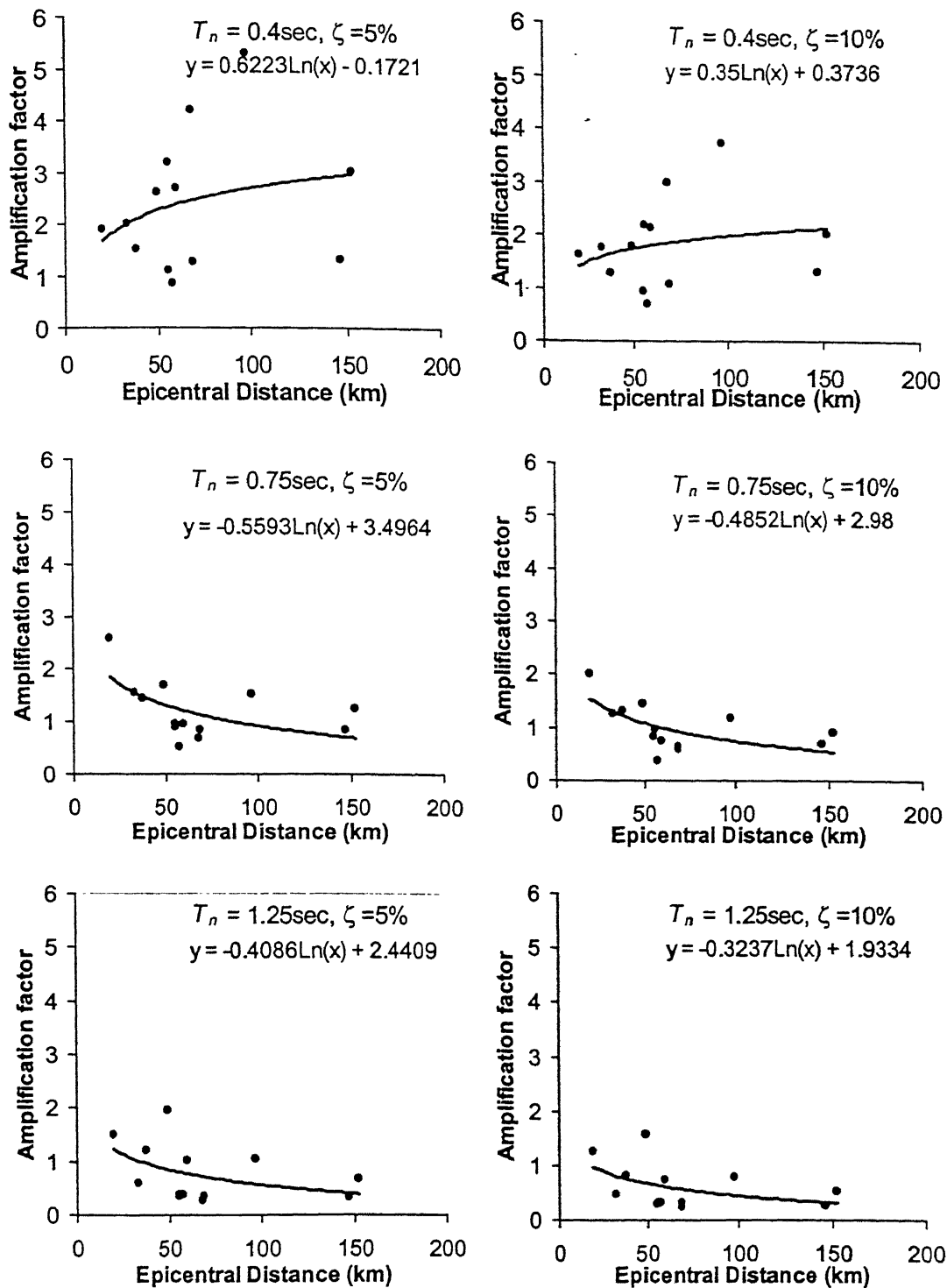


Figure 3.10(b): Amplification factor of the resultant spectral acceleration *versus* epicentral distance for the October, 1991 Uttarkashi earthquake, best fit line used $y = a \ln x + b$.

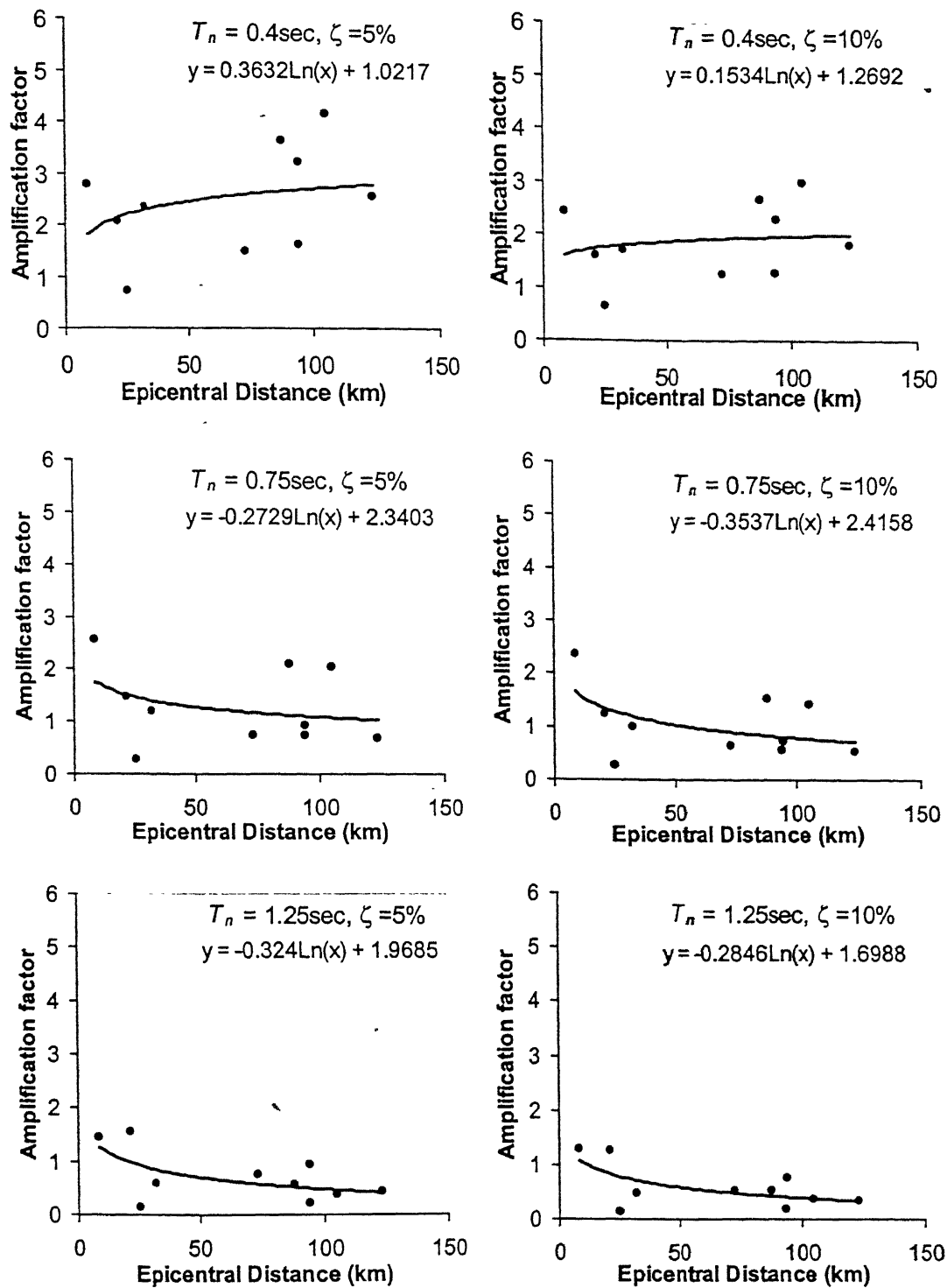


Figure 3.10(c): Amplification factor of the resultant spectral acceleration *versus* epicentral distance for the March, 1999 Chamoli earthquake, best fit line used $y = a \ln x + b$.

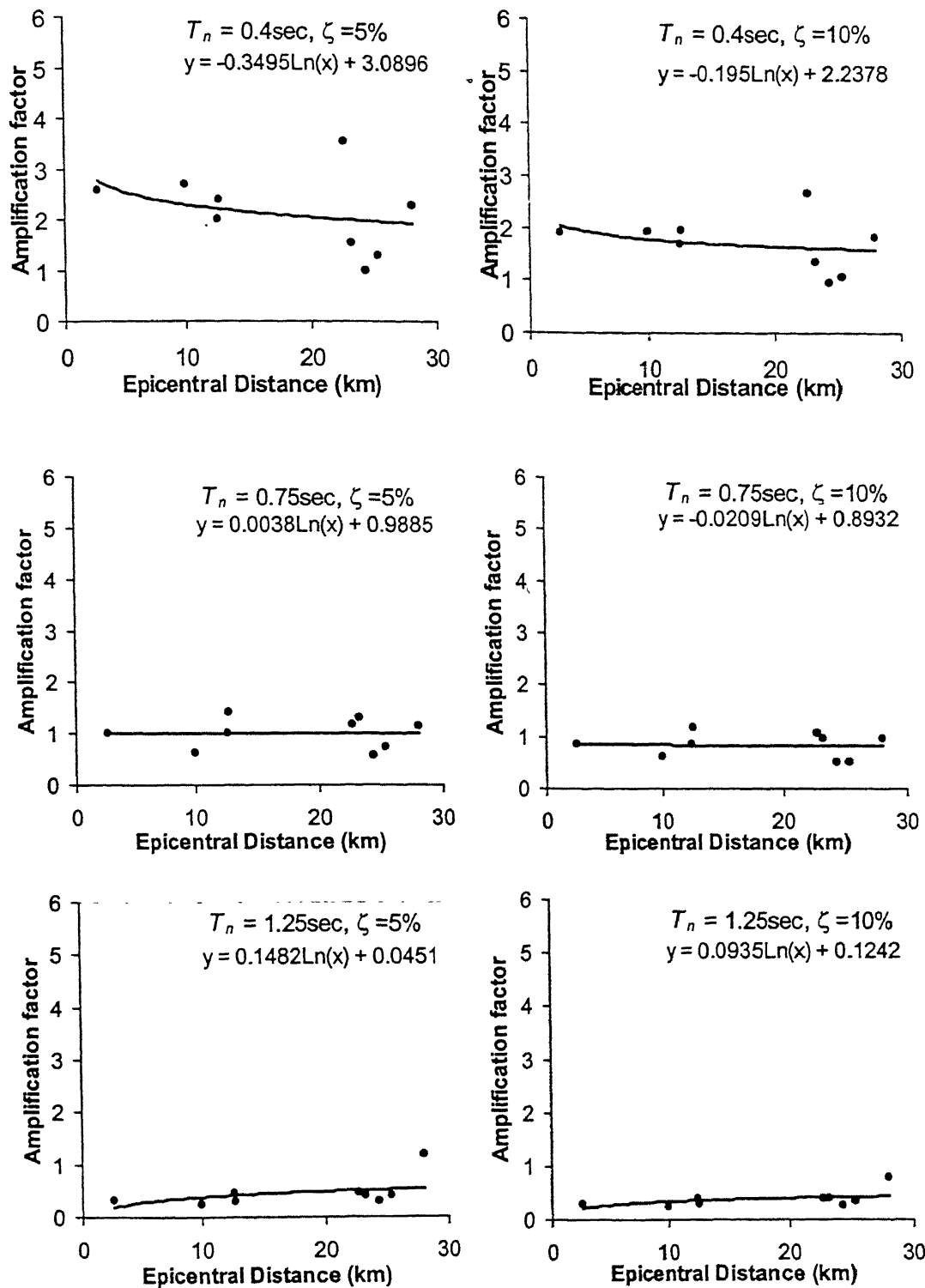
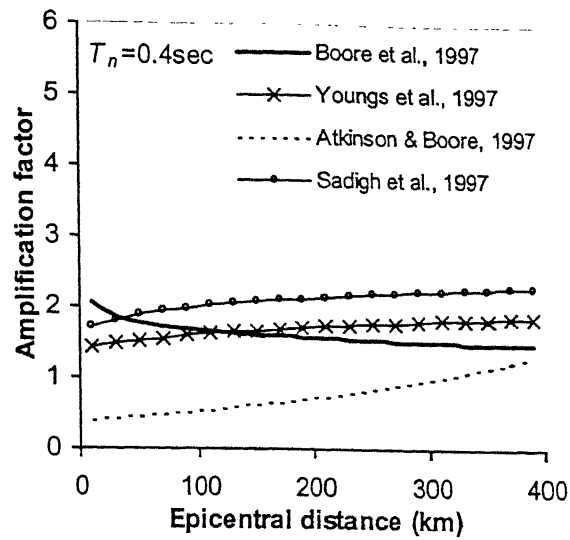
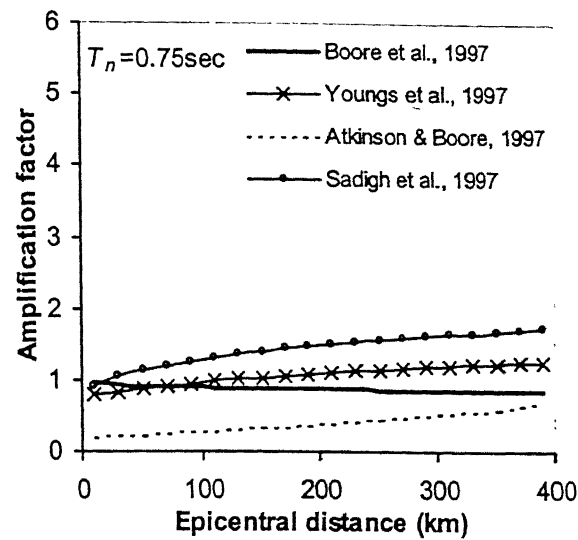


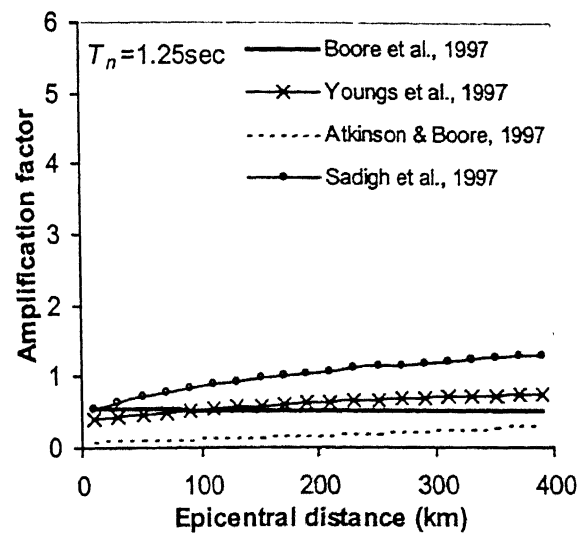
Figure 3.10(d): Amplification factor of the resultant spectral acceleration *versus* epicentral distance for the April, 1986 Kangra earthquake, best fit line used $y = a \ln x + b$.



(a)

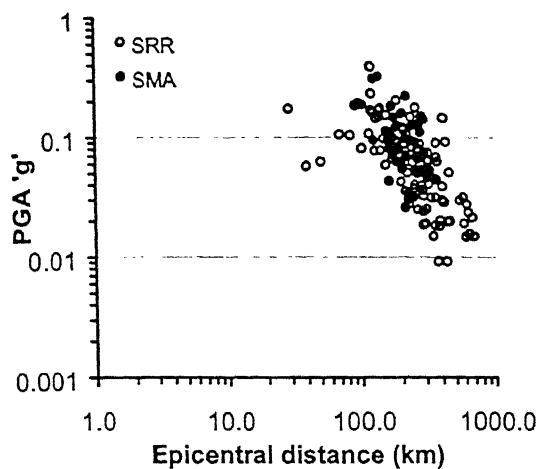


(b)

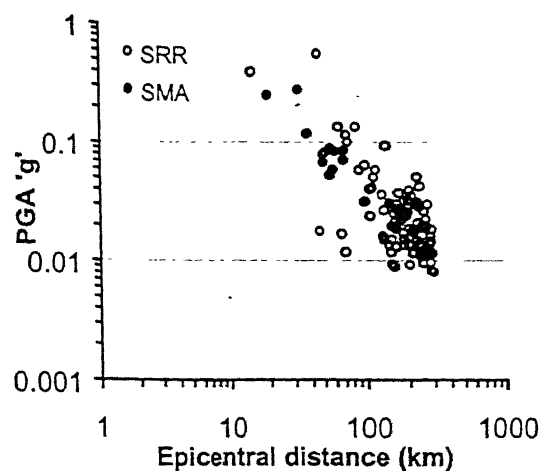


(c)

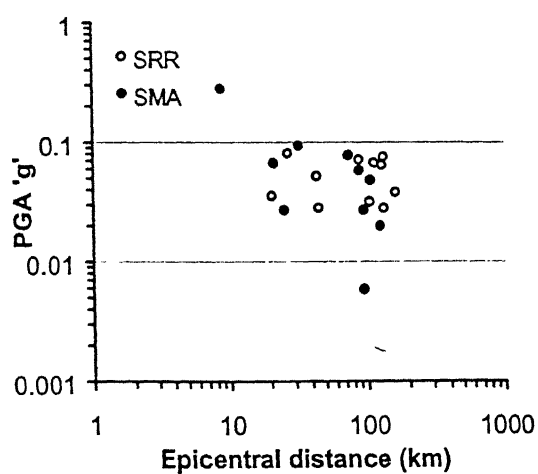
Figure 3.11 : Variation of amplification factors for spectral acceleration from different attenuation relationships available in the literature ($\zeta = 5\%$ of critical).



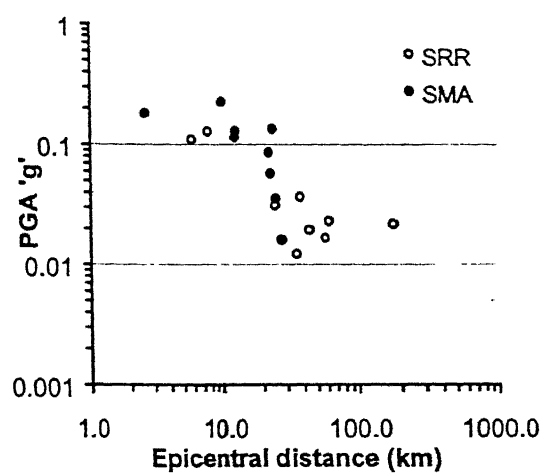
(a) 6 August, 1988



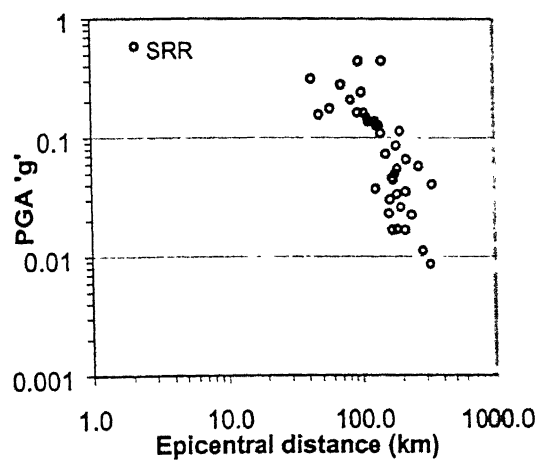
(b) 20 October, 1991



(c) 29, March, 1999 Chamoli



(d) 26 April, 1986 Kangra



(e) 6 August, 1988, Bihar

Figure 3.12 : Peak ground acceleration versus distance for different earthquakes.

Chapter 4

Development of Attenuation Relationships

4.0 Introduction

This chapter studies attenuation of Peak Ground Acceleration (PGA) from nine Himalayan earthquakes using data from strong motion accelerographs (SMAs) as well as structural response recorders (SRRs). The observed PGA values are compared with the existing attenuation relationships available in the literature. Considerable differences are observed in the attenuation characteristics for different tectonic regions. New attenuation relationships have been developed based on Indian ground motion data.

4.1 Indian Strong Motion data Versus Existing Attenuation Relationships

The Seismo-tectonical environment of Himalayan region can be divided into three classes based on geology. They are (1) The northern Himalayas (2) Central Himalayas and (3) North-Eastern Himalayas. Due to the constant thrust between Eurasian and Indian plate (Chandra, 1992), the rocks in the northern Himalayas are in a fractured state. Gangetic foredeep in Central Himalayas is characterized by the presence of a deep alluvial plane. In North-Eastern Himalayas, the base rocks are considered to more homogenous compared to that in northern Himalayas. Presence of a subduction process has also been reported along the Burmese arc in this region. So, the earthquakes included in the study can be divided in to three categories based on geology of region of recording. (1) Earthquakes of northern Himalayas (1991 Uttarkashi $M7.0$, 1999 Chamoli $M6.6$, and 1986 Dharmshala $M5.5$), (2) Earthquakes of Gangetic foredeep (1988 Bihar-Nepal $M6.8$), and (3) Earthquakes of North-East Himalayas (1986 NE $M5.2$, 1987 NE $M5.9$, 1988 NE $M5.8$, 1988 NE $M7.3$, 1990 NE $M6.1$). Two events in the NE Himalayan earthquakes have their predicted epicenters near the Burmese arc. Accelerations

observed during the earthquakes are compared with the existing attenuation relationships to assess the suitability of their application in Indian region.

The attenuation relationships used for comparison can be divided into three categories based on their origin. They are:

- (a) Relationships based on data from interplate earthquakes (Boore, 1997, Campbell, 1997 and Sadigh *et al.*, 1997)
- (b) Relationships based on data from subduction zone earthquakes (Young *et al.*, 1997 and Crouse, 1991)
- (c) Attenuation relationships based on data from intraplate earthquakes (Anders *et al.*, 1990; Toro *et al.*, 1997). The intraplate earthquakes exhibit lesser rate of attenuation compared to most of the attenuation relationships which are mostly developed based on the data from western America, where the base rocks exist in a highly fractured state.

Since different relationships require different types of parameters as input, the following assumptions were made for the parameters used in them for Indian earthquakes.

(1). The site conditions are assumed rocky (Shear wave velocity = 620m/s) for all events except for Bihar-Nepal event. Since the Bihar-Nepal earthquake originated in the Gangetic alluvium (Shear wave velocity = 310 m/s) propagation medium was soil.

(2) The information about the source mechanism of the most of the Indian earthquakes are not available. Hence, the source mechanism was assumed be reverse thrust faulting, for all events expect for the 1988 Bihar-Nepal $M6.8$ earthquake. It was observed that assumption of source mechanism as reverse fault predicted highest accelerations compared to all other mechanisms. The 1988 Bihar-Nepal $M6.8$ earthquake occurred in deep alluvium and fault mechanism identified was of strike-slip nature.

(3) Since the information about length and direction of fault was not available, the closest distance to surface projection of fault was assumed equal to epicentral distance.

(5) The closest distance to plane of rupture was assumed to be equal to hypocentral distance.

(6) Youngs *et al.*, (1997) have used the geometric mean of PGA as the predicted parameter. The maximum value of two horizontal components of PGA was used by Anders *et al.*, (1990) as the output parameter. But, these relationships have not provided any comparison of these parameters with respect to the average PGA, which is the parameter used in this study. So wherever these equations were used for predicting the PGA, the result was used without any modification.

The observed data points from different events in the Himalayan region and the predicted acceleration are shown in Figures 4.1 to 4.3. For ease of comparison the plots have been made based on their origin. The least square fit of each earthquake is also plotted to compare the deviation of the predicted data from the ideal relationship. Based on the plots, the following general observation can be made:

1. Interplate relationships give a better representation of the observed data for earthquakes in north & North-Eastern Himalayas compared to intra plate relationships.
 2. The accelerations predicted by the interplate relationships of Campbell, (1997) and Sadigh *et al.*, (1997) underestimate the accelerations observed from the earthquakes in the North-Eastern Himalaya. The difference in predictions is maximum for the earthquakes generated from Burmese arc. Of all the relationships used for comparison, Boore (1997) seems to give a better representation of the data.
-

3. Two North East events namely 1988 NE $M7.3$ and 1990 NE $M6.1$, whose epicenters were situated along the Burmese border, generated a much higher acceleration compared to the other events reordered in the region. For these events (1988 NE $M7.3$ and 1990 NE $M6.1$), the predictions by Youngs *et al.*, (1997) are found to be closer to the observed values compared to the relationship developed by Crouse, (1991). For $M7.3$ event, the rate of attenuation of PGA is found to be less than that predicted by these relationships.
4. For North India Earthquakes namely 1986 Dharmshala $M5.5$, 1991 Uttarkashi $M7.1$ and 1999 Chamoli $M6.6$, the existing interplate relationships are able to predict the accelerations without much error. But the optimum relationships are found to be different ones for each event. For Chamoli and Kangra events, the intraplate relationships predicted much higher accelerations compared to the observed values.
5. The rate of attenuation predicted by the intraplate relationships is in line with the attenuation observed in 1988 Bihar-Nepal $M6.8$ earthquake. The rate of attenuation of PGA for 1988 Bihar-Nepal $M6.8$ appears to be very rapid. An extrapolation of the observed acceleration indicates that the peak ground acceleration may have exceeded $1g$ near the source of the earthquake.
6. The North-East event with magnitude 6.1 has produced very high accelerations and all the relationships under-predict the accelerations.

The deviation of the points from the observed data was calculated by averaging the squares of their individual deviations from the observed values in logarithmic scale. The square root of the average can be used as a measure of average distance from the predicted curve and the observed data, *i.e.*,

$$Error = \sqrt{\frac{\sum_{i=1}^n (\ln(y_{observed}) - \ln(y_{predicted}))^2}{n}} \quad (4.1)$$

The results are given in Table 4.1. Most of the deviations observed in the data are greater than the standard deviation of the models considered. For the 1987 NE $M5.2$ 1988 NE and $M5.9$ events, the calculated deviation from the prediction was found to be close to the standard deviation predicted by the attenuation relationship of Boore *et al.* (1997). For all other events, the sample points were generally found to lie more than $\pm 1\sigma$ away from the predicted points. The relationship developed by Sadigh *et al.* (1997) and Campbell, (1997) gives a very high average error of prediction when compared with all the observed events. Thus, the earthquakes under consideration cannot be assumed to come from the same parent population as that used for the development of the various attenuation relationships.

The comparison of the Indian strong motion data with some of the existing attenuation relationships shows that in many cases the existing attenuation relationships have failed to represent the observed PGAs and a new attenuation relationship has to be generated for this region. The new attenuation relationship, which will be based on the enlarged database generated through the current work, can be used for prediction of the acceleration for future Himalayan earthquakes.

4.2 Development of Attenuation Model

4.2.1 Selection of Parameters

The parameter, which is being predicted, is known as dependent variable and the parameters used for the prediction are called independent variables. In the present study, average PGA is taken as the dependant variable.

4.2.1.1 Earthquake Parameters

Seismic moment is one of the ideal parameter, which can be used to represent the earthquake size. Because of the lack of information on the seismic moment of the earthquakes under consideration, earthquake magnitudes m_b and M_s are used in the

present study for characterizing the size of an earthquake. Magnitudes used in the analysis can be considered to be equivalent to moment magnitude because, below $m_b \sim 6.0$, m_b is considered to be equal to M_w and above $m_b \sim 6.0$, M_S is considered to be equal to the moment magnitude.

4.2.1.2 Source Parameters

In the present study, all the events occurred near the plate boundary and are interplate earthquakes. Since the fault mechanism of all the events are not well defined, the style of faulting is not included as a variable in the study.

4.2.1.3 Propagation Parameters

The propagation parameters characterize the effects due to wave scattering, inelastic attenuation and geometric attenuation of acceleration. Since the type and length of faulting, amount of slip etc. are not available, the distance measurements such as distance to horizontal projection of fault rupture, closest distance to rupture, distance to zone of maximum energy release etc. could not be used as the propagation parameter. In this analysis epicentral distance is used to represent the propagation parameter.

4.2.1.4 Site Parameters

Other than the broad classification on the local site conditions [Chandrasekaran and Das, 1994], no detailed information is available about the local site geology. Due to the lack of this information, all the events considered in this study, except the earthquake in Gangetic alluvium (1988 Bihar-Nepal $M6.8$), are assumed to be recorded on rocky strata since it is the general characteristic of the region.

4.2.1.5 Data Selection

The error in the predicted values of a parameter depends on the type of data that is used in the regression analysis. The scatter in the data to be analyzed is minimal if the recordings are taken from a tectonic region of similar attenuation-source features,

consistent record processing techniques are employed and recording instruments of similar dynamic characteristics [Campbell, 1985] are used. The database was assumed to be a homogenous one and no initial segregation of the data is done.

A plot of the epicentral distance vs. magnitude of the event was made for all the observations (Figure 4.4). It was found that a Magnitude of the earthquake and the distance to the farthest station follows a particular relationship i.e., there is a cutoff distance associated with each magnitude. For the data set used in the study, the cut-off line can be approximately denoted by $M = 4.8 + 0.0038R$, where R is the epicentral distance.

4.2.2 Selection of Attenuation Model

After deciding the data set as well as the group of independent variables that will be used in the analysis, it is necessary to select a proper attenuation model for the data. If the model is to be used for prediction using a data, which lies inside the range of parameters used for regression analysis, then a simple attenuation model can be used. In order to extrapolate the data from the observed ones, the model should have a physical basis during formulation [Campbell, 1985].

The amplitude of motion of a harmonic wave in an infinite elastic half space is given by [Dahle et al., 1990]

$$A = \frac{A_0}{R^b} e^{am+qR}, \quad (4.2)$$

where A is the observed ground motion amplitude, R is the hypocentral distance, m is the magnitude and A_0 , a , b and q are constants. The linearisation of Eq. (4.1) leads to

$$\ln A = \ln A_0 + am - b \ln R + qR. \quad (4.3)$$

Considering this as the basic form of attenuation, more variables can be added to represent the dependence between magnitude and distance, site parameters etc. So, the

attenuation relationship that can be used in a region can be of the form [Campbell, 1985]

$$Y = b_1 \cdot f_1(m) f_2(R) f_3(m, R) f_4 P, \quad (4.4)$$

where Y is the strong motion parameter predicted; $f_1(m)$ usually takes the form $f_1(m) = e^{b_2 m}$. This is based on the definition of magnitude as a logarithmic variation of amplitude [Richter, 1956]. Sometimes the quadratic form of magnitude is also used [Toro *et al.*, 1997; Spudich *et al.*, 1997], where the expression takes the form

$$f_1(m) = c_1(m - k) + c_2(m - k)^2 \quad (4.5)$$

where k is a constant. During analysis, k is selected in such a way that it gives the minimum squared error. A cubic term of magnitude has also been used, which is as follows [Joyner and Boore, 1991],

$$f_1(m) = c_1(m - k) + c_2(m - k)^2 + c_3(m - k)^3. \quad (4.6)$$

A third order equation was used instead of linear or second order equation, after it was found that the use of cubic term resulted in a better fit. The commonly used form of distance related term $f_2(R)$ is given by

$$f_2(R) = e^{b_4 R} (R + b_5)^{-b_3}. \quad (4.7)$$

The exponential term used in this equation represents the material damping and scattering, which is also known as inelastic attenuation of ground motion. The second term denotes for geometrical spreading of energy. The geometrical attenuation rate is given by the coefficient b_3 [Joyner and Boore, 1991]. The coefficient b_5 is used to limit the value of Y at zero distance. This becomes more significant when the distance parameter being used is epicentral distance or shortest distance to the surface projection of rupture. Another widely used form of $f_2(R)$ [Ambraseys, 1995; Joyner and Boore, 1981; Fukushima and Tanaka, 1990] is given by

$$f_2(R) = e^{b_4 R} \left(\sqrt{R^2 + b_5^2} \right)^{-b_3}. \quad (4.8)$$

The constant term in the brackets is considered analogous to hypocentral distance. In order to account for the combined effect of magnitude and distance, the form of the function used is given by [Campbell, 1997; Sadigh *et al.*, 1997]

$$f_3(m, R) = \left(R - b_6 e^{b_7 m} \right)^{-b_3}. \quad (4.9)$$

Depending on the effect of local site conditions, the style of faulting, soil structure interaction parameters and type of earthquake the variables, which can take pre-assigned values, can also be introduced in the formulation. This is done through the introduction of dummy variables corresponding to these parameters and is denoted through the term f_4P .

4.3 Attenuation model for Himalayan Earthquakes

The number of well-recorded earthquakes available for the Himalayan region is limited. So, the use of an exhaustive model including all the parameters mentioned above should be applied with caution. A simple form of attenuation equation compared to the one discussed above was chosen because of (a) lack of enough near source recordings, and (b) inadequate number of earthquakes to arrive at a meaningful nonlinear relationship with respect to magnitude, *i.e.*, the model contains only linear term in magnitude, $\ln R$ and R terms to incorporate the effect of attenuation due to geometric spreading as well as material damping, and a soil dependant parameter. The form of the attenuation model is given as

$$\ln Y = b_1 + b_2 M + b_3 R + b_4 \ln R + b_5 H + (b_6 + b_7 R) S. \quad (4.10)$$

The term H is added to include the effects of higher acceleration (if any) observed in the subduction zone earthquakes. The value of H is 1.0 for the earthquakes subduction zone earthquakes (1988 NE $M7.3$ and 1990 NE $M6.1$), and 0.0 for all other earthquakes.

A dummy value S is introduced to consider the change in the rate of attenuation in alluvial medium. S is equal to 1.0 for 1988 Bihar-Nepal $M6.8$ earthquake and for all other events which had rock as medium of propagation, S is zero.

4.3.1 Preliminary analysis of data

Before the data is regressed to get a particular attenuation model, it is necessary to do some preliminary analysis on the data to eliminate inconsistent data as well as to find the form of variables that gives a better fit for the data. The plot of PGA vs epicentral distance of the data used in the study is given in Figure 4.5.

The regression analysis for the model given by Eq. (4.10) was carried out using MATLAB subroutine REGRESS and G02DAF from NAG library. Both the subroutines use method of least squares for the regression analysis. The results of regression using the entire data of nine earthquakes are shown in Table 4.2. The table also gives the standard error, which denotes the amount of uncertainty in the calculated coefficients. This is generally not reported along with the attenuation relationships, but is useful for understanding the level of confidence that can be put on the predicted coefficients. This part can be dealt in detail after the regression form has been finalized.

The coefficient of earthquake magnitude is quite low indicating a very low dependence on magnitude or due to some error related to the sample considered in the analysis. For the model under consideration, a change of magnitude from 5.0 to 6.0 increases acceleration only by 12%, which is very less compared to the difference in amount energy released in the earthquake. For an increase in magnitude by 1.0, the average increase in acceleration predicted in the literature [e.g., Boore *et al.*, 1997; Spudich *et al.*, 1997; Ambraseys, 1995; Fukushima and Tanaka, 1990] is about 50% and it ranges from 25 to 75%. This anomaly may be attributed to the inconsistency of

observations in the data used, inability of the model to represent the complete database or the true characteristic of the region.

4.3.2 Study of Outliers

Any experimental data recorded will contain some outliers, which are to be removed before the data is analyzed. These can be either erroneous measurements, which are not consistent with the other observed points or points that get undue importance during analysis. When there are two or fewer explanatory variables, scatter plots will quickly reveal any outliers in X . When number of coefficients are greater than 2, scatter plots may not reveal multivariate outliers, which are separated from the bulk of X -points but do not appear as outliers in a plot of any single explanatory variable or pair of them. A least square projection matrix known as hat matrix $[H]$ [Belsley *et al.*, 1980] can be used as an indicator of the influence of the observation on the predicted value. The hat matrix is defined as

$$H = X(X^T X)^{-1} X^T, \quad (4.11)$$

where X is the $n \times p$ matrix containing explanatory variables. Hat matrix can be used to calculate the fitted predicted values, since

$$\hat{y} = Xb = Hy. \quad (4.12)$$

The contribution of each observation y_i in the prediction of \hat{y}_i is obtained from the hat matrix. The influence of the response value, y_i on the fit is most directly reflected in its impact on the corresponding fitted value \hat{y}_i . This information can be obtained from the diagonal elements of H , known as $\{h\}$ vector. This $\{h\}$ vector can be used as a tool to obtain the information about the over influencing observations. The proof for the fact that the average size of the diagonal element h_i is p/n and $2p/n$ provides a good cut-off for the removal of the influential data is available in literature [Belsley *et al.*, 1980].

For the model given in Eq. (4.9), the values of $\{h\}$ vector as computed are plotted with respect to epicentral distance of the observed points (Figure 4.6). It is seen that for each earthquake, the plot of $\{h\}$ vector follows almost a parabolic shape. It is evident from the plots that the near source recordings ($<10\text{km}$) by SMAs as well SRRs are highly influencing the predicted values. The recordings at distances more than 500kms were also found to be highly influential in prediction of the data and these were records corresponding to August 6, 1988 earthquake only. Majority of the points from 1988 Bihar-Nepal $M6.8$ earthquake is found to fail in satisfying the stipulated criteria. The failure of large number of points corresponding to a particular earthquake indicated a different behavior being exhibited by these points compared to the other events. The 1988 Bihar-Nepal $M6.8$ earthquake was the only event that was recorded after propagating through a deep alluvial plane. All other events had rock as the medium of propagation. Subsequently, 1988 Bihar-Nepal $M6.8$ earthquake data was removed from the database to be separately regressed later. The new database was regressed with the model without soil dependant coefficients as given below,

$$\ln Y = b_1 + b_2 M + b_3 R + b_4 \ln R + b_5 H. \quad (4.13)$$

The results are given in Table 4.3. The magnitude dependent coefficient did not show any marked improvement even after removal of Bihar-Nepal earthquake. This model also indicates that there are still data points, which have strong influence on the model.

The analysis of $\{h\}$ matrix indicates that, the influential observations are detected only at either extreme (with respect to epicentral distance) of the observations. One influential row from the matrix containing explanatory variables was deleted at a time and the values of $\{h\}$ were re-computed. In general the influential observations consisted of recordings at distances less than 10km and recordings at distances more than 500 km

(1 recording from 1986 NE $M5.2$, 14 from 1988 NE $M7.3$, 12 from Uttarkashi, 6 from Chamoli and 4 from Kangra events). The regression model after removal of the influential observations, showed an even weaker dependence (decreased to 8% from 12%) of peak ground acceleration on magnitude (Table 4.3). The coefficient b_5 , which was introduced to incorporate the difference in attenuation characteristics shown by the earthquakes from Burmese arc (subduction zone), was found to have a positive sign indicating magnification of the accelerations (about 300%) compared to a similar magnitude earthquake from a different source. Since the problem of magnitude independence persisted even after the removal of the influential data and the regression form did not seem to exclude any important parameter, the data was checked for any difference in characteristics, *i.e.*, the low magnitude dependence of the equation might be due inclusion of data with different characteristics in the same regression form.

The plot of PGA versus epicentral distance for all the earthquakes after removal of influential observations are shown in Figure 4.7. Figure 4.8 shows the PGA recorded for different events in the North East India and Figure 4.9 shows those for the North India events. Figure 4.10 shows the variation of PGA for Bihar-Nepal earthquake. Individual least-square fit lines of all the events are plotted and are given in Figure 4.11.

4.3.3 Observations on variation of PGA of different events:

Earthquakes recorded in the North-East India seem to have similar acceleration when compared to events with higher magnitude in North India. From Figure 4.11 it can be seen that an earthquake with a magnitude 5.2 in the North-East Himalayas has produced comparable acceleration with an earthquake of magnitude 6.6 (Chamoli) in northern Himalayas. Similarly, an earthquake with magnitude 5.8 in North-East Himalayas has produced similar acceleration for an earthquake of magnitude 7.0 (Uttarkashi) in northern Himalayas. Also, the acceleration recorded during Kangra

earthquake is lower than that of magnitude 5.2 earthquake in North-East. If a regression analysis is conducted without considering these characteristics, because of apparent independent behavior of acceleration with respect to magnitude, the magnitude related regression coefficient tends to become very low. So in order to get a meaningful magnitude dependant relationship, the separation of the database based on the region is required. Since the subduction zone events were found to produce higher acceleration, it was decided to have separate regression form for these events.

Though there is a large difference in earthquake magnitudes, the PGA generated by 1990 NE $M6.1$ are comparable with that produced by 1988 NE $M7.3$ earthquake. This anomaly can be attributed either to an error in magnitude measurement or error in the epicenter calculation. The average error in the calculation of magnitude by different agencies is ± 0.4 (Table 3.1a). Even if this variation is taken into consideration, there will be a difference of 0.8 in magnitude and the similarity in the order of accelerations cannot be explained.

It is also evident from Figures 3.5(a) to 3.5(d) that there is an error of 50-100km in locating the epicenters of North-East India earthquakes by different agencies. For events 1986 NE $M5.2$, 1987 NE $M5.9$, 1988 NE $M5.8$, and 1988 NE $M7.3$, the epicenters calculated using the strong motion data were found to lie closer to the recording site compared to the epicenter predicted by USGS. For January 20, 1990 earthquake, the only available location of the epicenter is from USGS. Thus, the best epicenter cannot be chosen from different locations available based on the correlation of distance and acceleration. There is a possibility that the error in locating the epicenter may have crept into the 1990 NE $M6.1$ event. Under these circumstances, it becomes necessary to remove the 1990 NE $M6.1$ event from the database.

Based on the above observations, the database can be classified into 4 categories corresponding to four regions. They are,

- (a) North India earthquakes,
- (b) North East India non-subduction zone earthquakes,
- (c) NE India subduction zone earthquakes, and
- (d) Earthquakes generated in the Gangetic foredeep, which is basically situated on alluvial plane.

4.4 Development of Attenuation Relationships

Tables 4.4 to 4.8 gives the coefficients of regression related to each region along with σ of the model. It can be observed from Table 4.4 that the regression predicts a negative value of material damping for North East India non-subduction earthquakes. Thus, the regression analysis for this region is carried out after removal of material damping term ($b_3 R$) from the model. The resulting regression coefficients along with the Standard Error (SE) in prediction of coefficients and SD of the model are given in Table 4.5. It can be observed that, the magnitude term has come out to be a significant value when the regression analysis was done separately for each region (Table 4.5 to 4.6).

For subduction zone event and earthquakes in alluvial planes, only single event is available. This necessitated the regression analysis of the data without magnitude term. The model used for regression analysis is given as

$$\ln Y = b_1 + b_2 R + b_3 \ln R \quad (4.14)$$

The results of regression analysis of these two groups are given in Tables 4.7 and 4.8. For the 1988 Bihar-Nepal $M6.8$ earthquake, both the coefficients corresponding to material damping as well as geometric spreading terms are higher compared to August 6,

1988 NE event. This implies a greater rate of attenuation in the alluvial planes as evident from Figure 4.10.

The results of the regression analysis on attenuation relationships of are summarised below:

Central Himalayan earthquakes

$$\ln(PGA) = -4.768 + 0.586M - 0.0032R - 0.481\ln(R); \quad \sigma = 0.597 \quad (4.15)$$

Non-Subduction earthquakes in North East India

$$\ln(PGA) = -3.441 + 0.706M - 0.828\ln(R); \quad \sigma = 0.437 \quad (4.16)$$

Subduction earthquake in North East India

$$\ln(PGA) = -0.42 - 0.004R - 0.241\ln(R); \quad \sigma = 0.578 \quad (4.17)$$

Bihar-Nepal Earthquake

$$\ln(PGA) = 2.103 - 0.006R - 0.76\ln(R); \quad \sigma = 0.696 \quad (4.18)$$

The predicted values of acceleration are plotted for different events along with the existing attenuation relationships (Figure 4.12). The predicted attenuation relationships give low values of standard error (Table 4.9). Figure 4.13 shows the comparison of the proposed attenuation relationships for a hypothetical earthquake of $M7.0$. Eq.4.17 for the subduction zone earthquake is for $M7.3$ and Eq.4.18 for the Bihar-Nepal region for $M6.8$ event. To plot equations for an $M7.0$ event for these two categories, the b_2 value was assumed as 0.70 and the value of b_1 adjusted accordingly.

Considering the epicentral distance range of 10km to 100km, which is of maximum engineering interest, motion is weakest in the Central Himalayan earthquakes and strongest in the Bihar-Nepal earthquake. For the same magnitude ($M7.0$), the ratio of PGA in the Indo-Gangetic plains to that in the Central Himalaya ranges from 5.2 (at 10km) to 3.4 (at 100km). The rate of attenuation with distance is lowest for the subduction event in North-East India and is highest for the Bihar-Nepal earthquake; ratio

of PGA at 10km to that at 100km is 2.6 for the former and 9.9 for the latter. Since the number of near source recordings was less, they were not included in the regression analysis. So this attenuation relationships may not be applicable in the near source region.

4.5 Adequacy of Model

The adequacy of the model can checked either by analysing the residuals or by testing the significance of each coefficient derived during the analysis.

4.5.1 Analysis of Residuals

The overall adequacy of the model is best assessed from an analysis of residuals. By the very nature of regression analysis, the residuals have a mean close to zero. If no apparent trend in the residuals is observed, then the model can be considered adequate [Draper and Smith, 1998]. A trend indicates an inadequacy in the model to predict the data and would require modification of the functional form. The residuals plotted with respect to epicentral distances (R) are given in Figures 4.14 to 4.17. No particular trend is shown by any of the plots from which we can ascertain that the models used in the regression analysis are adequate to represent the variation in data.

4.5.2 Significance Testing of Coefficients

The significance of the calculated coefficients can be estimated by means of a t -test. The t statistic is defined as [Draper and Smith, 1998]:

$$t = \frac{\hat{b}_1 - b_1}{SE(\hat{b}_1)} \quad (4.19)$$

Under the normality assumption, the variable \hat{b}_1 follows t distribution with $N-P$ degree of freedom, where P is the number of coefficients in the equation. If the true value of b_1 is specified in the null hypothesis, the t statistic can be computed from the available sample and used as a test statistic.

All the coefficients calculated are tested with a level of significance of 5% for the particular value being equal to zero. The null hypothesis being $H_0 : b_i = 0$ against the alternate hypothesis $H_1 : b_i \neq 0$. The calculated t -statistic as well as $t_{\alpha/2, N-P}$ for the data used in the analysis is given in Tables 4.5 to 4.8. All coefficients, which are calculated for North India as well as North East India non-subduction zone earthquakes, differ significantly from the assumed 0 with 5% level of significance. For North East Indian subduction zone earthquake (1988 NE $M7.3$) as well as for the 1988 Bihar-Nepal $M6.8$ earthquake, the null hypothesis of these coefficients being equal to zero cannot be rejected when tested with a level of significance of 5%. This implies, that the values obtained for these events should be used with caution.

• • •

Table 4.1: Average error of prediction from the observed data for different attenuation relationships.

<i>Events</i>	<i>Boore</i>	<i>Sadigh</i>	<i>Campbell</i>	<i>Young</i>	<i>Crouse</i>	<i>Anders</i>	<i>Toro</i>
10-Sep-86	0.5425	1.6036	0.9887	0.5043	0.6635	0.6864	0.7157
18-May-87	0.6132	2.4032	1.6330	1.0438	1.0846	1.3963	1.2375
06-Feb-88	0.4712	1.9119	1.2179	0.7449	0.8273	0.9456	0.8695
06-Aug-88	0.8678	2.4485	1.8430	1.0527	0.7943	2.2368	1.5719
20-Jan-90	1.2823	3.7612	2.7534	2.0318	1.8440	3.0760	2.3614
20-Oct-90	0.7160	1.0881	0.6726	0.6276	0.6438	0.7547	0.5923
29-Mar-99	0.7856	1.0988	0.8915	0.9294	0.9014	0.9148	1.0105
26-Apr-86	0.6993	0.8122	0.6924	0.9745	0.8331	0.8018	0.8138
21-Aug-88	0.9957	2.2212	1.7076	1.0168	0.9071	1.5284	1.3054

Table 4.2: Coefficients of regression for the model given below using the database containing accelerations from all the events.

$$\ln Y = b_1 + b_2 M + b_3 R + b_4 \ln R + b_5 H + (b_6 + b_7 R) S$$

<i>Value</i>	<i>Mean</i>	<i>Standard Error</i>
b_1	-1.5401	0.4259
b_2	0.1184	0.0668
b_3	-0.0019	0.0005
b_4	-0.5135	0.0715
b_5	1.2429	0.0818
b_6	1.8704	0.2549
b_7	-0.0058	0.0014

Table 4.3: Coefficients of regression for the model given below using the database after the removal of data obtained from 1988 Bihar-Nepal M6.8 earthquake.

$$\ln Y = b_1 + b_2 M + b_3 R + b_4 \ln R + b_5 H$$

Coeff.	Data with all points		Data after removal of outliers	
	Value	SE	Value	SE
b_1	-1.545	0.4188	-2.559	0.5751
b_2	0.1176	0.0657	0.0629	0.068
b_3	-0.002	0.0005	-0.005	0.0009
b_4	-0.511	0.0707	-0.145	0.136
b_5	1.2429	0.0804	1.2986	0.0814
SD	0.5887		0.5855	

Table 4.4: Coefficients of regression for the model given below using the accelerations recorded by 1986 NE M5.2, 1987 NE M5.9 and 1988 NE M5.8.

$$\ln Y = b_1 + b_2 M + b_3 R + b_4 \ln R$$

Coef.	Regression values	
	Value	SE
b_1	-3.1373	1.8548
b_2	0.7265	0.3362
b_3	0.0013	0.0050
b_4	-0.9515	0.4950
SD	0.4478	

Table 4.5: Coefficients of regression for the model given below using the database of accelerations recorded by 1986 NE M5.2, 1987 NE 5.9 and 1988 NE M5.8.

$$\ln Y = b_1 + b_2 M + b_3 \ln R$$

Number of observations = 43, $t_{5\%,40}=2.02$.

Coef.	Regression values		
	Value	SE	t Statistic
b_1	-3.441	1.4381	-2.393
b_2	0.706	0.3236	2.182
b_3	-0.828	0.1625	-5.096
SD	0.4368		

Table 4.6: Coefficients of regression for the model given below using the database of accelerations recorded by Uttarkashi, Chamoli and Kangra earthquakes.

$$\ln Y = b_1 + b_2 M + b_3 R + b_4 \ln R$$

Number of observations = 139, $t_{5\%,135} = 1.97$.

Coef.	Regression values		
	Value	SE	T Statistic
b_1	-4.7682	0.9755	-4.888
b_2	0.5856	0.1524	3.843
b_3	-0.0032	0.0019	-1.684
b_4	-0.4814	0.2396	-2.009
SD	0.5973		

Table 4.7: Coefficients of regression for the model given below with only subduction zone event (1988 NE M7.3).

$$\ln Y = b_1 + b_2 R + b_3 \ln R$$

Number of observations = 123, $t_{5\%,120} = 1.97$.

Coef.	Regression values		
	Value	SE	t Statistic
b_1	-0.420	1.5987	-0.262
b_2	-0.004	0.0017	-2.294
b_3	-0.241	0.3677	-0.655
SD	0.5776		

Table 4.8: Coefficients of regression for the model given below with only 1988 Bihar-Nepal M6.8.

$$\ln Y = b_1 + b_2 R + b_3 \ln R$$

Number of observations = 38, $t_{5\%,35} = 2.02$.

Coef.	Regression values		
	Value	SE	t Statistic
b_1	2.1034	3.1041	0.6776
b_2	-0.006	0.0054	-1.111
b_3	-0.76	0.7881	-0.965
SD	0.6968		

Table 4.9: Average error of prediction from the observed data for different attenuation relationships.

<i>Events</i>	<i>Boore</i>	<i>Sadigh</i>	<i>Campbell</i>	<i>Young</i>	<i>Crouse</i>	<i>Anders</i>	<i>Toro</i>	<i>New</i>
10-Sep-86	0.541	1.662	1.032	0.605	0.691	0.717	0.695	0.435
18-May-87	0.613	2.403	1.633	1.063	1.085	1.396	1.238	0.372
06-Feb-88	0.471	1.912	1.218	0.734	0.827	0.946	0.870	0.449
06-Aug-88	0.895	2.389	1.825	0.971	0.730	2.026	1.486	0.591
20-Oct-90	0.721	1.094	0.676	0.645	0.648	0.761	0.596	0.556
29-Mar-99	0.824	1.127	0.923	1.192	0.938	0.958	1.034	0.715
26-Apr-86	0.827	0.941	0.799	1.4455	1.000	0.939	0.911	0.633
21-Aug-88	0.996	2.221	1.708	0.959	0.907	1.528	1.305	0.669

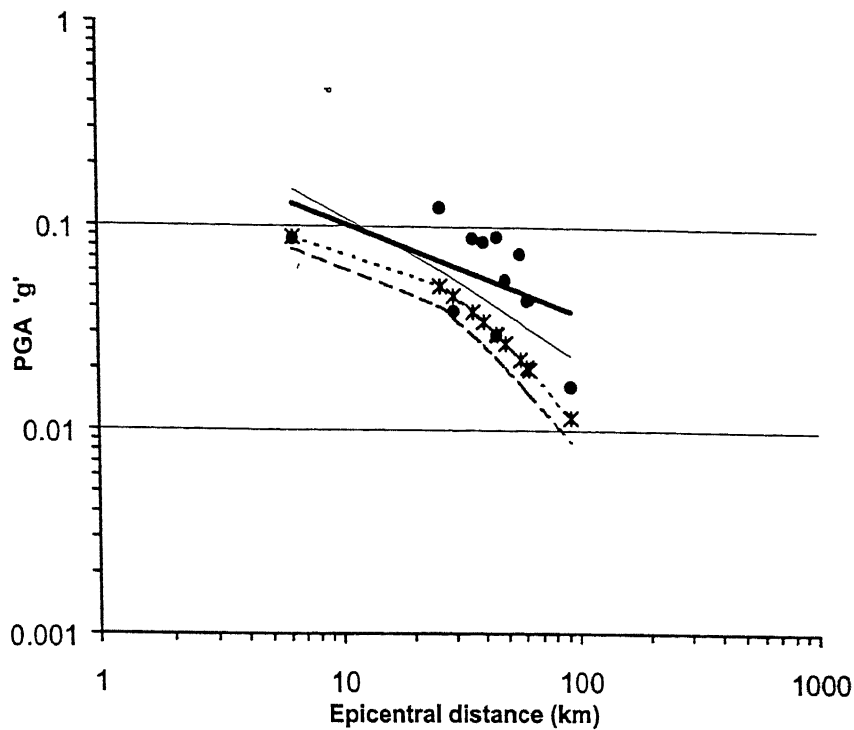


Figure 4.1(a): Distribution of peak ground acceleration for 10 September 1986, NE India earthquake and the predicted values of PGA using different relationships available for interplate earthquakes.

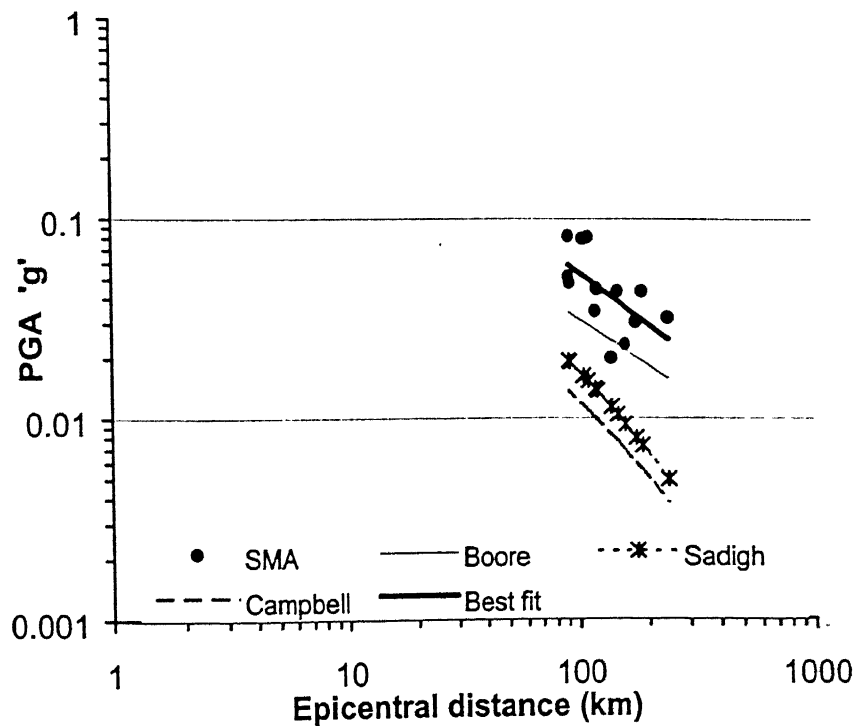


Figure 4.1(b): Distribution of peak ground acceleration for 14 May 1987, NE India earthquake and the predicted values of PGA using different relationships available for interplate earthquakes.

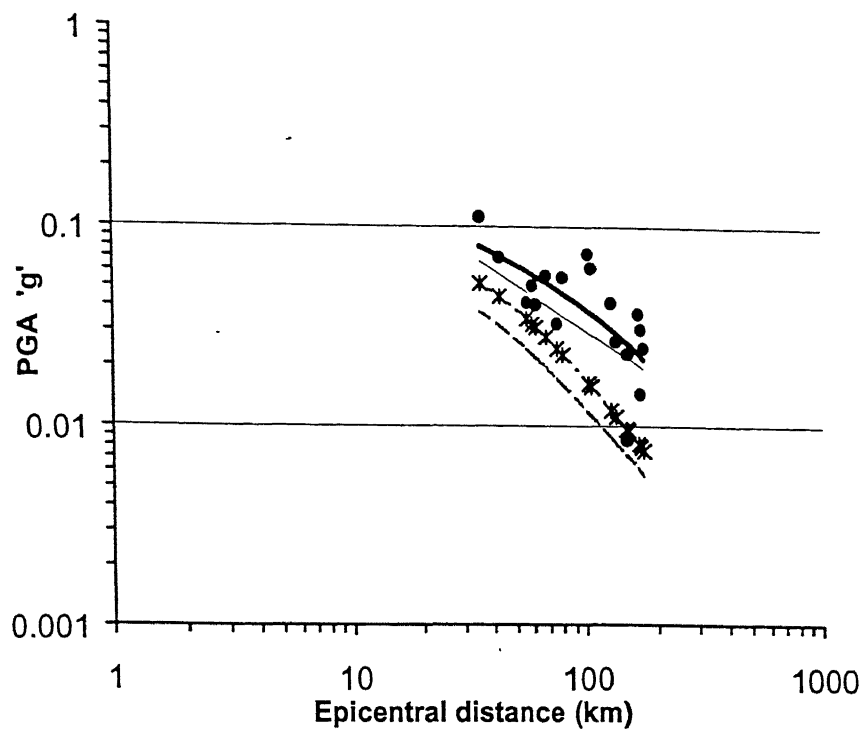


Figure 4.1(c): Distribution of peak ground acceleration for 6 February 1988, NE India earthquake and the predicted values of PGA using different relationships available for interplate earthquakes.

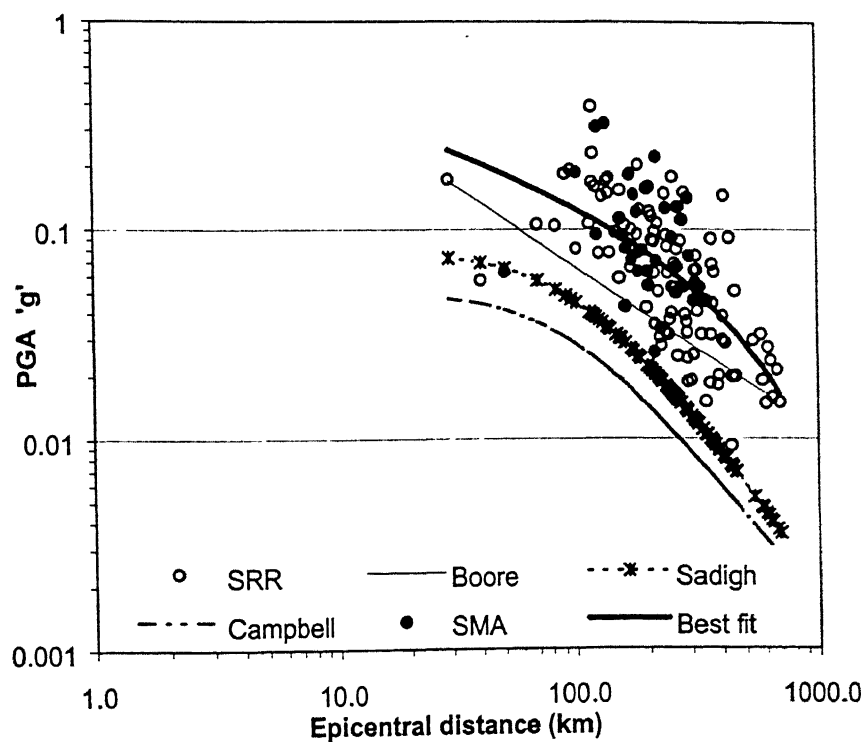


Figure 4.1(d): Distribution of peak ground acceleration for 6 August 1988, NE India earthquake and the predicted values of PGA using different relationships available for interplate earthquakes.

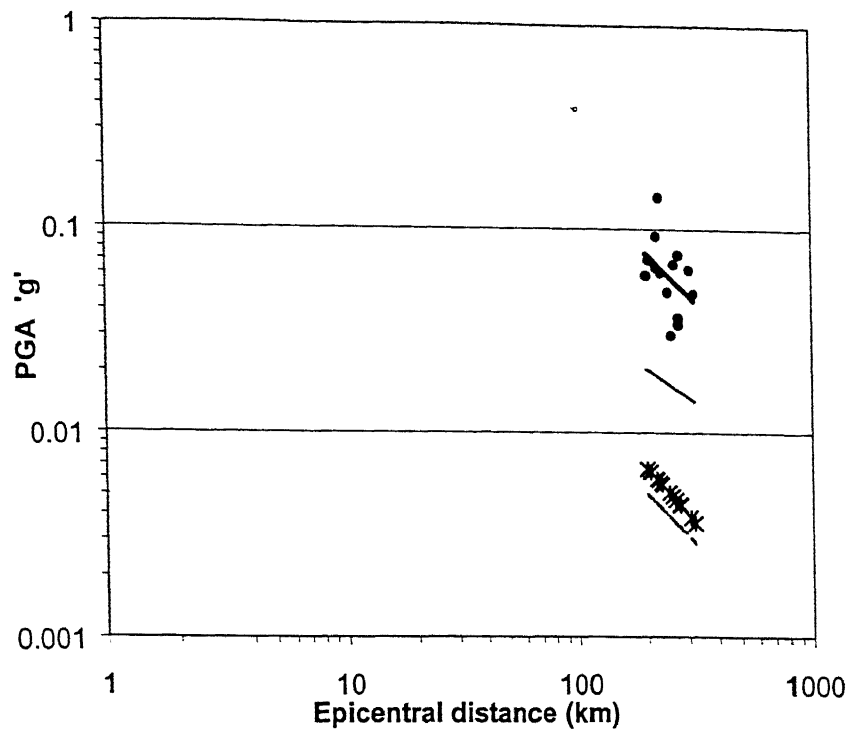


Figure 4.1(e): Distribution of peak ground acceleration for 10 January 1990, NE India earthquake and the predicted values of PGA using different relationships available for interplate earthquakes.

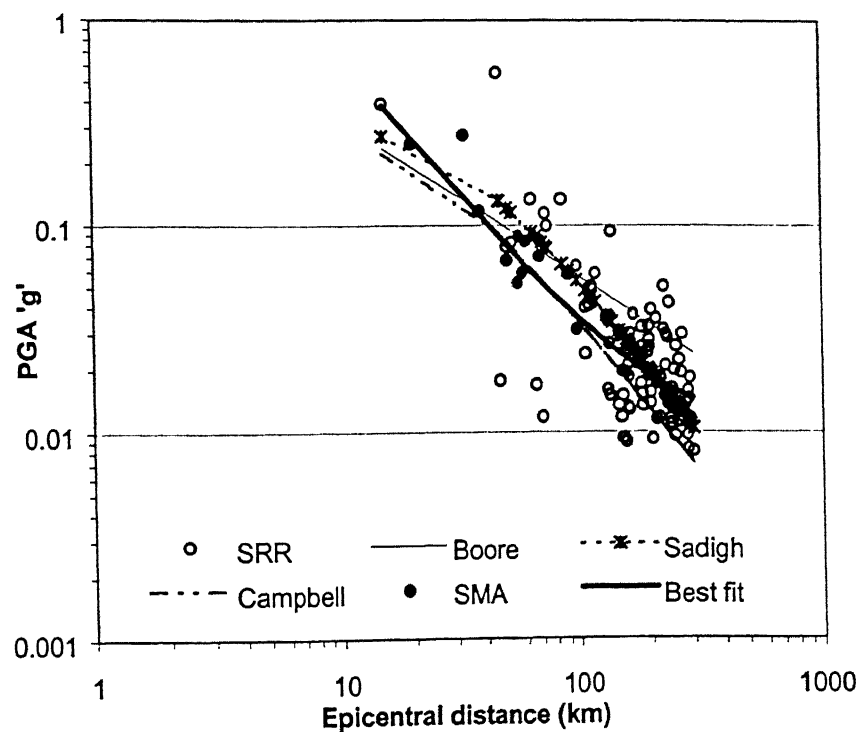


Figure 4.1(f): Distribution of peak ground acceleration for 20 October 1991, Uttarkashi earthquake and the predicted values of PGA using different relationships available for interplate earthquakes.

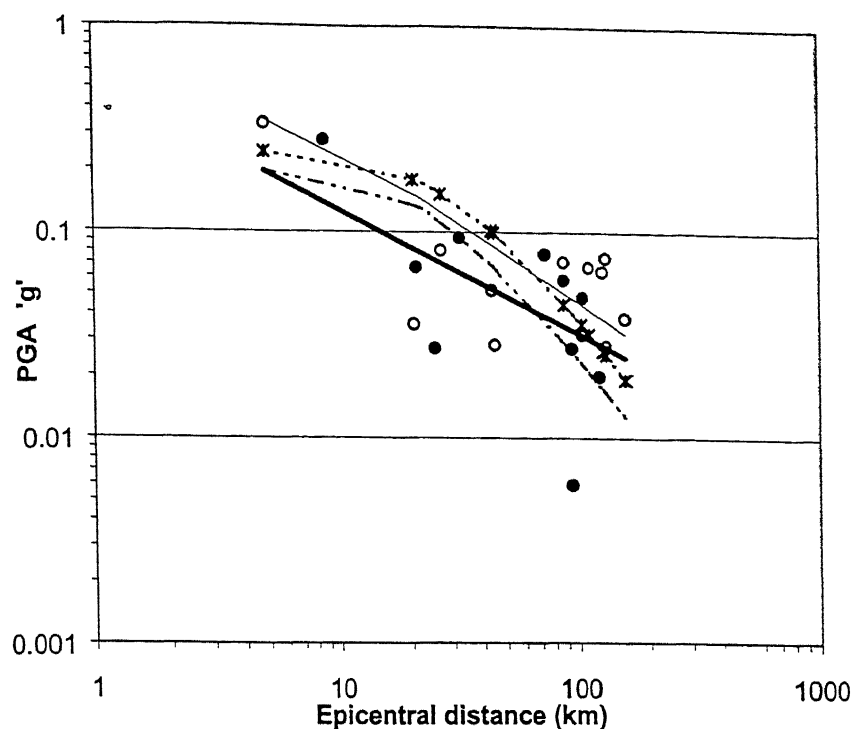


Figure 4.1(g): Distribution of peak ground acceleration for 29 March 1999, Chamoli earthquake and the predicted values of PGA using different relationships available for interplate earthquakes.

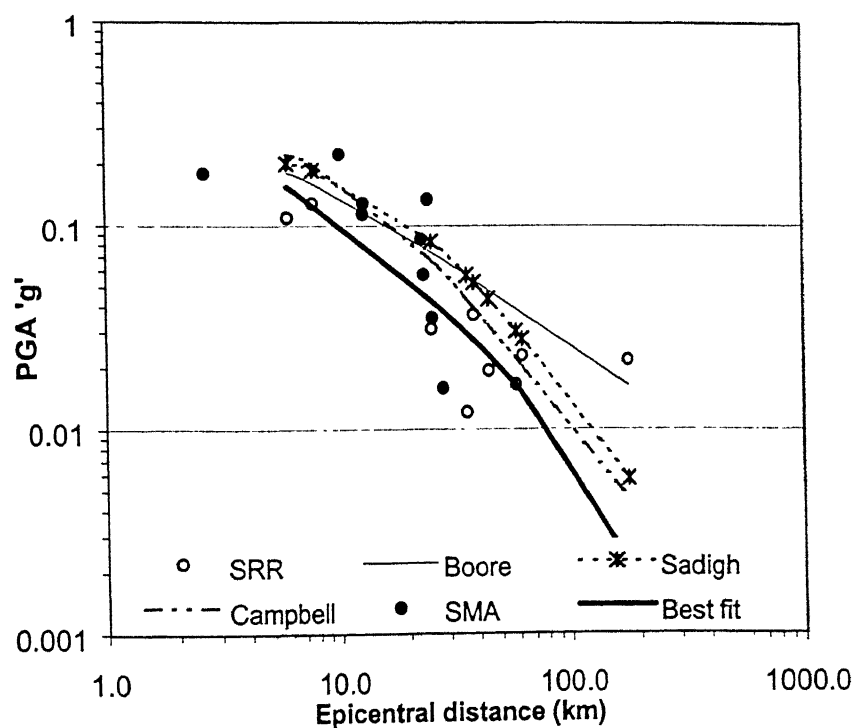


Figure 4.1(h): Distribution of peak ground acceleration for 26 April 1986 Kangra earthquake and the predicted values of PGA using different relationships available for interplate earthquakes.

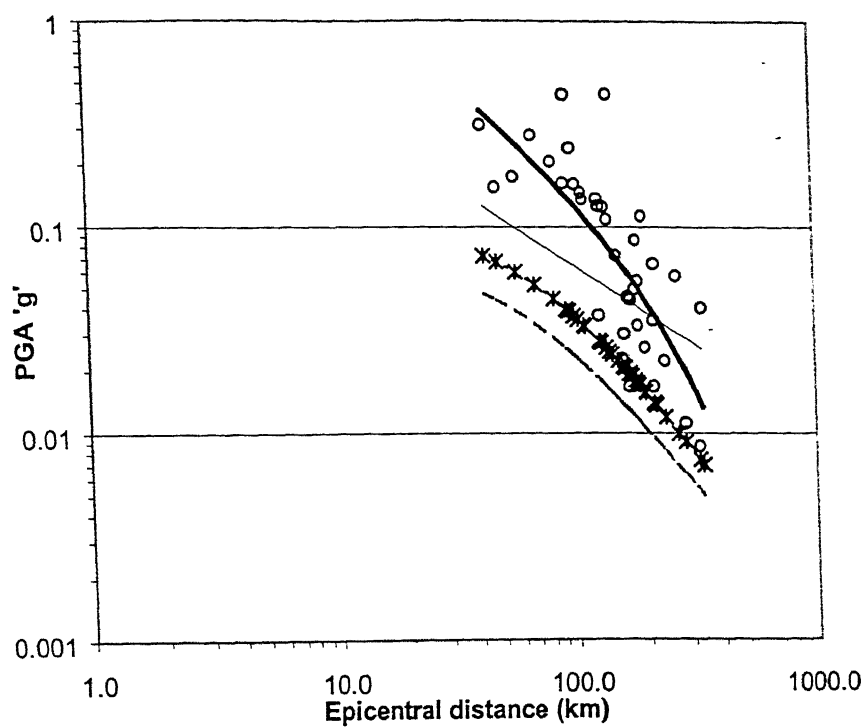


Figure 4.1(i): Distribution of peak ground acceleration for 21 August 1988, NE India earthquake and the predicted values of PGA using different relationships available for interplate earthquakes.

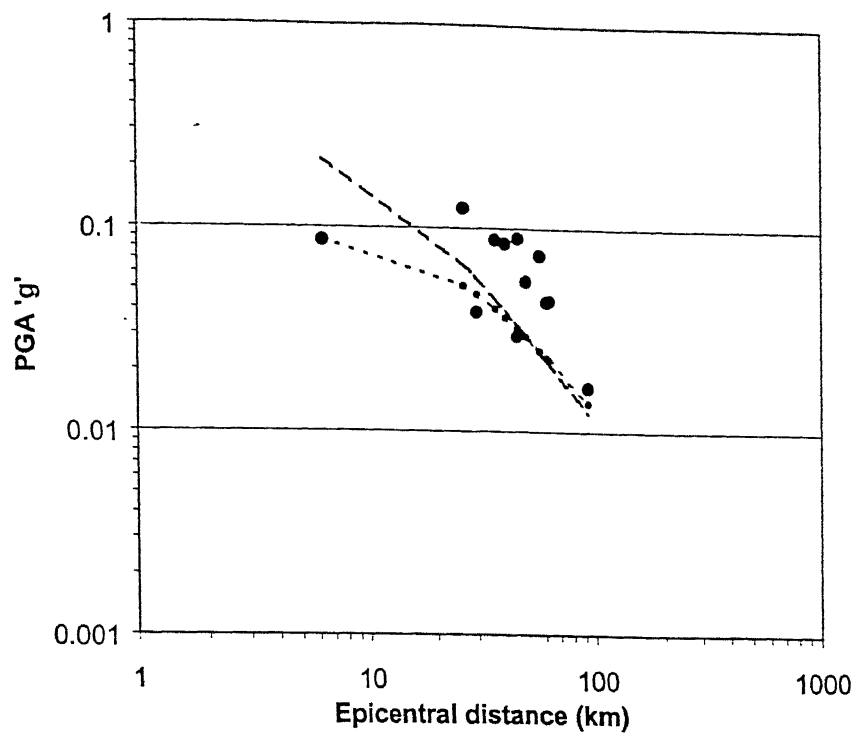


Figure 4.2(a): Distribution of peak ground acceleration for 10 September 1986, NE India earthquake and the predicted values of PGA using different relationships available for intraplate earthquakes.

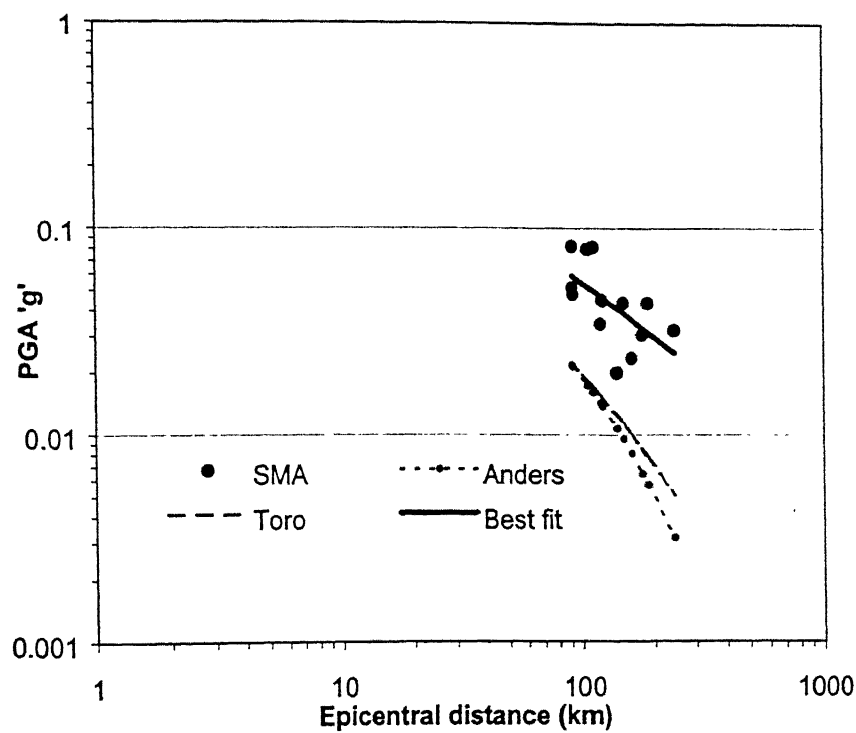


Figure 4.2(b): Distribution of peak ground acceleration for 14 May 1987, NE India earthquake and the predicted values of PGA using different relationships available for intraplate earthquakes.

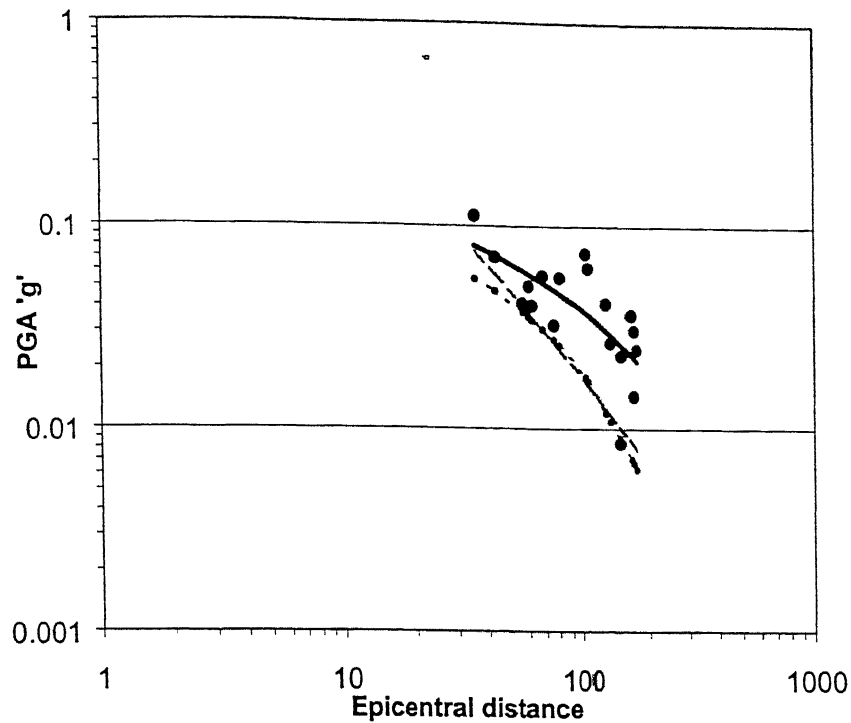


Figure 4.2(c): Distribution of peak ground acceleration for 6 February 1988, NE India earthquake and the predicted values of PGA using different relationships available for intraplate earthquakes.

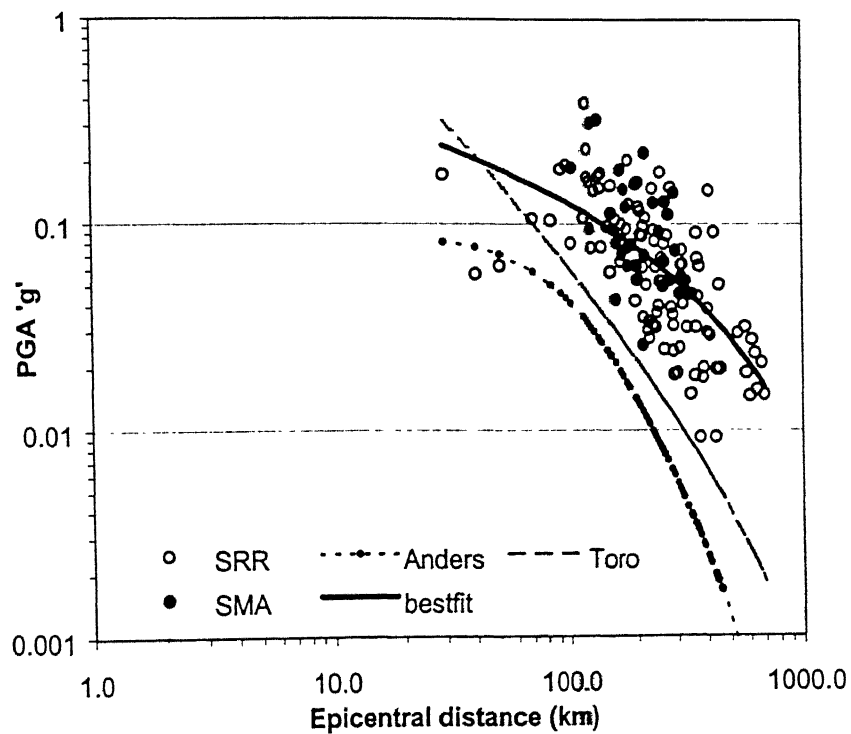


Figure 4.2(d): Distribution of peak ground acceleration for 6 August 1988, NE India earthquake and the predicted values of PGA using different relationships available for intraplate earthquakes.

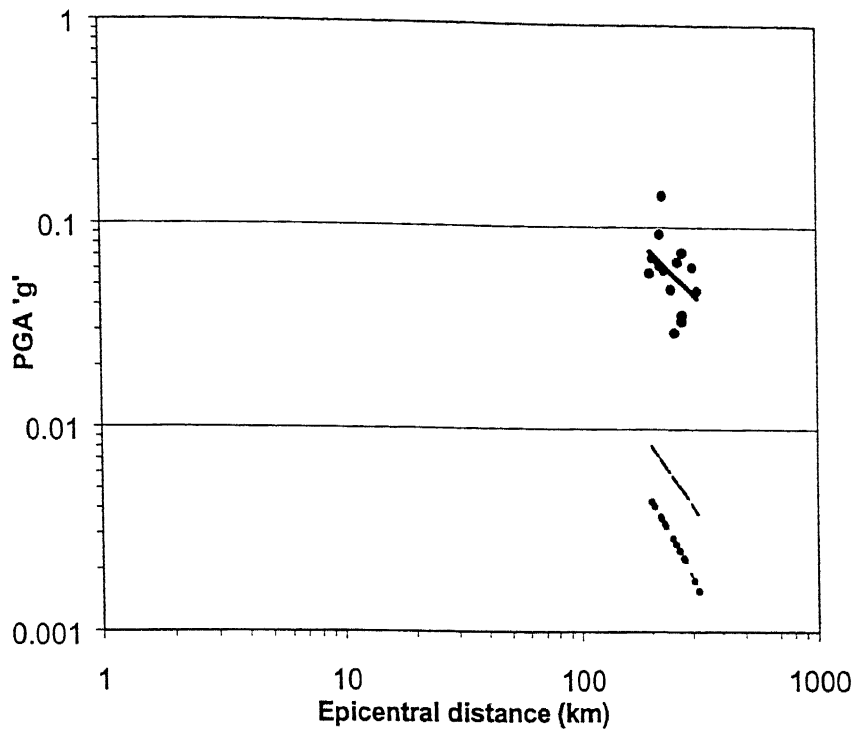


Figure 4.2(e): Distribution of peak ground acceleration for 10 January 1990, NE India earthquake and the predicted values of PGA using different relationships available for intraplate earthquakes.

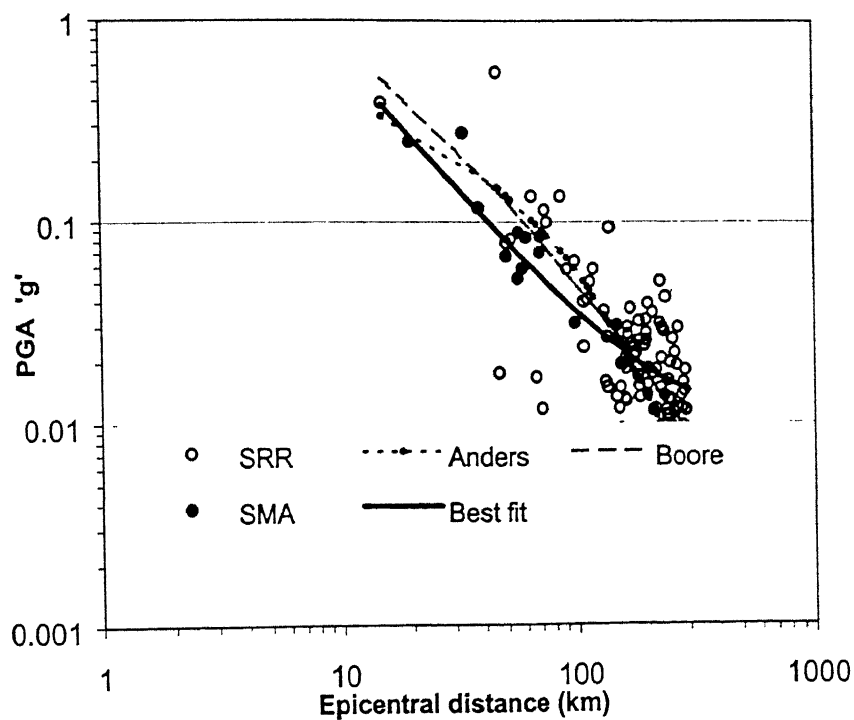


Figure 4.2(f): Distribution of peak ground acceleration for 20 October 1991, Uttarkashi earthquake and the predicted values of PGA using different relationships available for intraplate earthquakes.

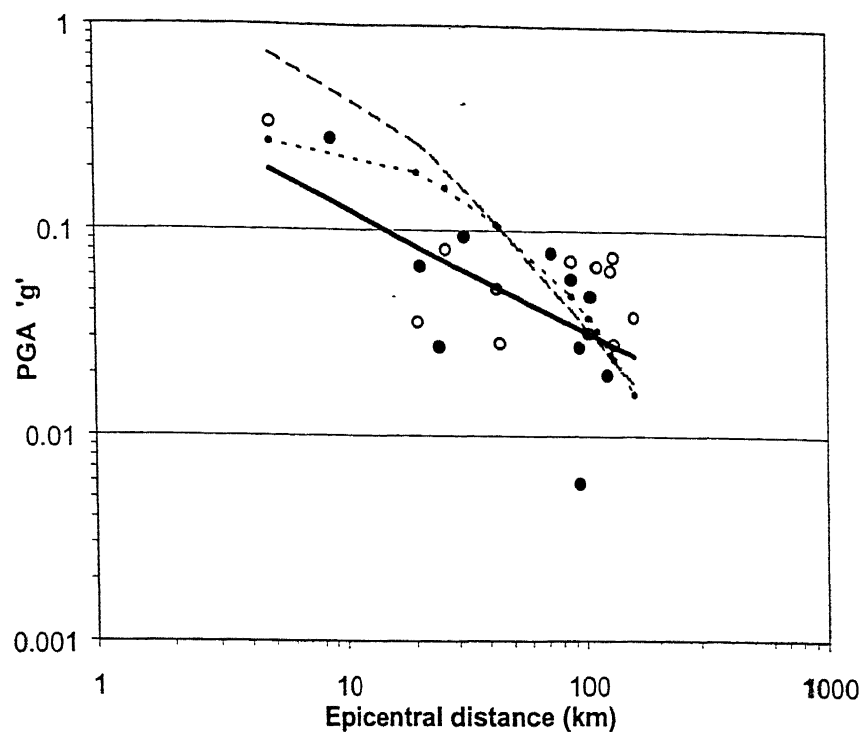


Figure 4.2(g): Distribution of peak ground acceleration for 29 March 1999, Chamoli earthquake and the predicted values of PGA using different relationships available for intraplate earthquakes.

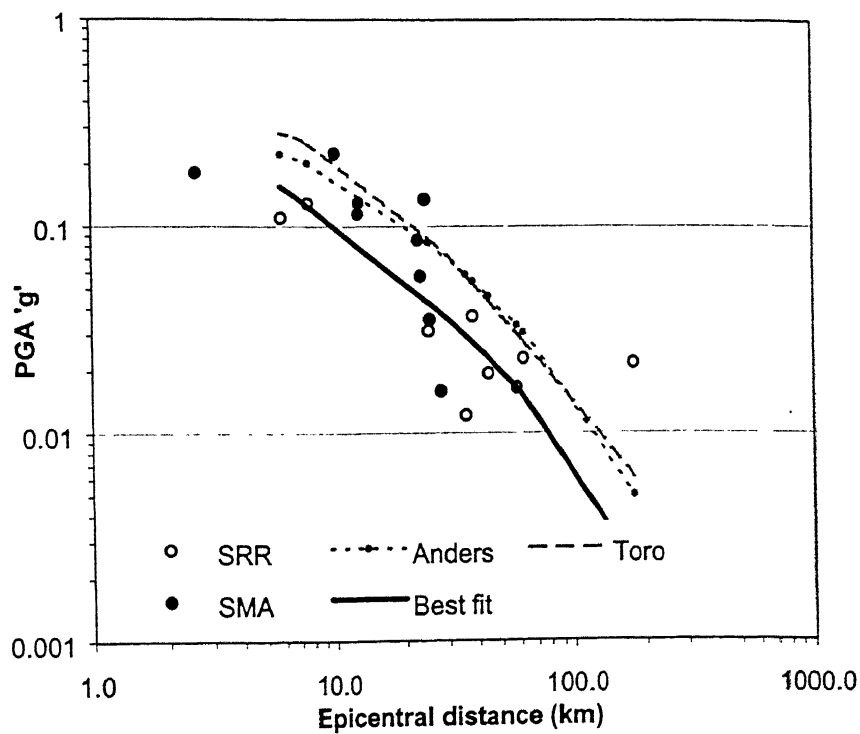


Figure 4.2(h): Distribution of peak ground acceleration for 26 April 1986 Kangra earthquake and the predicted values of PGA using different relationships available for intraplate earthquakes.

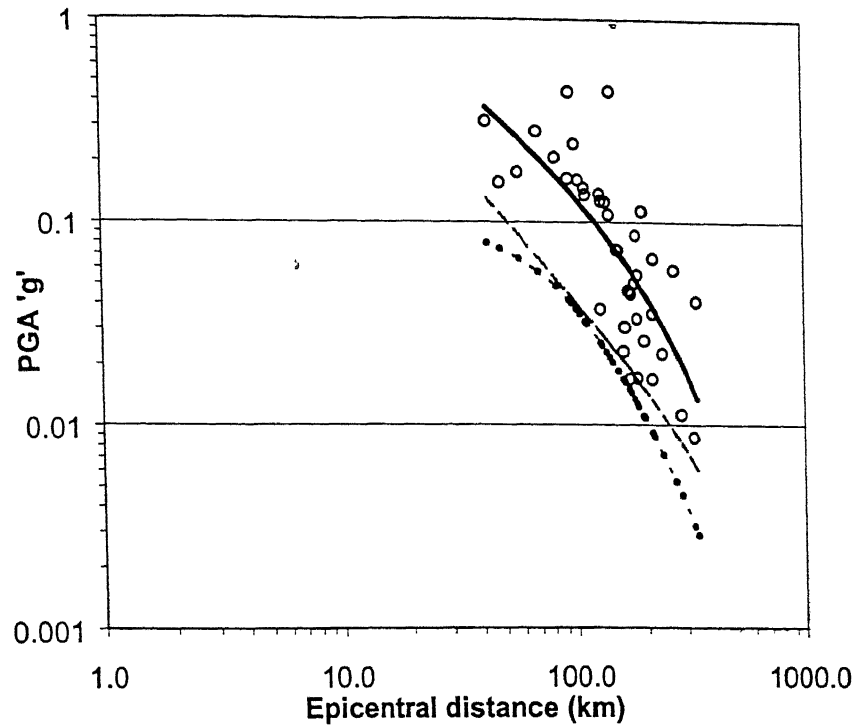


Figure 4.2(i): Distribution of peak ground acceleration for 21 August 1988, NE India earthquake and the predicted values of PGA using different relationships available for intraplate earthquakes.

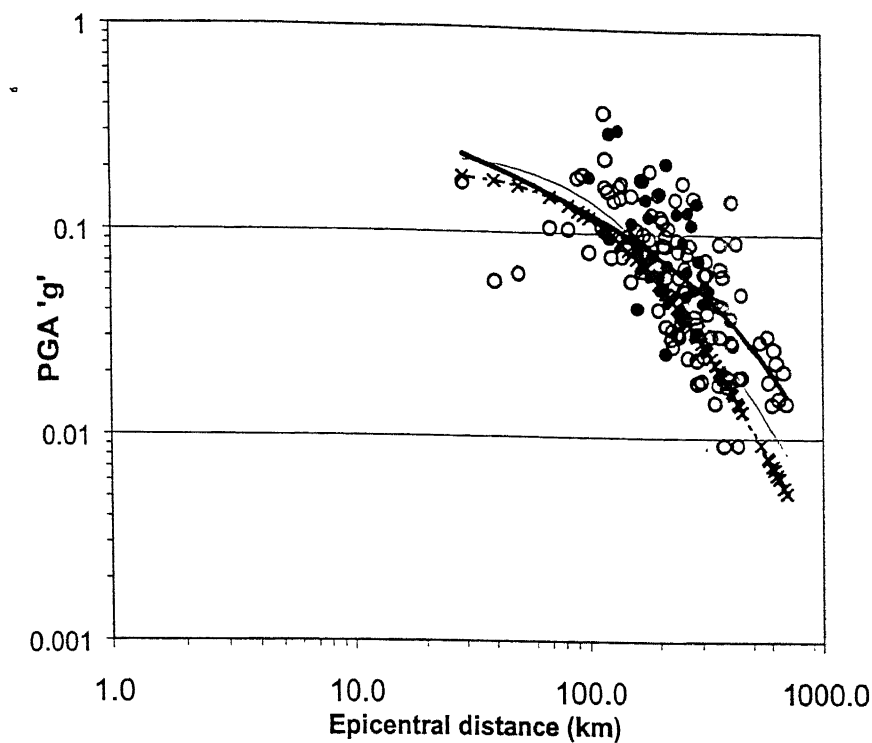


Figure 4.3(a): Distribution of peak ground acceleration for 6 August 1988, NE India earthquake and the predicted values of PGA using different relationships available for subduction zone earthquakes.

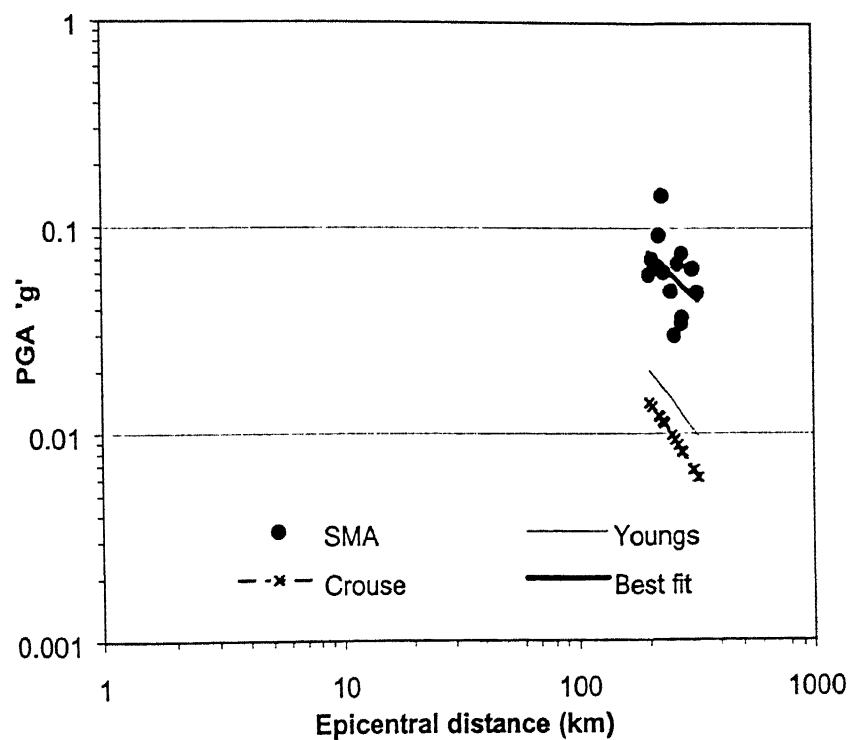


Figure 4.3(b): Distribution of peak ground acceleration for 10 January 1990, NE India earthquake and the predicted values of PGA using different relationships available for subduction zone earthquakes.

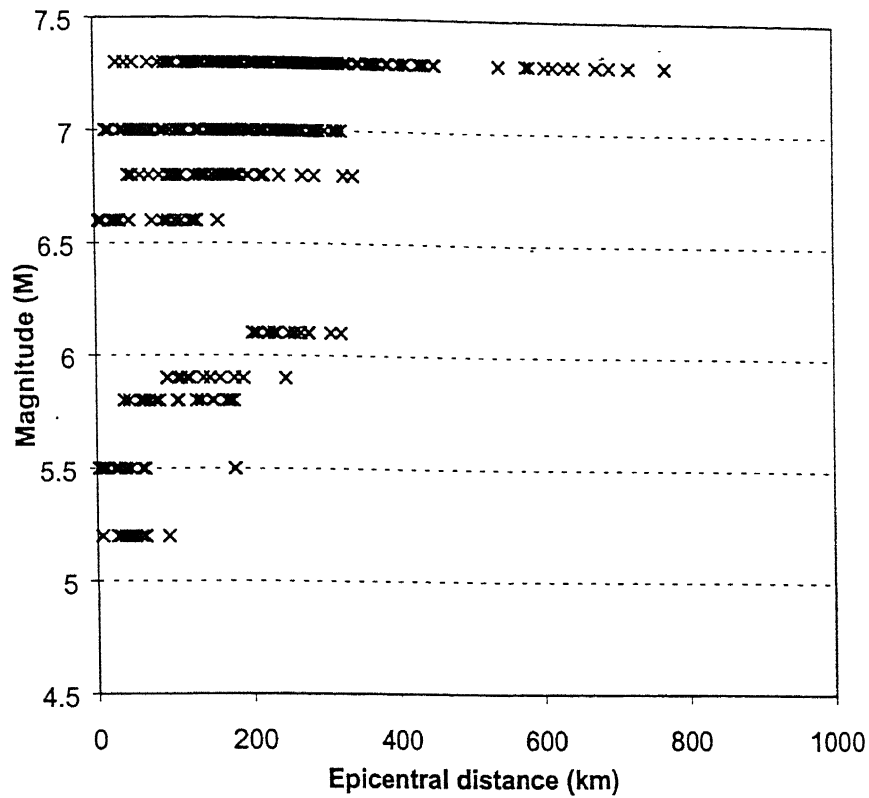


Figure 4.4: Scatter-graph of the epicentral distances from stations and magnitude of each events recorded by them.

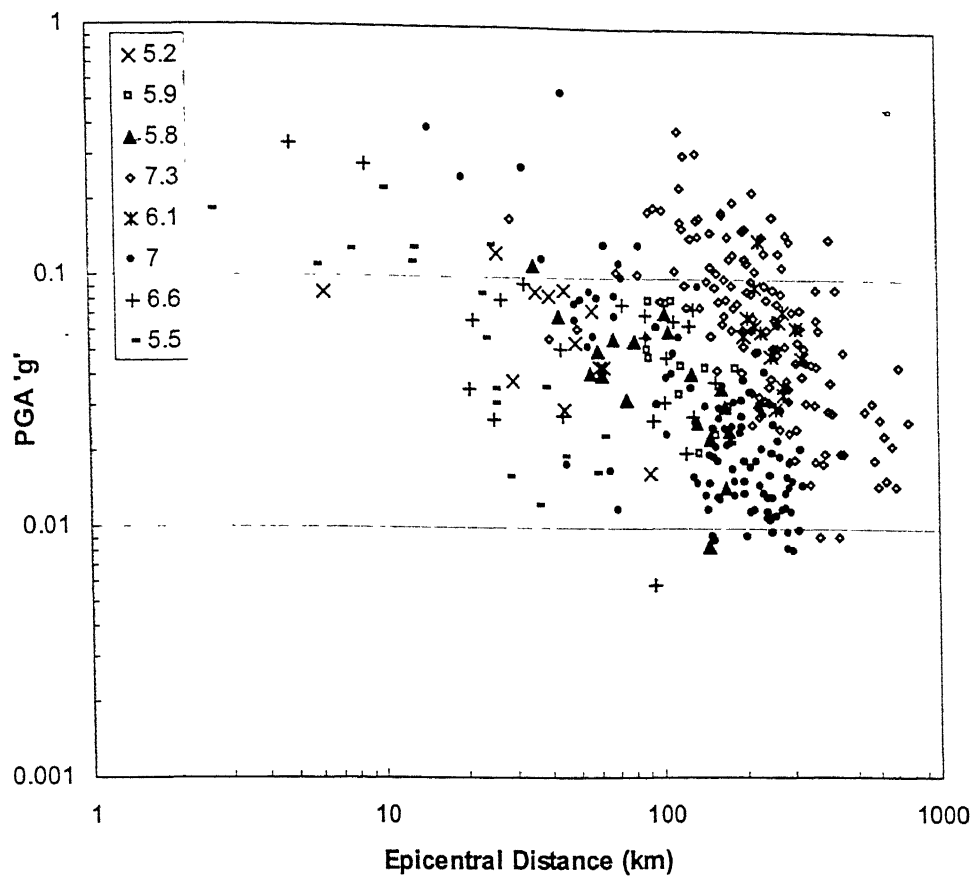


Figure 4.5: Plot of the variation of accelerations recorded in the different earthquakes. with respect to the epicentral distance. This includes database consisting accelerations from all events.

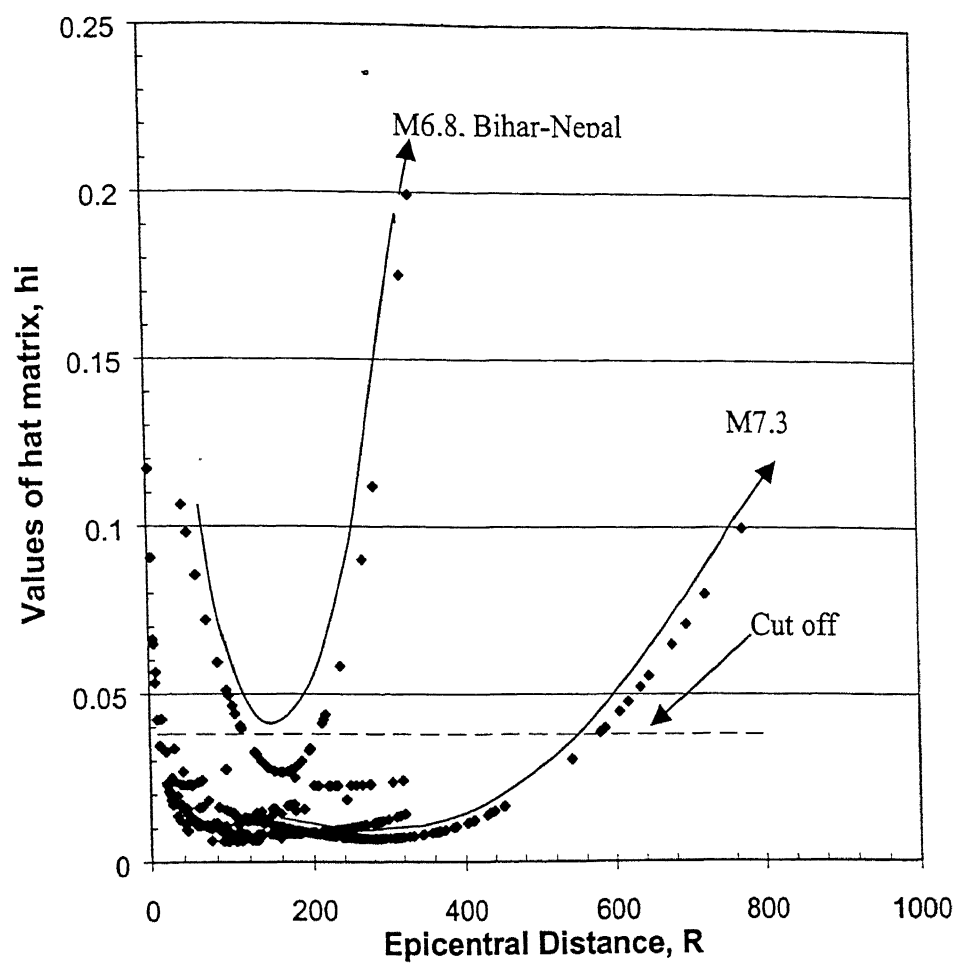


Figure 4.6: Distribution of h_i with respect to epicentral distance for the data set considered in the analysis. The dashed line gives theoretical cutoff for the data.

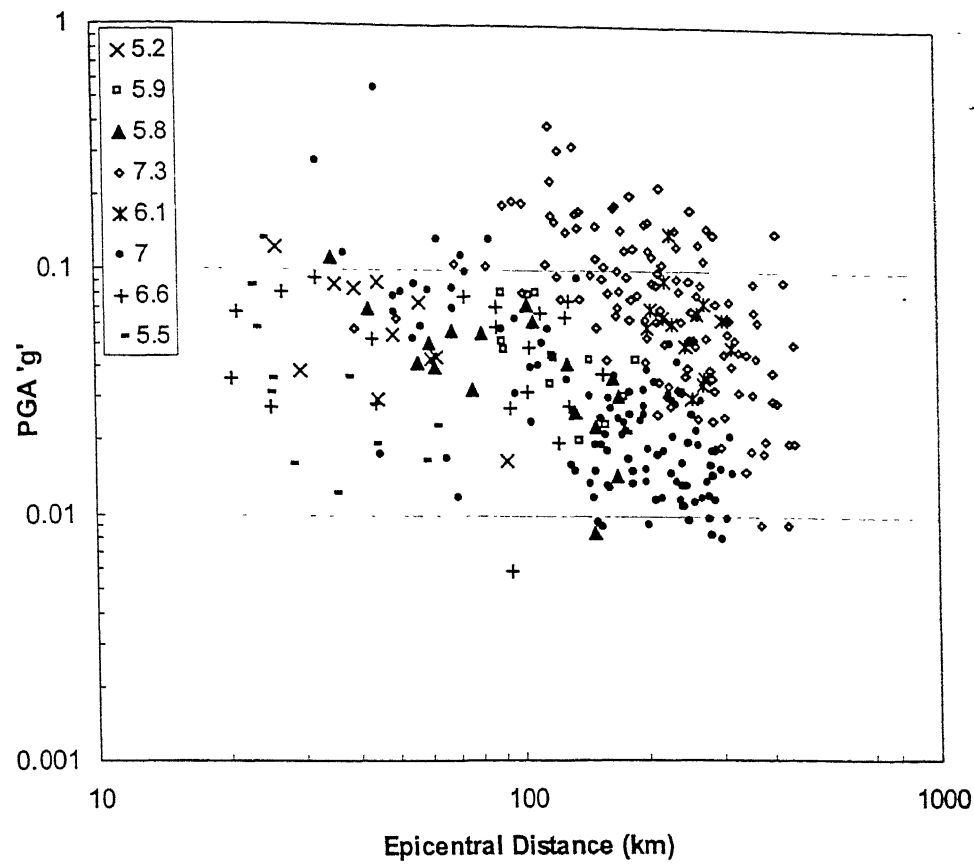


Figure 4.7: Plot of the variation of accelerations recorded in the different earthquakes. with respect to the epicentral distance. This includes database consisting accelerations from all events after removal of outliers.

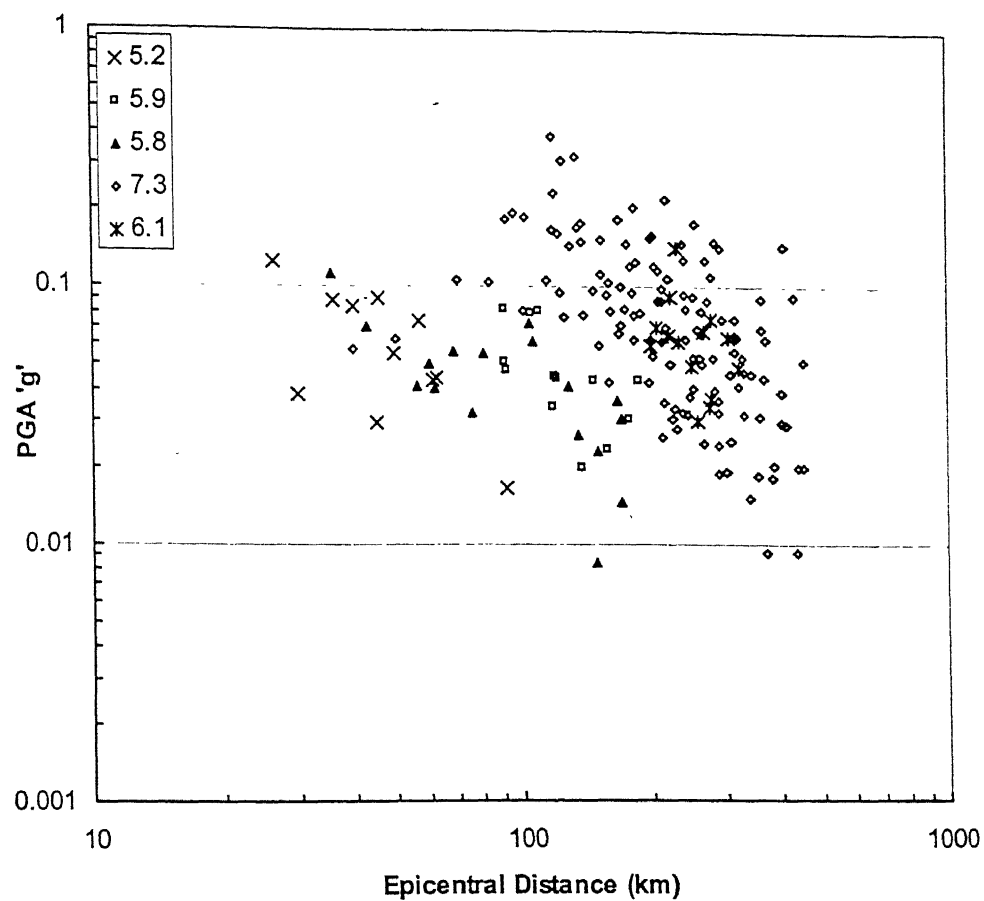


Figure 4.8: Plot of the variation of accelerations recorded in the NE Indian earthquakes with respect to the epicentral distance.

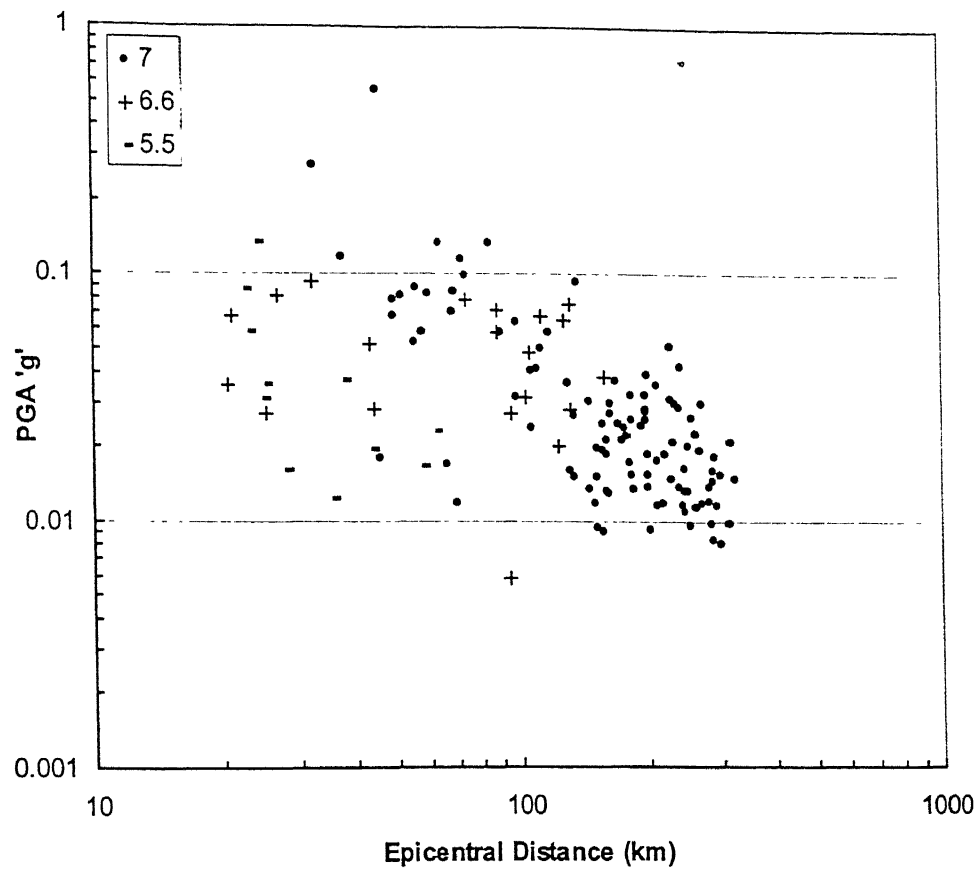


Figure 4.9: Plot of the variation of accelerations recorded in the N Indian earthquakes (Uttarkashi, Chamoli and Kangra).

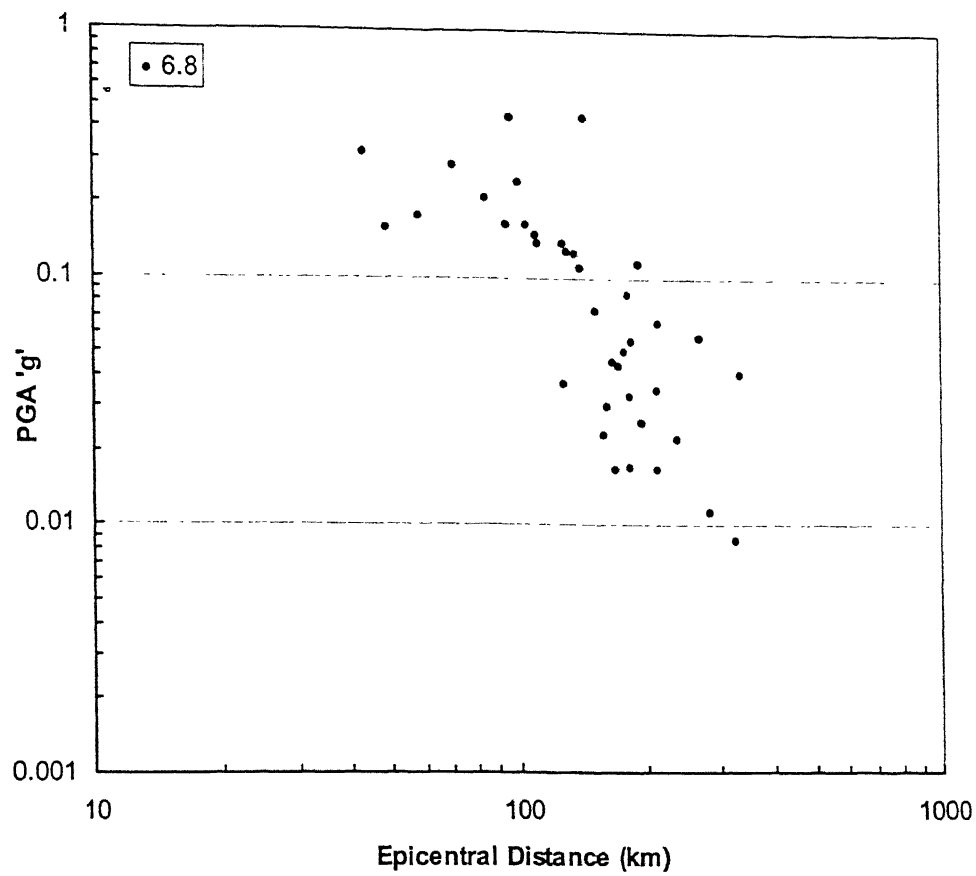


Figure 4.10: Plot of the variation of accelerations recorded in the Bihar- Nepal earthquake with respect to the epicentral distance.

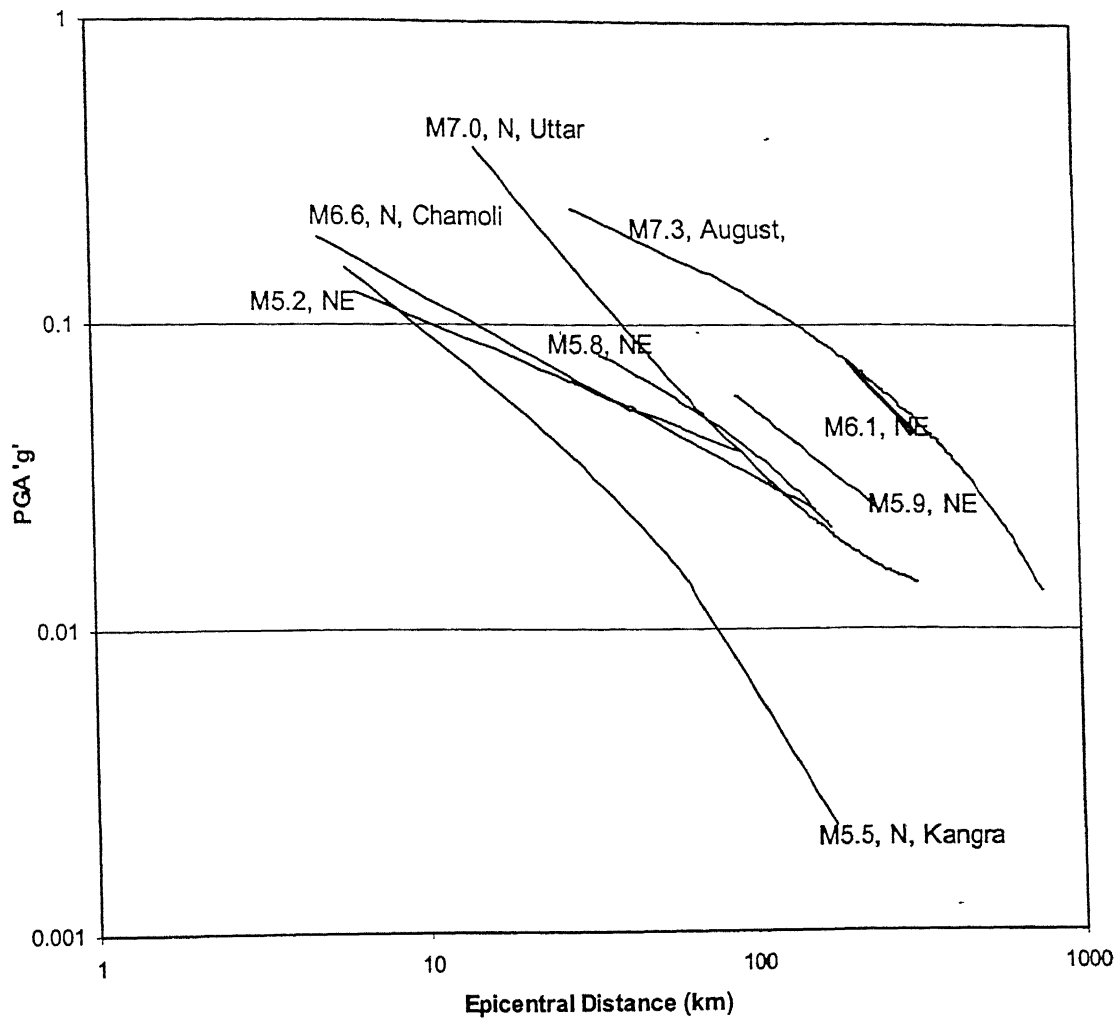
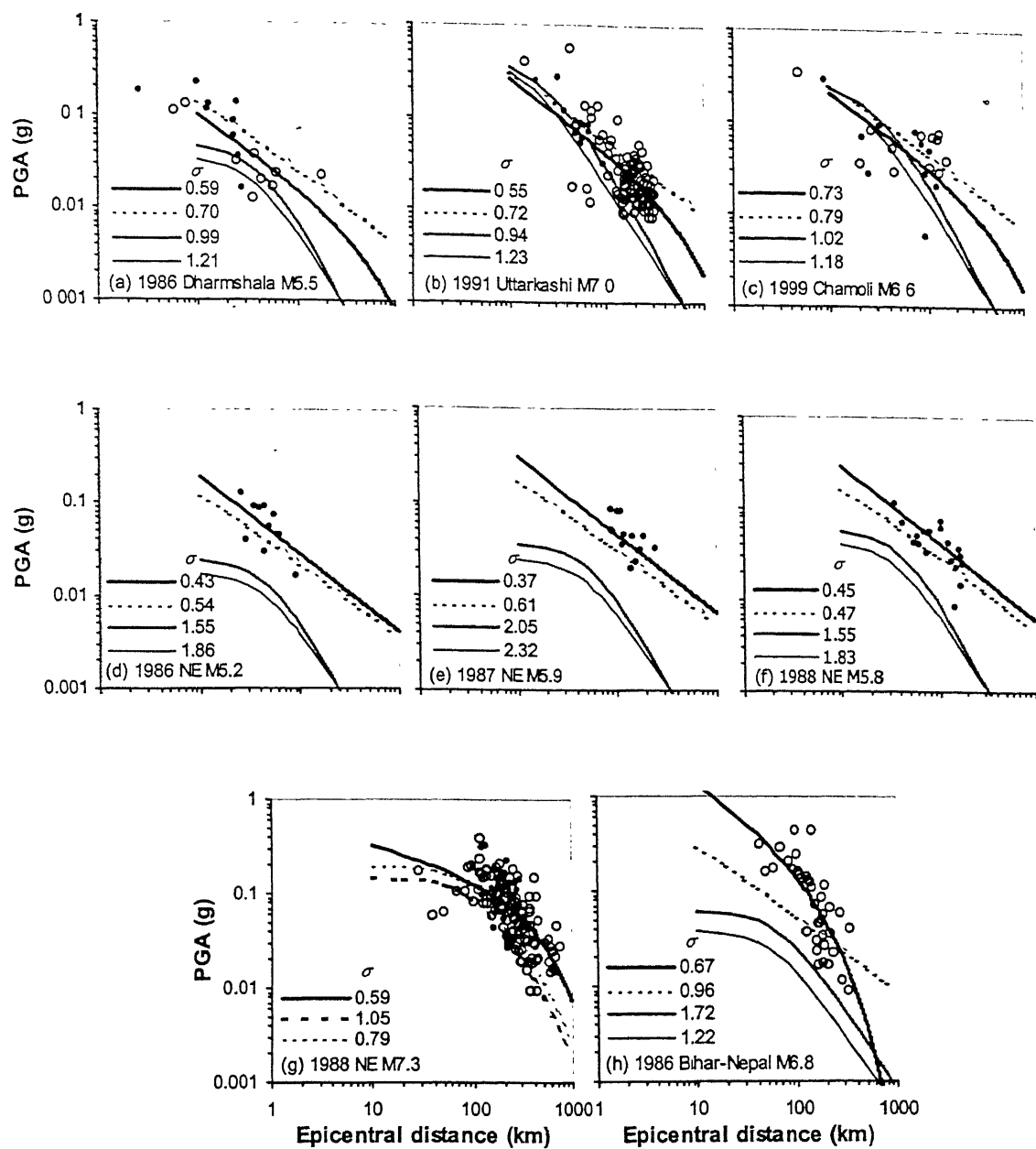


Figure 4.11: Plot of the best fit line of the accelerations recorded for each events with respect to the epicentral distance.



— Proposed, --- Boore, — Sadiq, — Campbell, --- Crouse, --- Youngs, • SMA, ° SRR.

Figure 4.12: The predicted values of acceleration using the new attenuation relationships plotted for different events along with the existing attenuation relationships.

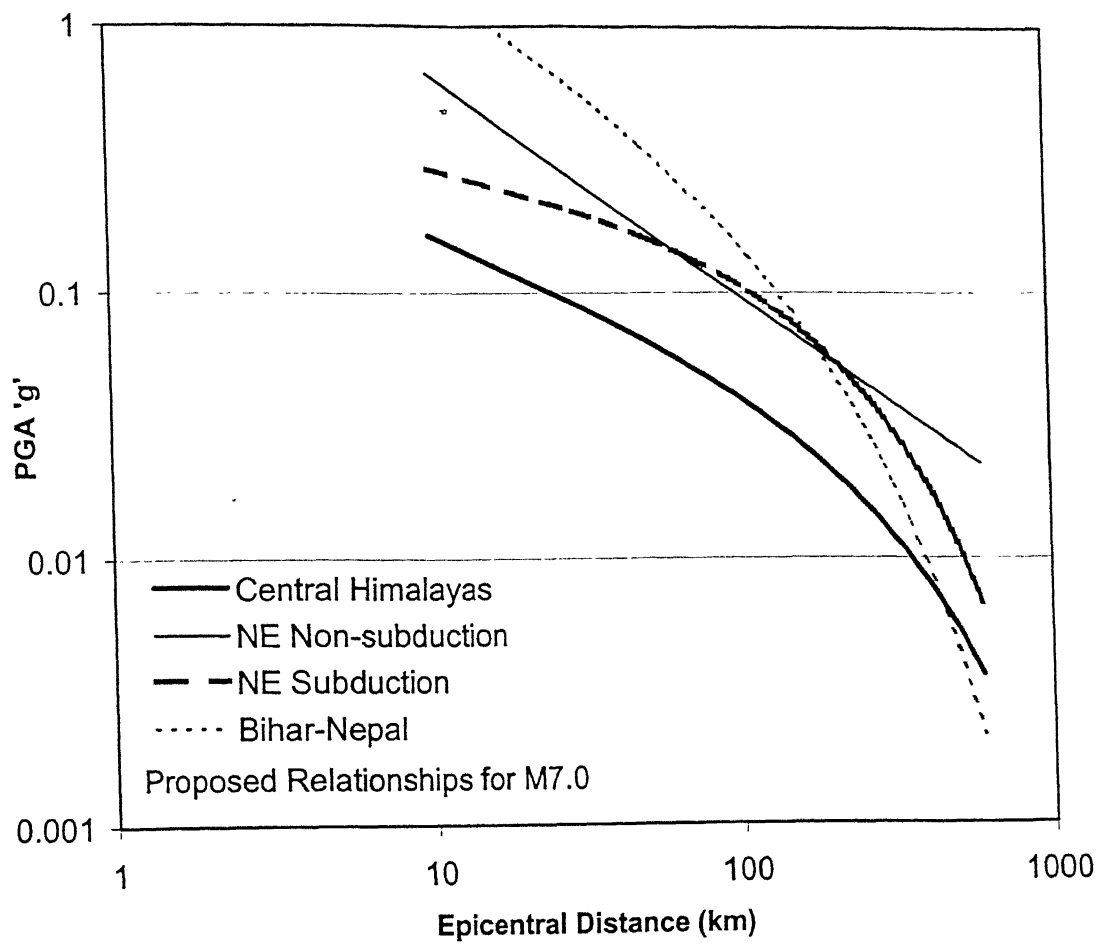


Figure 4.13 Comparison of the proposed equations for the four tectonic categories for a M7.0 event

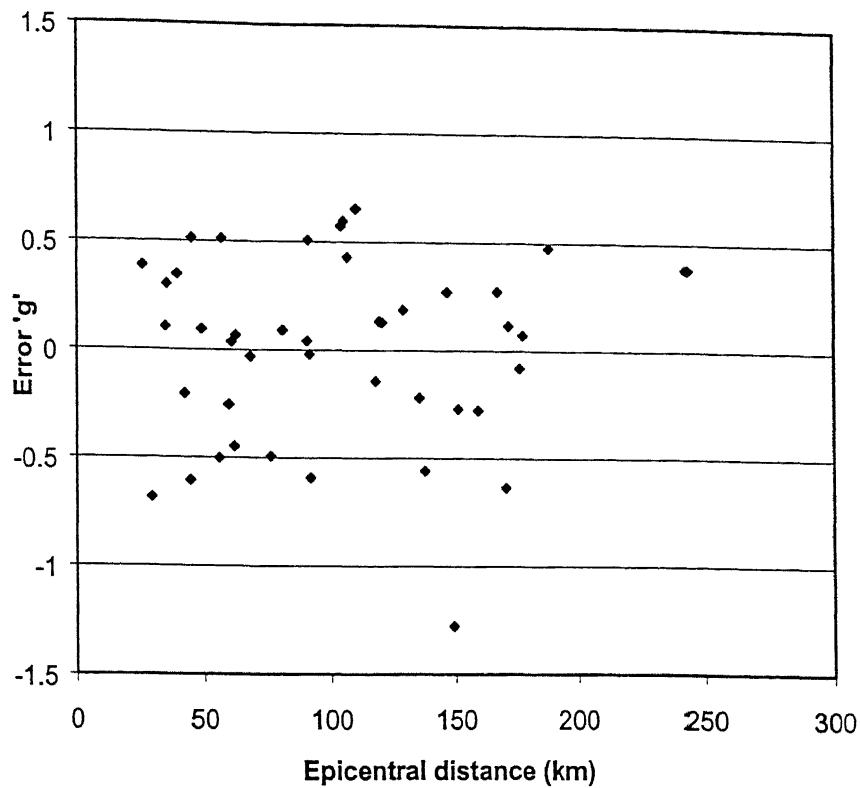


Figure 4.14: Plot of residues of the regression analysis for NE, non-subduction zone earthquakes.

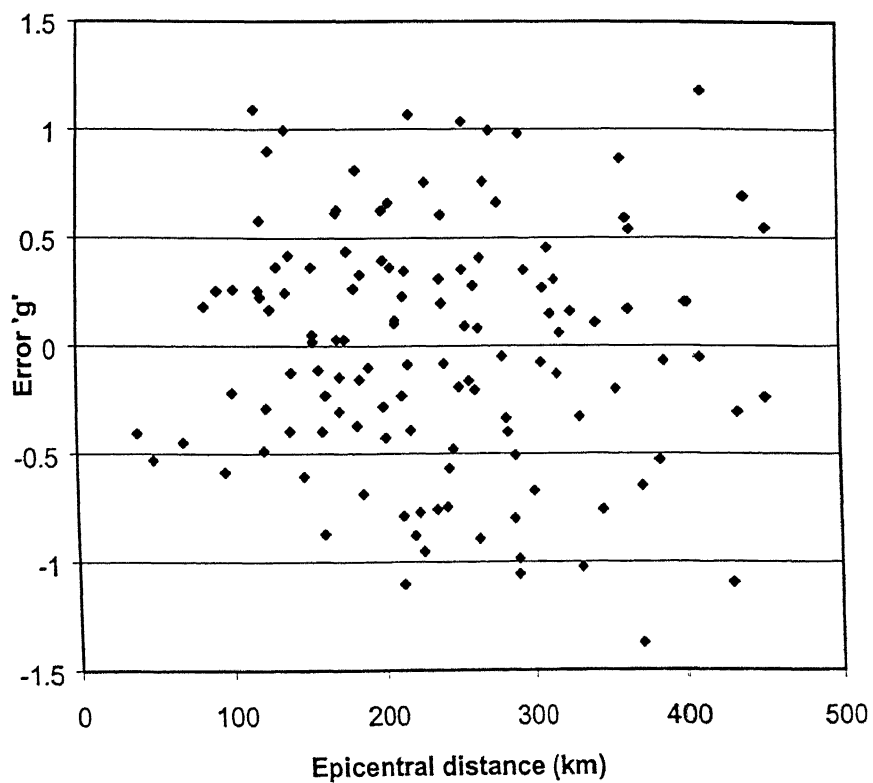


Figure 4.15: Plot of residues of the regression analysis for NE, subduction zone earthquake (August 6, 1988).

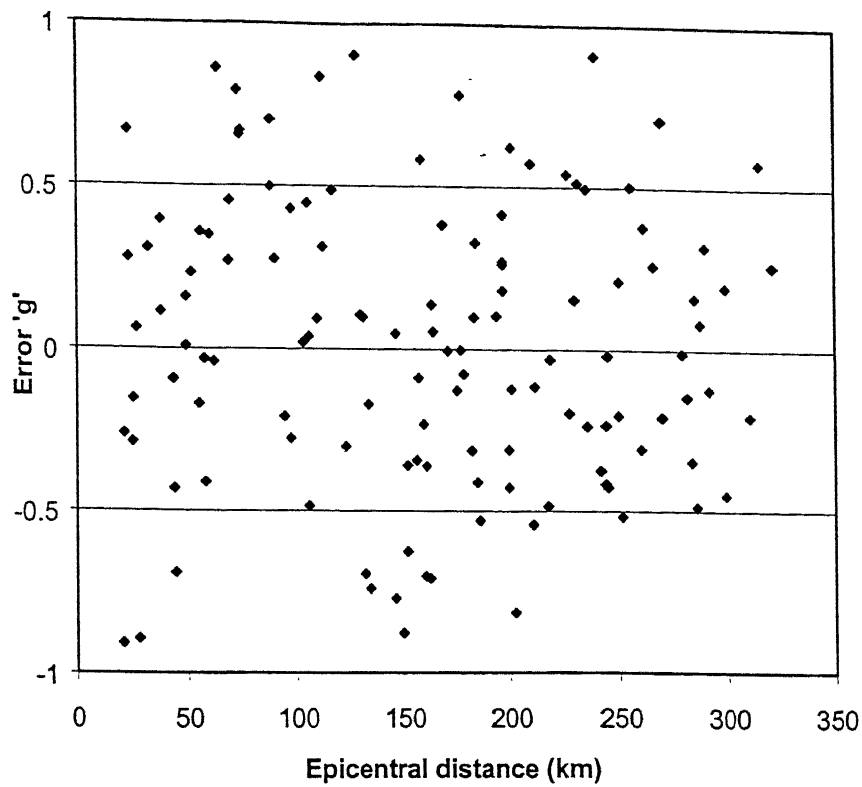


Figure 4.16: Plot of residues of the regression analysis for Central Himalayan earthquakes.

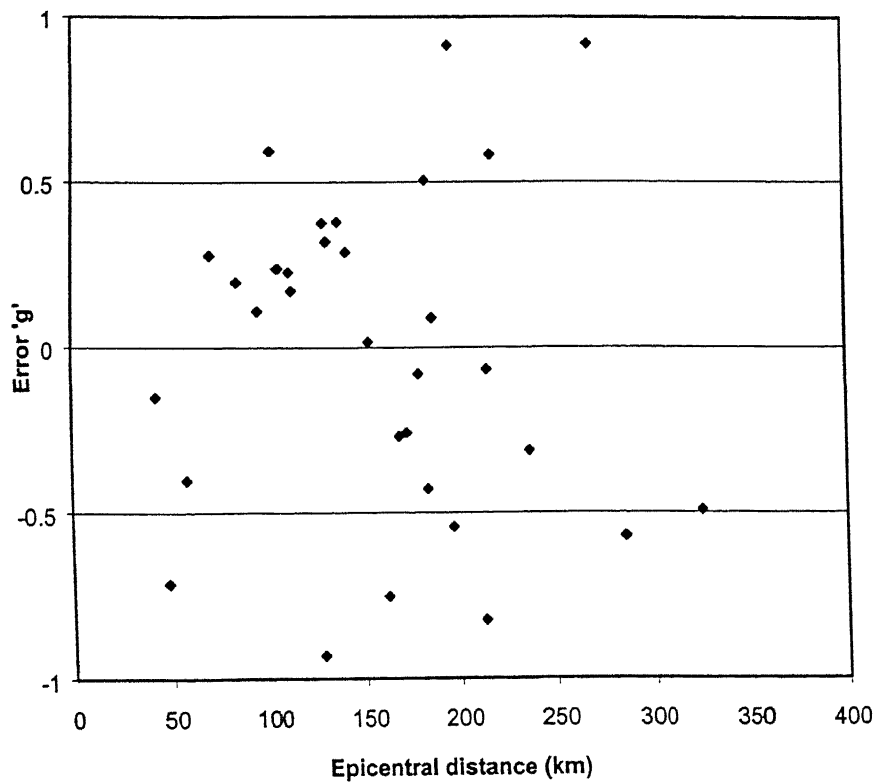


Figure 4.17: Plot of residues of the regression analysis for Bihar-Nepal earthquake

Chapter 5

Summary and Conclusions

From pre-historic times, earthquakes are considered as one of the most dreaded natural hazards. Apart from loss of human lives, earthquakes cause a lot of damage to the region in terms of collapse of dwellings, lifelines and loss of productivity. However, it is one of the few hazards, where humanity is winning the race in terms of the minimization of damages caused. This is achieved through the proper methodology followed in analysis, design, detailing and construction of structures. Estimation of reasonable level of peak ground acceleration for which the structure should be designed during an earthquake is an important step in the design process.

The available information about the attenuation of peak ground acceleration in Indian earthquakes is very limited. During the recent earthquakes in India, a large number of recordings from Structural Response Recorders have been generated as well as recordings from Strong Motion Accelerographs. The database of peak ground acceleration on Indian earthquakes can be increased if a proper method can be identified to relate the responses from structural response recorders to peak ground acceleration. The aims of the present study are as follows:

- Study the responses from Structural Response Recorders to validate their use in the analysis.
 - Study the similarity in responses obtained from Structural Response Recorders and Strong Motion Accelerographs.
 - Develop a methodology to arrive at an estimate of the peak ground acceleration at the recording site from responses recorded by Structural Response Recorders.
-

- Develop a database of peak ground accelerations observed during Indian earthquakes using the available observations from SMAs and the estimated values of peak ground accelerations from SRRs.
- Compare the attenuation of peak ground acceleration from different events with respect to the various attenuation relationships available in the literature, which are developed for different tectonic regions.
- Study the attenuation characteristics of peak ground accelerations recorded for Himalayan earthquakes for different geological regions in India and develop new attenuation relationships for peak round acceleration incorporating the data generated from the current study.

Following are the salient conclusions from the current study

- The SRR responses can be considered to come from the same sample space as that of Strong Motion Accelerograms.
- The methodology of using amplification factors of resultant spectral acceleration from Strong Motion Accelerograms to calculate the predicted values of PGA from SA values of SRRs along with the usage of correlation of responses with respect to PGA as weighing function seems to yield good results. The predicted peak ground acceleration using the methodology compares very well with the recorded PGA from Strong Motion Accelerographs.
- The amplification factors of the spectral acceleration for different natural periods of the structure indicated a decreasing trend for some natural periods and an increasing trend for some other natural periods for the same earthquake. The relationships for spectral acceleration available in the literature predict the relation of amplification factor with distance as one with a very weak negative dependence or a strong positive dependence. However, the trend predicted by these relationships is consistent for

periods 0.4sec, 0.75sec and 1.25 sec, which contradicts with the observations made for Indian earthquakes. Moreover, the correlation between epicentral distance and amplification factors was found very low. So, in the analysis of SRRs the effect of distance on amplification factors was not considered and it was taken as constant for each natural period. For SA corresponding to higher natural periods, the value of amplification factor with respect to epicentral distance is almost constant.

- The average of ratios of spectral acceleration between damping ratios of 5% and 10% critical damping for SRRs was found to lie between 1.4 to 1.5.
- The earthquakes in Himalayas can be classified into three different geographic regions with four different tectonic characteristics. The regions are Central Himalayas, Indo-Gangetic plains and North-East India. The earthquakes in North-East India can be divided into two categories. They are North East Indian Non-subduction zone earthquakes and North East Indian subduction zone earthquakes.
- Most of the available attenuation relationships underestimate the accelerations from Indian earthquakes. Attenuation relationships by Campbell, 1997 and Sadigh, 1997 significantly under-predict the ground motion (in terms of PGA) for Indian earthquakes. Boore *et al.*, 1997 relationship with assumed values of shear wave velocity gives somewhat reasonable estimates of acceleration except for Indo-Gangetic region and NE India.
- Youngs *et al.*, 1997, Crouse, 1990 equations underestimate the motions from subduction zone earthquakes in North-East India.
- Central Himalayan earthquakes produce the weakest motion while the Bihar-Nepal earthquake in the Indo-Gangetic plains has the strongest motion.
- The rate of attenuation with distance is lowest for the subduction zone earthquakes in North-East India and is highest for earthquakes in Indo-Gangetic plain.

The relationships derived for different regions in India can be summarised as follows:

Central Himalayan earthquakes

$$\ln(PGA) = -4.768 + 0.586M - 0.0032R - 0.481\ln(R); \quad \sigma = 0.597$$

Non-Subduction earthquakes in North-East India

$$\ln(PGA) = -3.441 + 0.706M - 0.828\ln(R); \quad \sigma = 0.437$$

Subduction earthquake in North-East India

$$\ln(PGA) = -0.42 - 0.004R - 0.241\ln(R); \quad \sigma = 0.578$$

Bihar-Nepal Earthquake

$$\ln(PGA) = 2.103 - 0.006R - 0.76\ln(R); \quad \sigma = 0.696$$

Due to rather limited data, the proposed relationships may be used only as first approximation for estimating ground motion.

Based on the present work the following areas are identified with scope of research and refinement.

- In the current study, only attenuation of peak ground acceleration was considered. To arrive at site dependant spectra, information about attenuation of spectral acceleration with respect to distance is very useful. The current work can be extended to derive the attenuation characteristics of the region in terms of spectral acceleration. The applicability and methodology of inclusion of recordings from Structural Response Recorders to the database of spectral accelerations computed from SMAs can also be looked into.
 - No segregation of amplification factor based on local site conditions was done. As the information on the local site conditions of SMA & SRR sites becomes available, an effort can be carried out to verify the assumption of zero correlation between amplification factor and site conditions.
-

- The effect of epicentral distance on amplification factors of spectral acceleration was not considered in the present study because it showed a trend not in line with the reported characteristics in the literature. When data of SMA from recent earthquakes becomes available, these characteristics can be verified.
- Method of least squares is used to carry out the regression analysis in the current study. However, most of the recent attenuation relationships make use of two-stage regression analysis or method of maximum likelihood for carrying out the regression analysis. These methods are reported to be more robust. When more data from the Indian earthquakes becomes available, these methods can be used to develop the attenuation relationships.
- A simple regression model was used in the current study to characterise the attenuation of acceleration. This may not give good estimate of acceleration in the near source region. To account for the data that will be obtained from near source region from future earthquakes and saturation of acceleration at near source region, a modified regression model can be used.
- As the fault parameters of the earthquakes become available, the distance terms used can be modified to account for the fault dimensions.



References

- Abrahamson N. A., and Shedlock K.M. (1997), "Overview", *Seismological Research Letters*, Vol.68, No. 1, pp.9-23.
- Abrahamson, N.A., and Litehiser, J.J. (1989), "Attenuation of Vertical Peak Acceleration", *Bulletin of the Seismological Society of America*, Vol. 79, No. 3, pp.549-579.
- Abrahamson, N.A., and Silva, W.J. (1997), "Empirical Response Spectral Attenuation Relations for Shallow Crustal Earthquakes", *Seismological Research Letters*, Vol.68, No. 1, pp.95-127.
- Abrahamson, N.A., Youngs, R.R. (1992), "A Stable Algorithm for Regression analyses Using The Random Effects Model", *Bulletin of the Seismological Society of America*, Vol. 82, No. 1, pp.505-510.
- Abramowitz M., and Stegun I.A. (1972), *Handbook of Mathematical Functions with Formulas, Graphs, and Mathematical Tables*, U.S. Department of Commerce, National Bureau of Standards, Applied Mathematics Series-55.
- Agarwal P.N., *Engineering Seismology*, Oxford & IBH publishing Co. Pvt. Ltd, 1991.
- Ambraseys, N.N. (1995), "The Prediction of Earthquake Peak Ground Acceleration in Europe", *Earthquake Engineering and Structural Dynamics*, Vol. 24, pp. 467-497.
- Atkinson, G.M., and Boore, D.M. (1997a), "Stochastic Point-Source Modeling of Ground Motions in the Cascadia Region", *Seismological Research Letters*, Vol.68, No. 1, pp.74-85.
- Atkinson, G.M., and Boore, D.M. (1997b), "Some Comparisons Between Recent Ground Motion Relations", *Seismological Research Letters*, Vol.68, No. 1, pp.24-40.
- Belsley D.A., Kuh E. and Welsch R.E. (1980), *Regression Diagnostics: Identifying Influential Data and Sources of Collinearity*, John Wiley & Sons.
- Bolt, B.A., and Abrahamson, N.A. (1982), "New Attenuation Relations for Peak and Expected Accelerations of Strong Ground Motion", *Bulletin of the Seismological Society of America*, Vol.72, No.6, pp.2307-2321.
- Bommer, J. (1999), "Seismic Hazard Assessment", *Practical Design for New and Existing Structures*, Centre for Continuing Education, Imperial College, London.
- Boore, D.M., and Joyner, W.B. (1991), "Estimation of Ground Motion at Deep Soil Sites in Eastern North America", *Bulletin of the Seismological Society of America*, Vol. 81, No. 6, pp.2167-2185.
- Boore, D.M., Joyner, W.B. and Fumal, T.E. (1997), "Equations for Estimating Horizontal Response Spectra and Peak Acceleration from Western North American Earthquakes: A Summary of Work", *Seismological Research Letters*, Vol.68, No. 1, pp.128-153.
- Caillot, V. and Bard, P.Y. (1993), "Magnitude, Distance and Site dependant spectra from Italian Accelerometric Data", *European Earthquake Engineering*, 1, pp.37-48.
-

- Campbell, K.W. (1985), "Strong Motion Attenuation Relations: A Ten -Year Perspective", *Earthquake Spectra*, Vol.1, No.4, pp.759-805.
- Campbell, K.W., and Bozorgnia, Y. (1994), "Near-Source Attenuation of Peak Horizontal Acceleration from Worldwide Accelerograms Recorded From 1957 to 1993", *Proceedings of the 5th U.S National Conference on Earthquake Engineering*, Vol III, pp.283-292.
- Campbell, W.K. (1997), "Empirical Near-Source Attenuation Relationships for Horizontal and Vertical Components of Peak Ground Acceleration, Peak Ground Velocity, and Pseudo- Absolute Acceleration Response Spectra", *Seismological Research Letters*, Vol.68, No. 1, pp.154-179.
- Chandak N.N and Jain S.K. (1994), "A Study of Strong Motion Accelerograms from Himalayan Earthquakes", Report, Department of Civil Engineering, Indian Institute of Technology, Kanpur, India.
- Chandra B., Basu S., Kumar A., Bansal M.K. (1994), "Strong motion information from structural response recorders during Uttarkashi earthquake", *Proceedings of Tenth Symposium on Earthquake Engineering, Roorkee*, pp.93-103
- Chandra B., Basu S., Kumar A., Bansal M.K, Das, J.D. (1997) "Ground Motion Characteristics from Strong Motion Instruments During April, 26 Himachal Earthquake", *Proceedings of workshop on Earthquake Disaster preparedness*, pp.19-30.
- Chandra, B., Basu S., Kumar A., Das, J.D., Bansal, M.K. (1996), "Strong Motion Studies at Department of Earthquake Engineering University of Roorkee", *Design Practices in Earthquake Geotechnical Engineering*, Swami Saran & R. Anbalagan (Eds).
- Chandra, U. (1992), "Seismotectonics of Himalaya", *Current Science*, Vol.62, Nos. 1&2, pp.40-71.
- Chandrasekaran, A.R. and Das J.D. (1994), "Analysis of Strong Motion Accelerograms of North-east Indian Earthquake of August 6, 1988", *Institution of Engineers (India) Journal*, Vol. 75, pp.1-11.
- Chandrasekaran, A.R. and Das, J.D. (1990), "Characteristics of Strong Motion Records of N.E. India", *Ninth Symposium on Earthquake Engineering, Roorkee*, Vol. 1, pp.2.23-2.32.
- Chandrasekaran, A.R., and Das, J.D. (1990), "Epicentral Evaluation from Strong Motion Data", *Proceedings of National Symposium on Recent Advances in Seismology and Their Application*, pp 1-20
- Chandrasekaran, A.R., and Das, J.D. (1992), "Strong Motion Arrays in India and Characteristics of Recent Recorded Events", *Memoir Geological Society of India*, No.23, pp.81-122.
- Clark, D., *Plane and Geodetic Surveying for Engineers*, Vol.II, 5ed, Constable & Company, London.
- Crouse, C.B. (1991), "Ground-Motion Equations for Earthquakes on the Cascadia Subduction Zone", *Earthquake Spectra*, Vol. 7, No. 2, pp.201-236.
-

- Dahle, A., Bungum, H., and Kvamme, L. (1990), "Attenuation Models Inferred from Intraplate Earthquake Recordings", *Earthquake Engineering and Structural Dynamics*, Vol. 19, pp.1125-1141.
- Dasgupta, S. (1993), "Tectono-Geologic Framework of the Eastern Gangetic Foredeep", *Bihar-Nepal Earthquake*, Special Publication 31, Geological Survey of India, pp.61-69.
- DEQ (1999), "Analysis of strong motion data of Chamoli earthquake of March 29, 1999", Earthquake Engineering Studies, EQ:99-08, Department of Earthquake Engineering, University of Roorkee.
- Draper, N.R., and Smith, H. (1998), *Applied Regression Analysis*, John Wiley & Sons.
- Fukushima, Y., and Tanaka, T. (1990), "A New Attenuation Relation for Peak Horizontal Acceleration of Strong Earthquake Ground Motion in Japan", *Bulletin of the Seismological Society of America*, Vol. 80, No. 4, pp.757-783.
- Gujarati, D. (1995), *Basic Econometrics*, McGraw-Hill Book Company
- Joyner, J.B., and Boore, D.M. (1981), "Peak Horizontal Acceleration and Velocity from strong motion Records Including Records from The 1979 Imperial Valley, California, Earthquake", *Bulletin of the Seismological Society of America*, Vol. 71, No. 6, pp.2011-2038.
- Kramer S.L., *Geotechnical Earthquake Engineering*, Prentice-Hall International Series, 1sted, 1996
- Kreyszig E., *Advanced Engineering Mathematics*, John Wiley & Sons, 4th ed, 1979.
- Loh C.H., Lee Z.K., Wu T.C. and Peng S.Y. (2000), "Ground motion characteristics of the Chi-Chi earthquake of 21 September 1999", *Earthquake Engineering and Structural Dynamics*, Vol. 29, pp.867-897.
- Miller I. and Freund J.E. (1977), "Probability and Statistics for Engineers", Prentice-Hall of India Pvt. Ltd., 2nd ed.
- Mukhopadhyay, M. (1992), "On Earthquake Focal Mechanism Studies for The Burmese Arc", *Current Science*, Vol.62, Nos. 1&2, pp.72-85.
- Newmark N.M. and Hall W.J. (1982), *Earthquake Spectra and Design*, Monograph series, EERI.
- Rajendran, K., Talwani, P., and Gupta, H.K. (1992), "State of Stress in the Indian Subcontinent: A Review", *Current Science*, Vol. 62, Nos. 1&2, pp. 86-93.
- Rajendran,K., Rajendran,C.P., Jain,S.K., Murty,C.V.R. and Arlekar,J.N. (2000), "The Chamoli Earthquake, Garhwal Himalaya: Field Observations and Implications for Seismic Hazards", *Current Science*, Vol.78, No.1, pp.45-51.
- Richter C.F., *Elementary Seismology*, Eurasia Publishing House (Pvt) Ltd., 1sted, 1969.
- Sabetta, F., and Pugliese, A. (1987), "Attenuation of Peak Horizontal Acceleration and Velocity from Italian Strong-Motion Records", *Bulletin of the Seismological Society of America*, Vol. 77, No. 5, pp.1491-1513.
- Sadigh, K., Chang, C.Y., Egan, J.A., Makdisi, F., and Youngs, R.R. (1997), "Attenuation Relationships for Shallow Crustal Earthquakes Based on California Strong Motion Data", *Seismological Research Letters*, Vol.68, No.1, pp.180-189.
-

- Sitaram, M.V.D and Saikia, M.M. (1992), "Results of a seismic network in North East India region", *Current Science*, Vol. 62, Nos. 1&2, pp. 177-182.
- Somerville, P.G., Smith, N.F., Graves, R.W., and Abrahamson, N.A. (1997), "Modification of Empirical Strong Ground Motion Attenuation Relations to Include the Amplitude and Duration Effects of Rupture Directivity", *Seismological Research Letters*, Vol.68, No.1, pp.199-222.
- Spudich, P., Fletcher, J.B., Hellweg, M., Boatwright, J., Sullivan, C., Joyner, W.B., Hanks, T.C., Boore, D.M., McGarr, A., Baker, L.M., and Lindh, A.G. (1997), "SEA96-A New Predictive Relation for Earthquake Ground Motions in Extensional Tectonic Regimes", *Seismological Research Letters*, Vol.68, No.1, pp.190-198.
- Tento, A., Franceschina, L., and Marcellini, A. (1992) "Expected Ground Motion Evaluation for Italian Sites", *Proceedings of the Tenth World Conference in Earthquake Engineering*, pp.489-494.
- Toro, G.R., Abrahamson, N.A., and Schneider, J.F. (1997), "Model of Strong Ground Motions from Earthquakes in Central and Eastern North America : Best Estimates and Uncertainties", *Seismological Research Letters*, Vol.68, No. 1, pp.41-57.
- Youngs, R.R., Chiou, S.J., Silva, W.J., and Humphrey, J.R. (1997), "Strong Ground Motion Attenuation Relationships for Subduction Zone Earthquakes", *Seismological Research Letters*, Vol.68, No.1, pp.58-73.
-

Table A1(a): Summary of strong motion data NE-India earthquake Sept.10, 1986

Sl. No.	Location	Component	Derived Maximum Peak Ground Acceleration In (cm/sec ²)	Derived Maximum Peak Ground Velocity (mm/sec)	Derived Maximum Peak Ground Displacement (mm)
1	Baithalangso	L-S 2 W	44.51	20.58	3.55
		V-VERT	24.58	10.91	4.74
		T-N 88 W	41.25	12.07	2.73
2	Dauki	L-S 72 E	87.61	32.40	3.00
		V-VERT	31.20	14.14	5.92
		T-S 8 W	88.65	37.33	2.56
3	Khliehriat	L-S 45 E	30.30	11.30	2.00
		V-VERT	1.45	7.71	1.95
		T-S 45 W	45.01	18.41	3.86
4	Mongkhlaw	L-N 80 W	53.87	33.09	9.32
		V-VERT	33.55	14.11	6.83
		T-S 10 E	90.96	48.08	5.47
5	Nongpoh	L-N 40 E	52.87	21.13	4.26
		V-VERT	32.86	11.25	2.64
		T-S 50 E	54.53	11.32	4.59
6	Nongstoin	L-N 65 E	19.01	10.04	4.90
		V-VERT	8.07	5.95	1.99
		T-S 25 E	13.59	6.48	1.66
7	Panimur	L-N 65 E	38.35	9.37	2.02
		V-VERT	22.80	5.61	1.40
		T-S 25 F	47.71	21.15	2.65
8	Pynursla	L-N 59 E	90.95	26.75	3.24
		V-VERT	29.68	9.28	3.80
		T-S 31 E	74.22	20.37	4.55
9	Saitsama	L-N 85 W	110.87	36.69	4.90
		V-VERT	60.72	20.06	3.22
		T-S 5 E	135.86	58.73	4.92
10	Ummulong	L-N 87 E	111.42	26.53	2.38
		V-VERT	47.91	14.25	3.21
		T-S 3 E	62.27	12.10	1.56
11	Umrongso	L-S 27 W	26.73	9.68	1.30
		V-VERT	13.86	7.81	2.26
		T-N 63 W	31.36	11.84	4.41
12	Umsning	L-N 45 E	99.49	28.72	3.42
		V-VERT	47.82	10.88	3.75
		T-S 45 E	74.89	25.67	3.93

Table A1(b): Summary of strong motion data NE-India earthquake May 18, 1987

Sl. No.	Location	Component	Derived Maximum Peak Ground Acceleration In (cm/sec ²)	Derived Maximum Peak Ground Velocity (mm/sec)	Derived Maximum Peak Ground Displacement (mm)
1	Baithalangso	L-S 2 W	33.59	15.53	4.15
		V-VERT	19.12	12.85	3.80
		T-N 88 W	26.26	21.56	8.11
2	Bamungao	L-N 19 W	19.42	12.22	4.24
		V-VERT	18.60	13.62	3.32
		T-S 71 W	19.37	22.00	6.78
3	Beriongfer	L-S 76 W	70.56	35.95	5.51
		V-VERT	45.19	19.24	7.47
		T-N 14 W	88.46	36.20	8.95
4	Bokajan	L-N 34 W	29.33	25.96	9.34
		V-VERT	19.43	13.20	5.25
		T-S 56 E	64.40	34.28	10.31
5	Diphu	L-N 90 E	84.33	27.69	5.80
		V-VERT	53.00	15.31	6.65
		T-S 0 W	71.93	23.92	11.54
6	Gunjung	L-N 15 E	41.39	23.04	5.55
		V-VERT	18.26	10.83	3.38
		T-S 75 E	48.4	28.56	5.51
7	Haflong	L-N 10 W	54.42	36.93	8.33
		V-VERT	14.79	12.15	3.06
		T-S 80 W	34.87	20.61	5.38
8	Hajadisa	L-S 20 W	76.95	38.07	7.50
		V-VERT	27.73	15.34	3.49
		T-N 70 W	83.86	28.07	5.00
9	Hatikhaii	L-N 40 E	30.49	14.55	5.55
		V-VERT	26.34	18.58	3.64
		T-S 50 E	37.04	17.71	3.48
10	Lalsong	L-S 45 E	41.49	32.35	7.84
		V-VERT	18.85	13.54	6.20
		T-S 4.5 W	60.07	23.69	9.42
11	Nongpoh	L-N 40 E	17.08	13.12	4.88
		V-VERT	13.75	9.55	3.13
		T-S 50 E	16.90	12.58	5.93
12	Panimur	L-N 65 E	39.14	18.00	4.10
		V-VERT	17.25	16.79	5.78
		T-S 25 E	46.43	18.11	2.99
13	Saitsama	L-N 85 E	36.40	13.92	3.36
		V-VERT	18.53	9.29	4.00
		T-S 5 E	48.53	22.84	8.91
14	Umrongso	L-S 27 W	20.01	13.79	2.76
		V-VERT	15.95	9.13	2.91
		T-N 63 W	25.02	14.5	5.69

Table A1(c): Summary of strong motion data NE-India earthquake Feb.6, 1988

Sl. No.	Location	Component	Derived Maximum PGA (cm/sec ²)	Derived Max PGV (mm/sec)	Derived Max PGD (mm)
1	Baigao	L-S 28 W	21.43	14.14	3.9
		V-VERT	9.61	11.27	3.26
		T-N 62 W	23.94	20.64	6.9
2	Baithalangso	L-S 2 W	29.59	13.65	3.81
		V-VERT	13.7	7.44	1.76
		T-S 88 W	21.78	12.26	3.33
3	Bamungao	L-N 19 W	16.04	5.08	1.3
		V-VERT	9.84	6.23	2.33
		T-S 17 W	13.05	10.35	2.3
4	Dauki	L-S 72 E	25.99	18.01	2.5
		V-VERT	30.2	8.57	3.41
		T-S 8 W	37.93	18.37	4.41
5	Gunjung	L-N 15 E	35.7	29.05	6.26
		V-VERT	19.14	12.87	3.3
		T-S 75 F	36.25	24.44	3.87
6	Haflong	L-N 10 W	33.97	19.42	3.13
		V-VERT	7.88	7.22	1.99
		T-S 80 W	26.82	14.02	3.34
7	Hatikhali	L-N 40 E	23.18	8.78	3.18
		V-VERT	20.95	7.29	1.98
		T-S 50 E	24.89	9.87	3.84
8	Katakhal	L-S 89 E	9.2	10.64	3.04
		V-VERT	9.65	9.88	4.0
		T-S 1 W	8.34	7.75	1.6
9	Khiliehriat	L-S 45 E	78.19	47.46	8.45
		V-VERT	28.93	15.91	2.94
		T-S 45 W	64.86	27.87	3.44
10	Mawphlang	L-S 35 W	79.61	43.85	7.97
		V-VERT	35.27	12.33	4.86
		T-N 55 W	57.68	24.89	10.14
11	Nongkhlaw	L-N 80 E	105.44	42.94	9.5
		V-VERT	100.76	35.1	11.23
		T-S 10 E	112.09	52.63	11.41
12	Nongpoh	L-N 40 E	26.9	15.89	4.64
		V-VERT	37.5	10.64	4.02
		T-S 50 E	84.62	26.45	3.75
13	Pynursla	L-N 59 E	48.75	21.24	4.99
		V-VERT	15.0	9.43	3.63
		T-S 31 E	30.42	11.95	4.93
14	Saitsama	L-N 85 E	64.58	22.38	4.5
		V-VERT	31.65	9.9	2.37
		T-S 5 E	57.06	32.43	4.37
15	Shillong	L-N 40 E	46.72	16.06	5.16
		V-VERT	13.41	14.42	5.19
		T-S 50 E	35.13	15.39	7.86
16	Ummulong	L-N 87 E	55.3	22.48	5.69
		V-VERT	23.74	10.89	4.37
		T-S 3 E	53.73	21.42	6.35
17	Umrongso	L-S 27 W	45.44	31.43	3.06
		V-VERT	21.68	12.26	2.38
		T-N 63 W	36.11	26.58	6.67
18	Umsning	L-N 45 E	39.01	16.62	3.14
		V-VERT	17.76	11.95	3.55
		T-S 45 E	59.74	36.73	5.03

Table A1(d): Summary of strong motion data for Aug 6, 1988 NE-India earthquake.

Sl. No.	Location	Component	Derived Maximum Peak Ground Acceleration In (cm/sec ²)	Derived Maximum Peak Ground Velocity (mm/sec)	Derived Maximum Peak Ground Displacement (mm)
1	Baigao	L-S 28 W V-VERT T-N 62 W	216.82 51.9 341.43	65.68 20.11 63.7	10.19 5.85 9.8
2	Baithalangso	L-S 2 W V-VERT T-N 88 W	150.99 80.4 162.06	75.52 36.12 117.05	12.36 6.98 15.45
3	Bamungao	L-N 19 W V-VERT T-S 71 W	91.5 64.29 68.59	64.03 25.06 49.8	8.96 4.23 10.23
4	Berlongfer	L-S 76 W V-VERT T-N 14 W	295.11 170.58 337.07	217.24 90.26 228.19	33.4 13.18 36.3
5	Bokajan	L-N 34 E V-VERT T-N 56 E	147.8 145.0 219.78	86.75 32.49 121.36	19.91 9.14 20.43
6	Cherrapunji	L-S 55 E V-VERT T-S 35 W	51.06 23.04 53.65	21.47 20.45 26.78	3.57 3.81 6.22
7	Dauki	L-S 72 E V-VERT T-S 8 W	106.6 29.88 71.7	46.87 20.74 44.53	7.56 6.52 5.78
8	Diphu	L-N 90 E V-VERT T-S 0 E	277.25 176.47 331.37	181.48 56.12 205.55	23.25 9 22.74
9	Doloo	L-S 41 E V-VERT T-S 49 W	63.05 37.94 60.99	58.89 33.83 53.49	14.4 7.63 12.61
10	Gunjung	L-N 2 E V-VERT T-S 75 E	91.88 60.98 130.21	44.19 25.56 52.05	8.54 6.74 8.58
11	Hajadisa	L-S 20 W V-VERT T-N 70 W	90.17 45.27 96.27	42.73 22.28 46.43	9.72 5.98 8.77
12	Harengajao	L-S 60 E V-VERT T-S 30 W	63.89 31.47 76.68	40.99 22.15 44.39	7.37 6.31 8.92
13	Hojai	L-S 82 W V-VERT T-N 8 W	105.68 59.71 131.05	31.88 25.25 65.61	14.06 7.83 11.61
14	Jellalpur	L-N 88 W V-VERT T-S 2 W	28.91 15.33 22.66	30.4 17.07 20.46	4.81 4.01 5.18
15	Jhirighat	L-N 47 W V-VERT T-S 43 W	95.71 30.26 87.47	88.3 30.38 70.35	11.15 8.21 10.05
16	Katain	L-S 64 E V-VERT T-S 26 W	55.8 28.12 50.25	77.76 43.21 51.09	15.87 10.89 15.71
17	Katakhal	L-S 89 E V-VERT T-S 1 W	65.55 17.6 58.28	110.74 33.72 93.56	23.34 10.11 25.26

18	Khliehriat	L-S 45 E	68.78	29.21	4.55
		V-VERT	33.83	16.11	3.44
		T-S 45 W	70.1	31.74	5.42
19	Koomber	L-S 72 E	48.24	39.04	9.86
		V-VERT	26.3	23.23	3.57
		T-S 18 W	36.02	34.88	7.14
20	Loharghat	L-N 54 E	56.78	36.58	8.58
		V-VERT	21.78	20.42	5.06
		T-S 36 E	53.42	48.61	9.91
21	Mawkyrwat	L-N 20 E	45.12	25.18	3.1
		V-VERT	31.57	17.51	4.69
		T-S 70 E	45.33	21.98	4.8
22	Mawpblang	L-S 35 W	113.14	39.37	6.78
		V-VERT	35.47	12.52	3.85
		T-N 55 W	104.75	38.99	5.34
23	Mawsynram	L-S 58 W	83.63	33.67	8.29
		V-VERT	33.17	21.45	5.89
		T-N 32 W	63.3	28.61	5.47
24	Nongkhlaw	L-N 80 E	135.35	64.5	6.02
		V-VERT	81.62	34.17	9.46
		T-S 10 E	143.47	55.66	11.07
25	Nongstoin	L-N 65 E	53.23	24.09	9.54
		V-VERT	40.84	14.8	6.14
		T-S 25 E	50.67	31.04	11.16
26	Panimur	L-N 65 E	165.44	55.19	5.29
		V-VERT	71.62	20.85	6.14
		T-S 25 E	122.41	44.38	6.06
27	Pynursla	L-N 59 E	48.41	42.13	5.92
		V-VERT	35.31	31.55	6.35
		T-S 31 E	50.37	32.24	7.22
28	Saitsama	L-N 85 E	207.04	87.31	7.83
		V-VERT	96.73	33.77	4.82
		T-S 5 E	228.28	103.63	33.89
29	Shillong	L-N 40 E	73.5	20.44	3.24
		V-VERT	35.12	9.75	3.31
		T-S 50 E	56.16	17.55	5.86
30	Silchar	L-N 60 E	63.18	71.52	21.1
		V-VERT	24.76	29.98	8.62
		T-S 30 E	89.38	98.76	21.13
31	Ummulong	L-N 87 E	98.14	30.76	7.86
		V-VERT	60.8	27.33	11.28
		T-S 3 E	149.76	43.95	12.8
32	Umrongso	L-S 27 W	76.91	51.66	6.46
		V-VERT	43.67	17.48	4.46
		T-N 63 W	79.04	39.98	7.76
33	Umsning	L-N 45 E	133.27	41.46	7.88
		V-VERT	69.78	38.31	12.5
		T-S 45 E	150.16	51.94	10.12

Table A1(e): Summary of strong motion data Jan 10, 1990 NE-India earthquake.

Sl. No.	Location	Component	Derived Maximum Peak Ground Acceleration In (cm/sec ²)	Derived Maximum Peak Ground Velocity (mm/sec)	Derived Maximum Peak Ground Displacement (mm)
1.	Baigo	L - S 28 W V - VERT T - N 62 W	55.19 15.31 41.55	15.92 5.58 11.69	3.21 2.02 2.20
2.	Baithalangso	L - S 02 W V - VERT T - N 88 W	60.33 32.49 86.41	31.45 13.59 44.83	7.46 3.97 6.00
3.	Bamungao	L - N 19 W V - VERT T - S 71 W	29.30 20.16 29.74	11.95 10.43 13.72	2.70 3.28 4.33
4.	Berlongfer	L - S 76 W V - VERT T - N 14 W	142.04 61.50 138.49	79.55 32.91 95.26	10.75 5.23 16.17
5.	Diphu	L - N 90 E V - VERT T - S 00 W	89.83 52.10 91.10	47.31 18.04 38.50	4.89 4.57 9.98
6.	Gunjung	L - N 15 E V - VERT T - S 75 E	49.65 18.29 70.17	24.65 8.17 24.85	3.06 1.85 5.87
7.	Hajadisa	L - S 20 W V - VERT T - N 70 W	53.53 23.62 84.57	21.78 7.88 26.55	2.61 2.69 3.31
8.	Hojai	L - S 82 W V - VERT T - N 08 W	40.51 18.36 31.61	15.49 8.61 15.44	2.94 2.09 6.44
9.	Laisong	L - S 45 E V - VERT T - S 45 W	60.86 25.72 55.39	22.82 9.92 15.61	3.89 2.48 2.68
10.	Maibang	L - N 87 E V - VERT T - S 03 E	62.43 26.99 64.71	30.85 8.38 19.18	6.41 1.86 4.61
11.	Panimur	L - N 65 E V - VERT T - S 25 E	75.28 22.49 56.52	19.68 8.32 15.99	3.00 2.49 3.11
12.	Saitsama	L - N 85 E V - VERT T - S 05 E	60.99 35.83 63.41	27.59 10.64 26.00	1.88 2.40 2.98
13.	Ummulong	L - N 87 E V - VERT T - S 03 E	44.80 18.65 50.28	9.64 6.08 12.13	1.87 1.87 2.26
14.	Umrongo	L - S 27 E V - VERT T - N 63 W	35.21 18.35 32.01	17.76 8.03 25.76	4.07 2.85 3.43

Table A1(f): Summary of strong motion data for October 20,1991 Uttarkashi earthquake.

Sl. No.	Location	Component	Derived Maximum Peak Ground Acceleration In (cm/sec ²)	Derived Maximum Peak Ground Velocity (mm/sec)	Derived Maximum Peak Ground Displacement (mm)
1.	Almora	L - N 53 W V - VERT T - N 37E	17.41 18.44 21.02	13.32 15.48 12.62	3.42 3.98 4.50
2.	Barkot	L - N 10E V - VERT T - N 80 E	93.18 43.65 80.47	57.87 27.53 44.84	10.93 5.62 6.98
3.	Bhatwari	L - N 85E V - VERT T - N 05 W	248.37 288.78 241.89	178.73 133.65 297.78	37.54 23.53 53.23
4.	Ghansiali	L - N 00 E V - VERT T - N 90 E	115.59 99.23 114.89	80.44 95.94 78.21	13.57 25.90 13.37
5.	Karnprayag	L - N ---- V - VERT T - N ----	60.99 25.96 77.35	36.90 14.98 37.30	5.90 2.17 4.02
6.	Kosani	L - N 25 E V - VERT T - N 65 E	28.34 11.04 31.50	18.82 9.17 15.55	3.77 2.41 2.86
7.	Koteshwar	L - N 30 E V - VERT T - N 60 E	98.85 74.34 65.23	51.55 85.25 39.27	11.41 20.47 6.78
8.	Koti	L - N 10 E V - VERT T - N 80 E	20.64 14.26 40.95	23.43 17.65 28.60	4.27 5.05 3.40
9.	Purola	L - N 65 E V - VERT T - N 25 E	73.95 51.74 91.68	48.13 25.57 45.91	8.44 4.49 9.22
10.	Rudraprayag	L - N ---- V - VERT T - N ----	52.29 44.13 50.76	20.70 17.92 27.06	7.85 3.83 4.01
11.	Srinagar	L - N ---- V - VERT T - N ----	65.44 33.09 49.45	19.45 35.25 20.20	5.86 7.62 5.07
12.	Tehri	L - N 63 E V - VERT T - N 27 E	71.41 57.82 61.13	42.15 88.41 92.30	8.17 23.68 19.84
13.	Uttarkashi	L - N 15 E V - VERT T - N 75 E	237.27 192.62 303.99	169.56 141.56 194.68	21.15 22.98 19.85

Table A1(g): Summary of strong motion data for march 29,1999 Chamoli (U.P. hills) earthquake .

Sl. No.	Location	Component	Derived Maximum Peak Ground Acceleration In (cm/sec ²)	Derived Maximum Peak Ground Velocity (mm/sec)	Derived Maximum Peak Ground Displacement (mm)
1.	Almora	L - N 53W	26.17	23.50	3.70
		V - VERT	26.89	12.70	0.90
		T - N 37E	27.74	18.90	3.00
2.	Barkot	L - N 10E	16.88	8.30	0.40
		V - VERT	19.59	7.70	0.30
		T - N 80 E	22.26	12.40	0.50
3.	Chinyalisaur	L - N43 E	50.65	31.20	2.50
		V - VERT	48.64	31.40	2.70
		T - N 47 W	43.92	33.10	3.10
4.	Ghansiali	L - N 00 E	71.42	33.10	5.00
		V - VERT	38.74	20.00	5.30
		T - N 90 E	81.84	40.80	0.70
5.	Gopeshwar	L - N 70 W	195.08	225.50	52.20
		V - VERT	153.73	75.00	20.90
		T - N 20 E	352.83	453.10	122.80
6.	Joshimath	L - N 80 E	69.55	31.80	5.50
		V - VERT	40.45	27.20	3.50
		T - N 10 W	62.28	89.40	23.20
7.	Lansdown	L - N 70 E	5.24	1.80	0.20
		V - VERT	11.01	2.50	0.10
		T - N 20 W	6.32	2.10	0.10
8.	Roorke	L - N 55 W	55.39	42.80	8.70
		V - VERT	17.25	12.20	2.70
		T - N 35 E	45.89	32.90	5.50
9.	Tehri	L - N 63 W	53.43	46.00	4.70
		V - VERT	33.54	21.10	3.20
		T - N 27 E	61.06	53.80	6.40
10.	Ukhimath	L - N 15 E	89.06	68.50	12.90
		V - VERT	46.45	40.50	8.50
		T - N 75 W	94.71	54.50	17.40
11.	Uttarkashi	L - N 15 W	52.74	35.50	4.50
		V - VERT	22.22	15.80	3.60
		T - N 75 E	62.32	46.70	7.00

Table A1(h): Summary of strong motion data, March 29,1999 Kangra (U.P. hills) earthquake.

Sl. No.	Location	Component	Derived Maximum Peak Ground Acceleration In (cm/sec ²)	Derived Maximum Peak Ground Velocity (mm/sec)	Derived Maximum Peak Ground Displacement (mm)
1	Bandlakhas	L-S 27 E	142.49	83.13	20.08
		V-VERT	22.07	15.63	6.33
		T-N 63 E	122.36	50.75	5.85
2	Baroh	L-N 25 W	57.56	36.8	6.55
		V-VERT	22.31	15.07	3.64
		T-N 65 E	56.17	27.62	4.58
3	Bhawarna	L-N 82 E	36.49	11.7	2.73
		V-VERT	35.36	9.34	21.13
		T-N 8 W	34.72	19.21	4.2
4	Dharnsala	L-N 76 W	172.21	72.97	7.76
		V-VERT	80.94	27.39	4.19
		T-N 14 E	182.89	94.9	24.79
5	Jawali	L-S 86 W	14.87	19.2	4.9
		V-VERT	10.81	14.39	7.53
		T-N 4 W	16.55	15.18	9.56
6	Kangra	L-N 43 W	144.97	50.57	5.23
		V-VERT	70.77	31.93	5.37
		T-N 47 E	109.43	95.75	9.62
7	NagrotaBagwan	L-S 85 W	145.53	94.17	13.09
		V-VERT	49.73	18.19	6.51
		T-N 5 W	78.59	25.4	6.14
8	Shahpur	L-N 75 E	200.17	59.21	7.26
		V-VERT	64.31	28.04	5.25
		T-N 15 W	243.2	147.8	10.85
9	Sihunta	L-N 25 W	50.41	26.72	4.71
		V-VERT	38.25	27.73	4.74
		T-N 65 E	35.32	33.88	3.67

Table A2 (b): SMA stations installed in Uttarpradesh array and their geographical coordinates

Sl No:	Station	Longitude		Latitude	
		Deg.	Min.	Deg.	Min.
1	Almora	79	66	29	58
2	Bageswar	79	77	29	83
3	Barkot	78	22	30	80
4	Bhatwari	78	62	30	81
5	Chak	77	88	30	70
6	Chamoli	80	10	29	32
7	Chau	79	36	29	85
8	Chinsyali	78	34	30	56
9	Didihat	80	27	29	80
10	Gwal	79	58	30	2
11	Haldwani	79	54	29	22
12	Kapk	79	90	29	95
13	Karnaprayag	79	24	30	26
14	Kosani	79	72	29	68
15	Koteswar	78	58	30	23
16	Koti	77	80	30	59
17	Lansdowne	78	71	29	84
18	Nainital	79	46	29	38
19	Pithogarh	80	22	29	57
20	Purola	78	10	30	88
21	Ramnagar	79	12	29	39
22	Ranikhet	79	43	29	63
23	Rati	79	49	29	48
24	Roorkee	79	0	30	28
25	Srinagar	78	78	30	23
26	Uttarklashi	78	46	30	73

Table A2(c): SMA stations installed in Kangra array and their geographical coordinates

Sl No:	Station	Longitude		Latitude	
		Deg.	Min.	Deg.	Min.
1	Aghar	76	34	31	36
2	Bagsiad	77	7	31	33
3	Bagi	77	33	31	14
4	Bajaura	77	9	31	50
5	Bali	77	16	31	41
6	Bandlakhas	76	32	32	7
7	Baroh	76	18	31	59
8	Bhajradu	76	9	32	50
9	Bhawarna	76	29	32	2
10	Bir	76	43	32	2
11	Chamba	76	7	32	33
12	Choridhar	77	18	31	21
13	Chuwarikhas	76	1	32	25
14	Dadasiba	76	5	31	55
15	Dalash	77	25	31	23

16	Dalhousie	75	58	32	32
17	Dharmpur	76	45	31	48
18	Dharmsala	76	19	32	12
19	Drang	76	56	31	48
20	Chumarwin	76	42	31	26
21	Hamirpur	76	31	31	41
22	Jawali	76	0	32	8
23	Jhatingri	76	53	31	56
24	Jhungi	77	5	31	25
25	Kangra	76	15	32	5
26	Kotla	76	3	32	14
27	Kulu	77	6	31	57
28	Kunihar	76	56	31	4
29	Ladbharol	76	42	31	56
30	Lambagaon	76	33	31	53
31	Nadaun	76	20	31	46
32	Nagrota Bagwan	76	22	32	6
33	Nagrota Bagwan	76	5	32	3
34	Namhol	76	52	31	15
35	Nurpur	75	53	32	18
36	Pandoh	77	3	31	40
37	Patlander	76	32	31	46
38	Pragpur	76	12	31	49
39	Rakh	76	14	32	28
40	Rewalsar	76	50	31	37
41	Rirkmar	76	11	32	18
42	Sandhu	77	22	31	9
43	Sarkaghat	76	44	31	42
44	Shahpur	76	11	32	12
45	Shimla	77	13	31	6
46	Sihunta	76	5	32	18
47	Sundernagar	76	54	31	33
48	Sundla	76	2	32	40
49	Sunni	77	7	31	14
50	Surani	76	20	31	53

Table B1(a): Recorded SRR values and the predicted PGA's for August 6, 1988 N-E India earthquake

Sl. No.	Station	Dist. (km)	accelerations in %g						PGA
			5% damping			10% damping			
			0.4 sec	0.75sec	1.25sec	0.4sec	0.75sec	1.25sec	
1	Along	308.2	8.18	2.89	1.23	6.22	1.57	0.74	2.53
2	Bilat	288.0	11.29	3.49	2.41	8.99	1.56	1.73	3.64
3	Choukham	303.7	6.89	2.58	1.5	5.26	1.57	0.56	2.24
4	Daring	275.5	10.12	2.76	0.93	9.89	4.22	0.92	3.59
5	Hapoli	258.1	27.43	6.23	2.05	15.66	4.06	2.26	6.87
6	Itanagar	221.4	13.75	5.49	5.6	9.53	3.56	2.41	5.07
7	Khonsa	198.6	8.46	5.45	4.5	5.07	5.06	3.64	4.25
8	Oyan	343.9	4.5	1.09	1.06	3.59	0.89	0.82	1.50
9	Pangin	319.9	12.61	4.41	1.53	11.32	2.59	1.19	4.10
10	Pasighat	301.3	5.29	2.2	0.85	5.13	1.31	0.65	1.90
11	Roing	332.7	10.27	1.86	1.9	9.52	1.28	0.94	3.16
12	Yembeung	265.1	7.7	2.02	1.34	5.98	1.86	1.08	2.48
13	Abhayapuri	402.9	7.76	4.36	2.45	4.76	3.61	1.01	2.98
14	Amguri	157.8	25.67	26.42	10.78	15.4	11.64	5.68	11.89
15	Badarpur	224.9	4.42	3.92	3.98	3.92	2.93	3.31	3.07
16	Badulipur	139.9	21.26	7.2	7.81	17.71	5.14	2.87	7.76
17	Barpathar	119.4	42.3	23.15	35.14	37.96	22.17	14.74	23.20
18	Barpeta	364.1	28.8	5.7	5.26	23.56	6.16	3.49	9.05
19	Bihpuria	184.5	60.99	22.14	9.38	46.54	18.83	7.43	20.39
20	Bijini	404.2	16.85	9.28	6.04	8.45	4.73	1.5	5.69
21	Bijoynagar	289.0	3.49	5.14	2.06	2.56	2.58	2.52	2.43
22	Bilasipara	440.0	5.61	2.3	0.71	4.41	2.35	0.67	1.99
23	Bokakhat	171.8	27.43	18.59	5.25	20.27	6.67	3.93	10.00
24	Bongaigaon	411.0	54.93	22.05	3.39	30.06	12.11	1.96	14.57
25	Dangari	285.2	28.29	14	7.18	19.52	8.93	2.78	9.88
26	Bergaon	160.6	32.88	10.12	4.63	29.23	6.61	2.69	10.51
27	Dhakiajuli	251.5	13.31	4.46	2.21	5.91	4.74	1.93	4.02
28	Dhemaji	239.1	25.79	11.27	8.56	18.73	7.06	3.88	9.38
29	Dhing	236.3	50.31	13.45	7.68	34.91	11.57	4.19	14.85
30	Digboi	243.7	6.98	2.59	1.56	7.7	2.85	1.53	2.97
31	Diphu	118.0	95.41	63.29	15.66	81.45	46.54	12.41	38.98
32	Doomdooma	264.1	24.43	7.57	3.09	23.74	4.36	2.51	8.05
33	Dudhnoi	378.3	8.69	4.74	1.3	4.62	1.73	0.98	2.64
34	Dullabchera	235.3	8.1	9.77	3.76	7.11	2.32	0.89	3.88
35	Furkating	129.7	27.72	29.35	10.08	25.88	16.19	6	14.47
36	Goalparag	398.9	8.73	3.75	3.44	2.97	1.98	3.11	3.09
37	Golaghat	135.8	65.11	18.48	6.98	32.6	12.32	6.68	17.05
38	Guwahati	290.5	4.5	2.18	1.16	3.61	2.21	1	1.87
39	Haflong	152.6	12.93	14.72	1.06	12.75	6.52	0.85	5.88
40	Hailakandi	213.0	29.09	11.58	5.69	12.63	8.82	4.15	8.81
41	Hojai	181.7	32.79	8.61	6.81	15.53	5.73	6.78	9.49
42	Jamugiri	214.0	23.74	10.11	8.92	15.96	8.32	8.32	9.81
43	Jorhai	154.0	42.57	16.66	8.97	32.24	15.15	7.17	15.38
44	Kamargaon	148.0	25.6	17.64	3.94	20.04	9.7	2.91	9.74
45	Kampur	208.0	31.42	19.68	5.72	19.88	14.52	3.18	11.55
46	Karimganj	227.0	16.06	0	3.05	0	5.76	2.38	3.38
47	Koliabar	199.6	29.87	34.19	8.89	22.94	21.84	7.01	15.68
48	Kukichera	228.3	7.4	3.54	1.4	6.67	2.17	1.3	2.80
49	Lakhipur	413.9	10.74	12.9	4.91	12.9	4.06	2.2	5.95
50	Lalaghat	214.5	9.63	4.36	1.9	6.4	1.59	3.66	3.54

51	Lanka	169.4	19.65	7.18	4.47	11.47	4.84	4.79	6.61
52	Ledo	247.6	13.03	3.17	1.08	10.12	2.67	0.91	3.74
53	Likhapani	244.8	8.14	3.65	1.81	6.54	2.81	2.02	3.17
54	Lumding	121.9	49.19	21.41	9.61	33.7	12.22	5.44	16.05
55	Mairabari	255.6	65.85	17.27	6.04	40.66	13.27	5.51	17.86
56	Makum	247.8	25.56	10.21	7.68	15.36	3.73	1.25	7.63
57	Mangaldai	290.3	9.6	4.99	0.67	6.72	4.24	0.55	3.24
58	Marghetia	237.8	8.18	3.33	3.41	3.94	2.84	3.1	3.24
59	Mariani	139.2	42.23	30.59	10.31	32.48	19.01	7.07	17.61
60	Nagora	118.6	48.54	19.51	9.61	38.18	12.26	7.76	16.86
61	Maharkatiya	213.3	19.52	7.71	4.16	10.36	5.95	2.73	6.21
62	Nazira	169.7	56.72	25.93	9.11	34.91	16.62	7.26	18.39
63	Nilbagan	101.2	23.61	8.92	5.14	19.95	5.69	2.52	8.10
64	N.Lakhimpur	204.5	37.61	9.86	5.92	32.21	7.82	4.82	12.15
65	Paneri	295.1	13.22	3.26	1.19	4.92	1.6	0.66	2.87
66	Rangia	311.1	16.51	2.82	7.62	11.92	2.41	6.71	6.37
67	Rangpara	241.3	19.88	8.83	6.46	16.87	5.95	6.28	8.29
68	Sarupeta	365.4	19.69	8.81	5.31	10.83	4.65	4.97	6.83
69	Shilapatha	271.8	21.15	13.74	2.32	17.21	13.8	2.61	8.82
70	Sibsagar	174.8	16.43	6.57	8.63	13.09	6.09	9.89	8.26
71	Silghat	208.0	19.18	14.67	6.3	13.67	11.5	4.76	8.91
72	Silichar	186.7	28.75	14.6	9.86	19.34	12.17	10.91	12.48
73	Sonapur	315.9	12.83	10.8	6.64	11.08	10.03	5.51	7.50
74	Subankhat	346.9	15.75	2.69	5.19	6.02	1.9	4.36	4.58
75	Tezpur	219.3	26.33	10.79	8.78	19.57	11.07	6.9	10.73
76	Tinsukia	243.1	13.35	5.75	9.28	8.48	3.7	6.12	6.22
77	Titabar	137.9	41.38	18.9	9.85	29.6	11.32	8.35	14.93
78	Udalguri	283.2	35.72	24.75	8.37	23.84	23.34	4.44	15.01
79	V.Charali	200.5	2.98	1.04	2.37	1.7	0.74	0.92	1.28
80	Ararhia	721.0	9.19	5.63	3.15	8.98	5.13	2.49	4.45
81	Bahadurganj	676.5	5.65	2.16	1.33	4.91	1.88	1.02	2.14
82	Biharganj	771.9	7.4	3.17	1.79	4.65	2.91	1.58	2.72
83	Katihar	695.1	4.62	1.1	0.79	4.11	0.71	0.69	1.49
84	Baghmara	404.7	13.82	5.53	0.89	8.06	3.64	0.73	3.87
85	Barengpara	434.6	2.05	1.11	0.8	1.48	0.93	0.74	0.93
86	Dalu	429.7	17.45	2.87	0.9	3.23	2.3	0.75	3.10
87	Dauki	253.3	11.43	10.1	2.28	11.14	5.61	2.04	5.30
88	Mehendraganj	453.9	5.81	1.07	1.93	3.93	0.84	1.83	2.00
89	Mendipathar	395.4	3.94	2.63	2.77	3.12	1.16	0.94	1.36
90	Nangwalbibra	356.8	6.98	1.14	1.96	3.74	1.6	0	1.35
91	Mongpoh	284.2	6.9	2.83	4.72	4.86	1.89	6.63	3.95
92	Phulbari	452.4	10.58	5.42	4.97	7.76	5.59	4.3	5.10
93	Resubelpara	413.0	9.27	2.02	2.44	6.62	1.85	1.14	2.39
94	Shillong	260.5	0	2.03	2.33	31.09	1.87	1.09	5.27
95	Tura	430.3	32.34	8.31	5.06	19.23	6.52	3.79	9.17
96	Chrachandpur	218.3	13.75	7.6	8.62	6	6.11	2.54	5.67
97	Imphal	91.5	36.96	31.58	17.02	28.35	17.24	12.83	18.50
98	Kangpokbi	69.7	24.33	14.12	7.33	23.85	7.93	5.98	10.50
99	Maosongsang	39.6	14.18	6.17	4.21	14.08	5.2	1.93	5.75
100	Moirang	125.7	9.14	18.99	6.8	9	10.7	4.77	7.69
101	Pallel	114.9	23.27	17.45	4.53	22.69	14.15	3.49	10.72
102	Ukhrul	29.1	22.44	43.53	16.58	19.95	25.88	7.48	17.35
103	Chumukedima	83.2	21.44	19.42	6.63	16.08	15.98	3.59	10.45
104	Dimapur	96.3	54.17	25.32	12.22	39.56	12.47	11.17	19.32
105	Kohima	50.2	8.73	0	8.47	11.48	9.08	6.4	6.30
106	Agartala	373.8	1.99	1.25	0.71	1.75	0.94	0.55	0.92

107	Amarpur	361.1	11.47	3.75	1.12	6.16	2.79	1.02	3.16
108	Belonia	388.6	6.54	1.75	1.18	5.07	0.86	0.93	2.01
109	Bishalgarh	376.3	7.48	4.52	1.6	5.24	0.98	0.93	2.50
110	Kailashahar	278.8	7.44	6.73	2.42	4.07	2.38	1.18	2.95
111	Kamalpur	317.8	19.04	6.59	2.67	15.27	5.7	2.53	6.41
112	Khowai	332.6	12.95	3.35	1.26	9.82	9.31	0.62	4.68
113	Matarbari	366.6	11.82	4.36	4.63	6.98	3.56	3.34	4.46
114	Radhakishorpur	372.5	21.16	5.5	3.32	16.04	4.36	1.4	6.28
115	Sabrum	385.0	4.76	1.65	1.19	4.36	1.3	1.03	1.81
116	Belakoba	606.1	4.91	1.48	0.5	4.11	0.81	0.4	1.48
117	Haldibari	585.7	4.91	2.16	1.62	3.61	1.47	1.2	1.90
118	Kalimpong	633.7	5.98	2.71	1.5	5.82	1.64	1.16	2.37
119	Kurseong	645.3	4.62	1.79	0.88	2.95	1.21	1.08	1.57
120	Madarihat	541.7	12.97	1.94	0.93	6.7	1.71	0.89	2.97
121	Ramshai	579.8	11.64	2.52	2.15	5.73	2.18	1.65	3.17
122	Siliguri	617.5	7.93	2.86	2.27	5.11	2.16	1.55	2.75

Table B1(b): Recorded SRR values and the predicted PGA's for August 21, 1988, Bihar-Nepal earthquake.

Sl. No:	Stations	dist.	Accelerations in %g						
			5% damping			10% damping			PGA
			0.4	0.75	1.25	0.4	0.75	1.25	
1	Ararhia	100.8	42.71	25.52	26.18	33.91	26.69	24.03	24.18
2	Bahardur	130.1	26.69	17.99	13.65	21.27	13.7	6.01	12.69
3	Bairagnia	136.0	24.8	22.36	7.32	23.59	16.9	4.59	12.55
4	Barauni	152.3	18.62	10.71	2.87	14.96	9.23	2.28	7.27
5	Bettiah	213.0	6.54	2.09	0.87		0.97	0.77	1.68
6	Biharganj	110.7	35.96	19.2	8.06	30.25	16.22	6.96	14.71
7	Chapra	214.9	12	3.32	2.01	7.56	2.44	1.5	3.53
8	Darbhanga	96.3	74.8	66.21	39.04	58.18	61.18	33.53	43.92
9	Forbsganj	83.8	58.79	44.98	8.28	33.96	19.07	7.23	20.73
10	Jayanagar	48.5	36.28	24.8	12.62	29.45	14.73	6.84	15.64
11	Jogbani	144.3	141.5	69.81	17.34	78.8	48	11.64	44.20
12	Katibar	162.3	11.29	2.76	1.02	8.21	1.23	0.8	3.02
13	Kesaria	178.8	12.64	5.2	3.12	11.84	3.7	2.8	4.98
14	Lalganj	172.7	18.51	2.67	1.45	12.04	1.76	1.04	4.44
15	Lauria	237.2	7.09	2.67	1.36	3.82	2.02	1.15	2.24
16	Madhubani	58.3	35.8	28.41	14.16	28.41	16.51	12.65	17.50
17	Motipur	128.1	12.47	2.2	0.89	12.16	2	0.85	3.72
18	Murliganj	104.6	32.18	17.45	19.72	29.28	13.75	10.79	16.11
19	Muzzafarpur	141.3	10.18	8.9	3.32	16.6	7.16	3.12	6.39
20	Nirmali	42.8	36.85	56.3	31.77	38.18	46.67	24.15	31.28
21	Purnia	140.6	37.99	12.94	3.55	27.27	6.3	2.88	10.88
22	Raxaul	168.7	16.36	3.71	0.72	12.95	3.19	1.09	4.58
23	Sangauli	185.0	4.07	2.03	0.88	3.38	1.96	0.98	1.70
24	Saharsa	94.2	44.72	15.47	6.16	43.63	14.39	6.35	16.33
25	Samastipur	128.4	45.3	9.62	12.61	31.58	7.2	4.87	13.69
26	Shakarpur	169.2	5.82	1.05	1.28	3.7	0.88	0.86	1.68
27	Sitamarhi	112.1	31.58	21.29	9.03	22.14	17.99	6.2	13.65
28	Siwan	236.0	6.35	3.75	1.45	3.94	1.57	0.9	2.19
29	Sonpur	184.1	11.45	2.97	0.91	9.03	2.37	0.82	3.33
30	Supaul	70.3	47.71	49.3	20.9	42.54	40	15.64	27.91
31	Gorakhpur	337.4	9.19	6.48	0.86	9.21	6.39	0.62	4.06
32	Nautanwa	324.8	2.82	0.54	0.6	2.41	0.38	0.29	0.87
33	Nichaul	285.4	2.71	0.91	1.22	2.48	0.74	0.65	1.12
34	Belakoba	195.6	38.18	9.24	5.26	27.72	8.28	3.97	11.33
35	Englishmalda	254.0	9.97	11.41	3.93	5.91	2.94	2.37	4.49
36	Haldibari	217.2	16.36	9.61	6.61	9.75	7.07	3.07	6.60
37	Kalimpong	182.5	23.27	15.56	4.36	15.27	9	2.91	8.60
38	Kurseong	159.6	4.62	4.3	1.47	2.73	3.6	1.29	2.30
39	Maadrihat	268.5	22.94	3.88	1.52	16.75	2.74	0.89	5.77
40	Raiganj	197.3	2.61	4.2	3.62	1.94	4.53	2.11	2.60
41	Siliguri	186.1	12.4	6.44	5.21	10.22	6.13	2.49	5.48

Table B1(c): Recorded SRR values and the predicted PGA's for October 20, 1990, Uttarkashi earthquake.

Sl. No.	Stations	Dist. (km)	accelerations %g						
			5% damping			10% damping			PGA
			0.4	0.75	1.25	0.4	0.75	1.25	
1	Aut	150.0	2.83	1.15	0.93	2.49	0.99	0.85	1.18
2	Bainath	244.2	6.67	2.52	0.87	2.73	1.28	0.77	1.70
3	Bajaura	197.2	10.70	2.21	1.95	5.61	2.03	1.66	2.79
4	Barjar	168.8	15.46	1.99	1.54	14.10	1.75	1.35	3.71
5	Bilaspur	201.1	8.06	6.01	1.65	7.76	5.89	1.37	3.91
6	Deragopipur	269.7	2.99	1.23	1.03	2.57	0.92	0.72	1.19
7	Dharamashala	291.7	3.88	1.18	0.76	2.49	0.99	0.58	1.16
8	Drang	235.6	8.21	2.39	1.72	8.18	2.28	1.56	2.86
9	Ghuinarwin	212.1	3.27	0.98	2.34	2.49	0.60	2.29	1.76
10	Hamirpur	241.8	3.58	0.97	1.23	2.76	0.79	0.45	1.16
11	Jogindranagar	234.8	3.88	2.71	2.33	3.08	1.18	1.04	1.90
12	Jwalamukhi	266.1	6.43	1.59	1.12	6.16	1.04	0.97	1.93
13	Kandaghat	159.7	4.85	2.14	2.01	3.32	1.68	1.79	2.12
14	Kangra	285.7	2.18	0.87	0.59	1.89	0.73	0.49	0.83
15	Kasull	171.2	8.48	2.41	1.86	4.62	1.62	1.70	2.48
16	Kulu	211.3	2.46	1.30	1.04	2.13	0.95	0.84	1.16
17	Largi	184.2	7.81	2.13	3.19	7.76	1.59	2.69	3.21
18	Manall	232.0	6.98	3.49	2.69	4.99	2.46	2.04	2.97
19	Mandi	202.6	1.94	2.21	0.45	1.06	1.04	0.35	0.92
20	nachar	116.8	11.82	14.09	2.45	8.10	7.66	1.21	5.81
21	Naduan	255.6	8.43	2.27	1.82	6.86	1.62	1.43	2.60
22	Naban	197.1	12.54	3.25	1.15	4.65	2.94	1.00	2.81
23	Nalagarh	197.1	6.18	3.06	1.55	5.53	2.65	1.49	2.57
24	Narkanda	197.1	8.10	2.69	3.49	5.82	2.23	2.53	3.25
25	Nurpur	320.6	2.49	0.78	1.16	1.09	0.40	0.72	0.88
26	Palampur	261.4	3.32	4.26	1.30	2.91	3.36	0.97	2.23
27	Pandoh	189.9	3.30	1.18	0.34	2.91	0.40	0.23	0.88
28	Parwaiioo	178.6	9.01	1.00	1.43	7.48	0.62	1.21	2.21
29	pooli	132.0	3.82	1.76	1.51	2.33	1.39	1.20	1.60
30	Rampur	133.8	8.14	2.64	2.31	7.11	1.66	1.06	2.67
31	Rohru	110.0	3.49	4.76	5.26	1.81	4.36	4.73	4.12
32	Shimla	112.6	15.71	6.25	2.61	12.86	4.55	1.75	5.03
33	Sirkaghat	218.1	1.84	1.32	1.26	1.54	1.07	1.06	1.18
34	Suganpur	244.9	2.91	1.22	0.73	2.05	1.13	0.63	1.09
35	Sundarnagar	199.8	5.49	1.36	0.98	4.11	1.10	0.70	1.55
36	Una	249.7	3.83	1.41	0.93	3.77	0.73	0.65	1.32
37	Ambala	194.2	7.48	2.31	1.91	5.82	1.72	1.21	2.42
38	Bahadurgarh	287.5	3.64	1.72	1.01	3.04	1.31	0.87	1.45
39	Ballabhgarh	299.4	3.08	1.36	1.86	2.91	0.98	1.18	1.54
40	Faridabad.	289.8	4.91	1.75	1.85	2.91	1.51	1.23	1.83
41	Gohana	269.5	5.90	2.37	3.25	4.21	2.05	3.17	2.98
42	Jagadhari	154.6	10.47	5.76	1.72	6.02	1.16	1.09	2.98
43	JhaJJar	310.8	1.98	1.67	0.58	1.84	0.94	0.53	0.97
44	Jind	279.3	2.91	2.00	1.45	2.57	1.00	0.68	1.38
45	Kaittial	244.9	3.82	2.03	0.90	3.49	1.96	0.79	1.63
46	Ktirukst,ietra	227.3	4.50	6.29	2.82	3.88	2.46	2.08	3.12
47	Narwana	284.9	5.42	2.23	0.78	3.74	1.09	0.70	1.59
48	Panipat	228.1	5.98	1.38	1.13	2.12	1.08	0.97	1.49
49	Rohtak	299.3	3.18	0.52	0.53	2.33	0.36	0.44	0.81
50	Sohna	321.9	2.41	1.92	2.01	1.25	1.45	1.00	1.48

51	Afzalgarh	161.2	5.65	1.73	1.25	4.99	0.99	1.15	1.85
52	Almora	152.7	1.89	1.62	0.78	1.06	0.83	0.63	0.93
53	Amroha	210.6	4.14	5.35	3.93	3.56	3.08	3.17	3.54
54	Askot	184.8	3.29	1.24	1.62	2.62	0.97	1.45	1.53
55	Badaun	299.2	2.76	1.42	0.69	1.25	0.65	0.50	0.90
56	Badrinath	106.2	6.16	4.32	0.83	4.36	3.10	0.72	2.38
57	Bagpat	250.2	4.80	2.05	2.18	3.88	1.41	1.18	1.99
58	Banbasa	228.1	5.82	7.80	4.97	4.92	5.31	4.45	5.07
59	Baraut	244.2	1.94	1.90	1.40	1.45	1.19	1.11	1.32
60	Batkot	63.6	17.51	14.51	14.40	17.45	13.96	12.06	13.41
61	Bhatwari	14.8	46.25	57.02	37.62	38.49	49.48	29.85	39.02
62	Rijnor	157.3	5.82	3.05	2.21	4.91	2.09	1.37	2.49
63	Bilaspur		4.87	2.53	1.59	2.76	2.12	0.75	1.86
64	Champawat	199.8	3.13	1.09	1.81	1.38	0.97	1.33	1.38
65	Chandausi	251.6	1.89	1.19	1.03	1.45	0.62	0.77	0.96
66	Chandpur	183.4	5.33	3.04	3.12	2.73	1.59	2.31	2.56
67	Dakpathar	98.8	8.91	4.04	3.36	1.52	2.38	1.30	2.78
68	Dehradun	84.8	34.91	14.48	9.23	33.66	14.42	4.64	13.40
69	Deoband	152.2	3.22	2.71	0.94	3.08	1.19	0.73	1.50
70	Dhampur	164.6	7.61	3.45	1.70	7.19	1.96	1.27	2.74
71	Dharasu	51.7	20.56	8.64	6.08	13.86	8.01	6.07	8.21
72	Dharchula	156.7	2.05	0.64	1.12	1.08	0.44	1.02	0.90
73	Didihat	177.3	7.12	2.86	1.60	6.16	1.33	1.31	2.40
74	Gopeshwar	66.2	4.15	1.88	1.33	3.79	1.45	0.93	1.69
75	Haldwani	182.3	3.25	1.78	1.45	3.13	1.65	1.33	1.71
76	Hapur	244.0	2.63	0.89	1.03	2.18	0.74	0.95	1.10
77	Hardwar	105.8	7.32	2.81	4.78	3.49	0.82	3.64	3.27
78	Joshimath	84.4	3.48	2.36	1.51	1.19	0.92	0.94	1.40
79	Kairna	235.9	3.49	2.20	0.84	1.90	1.75	0.58	1.37
80	Kalagarh	137.2	4.26	14.22	12.47	2.69	7.92	11.25	9.33
81	Karanprayag	70.2	2.33	0.86	1.51	1.98	0.70	1.10	1.18
82	Kashipur	281.3	3.13	1.15	1.06	2.83	0.78	0.73	1.19
83	Kausani	160.7	2.49	1.10	1.72	2.36	0.93	0.98	1.32
84	Koti	97.6	20.21	7.53	5.34	11.64	4.46	3.42	6.36
85	Lansdowne	106.1	16.00	2.70	1.42	14.48	2.61	1.34	4.02
86	Meerut	219.2	4.11	2.23	1.78	3.27	1.53	1.13	1.84
87	Moradabad	212.8	3.04	1.34	1.57	2.05	0.35	0.45	1.10
88	Mussorie	74.0	16.81	11.64	11.89	16.11	8.14	6.82	9.96
89	Muzzafarnagar	175.4	4.11	3.37	1.54	3.15	2.57	1.18	2.14
90	Pagina	148.8	8.73	3.16	1.72	3.59	1.36	1.28	2.33
91	Nainabaq	72.4	24.43	14.54	10.31	18.37	10.17	7.85	11.45
92	Nainital	163.9	6.98	4.31	1.40	6.19	4.21	0.98	2.99
93	Narendra		5.97	3.21	3.83	3.49	1.16	3.45	3.06
94	Narora nagar	283.3	1.49	1.37	0.93	1.19	0.99	0.75	0.97
95	Paurt	45.8	4.89	1.43	2.03	2.14	1.09	1.66	1.77
96	Pilibhit	254.1	17.88	5.88	3.99	6.11	4.69	2.79	5.03
97	Pithoragarh	185.9	1.99	0.79	2.36	1.01	0.59	1.67	1.35
98	Puranpur	315.8	5.98	2.49	1.70	2.05	1.94	1.67	2.09
99	Rampur	230.5	8.21	2.14	0.77	5.45	1.96	0.66	2.09
100	Ranikhet	134.5	2.91	0.91	2.80	2.12	0.78	1.06	1.50
101	Rishikesh	90.0	15.65	8.17	2.72	15.58	4.93	2.33	5.81
102	Roorkee	130.0	4.81	4.01	5.42	3.36	2.49	3.35	3.61
103	Rudraprayag	52.2	4.72	1.71	2.31	1.99	1.11	1.38	1.78
104	Saharanpur	146.3	5.17	1.87	0.53	3.09	1.10	0.44	1.35
105	Sambhal	239.7	8.73	7.48	2.40	6.23	5.53	1.84	4.23

106	Shamli	202.0	5.69	9.86	1.16	4.25	4.55	0.43	3.39
107	Tehri	49.4	14.77	7.43	7.02	13.32	7.31	6.94	7.85
108	Tezam	156.4	5.51	1.71	1.82	3.28	1.37	1.50	1.94
109	Thal	162.8	4.72	1.48	0.71	2.60	1.37	0.43	1.29
110	Uttarkashi	45.3	106.21	65.24	45.73	95.84	64.76	33.79	55.35
111	Delhi	260.2	3.32	1.84	0.58	1.94	1.11	0.50	1.13

Table B1(d): Recorded SRR values and the predicted PGA's for March, 29 1999, Chamoli earthquake.

Sl. No.	Stations	Dist. (km)	Acceleration in %g						PGA
			5%			10%			
			0.4 sec	0.75 sec	1.25 sec	0.4 sec	0.75 sec	1.25 sec	
1	Barkot	131.3	10.19	3.26	1.22	7.03	3.06	1.12	2.81
2	Bhatwari	81.5	7.34	2.55	1.12	3.36	1.12	0.71	1.76
3	Dehradun	131.3	21.51	9.99	3.67	18.65	8.87	3.16	7.52
4	Dharasu	118.4	3.98	1.43	1.53	1.22	1.22	0.92	1.35
5	Gopeshwar	4.8	64.53	45.16		64.12	42.92	20.59	33.53
6	Joshimath	26.9	14.07	9.28	9.99	8.36	7.54	6.63	8.12
7	Karnprayag	20.6	6.93	2.24	4.28	5.91	2.14	3.77	3.57
8	Kausani	103.5	9.17	2.96	2.75	8.46	2.55	1.43	3.18
9	Lansdown	106.1	3.98	2.04	0.92	1.83	1.02	0.61	1.23
10	Mussourie	127.8	19.88	9.17	2.55	17.13	7.75	2.04	6.44
11	Narendranagar	43.6	17.43	7.44	2.96	11.93	4.28	2.45	5.22
12	Pauri	108.6	7.65	3.57	4.49	4.28	1.12	4.18	3.63
13	Roorkee	158.7	13.25	4.38	2.85	6.73	3.36	2.14	3.82
14	Rudraprayag	44.7	4.69	2.04	3.98	4.28	1.53	2.75	2.83
15	Tehri	88.0	25.08	9.28	3.16	16.11	8.56	2.75	7.17
16	Uttarkashi	111.8	28.95	5.81	5.50		5.40	2.96	6.77

Table B1(e): Recorded SRR values and the predicted PGA's for April 26 1986, Kangra earthquake.

Sl. No.	Stations	Dist. (km)	Acceleration %g						PGA
			SA 5% damping			10% damping			
			0.4	0.75	1.25	0.4	0.75	1.25	
1	Bakloh	62.0	5.68	1.05	1.06	3.08	1.44	1.58	2.30
2	Bajjnath	44.1	4.53	1.52	0.82	3.66	0.65	1.23	1.94
3	Chamba	44.4	8.25	2.65	1.98	3.57	1.42	1.05	2.88
4	Deragopipur	36.2	1.67	1.26	0.94	0.74	0.79	0.38	1.08
5	Hamirpur	58.1	0.39	2.1	1.37	0.68	0.57	1.33	1.66
6	Nurpur	35.5	2.04	0.41	0.49	5.48	0.94	0.17	1.22
7	Palampur	25.0	5.18	2.13	1.87	3.76	1.76	2.15	3.13
8	Pathankot	55.9	1.2	0.36	0.48	2.05	1.49	0.41	1.02
9	Shimla	177.3	4.47	1.13	0.61	9.98	1.5	0.29	2.18
10	Sundarnagar	92.9	1.8	0.48	0.39	2.38	0.78	0.33	0.90
11	Bilaspur	107.6	4.95	3.88	2	5.19	0.92	1.68	3.20
12	Jawalamukhi	38.0	6.11	2.88	2.65	3.23	2.52	2.07	3.67
13	Joginder Nagar	51.8	5.03	1.59	0.64	4.09	1.28	1.67	2.30
14	Sarkaghat	71.6	5.14	1.82	0.63	7.01	1.61	1.03	2.42
15	Tira Sujanpur	47.5	1.81	1.38	0.51	1.83	0.38	0.33	0.96
16	Dharamstjala	5.8	22.8	15.8	4.64	16.66	11.1	2.34	10.99
17	Kangra	7.6	27.29	17.81	5.3	15.47	11.53	4.54	12.86

Table B2: SRR stations installed and their geographical coordinates

Sl. No.	Station	State	Longitude		Latitude	
			Deg.	Min.	Deg.	Min.
1	Along	Arunachal	94	46	28	10
2	Bilat	Arunachal	95	9	27	56
3	Bomdila	Arunachal	92	20	27	20
4	Choukham	Arunachal	96	2	27	47
5	Daring	Arunachal	94	49	27	52
6	Dirang	Arunachal	92	17	27	25
7	Gensi	Arunachal	94	25	27	47
8	Hapeli	Arunachal	93	42	27	36
9	Itanagar	Arunachal	93	35	27	12
10	Khonsa	Arunachal	95	25	27	0
11	Oyan	Arunachal	95	1	28	28
12	Pangin	Arunachal	95	0	28	15
13	Pasighat	Arunachal	95	20	28	1
14	Raga	Arunachal	94	1	28	31
15	Roing	Arunachal	95	52	28	9
16	Tawang	Arunachal	91	52	27	35
17	Yembeung	Arunachal	93	12	27	28
18	Abhayapuri	Assam	90	38	26	21
19	Amguri	Assam	94	31	26	49
20	Badarpur	Assam	92	22	24	52
21	Baduliipur	Assam	94	1	26	34
22	Barpathar	Assam	93	50	26	16
23	Barpeta-road	Assam	91	2	26	20
24	Bihpuria	Assam	93	59	26	59
25	Bijni	Assam	90	40	26	30
26	Bijoynagar	Assam	91	45	26	7
27	Bilasipara	Assam	90	13	26	13
28	Bokakrat	Assam	93	27	26	36
29	Bongaigaon	Assam	90	35	26	28
30	Chaparmukh	Assam	92	30	26	11
31	Dangari	Assam	95	36	27	47
32	Dergaon	Assam	93	58	26	45
33	Dhakiajuli	Assam	92	28	26	42
34	Dhemaji	Assam	94	36	27	33
35	Di-iing	Assam	92	29	26	28
36	Dibrugarh	Assam	94	54	27	29
37	Digboi	Assam	95	37	27	22
38	Diphu	Assam	93	28	25	51
39	Doomdooma	Assam	95	40	27	33
40	Dudhnoi	Assam	90	48	25	59
41	Dullabchera	Assam	92	26	24	27
42	Furkating	Assam	94	1	26	28
43	Goalpara	Assam	90	37	26	7
44	Golaghat	Assam	93	57	26	30
45	Golakgang	Assam	89	55	26	9
46	Goriipur	Assam	89	58	26	5
47	Guwahati	Assam	91	45	26	10
48	Haflong	Assam	93	1	25	15
49	Hailakandi	Assam	92	35	24	38
50	Hojai	Assam	92	51	26	1

Sl. No.	Station	State	Longitude		Latitude	
			Deg.	Min.	Deg.	Min.
51	Jamugiri	Assam	92	57	26	42
52	Jamunamukh	Assam	92	46	26	8
53	Jorhat	Assam	94	12	26	45
54	Kamargaon	Assam	93	59	26	38
55	Kampur	Assam	92	38	26	10
56	Karimganj	Assam	92	21	24	51
57	Kollabar	Assam	92	58	26	31
58	Kukichera	Assam	92	35	24	20
59	Lakhipur	Assam	90	27	26	3
60	Lalagiat	Assam	92	36	24	34
61	Lanka	Assam	92	56	25	54
62	Ledo	Assam	95	50	27	18
63	Likhapani	Assam	95	48	27	17
64	Lumding	Assam	93	19	25	27
65	Mairabari	Assam	92	29	26	47
66	Makum	Assam	95	28	27	28
67	Magaldai	Assam	92	2	26	45
68	Mariani	Assam	94	19	26	38
69	Moranhat	Assam	94	10	27	17
70	Naharkatiya	Assam	95	22	27	10
71	Nalbari	Assam	91	14	26	25
72	Nazira	Assam	94	50	26	54
73	Neamati	Assam	94	18	26	46
74	Nilbagan	Assam	93	40	25	52
75	Nogora	Assam	93	58	26	20
76	North-lakhimpur	Assam	94	7	27	12
77	Paneri	Assam	91	57	26	42
78	Rangapara	Assam	92	40	26	47
79	Rangia	Assam	91	38	26	26
80	Sarupeta	Assam	91	5	26	31
81	Shilapathar	Assam	95	14	27	47
82	Sibsagar	Assam	94	39	26	58
83	Silchar	Assam	92	47	24	49
84	Silgrat	Assam	92	56	26	36
85	Sonapur	Assam	92	0	27	7
86	Subankrata	Assam	91	24	26	46
87	Tezpur	Assam	92	49	26	38
88	Tinsukia	Assam	95	20	27	28
89	Titabar	Assam	94	12	26	36
90	Udalguri	Assam	92	8	26	46
91	Ararira	Bihar	87	21	26	7
92	Bahadurganj	Bihar	87	49	26	16
93	Bairagania	Bihar	85	15	26	39
94	Barauni	Bihar	85	59	25	30
95	Bettiah	Bihar	84	28	26	47
96	Bihariganj	Bihar	86	49	25	46
97	Chapra	Bihar	84	44	25	48
98	Darbhanga	Bihar	85	54	25	10
99	Jaynagar	Bihar	86	10	26	35
100	Jogbani	Bihar	85	13	26	24

Sl. No.	Station	State	Longitude		Latitude	
			Deg.	Min.	Deg.	Min.
101	Katihar	Bihar	87	35	25	34
102	Kesariya	Bihar	84	52	26	22
103	Kishanganj	Bihar	88	9	26	5
104	Lalganj	Bihar	85	12	25	51
105	Lauriya	Bihar	84	14	26	59
106	Madhubani	Bihar	86	5	26	32
107	Motipur	Bihar	85	24	26	22
108	Murliganj	Bihar	87	0	25	52
109	Muzzafarpur	Bihar	85	23	26	7
110	Nirmali	Bihar	86	34	26	22
111	Purnea	Bihar	87	28	25	44
112	Raxaul	Bihar	84	56	26	59
113	Sagauli	Bihar	84	45	26	46
114	Sahrasa	Bihar	86	36	25	54
115	Samastipur	Bihar	85	47	25	52
116	Shikarpur	Bihar	84	55	26	37
117	Sitamarhi	Bihar	85	30	26	36
118	Siwan	Bihar	84	22	26	4
119	Sonpur	Bihar	85	11	25	42
120	Supaul	Bihar	86	35	26	7
121	Ahemdabad	Gujarat	72	38	23	2
122	Amreli	Gujarat	71	19	21	33
123	Anand	Gujarat	73	1	22	34
124	Anjar	Gujarat	70	5	23	6
125	Bhachau	Gujarat	71	23	23	12
126	Bhuj	Gujarat	69	54	23	12
127	Caimay	Gujarat	72	39	22	19
128	Dwarka	Gujarat	69	3	22	15
129	Janujodhpur	Gujarat	70	20	21	56
130	Jamnagar	Gujarat	70	4	22	4
131	Junagadh	Gujarat	70	30	21	25
132	Aliya	Gujarat	69	42	22	13
133	Mandavi	Gujarat	73	22	21	16
134	Morvi	Gujarat	70	50	22	50
135	Naliga	Gujarat	68	51	23	19
136	Niruna	Gujarat	69	12	22	43
137	Porbandar	Gujarat	69	40	21	40
138	Aut	Himachal	77	13	30	44
139	Balnath	Himachal	76	43	32	3
140	Bajaura	Himachal	77	9	31	50
141	Bakloh	Himachal	75	41	32	25
142	Banjar	Himachal	77	21	31	38
143	Bilaspur	Himachal	76	47	31	19
144	Dalhousie	Himachal	75	58	32	37
145	Deragopwm	Himachal	76	16	31	52
146	Dharamsala	Himachal	76	15	32	14
147	Drang	Himachal	76	35	31	43
148	Gumarwin	Himachal	76	43	31	27
149	Hamirpur	Himachal	76	30	31	42
150	Jogindranagar	Himachal	76	47	31	59

Sl. No.	Station	State	Longitude		Latitude	
			Deg.	Min.	Deg.	Min.
151	Jwalamuki	Himachal	76	18	31	51
152	Kandaghat	Himachal	77	8	30	58
153	Kangra	Himachal	76	15	32	8
154	Kasuali	Himachal	77	0	30	53
155	Keylong	Himachal	77	5	32	35
156	Khoksar	Himachal	77	15	32	27
157	Kulu	Himachal	77	6	31	59
158	Larji	Himachal	77	14	31	44
159	Manali	Himachal	77	8	32	17
160	Mandi	Himachal	76	57	31	40
161	Nachar	Himachal	77	59	31	32
162	Naduan	Himachal	76	22	31	45
163	Nahan	Himachal	77	18	30	35
164	Nalagarh	Himachal	76	45	31	3
165	Narkanda	Himachal	77	25	31	15
166	Nurpur	Himachal	75	56	32	18
167	Palawur	Himachal	76	32	32	6
168	Pandoh	Himachal	77	5	31	38
169	Parwanoo	Himachal	76	55	30	48
170	Pooh	Himachal	78	35	31	55
171	Rampur	Himachal	77	40	31	28
172	Rohru	Himachal	77	46	31	12
173	Sirkhaghat	Himachal	76	47	31	42
174	Sujanpur	Himachal	76	32	31	49
175	Sundarnagar	Himachal	76	54	31	32
176	Una	Himachal	76	18	31	28
177	Talwara	Punjab	75	56	31	57
178	Ambala	Haryana	76	49	30	19
179	Bahaurgarh	Haryana	76	58	28	41
180	Ballabhgarh	Haryana	77	16	28	23
181	Faridabad	Haryana	77	14	28	30
182	Gohana	Haryana	76	43	29	6
183	Gurgaon	Haryana	77	1	28	27
184	Jagadhari	Haryana	77	20	30	8
185	Jhajjar	Haryana	76	42	28	36
186	Jind	Haryana	76	24	29	18
187	Kaithal	Haryana	76	29	29	47
188	Kurukshetra	Haryana	76	49	29	36
189	Narwana	Haryana	76	8	29	35
190	Panepat	Haryana	76	59	29	24
191	Rohtak	Haryana	76	35	28	50
192	Sohna	Haryana	77	4	28	15
193	Bagmara	Meghalaya	90	30	25	10
194	Barengpara	Meghalaya	90	12	25	11
195	Cherapunji	Meghalaya	91	43	25	16
196	Dalu	Meghalaya	90	15	25	10
197	Dauki	Meghalaya	92	1	25	10
198	Jowai	Meghalaya	92	16	25	25
199	Mawplang	Meghalaya	91	36	25	22
200	Mehendraganj	Meghalaya	90	0	25	17

Sl. No.	Station	State	Longitude		Latitude	
			Deg.	Min.	Deg.	Min.
201	Mendipathar	Meghalaya	90	35	25	34
202	Nangwalbibra	Meghalaya	90	58	25	28
203	Nongpoh	Meghalaya	91	43	25	45
204	Nongstoin	Meghalaya	91	14	25	25
205	Phulbari	Meghalaya	90	2	25	52
206	Resubelpara	Meghalaya	90	25	25	44
207	Tura	Meghalaya	90	14	25	32
208	Chandigarh	Chandigarh	76	47	30	43
209	Chura-chandpur	Manipur	92	50	24	10
210	Iwhal	Manipur	93	55	24	47
211	Kangpokbi	Manipur	93	53	25	10
212	Maosongsang	Manipur	94	9	25	29
213	Moirang	Manipur	93	47	24	29
214	Pallel	Manipur	94	1	24	28
215	Tamenglong	Manipur	93	30	25	0
216	Thoubal	Manipur	94	0	24	40
217	Ukhrul	Manipur	94	23	25	10
218	Aijawl	Mizoram	92	45	23	45
219	Kalosib	Mizoram	92	40	24	17
220	Lungleh	Mizoram	92	49	22	55
221	N.vanlaiphm	Mizoram	93	4	23	7
222	Sairang	Mizoram	92	42	23	50
223	Tlabang	Nfizoram	92	29	22	53
224	Chumukedima	Nagaland	93	50	25	48
225	Dimapur	Nagaland	93	45	25	54
226	Kohims	Nagaland	94	8	25	40
227	Mokokchung	Nagaland	94	31	26	23
228	Nagnimara	Nagaland	94	48	26	49
229	Tuensang	Nagaland	94	52	26	16
230	Amritsar	Punjab	74	56	31	35
231	Batala	Punjab	75	18	31	47
232	Biiatinda	Punjab	74	58	30	13
233	Dasuya	Punjab	75	44	31	48
234	Derababananak	Punjab	75	2	32	3
235	Dinanagar	Punjab	75	35	32	10
236	Fazilka	Punjab	74	1	30	26
237	Ferozpur	Punjab	74	35	30	52
238	Gurdaspur	Punjab	75	27	32	3
239	Hosiharpur	Punjab	76	1	31	45
240	Mlundar	Punjab	75	35	31	20
241	Kapurthala	Punjab	75	22	31	25
242	Ludhiana	Punjab	75	52	30	56
243	Moga	Punjab	75	10	30	49
244	Mukerian	Punjab	75	42	31	56
245	Patiala	Punjab	76	27	30	22
246	Patn	Punjab	74	52	31	17
247	Phagwara	Punjab	75	48	31	15
248	Gangtok	Sikkim	88	42	27	12
249	Agartala	Tripura	91	15	23	49
250	Amarpur	Tripura	91	37	23	30

Sl. No.	Station	State	Longitude		Latitude	
			Deg.	Min.	Deg.	Min.
251	Belonia	Tripura	91	29	23	15
252	Bishalgarh	Tripura	91	17	23	43
253	Kailashahar	Tripura	92	1	24	20
254	Kamalpur	Tripura	91	40	24	11
255	Kiiowai	Tripura	91	34	24	4
256	Nutarbari	Tripura	91	33	23	30
257	Radhakishorepur	Tripura	91	28	23	31
258	Sabrum	Tripura	91	45	23	1
259	Afazalgarh	Uttar	78	32	29	18
260	Almora	Uttar	79	38	29	34
261	Amroha	uttar	78	14	28	54
262	Askot	Uttar	80	20	29	44
263	Badaun	Uttar	79	6	28	3
264	Badrinath	Uttar	79	54	30	38
265	Bagpat	Uttar	77	12	28	57
266	Baharaich	Uttar	81	55	27	35
267	Balrampur	Uttar	82	10	27	25
268	Banbassa	Uttar	80	4	29	0
269	Baraut	Uttar	77	8	29	4
270	Barkot	Uttar	78	8	30	50
271	Barriely	Uttar	79	18	31	47
272	Bhatwari	Uttar	78	45	30	52
273	Bijnor	Uttar	78	6	29	27
274	Buaspur	Uttar	79	29	28	10
275	Bulandshahar	Uttar	77	59	28	9
276	Chawawat	Uttar	80	6	29	20
277	Chandausi	Uttar	78	48	28	28
278	Chandpur	Uttar	78	15	29	9
279	Dakpathar	Uttar	78	8	30	3
280	Dehradun	Uttar	78	3	30	19
281	Deoband	Uttar	77	45	29	42
282	Dhamapur	Uttar	78	33	29	16
283	Dharasu	Uttar	78	15	30	46
284	Dharchula	Uttar	80	10	29	58
285	Didihat	Uttar	80	15	29	45
286	Domariyaganj	Uttar	82	39	27	12
287	Gonda	Uttar	81	58	27	4
288	Gopeshwar	Uttar	79	24	30	27
289	Haldwani	Uttar	79	31	29	13
290	Hapur	Uttar	77	47	28	43
291	Hardwar	Uttar	78	10	29	57
292	Jarwal-road	Uttar	81	32	27	9
293	Joshimath	Uttar	79	39	30	33
294	Kairana	Uttar	77	8	29	10
295	Kaisarganj	Uttar	81	33	27	15
296	Karanprayag	Uttar	79	17	30	16
297	Kashipur	Uttar	78	53	28	12
298	Kausani	Uttar	79	40	29	30
299	Lansdowne	Uttar	78	34	29	48
300	Mithura	Uttar	77	46	27	28

Sl. No.	Station	State	Longitude		Latitude	
			Deg.	Min.	Deg.	Min.
301	Meerut	Uttar	77	42	29	0
302	Moradabad	Uttar	78	49	28	49
303	Mussorie	Uttar	78	5	30	28
304	Muzzafarnagar	Uttar	77	42	29	28
305	Nagina	Uttar	78	21	29	27
306	Nainabag	Uttar	78	2	30	47
307	Nainital	Uttar	79	26	29	22
308	Nanpara	Uttar	81	30	27	51
309	Narora	Uttar	78	18	28	13
310	Nautanwa	Uttar	83	25	27	26
311	Nepalgarh	Uttar	81	0	28	10
312	Nicblaul	Uttar	83	47	27	15
313	Pauri	Uttar	78	39	31	8
314	Pilibhit	Uttar	79	45	28	36
315	Pithoragarh	Uttar	80	12	29	35
316	Puranpur	Uttar	80	2	28	6
317	Rampur	Uttar	79	1	28	40
318	Raniketh	Uttar	79	25	29	39
319	Rishikesh	Uttar	78	14	30	5
320	Saharanpur	Uttar	77	33	29	58
321	Sambhal	Uttar	78	34	28	35
322	Shamli	Uttar	77	18	29	27
323	Teiuu	Uttar	78	29	30	21
324	Tejam	Uttar	80	9	29	57
325	Thal	Uttar	80	8	29	50
326	Uska-bazar	Uttar	82	12	27	4
327	Uttarkasi	Uttar	78	19	30	45
328	Alipurdwar	West	89	38	26	29
329	Belakoba	West	88	35	26	33
330	English-bazar	West	88	16	25	0
331	Haldibari	West	88	44	26	14
332	Jalpaiguri	West	88	50	26	30
333	Kalimpong	West	88	26	27	4
334	Kurseong	West	88	14	26	47
335	Madarihat	West	89	20	26	51
336	Raiganj	West	88	10	25	38
337	Ramshai	West	88	54	26	44
338	Siliguri	West	88	30	26	42
339	Champa		76	11	32	35
340	Pathankot		75	42	32	16
341	Shimla		77	42	31	8
342	Sujanpur		76	32	31	49
343	Forbesganj		87	18	26	18
344	Marghetia		95	40	27	17
345	Delhi		77	31	28	40
346	Gorakhpur		83	23	26	45
347	Kalagarh		78	45	29	30
348	Shillong		91	53	25	34
349	V.charali		93	12	26	45
350	Koti		77	48	30	35